EMERGING INFECTIOUS DISEASES®

U.S. CENTERS FOR DISEASE CONTROL AND PREVENTION

Fungal Infections

September 2026

Jörg Braumeister, *Stadtbibliothek im Bildungscampus Nürnberg*, Amb. 317.2°, *Folio 60 recto*, 1437. Pen and ink on parchment. 287 mm × 205 mm (11.3 in × 8.1 in). Collection: The Hausbücher der Nürnberger Zwölfbrüderstiftungen. Nuremberg Twelve Brothers House Books, Nuremberg, Germany.

Pages 1391–1536

EMERGING INFECTIOUS DISEASES

A Peer-Reviewed Journal Tracking and Analyzing Disease Trends

Emerging Infectious Diseases is published monthly by the Centers for Disease Control and Prevention, 1600 Clifton Rd NE, Mailstop H16-2, Atlanta, GA 30329-4018, United States. Telephone 404-639-1960; email eideditor@cdc.gov

EMERGING INFECTIOUS DISEASES®

Fungal Infections **September 2026**

On the Cover

Jörg Braumeister, *Stadtbibliothek im Bildungscampus Nürnberg, Amb. 317.2°, Folio 60 recto,* 1437 (detail). Pen and ink on parchment. 287 mm × 205 mm (11.3 in × 8.1 in). Collection: The Hausbücher der Nürnberger Zwölfbrüderstiftungen. Nuremberg Twelve Brothers House Books, Nuremberg, Germany.

About the Cover p. 1533

Synopses

Medscape EDUCATION ACTIVITY

Research

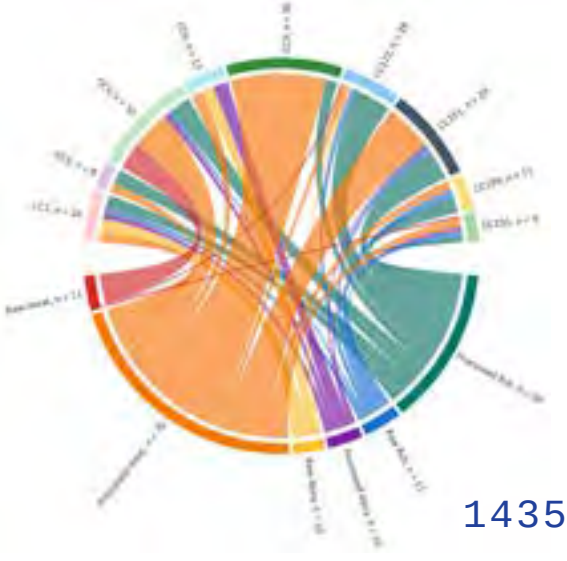

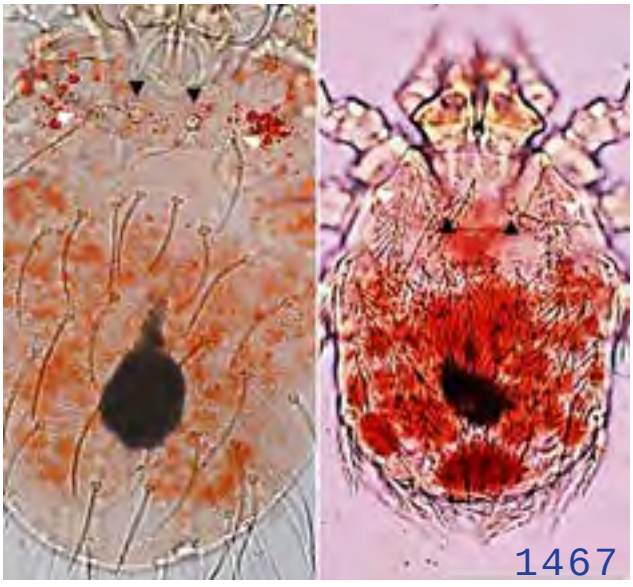

Dispatches

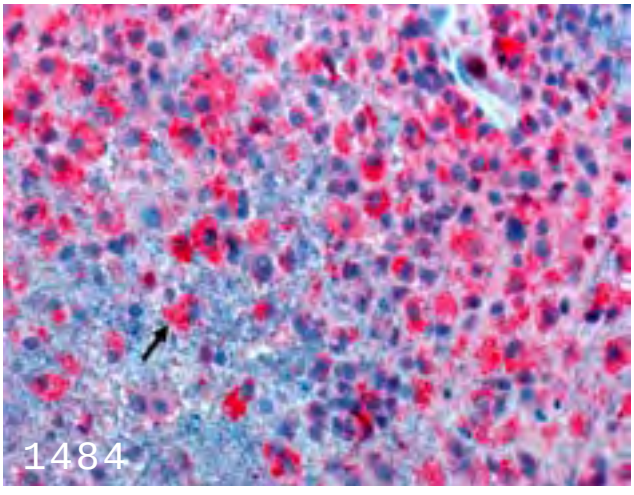

EMERGING INFECTIOUS DISEASES®
September 2026

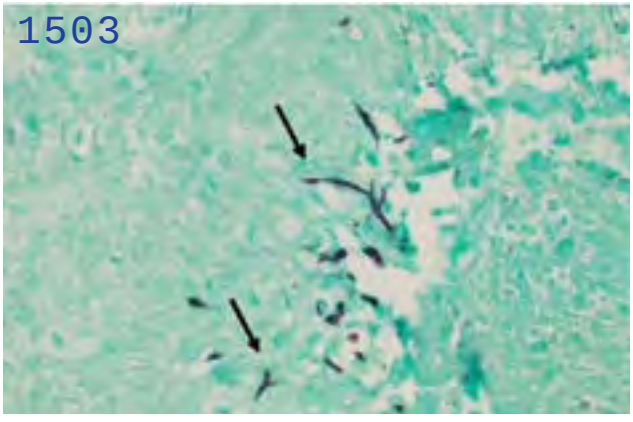

Research Letters

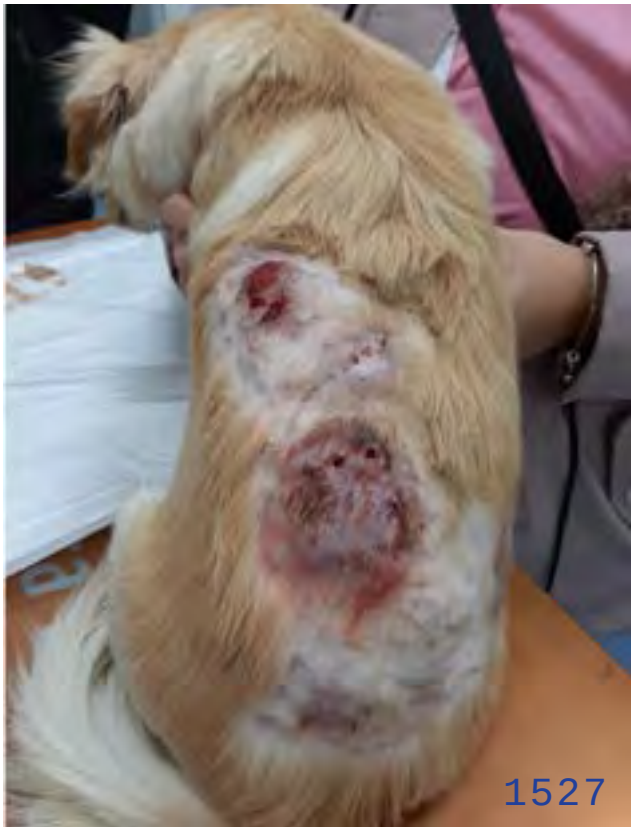

EMERGING INFECTIOUS DISEASES®
September 2026

Comment Letters

About the Cover

Emerging Infectious Diseases
Photo Quiz Articles

Volume 14, Number 9
September 2008

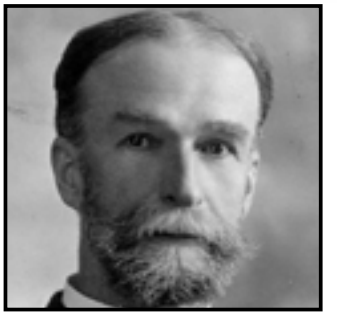

Volume 14, Number 12
December 2008

Volume 15, Number 9
September 2009

Volume 15, Number 10
October 2009

Volume 16, Number 6
June 2010

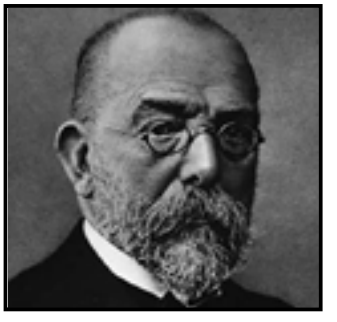

Volume 17, Number 3
March 2011

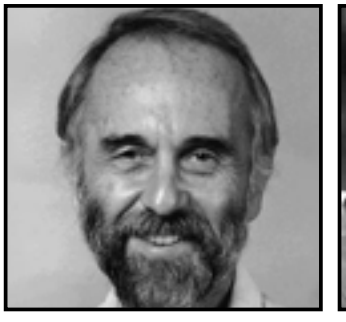

Volume 17, Number 12
December 2011

Volume 19, Number 4
April 2013

Volume 20, Number 5
May 2014

Volume 21, Number 9
September 2015

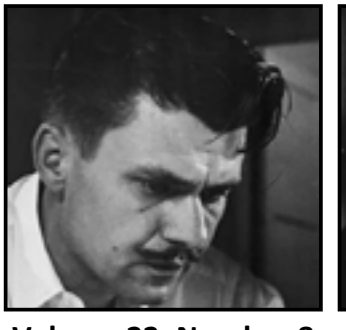

Volume 22, Number 8
August 2016

Volume 28, Number 3
March 2022

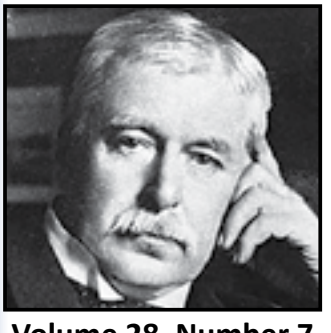

Volume 28, Number 7
July 2022

Click on the link below to read about the people behind the science.

https://bit.ly/3LN02tr

See requirements for submitting a photo quiz to EID.

https://bit.ly/3VUPqfj

Volume 32, Number 6
June 2026

Neoehrlichiosis Causing Hemolytic Anemia in Patients Treated with Rituximab, Norway, 2024–2025

Martin Paulson, Christine Wennerås, Hanne Quarsten, Kristine K. Berg, Anders L. Drivenes, Magnus Moksnes, Tor Henrik A. Tvedt

CDC Continuing Education (CE) ACTIVITY

PROGRAM DESCRIPTION: This activity provides the target audience with quality research to further their knowledge in neoehrlichiosis and will inform readers of the latest findings on this tickborne infection and a complication for patients taking rituximab. **INTENDED AUDIENCE:** Clinicians; epidemiologists; Public health departments.

Learning Objectives

Upon completion of this activity, participants will be able to:

- Describe characteristics of neoehrlichiosis
- Identify variables that put the three case-patients at risk for neoehrlichiosis
- Discuss recommended treatments for neoehrlichiosis

For complete instructions and CE quiz, see page 1536.

Release date: August 31, 2026; Expiration date: August 31, 2027

CME Authors

Martin Paulson, MD, *Consultant Hematologist, Vestfold Hospital Trust;* ***Christine Wennerås, MD, PhD,*** *Professor, Senior Consultant, Sahlgrenska University Hospital;* ***Hanne Quarsten, MsC, PhD,*** *Head of the Molecular Biology Unit/Researcher, Sørlandet Hospital Trust;* ***Kristine K. Berg, MD,*** *Consultant MD, Sørlandet Hospital Trust, Department of Medical Microbiology;* ***Anders L. Drivenes, MD,*** *Resident MD, Oslo University Hospital;* ***Magnus Moksnes, MD,*** *Consultant MD, Vestfold Hospital Trust;* ***Tor Henrik A. Tvedt, MD, PhD,*** *Consultant Hematologist and Associate Professor, Oslo University Hospital, Department of Hematology.*

In support of improving patient care, the Centers for Disease Control and Prevention is jointly accredited by the Accreditation Council for Continuing Medical Education (ACCME), the Accreditation Council for Pharmacy Education (ACPE), and the American Nurses Credentialing Center (ANCC) to provide continuing education for the healthcare team.

CME: The Centers for Disease Control and Prevention designates this enduring activity for a maximum of **0.75 AMA PRA Category 1 Credits™**. Physicians should claim only the credit commensurate with the extent of their participation in the activity. **AAPA CME:** Credit Designation Statement—Enduring Materials: The Centers for Disease Control and Prevention has been authorized by the American Academy of PAs (AAPA) to award AAPA Category 1 CME credit for activities planned in accordance with AAPA CME Criteria. This activity is designated for **0.75 AAPA Category 1 CME credits**. Approval is valid until August 31, 2029. PAs should only claim credit commensurate with the extent of their participation. **CNE:** The Centers for Disease Control and Prevention designates this activity for **0.75 nursing contact hours**. **CEU:** The Centers for Disease Control and Prevention is authorized by IACET to offer **0.1 CEUs** for this program. **AAVSB/RACE:** This program was reviewed and approved by AAVSB RACE program for **1.0 hours of continuing education**. Participants should be aware that some boards have limitations on the number of hours accepted in certain categories or restrictions on certain methods of delivery of continuing education. Please contact the AAVSB RACE program if you have any comments or concerns regarding this program's validity or relevancy to the veterinary profession. **CPH:** The Centers for Disease Control and Prevention is a preapproved provider of Certified in Public Health (CPH) recertification credits and is authorized to offer **1 CPH recertification credits** for this program.

DISCLOSURE: *In compliance with continuing education requirements, all planners and presenters must disclose all financial relationships, in any amount, with ineligible companies during the previous 24 months as well as any use of unlabeled product(s) or products under investigational use. CDC, our planners, and content experts wish to disclose they have no financial relationship(s) with ineligible companies with the exception of Dr. Magnus Moksnes and Dr. Tor Henrik Anderson Tvedt, and they wish to disclose the following relationships: Dr. Magnus Moksnes disclosures: Johnson & Johnson, Honoraria & advisory board; Abbvie, Honoraria; Pfizer, Honoraria; Sanofi, Advisory board; Eli Lilly, Advisory board; MDS, Advisory board; AstraZeneca, Honoraria. Dr. Tor Henrik Anderson Tvedt disclosures: Janssen, Educational material; Takeda, Advisory board/educational material. All the relevant financial relationships listed for these individuals have been mitigated. Content will not include any discussion of the unlabeled use of a product or a product under investigational use.*

The Centers for Disease Control and Prevention (CDC) complies with applicable Federal civil rights laws and does not discriminate based on race, color, national origin, age, disability, religion, or sex. To learn more visit: https://www.hhs.gov/civil-rights/for-individuals/nondiscrimination/index.html.

CONTACT INFORMATION: ***Emerging Infectious Diseases*** **Journal, eideditor@cdc.gov**

Author affiliations: Vestfold Hospital Trust, Tønsberg, Norway (M. Paulson, M. Moksnes); University of Gothenburg, Gothenburg Sahlgrenska Academy, Gothenburg, Sweden (C. Wennerås); Sahlgrenska University Hospital, Gothenburg (C. Wennerås); Sørlandet Hospital Trust, Kristiansand, Norway (H. Quarsten, K.K. Berg); Oslo University Hospital, Oslo, Norway (A.L. Drivenes, T.H.A. Tvedt); University of Oslo Institute of Clinical Medicine, Oslo (T.H.A. Tvedt)

DOI: https://doi.org/10.3201/eid3209.260553

Neoehrlichiosis is caused by infection with the tickborne intracellular bacterium *Neoehrlichia mikurensis*. We describe 3 cases of direct antiglobulin test–negative hemolytic anemia in rituximab-treated patients infected with tickborne *N. mikurensis* bacteria in Norway during 2024–2025. All 3 patients had splenomegaly and night sweats. The hemolysis ranged from mild with compensated hemolysis to severe transfusion-dependent hemolysis that resulted in splenectomy in 1 case. All patients experienced complete resolution of hemolytic anemia and other symptoms of infection after eradication therapy with doxycycline for 21 days. Neoehrlichiosis should be considered as a curable cause of hemolytic anemia in *N. mikurensis*–endemic regions.

The tickborne intracellular bacterium *Neoehrlichia mikurensis* is the cause of the infectious disease neoehrlichiosis (*1*). The initial case reports of neoehrlichiosis were published from various countries in Europe in 2010 (*2*–*4*). The typical manifestations of neoehrlichiosis includes signs and symptoms of systemic inflammation, such as fever, malaise, fatigue, and nightly sweats, as well as myalgia, skin rashes and vascular events (e.g., venous thromboembolism and vasculitis) (*1*,*5*,*6*). Vascular manifestations probably are attributable to *N. mikurensis* being an intracellular pathogen that can grow and propagate in vascular endothelium (*7*). The infection has a variable clinical manifestation, ranging from asymptomatic carriage to life-threatening disease (*3*,*4*,*8*,*9*). The heterogenous clinical features of the disease, including manifestations such as vasculitis resembling giant cell arteritis and polyarteritis nodosa and life-threatening hemophagocytic lymphohistiocytosis, illustrate the complexity of neoehrlichiosis (*6*,*9*).

Compromised B-cell immunity and splenectomy are risk factors for neoehrlichiosis (*5*). Of the published cases of neoehrlichiosis, most were in patients who were immunocompromised and had frequently been treated with the B-cell lymphocyte–depleting agent rituximab (*9*–*12*). Secondary anemia is a frequent finding in patients with neoehrlichiosis that could be caused by long duration of the infection attributable to diagnostic delay (*1*,*9*,*13*). Neoehrlichiosis is not detected by blood culture and currently only can be diagnosed by molecular detection of bacterial DNA. One study of 103 patients with neoehrlichiosis in Sweden found a 3% prevalence of autoimmune hemolytic anemia (*5*). In addition, a case report describes Coombs test-positive hemolytic anemia, neutropenia, and thrombocytopenia in a dog infected with *N. mikurensis* (*14*). We describe 3 patients from southeastern Norway who had been treated with rituximab and who had splenomegaly, direct antiglobulin test (DAT)–negative hemolytic anemia, and infection with *N. mikurensis*.

Methods and Patients

All 3 patients were treated at Vestfold Hospital Trust, Tønsberg, Norway. Patient 1 also underwent diagnostic workup and treatment at Oslo University Hospital's Department of Hematology (Oslo, Norway). We obtained written informed consent from all patients for the publication of their case reports.

We performed the polyspecific DAT tests for IgG and C3d at Vestfold Hospital Trust. We performed DAT tests for IgG, C3d, IgM, and IgA at Oslo University Hospital, Rikshospitalet (Oslo).

PCR

We tested DNA isolated from the plasma or buffy coat fractions of whole blood by using real-time reverse transcription PCR for the detection of *Borrelia burgdorferi* (*ospA* and 16S rRNA genes), *Borrelia miyamotoi* (16S rRNA gene), *Anaplasma phagocytophilum* (*groEL* gene), *Rickettsia* spp. (*gltA* gene), and *N. mikurensis* (*groEL* gene, named CNM-II in the reference article) at the Department of Medical Microbiology at Sørlandet Hospital (Kristiansand, Norway) using primers and probes as described previously (*8*). We performed *Babesia* subspecies DNA PCR at Statens Serum Institut (Copenhagen, Denmark). We established a diagnosis of hemolysis on the basis of reduced hemoglobin, reduced plasma haptoglobin, increased plasma lactate dehydrogenase, and increased blood reticulocytes.

Case Reports

Patient 1

A 61-year-old woman sought care for rapid-onset dyspnea, fatigue, palpitations, dizziness, and a 6-month history of infrequent febrile episodes. Her medical history included rheumatoid arthritis for 17 years, breast cancer treated 16 years previously, and episodic severe depression for 1.5 years. Her arthritis initially was treated with oral methotrexate, salazopyrine, and hydroxychloroquine. Methotrexate temporarily was withdrawn because of cytopenias after a year and permanently withdrawn when she had breast cancer diagnosed. Her breast cancer was treated with surgery after 6 courses of neoadjuvant chemotherapy with fluorouracil, epirubicin hydrochloride, and cyclophosphamide, followed by postoperative radiotherapy. After completion of breast cancer treatment, treatment for rheumatoid arthritis commenced with rituximab infusions (1,000 mg 2×/y). She also was treated with venlafaxine for depression and anxiety.

At admission, we diagnosed severe transfusion-dependent direct antiglobulin test (DAT)–negative hemolytic anemia in the patient (Table). We suspected drug-induced hemolytic anemia and discontinued venlafaxine and rituximab, which later were reinstated because of lack of improvement. Two months after initially seeking care, the patient was admitted to a hospital with acute appendicitis and worsened hemolysis. After appendectomy, we initiated prednisolone (1 mg/kg/d), which resulted in partial reduction of hemolysis. We introduced the interleukin 1 receptor inhibitor anakinra 7 months later as a steroid-sparing agent after relapses of fever and worsened hemolysis during the tapering of prednisolone.

Diagnostic tests of blood and bone marrow revealed no evidence of congenital or acquired erythrocyte membrane defects, including paroxysmal nocturnal hemoglobinuria (PNH), lymphoproliferative disorders, or other hematologic neoplasia. Results of a 184-gene panel of hereditary causes of anemia and bone-marrow failure (e.g., Fanconi anemia, Diamond-Blackfan anemia, and hereditary stomatocytosis) were negative. No findings were suggestive of Wilson disease (i.e., normal ceruloplasmin and copper serum and urine levels) or of zinc- or arsenic-related poisoning. Computed tomography (CT) scans of the neck to pelvis were unremarkable, whereas a fluorodeoxyglucose (FDG) positron emission tomography (PET)–CT scan showed a slight uptake in the spleen initially deemed to be reactive. When a repeat FDG PET–CT scan 3 months later showed a maintained slight uptake in the spleen, the patient underwent diagnostic splenectomy because of a continued suspicion of underlying lymphoproliferative disorder. Before splenectomy, the patient had thrombophlebitis in the right cubital fossa and right ankle diagnosed. After splenectomy, hemoglobin levels improved for a period, but evidence of hemolysis remained. Histopathologic examination of the spleen showed depletion of B cells in the white pulp, secondary to

Table. Characteristics, reported symptoms, and biochemical test results at admission, during disease course, and post-treatment with antibiotics for 3 patients with neoehrlichiosis, hemolytic anemia, and splenomegaly, Norway, 2024–2025*

Characteristic	Patient 1	Patient 2	Patient 3
Age, y/sex	61/F	62/M	48/M
Indication for rituximab	Rheumatoid arthritis	Myasthenia gravis	Multiple sclerosis
Immunosuppression	Rituximab 1,000 mg 2×/y	Rituximab 1,000 mg 2×/y	Rituximab, 1,000 mg 1×/y
Signs and symptoms			
Fever	Yes	No	Yes
Night sweats	Yes	Yes	Yes
Weight loss	Yes	No	Yes
Fatigue	Yes	No	Yes
Skin involvement	No	Hyperpigmented rash of the lower extremities	No
Vascular involvement	Yes	No	No
Hemolysis	Yes	Yes	Yes
Direct antiglobulin test	Negative	Negative	Negative
Blood biochemistry at admission/peak or nadir during disease course/after treatment (reference range)			
Blood Hb, g/dL	6.4/5.8/12.1 (11.7–15.3)	9.6/8.8/14.7 (13.4–17.0)	13.8/17.5/17.5 (13.4–17.0)
Blood platelets × 10^9/L (145–390)	416/932/373	234/154/314	186/241/241
Blood leukocytes × 10^9 cells/L (3.5–10.0)	4.75/2.74/6.0	4.93/3.32/5.97	5.32/5.72/4.19
Blood reticulocytes × 10^9 cells /L (30–100)	336/70/120	180/48/78	103/52/84
Plasma C-reactive protein, mg/L (<5)	15/92/<1.0	3.1/3.4/<1.0	11/1.7/<1.0
Plasma ferritin, µg/L (30–400)	950/8,004/3,274	92/41/106	362/NA/NA
Plasma haptoglobin, g/L (0.50–2.10)	0.34/<0.10/0.45	<0.1/<0.1/0.24	<0.1/<0.1/0.54
Plasma, LDH, U/L (35–210)	189/261/138	286/159/188	288/164/173
Plasma, bilirubin (total) µmol/L (<25)	77/100/20	19/10/12	19/22/16
Blood type	A RhD+	NA	NA
Plasma IgG, g/L (6.10–14.9)	7.29/6.91/8.68	10.4/NA/NA	8.63/8.63/9.42
Neoehrlichia mikurensis PCR Ct value (at admission)	22	28	25
Largest spleen size before treatment (radiologic imaging)	13.8-cm coronal length	17-cm coronal length	17.7-cm coronal length, hilar width 7.4 cm
Treatment and results			
Time from treatment start to improved hemolysis	30 d to normalization of reticulocytosis and Hb increase >2 g/dL	60 d to normalization of reticulocytosis and Hb increase >2g/dL	47 d to normalization of reticulocytosis and Hb increase >2 g/dL
Time from treatment to improved symptoms	Cessation of fever after 3 d	NA	Cessation of night sweats and fatigue after 7 d
Spleen size posttreatment (radiologic imaging)	Splenectomized	Not evaluated	14 cm coronal length, hilar width 5.2 cm

*Ct, cycle threshold; Hb, hemoglobin; LDH, lactate dehydrogenase; NA, not available.

rituximab treatment, and expanded red pulp with extramedullary hematopoiesis but no evidence of lymphoma. Within 2 months, the patient's hemolytic anemia relapsed. Because of a history of tick exposure and erythema migrans a few years prior, we sent EDTA blood samples for PCR testing for tickborne microbes, including *Rickettsia* spp., *B. miyamotoi*, *B. burgdorferi*, *A. phagocytophilum, N. mikurensis* (*8*), and *Babesia* subsp. The patient tested positive for *N. mikurensis*, upon which we initiated oral doxycycline (100 mg 2×/d for 21 d). Her symptoms, most prominently fever, night sweats and fatigue, as well as all signs of hemolysis, rapidly improved and cleared completely (Table; Figure). She tested negative for *N. mikurensis* DNA by PCR after the course of antibiotics. We also detected *N. mikurensis* DNA in historical serum samples drawn 22, 11, and 6 months before the time of diagnosis. At a 12-month follow-up, no evidence of hemolytic anemia remained.

Patient 2

A 62-year-old man was referred to our outpatient clinic with a 4-month history of gradually progressive symptomatic anemia, prominent fatigue, and night sweats. He did not have fever, weight loss, nor any current or previous vascular events. His medical history included myasthenia gravis for 14 years that had been treated with rituximab infusions (1,000 mg 2×/y) for the previous 5 years. One year earlier, he had a prolonged SARS-COV-2 infection, evaluated with a chest CT, with an incidental finding of a slightly enlarged spleen. Laboratory findings at referral showed mild DAT-negative hemolytic anemia (Table). A peripheral blood smear showed no evidence of cellular dysplasia, blasts, or schistocytes. A test result for PNH was negative. We performed coagulation tests because of easy bruising, but we detected no coagulation defect. The patient had had no recall of tick bites. We performed no testing for SARS-COV-2. Because of several similarities to the first patient case (e.g., a probable nonimmunologic hemolytic anemia, treatment with rituximab, and slight splenomegaly), we performed PCR testing for tickborne microbes, including *Rickettsia* spp., *B. miyamotoi*, *B. burgdorferi*, *A. phagocytophilum, N. mikurensis*, and *Babesia* subsp. The patient was positive by PCR for *N. mikurensis*, and we initiated oral doxycycline (100 mg 2×/d for 21 d). A month later, his anemia had improved, although haptoglobin still was suppressed slightly, indicating low-grade hemolysis. Two months after the patient finished doxycycline treatment, hemoglobin and haptoglobin levels were normal (Table). At 12-month follow-up, no evidence of hemolytic anemia remained.

Patient 3

A 48-year-old man was referred our care with splenomegaly and profuse night sweats that had started 1 year earlier. His medical history included relapsing or remitting multiple sclerosis 5 years prior, which had been treated with rituximab infusions (1,000 mg 1×/y) for the previous 2 years. CT imaging of the thorax, abdomen, and pelvis done a few months before referral revealed no pathologic lymphadenopathy but substantial splenomegaly (largest diameter 17.7 cm). One month before his first episode of night sweats, he had traveled to the southern United States, Caribbean, and South America, none of which warranted malarial chemoprophylaxis. He had not contracted fever, insect bites, or rashes during his travels. He had a history of tick bites after hiking trips in southeastern Norway but no erythema migrans. Blood chemistry taken a week before the appointment at our facility showed mild and fully compensated DAT-negative hemolytic anemia (Table). The levels of haptoglobin, reticulocytes, and lactate dehydrogenase normalized spontaneously 10 days later.

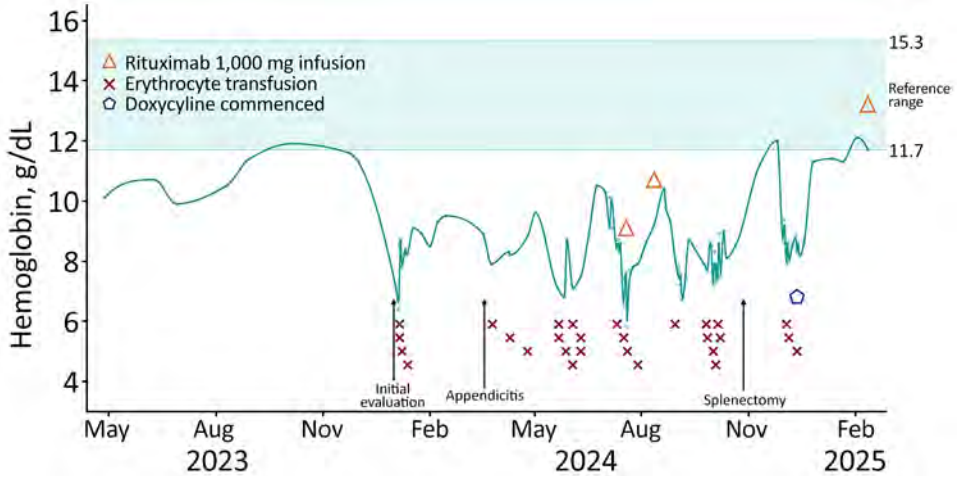

Figure. Hemoglobin levels (blue line) for patient 1 in a case series of 3 patients with neoehrlichiosis and hemolytic anemia at admission, during disease course, and after treatment with antibiotics, Norway, 2024–2025.

An ultrasound at the time of the first consultation showed a reduction of spleen size to 15.1 cm (largest diameter). PNH test result was negative, and peripheral blood smears results were normal. Bone marrow trephine biopsy showed a very slight increase of intrasinusoidal T-lymphocytes of uncertain importance. Repeated bone marrow trephine biopsies and bone marrow aspirate analyses by flow cytometry yielded similar results. A FDG PET or CT scan showed no pathologic FDG uptake in the liver, spleen, or bone marrow and a maximal spleen diameter of 15.8 cm. We noted only a slight clonal T-cell receptor rearrangement in the bone marrow and normal results in peripheral blood, consistent with a reactive cause with no conclusive evidence of lymphoproliferative disorder. A repeat ultrasound of the spleen a few months later showed a spleen size of 14.3 cm. Six months after the initial diagnostic work-up and 2 months after receiving his yearly rituximab infusion, the patient experienced a relapse of symptoms with increasing night sweats, increase in spleen size to 17.4 cm on ultrasound, and hemolysis with a substantial reduction in hemoglobin levels and signs of intravascular hemolysis (Table).

We performed testing for tickborne microbes, including *Rickettsia* spp., *B. miyamotoi*, *B. burgdorferi*, *A. phagocytophilum* and *N. mikurensis*, and the patient was positive by PCR for *N. mikurensis*. We did not test for *Babesia* subsp. We initiated treatment of the patient with oral doxycycline (100 mg 2×/d for 21 d). A repeat ultrasound of the spleen performed 6 weeks later showed a reduction in size to 14 cm. His symptoms improved and resolved within a week of antibiotic treatment. A PCR test for *N. mikurensis* was negative after treatment. We also detected *N. mikurensis* DNA in stored serum samples drawn 12 and 8 months before the time of diagnosis. At 12-month follow-up, no evidence of hemolytic anemia remained.

Discussion

We describe 3 patients with a diagnosis of DAT-negative hemolysis, splenomegaly, and infection with *N. mikurensis*. We considered neoehrlichiosis to be the cause of their hemolysis, and all patients went into remission after treatment with doxycycline. Receipt of rituximab is a risk factor for neoehrlichiosis, and splenomegaly and systemic symptoms are established features of neoehrlichiosis. Two of the 3 patients had documented *N. mikurensis* DNA in archival serum samples up to 2 years before the time of diagnosis. Although no archived blood samples from the second patient were available, he had splenomegaly of unknown cause 1 year previously, which in retrospect might have been caused by *N. mikurensis*. Neoehrlichiosis may progress from asymptomatic latent infection to symptomatic acute infection. A recent study showed that *N. mikurensis* causes latent infections that can reactivate when B-cell immunity is suppressed by rituximab (*15*). The mechanism by which *N. mikurensis* causes hemolysis is unclear but does not seem to involve either complement antibodies or IgG.

Hemolytic anemia invariably entails thorough review by a hematologist, especially when splenomegaly is present because lymphoproliferative disorders are a differential diagnosis. We recommend testing patients with hemolytic anemia residing in regions endemic for *N. mikurensis* (i.e., large parts of Europe and northern Asia) for this emerging zoonotic infection that can easily be treated and cured by oral antibiotics.

About the Author

Mr. Paulson is a specialist in hematology and internal medicine at the Cancer and Hematology Center, Vestfold Hospital Trust, Tønsberg, Norway. His primary research interests include hemolytic anemia and the use of artificial intelligence in hematologic diagnostics.

References

1. Grankvist A, Andersson PO, Mattsson M, Sender M, Vaht K, Höper L, et al. Infections with the tick-borne bacterium "*Candidatus* Neoehrlichia mikurensis" mimic noninfectious conditions in patients with B cell malignancies or autoimmune diseases. Clin Infect Dis. 2014;58:1716–22. https://doi.org/10.1093/cid/ciu189
2. Welinder-Olsson C, Kjellin E, Vaht K, Jacobsson S, Wennerås C. First case of human "*Candidatus* Neoehrlichia mikurensis" infection in a febrile patient with chronic lymphocytic leukemia. J Clin Microbiol. 2010;48:1956–9. https://doi.org/10.1128/JCM.02423-09
3. von Loewenich FD, Geissdörfer W, Disqué C, Matten J, Schett G, Sakka SG, et al. Detection of "*Candidatus* Neoehrlichia mikurensis" in two patients with severe febrile illnesses: evidence for a European sequence variant. J Clin Microbiol. 2010;48:2630–5. https://doi.org/10.1128/JCM.00588-10
4. Fehr JS, Bloemberg GV, Ritter C, Hombach M, Lüscher TF, Weber R, et al. Septicemia caused by tick-borne bacterial pathogen *Candidatus* Neoehrlichia mikurensis. Emerg Infect Dis. 2010;16:1127–9. https://doi.org/10.3201/eid1607.091907
5. Wennerås C, Wass L, Bergström B, Grankvist A, Lingblom C. Ten years of detecting *Neoehrlichia mikurensis* infections in Sweden: demographic, clinical and inflammatory parameters. Eur J Clin Microbiol Infect Dis. 2024;43:2083–92. https://doi.org/10.1007/s10096-024-04909-5
6. Höper L, Skoog E, Stenson M, Grankvist A, Wass L, Olsen B, et al. Vasculitis due to *Candidatus* Neoehrlichia mikurensis: a cohort study of 40 Swedish patients. Clin Infect Dis. 2021;73:e2372–8. https://doi.org/10.1093/cid/ciaa1217
7. Wass L, Grankvist A, Bell-Sakyi L, Bergström M, Ulfhammer E, Lingblom C, et al. Cultivation of the causative agent of human neoehrlichiosis from clinical isolates

identifies vascular endothelium as a target of infection. Emerg Microbes Infect. 2019;8:413–25. https://doi.org/10.1080/22221751.2019.1584017
8. Quarsten H, Salte T, Lorentzen ÅR, Hansen IJW, Hamre R, Forselv KJN, et al. Tick-borne pathogens detected in the blood of immunosuppressed Norwegian patients living in a tick-endemic area. Clin Infect Dis. 2021;73:e2364–71. https://doi.org/10.1093/cid/ciaa971
9. Gynthersen RMM, Stensvold CR, Nielsen SL, Møller HJ, Nielsen HV, Lebech AM, et al. *Neoehrlichia mikurensis*—an emerging opportunistic tick-borne infection in immunosuppressed patients. J Intern Med. 2023;293:782–90. https://doi.org/10.1111/joim.13638
10. Ditlevsen Regen E, Victor D, Hendrikx T. Neoehrlichiosis in patients with multiple sclerosis in Halmstad, Sweden: a case series. J Neuroimmunol. 2026;410:578787. https://doi.org/10.1016/j.jneuroim.2025.578787
11. Da Silva Duarte M, Hennebel C, Fourré N, Greub G, Opota O, Merz L. *Neoehrlichia mikurensis*–associated secondary capillary leak syndrome and septic shock: a case report. J Med Case Rep. 2025;19:498. https://doi.org/10.1186/s13256-025-05552-0
12. Margini C, Maldonado R, Keller P, Banz Y, Escher R, Waldegg G. Fever of unknown origin, a vascular event, and immunosuppression in tick-endemic areas: think about neoehrlichiosis. Cureus. 2023;15:e40617. https://doi.org/10.7759/cureus.40617
13. Wennerås C. Infections with the tick-borne bacterium *Candidatus* Neoehrlichia mikurensis. Clin Microbiol Infect. 2015;21:621–30. https://doi.org/10.1016/j.cmi.2015.02.030
14. Diniz PP, Schulz BS, Hartmann K, Breitschwerdt EB. "*Candidatus* Neoehrlichia mikurensis" infection in a dog from Germany. J Clin Microbiol. 2011;49:2059–62. https://doi.org/10.1128/JCM.02327-10
15. Wass L, Lewerin C, Jaén-Luchoro D, Lingblom C, Wennerås C. Latent *Neoehrlichia mikurensis* infections may be reactivated in patients with B-cell lymphomas treated with rituximab. Immunology. 2026;178:307–17. https://doi.org/10.1111/imm.70120

Address for correspondence: Martin Paulson, Cancer and Hematology Center, Vestfold Hospital Trust, Halfdan Wilhelmsens allé 17, 3103 Tønsberg, Norway; email: martin.paulson@siv.no

etymologia revisited

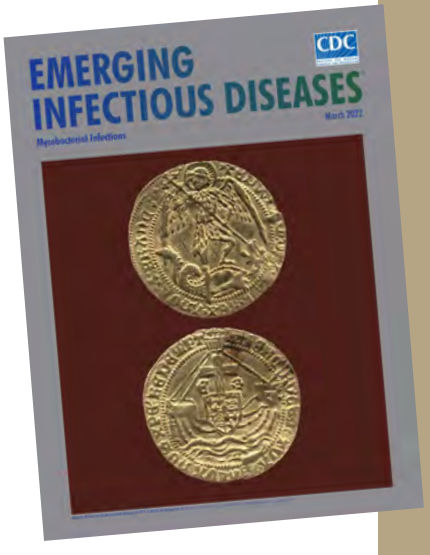

Originally published in March 2022

Schizophyllum commune

[skiz-of′-ĭ-ləm kom′-yoon]

Schizophyllum commune, or split-gill mushroom, is an environmental, wood-rotting basidiomycetous fungus. *Schizophyllum* is derived from "*Schíza*" meaning split because of the appearance of radial, centrally split, gill like folds; "*commune*" means common or shared ownership or ubiquitous. Swedish mycologist, Elias Magnus Fries (1794–1878), the Linnaeus of Mycology, assigned the scientific name in 1815. German mycologist Hans Kniep in 1930 discovered its sexual reproduction by consorting and recombining genomes with any one of numerous compatible mates (currently >2,800).

References

1. Chowdhary A, Kathuria S, Agarwal K, Meis JF. Recognizing filamentous basidiomycetes as agents of human disease: a review. Med Mycol. 2014;52: 782–97. https://doi.org/10.1093/mmy/myu047
2. Cooke WB. The genus *Schizophyllum*. Mycologia. 1961;53:575–99. https://doi.org/10.1080/00275514.1961.12017987
3. Greer DL. Basidiomycetes as agents of human infections: a review. Mycopathologia. 1978;65:133–9. https://doi.org/10.1007/BF00447184
4. O'Reilly P. *Schizophyllum commune*, split gill fungus, 2016 [cited 2021 Aug 23]. https://www.first-nature.com/fungi/schizophyllum-commune.php
5. Raper CA, Fowler TJ. Why study *Schizophyllum*? Fungal Genet Rep. 2004;51:30–6. https://doi.org/10.4148/1941-4765.1142

https//wwwnc.cdc.gov/eid/article/28/3/et-2803_article

Investigation of *Mycobacterium abscessus* Cluster in Hospital, Maryland, USA, 2024

Sarah Ludmer, Monique Duwell, Tracie Harris, Surbhi Leekha, Allison Slater, Vincent Escuyer, Joseph Shea, Pascal Lapierre, Jamie Rubin, Rebecca Perlmutter, Donna Kohlershmidt, Michelle Dickinson

Mycobacterium abscessus infections are frequently drug resistant and can cause severe disease, particularly among vulnerable populations in healthcare settings. In June 2024, a cluster of *M. abscessus* infection cases was reported at a hospital in Maryland, USA. An investigation involving hospital infection prevention staff, the Maryland Department of Health, the Centers for Disease Control and Prevention, and the Wadsworth Laboratory of the New York State Department of Health included initiation of mitigation efforts such as tap water use restrictions, point-of-use water filters, hospitalwide water flushing, and staff education regarding sink safety. Whole-genome sequencing of patient and environmental isolates, coupled with epidemiologic data, revealed a strong association (0–24 single-nucleotide polymorphism differences) between environmental and patient samples, indicating that infections were likely a result of patient exposure to *M. abscessus*. Ensuring initiation of mitigation initiatives likely prevented additional patient infections. Although effective in this investigation, not all mitigation strategies are equal or sustainable.

Nontuberculous mycobacteria (NTM) are a group of bacteria found naturally in soil, dust, and water; infections caused by NTMs are increasing globally (*1*–*3*). The NTM *Mycobacterium abscessus* and its subspecies are classified as rapid growers and are responsible for skin and soft tissue infections, bacteremia, and pulmonary infections, among other conditions (*4*). *M. abscessus* infections are difficult to treat because of intrinsic drug resistance that limits treatment options (*2*). The environmental persistence of *M. abscessus* and the often treatment-resistant infections it can cause make it an emerging bacterium of concern. *M. abscessus* outbreaks have been reported in healthcare settings, often involving exposure to contaminated water sources (*5*–*8*).

In June 2024, hospital infection prevention (IP) staff at a hospital in Maryland, USA, notified the Maryland Department of Health (MDH) of 10 patients with cultures positive for *M. abscessus*. The ensuing investigation involved the IP staff, MDH, the Centers for Disease Control and Prevention (CDC), and the Wadsworth Laboratory of the New York State Department of Health. This activity was reviewed by the CDC Public Health Infrastructure Center's human subjects review staff, was deemed not research, and was conducted consistent with applicable federal law and CDC policy (e.g., 45 C.F.R. part 46, 21 C.F.R. part 56; 42 U.S.C. §241(d); 5 U.S.C. §552a; 44 U.S.C. §3501 et seq.).

Methods

Epidemiologic Investigation

After they identified an initial case of *M. abscessus* infection in May 2024, hospital IP staff initiated retroactive case finding. The hospital had a previous cluster of 3 cases of *M. abscessus* (2 positive CSF cultures, 1 positive sputum culture) in 2021, shortly after occupancy of a newly constructed building. Preoccupancy water quality testing was within acceptable ranges but did not include specific testing for *M. abscessus*. With guidance from MDH and CDC, water samples from the 2021 outbreak were tested at CDC, where NTM was identified, but not *M. abscessus*.

Author affiliations: Centers for Disease Control and Prevention, Atlanta, Georgia, USA (S. Ludmer); Maryland Department of Health, Baltimore, Maryland, USA (S. Ludmer, M. Duwell, J. Rubin, R. Perlmutter); University of Maryland Capital Region Health, Largo, Maryland, USA (T. Harris, A. Slater); University of Maryland School of Medicine, Baltimore (S. Leekha); Wadsworth Center, New York State Department of Health, Albany (V. Escuyer, J. Shea, P. Lapierre, D. Kohlershmidt, M. Dickinson)

DOI: https://doi.org/10.3201/eid3209.260093

In the cluster reported in 2024, a total of 10 patients had *M. abscessus* identified from clinical cultures during March 28, 2023–June 5, 2024. Hospital IP staff identified 1 additional patient in September 2024 and reported that case to MDH, bringing the total to 11 patients. The hospital implemented mitigation strategies after the first 2 cases were identified in 2024, including hospitalwide water flushing, increased point-of-entry supplemental disinfectant (monochloramine) levels, restrictions on use of tap water and ice machines, and staff education and monitoring of sink safety. The hospital also installed PALL point-of-use filters (https://www.pall.com) in sinks and medication rooms in high-risk patient care areas, including intensive care unit patient rooms, operating room (OR) scrub sinks, and cancer centers. The hospital water management plan guided some of the mitigation strategies and was ultimately updated to include more frequent building flushes, residual disinfectant testing, and inclusion of *M. abscessus* in water microbial testing. All those measures have been shown to reduce risk for patient exposure to contaminated water sources (*6*). Investigators also collected information regarding timing of clinical culture collection, patient location within the facility, and clinical manifestations (including patient procedures).

Laboratory Testing

Before initiating mitigation strategies, the hospital water management team completed environmental sampling to attempt to identify potential sources of *M. abscessus* in the hospital. Water sampling included bulk water samples (1 L, mixed hot and cold) and swab specimens from faucets, sinks, and ice machines; testing was conducted by an accredited commercial environmental microbiology laboratory. The team chose locations for water samples on the basis of patient location in the hospital, high-risk patient care areas, and sources implicated in reports of other *M. abscessus* outbreaks (*5*). In addition to cultures, supplemental disinfectant levels were measured for faucets inside patient rooms, medication rooms, ice machine water, and OR scrub sinks. Heater-cooler machines have been implicated in other outbreaks of NTM (*8*–*9*), and a bulk water sample from a heater-cooler machine (CardioQuip, https://www.cardioquip.com) used during 1 patient's hospitalization was included; that case-patient was the only one with heater-cooler machine exposure. After mitigation methods were implemented, resampling was conducted to determine effectiveness. For point-of-use filters, sampling was done before and after filter installation.

Whole-Genome Sequencing

Whole-genome sequencing (WGS) was performed at the New York State Department of Health Wadsworth Center for both clinical and environmental isolates using the Next¬Seq platform (Illumina, https://www.illumina.com) (10,11). De novo genome assemblies were performed using the Shovill pipeline version 1.1.0, default parameters (https://github.com/tseemann/shovill). No postmitigation isolates were sequenced.

Results

Epidemiologic Investigation

Among 11 patients identified, median age was 40 (range 24–76) years. Five patients underwent surgical procedures; 2 had procedures in OR A, 2 in OR B, and 1 in OR C. No patients had the same procedure; however, the 2 patients in OR A each had cardiac surgery. One patient had a heater-cooler machine used during the cardiac procedure. Two rooms housed multiple affected patients; however, their admissions did not overlap in time. Otherwise, we identified no shared patient ward or unit locations. Six (55%) of the 11 patients were treated with antimicrobial therapy as directed by infectious disease physicians, after positive culture results. One (9%) patient died within 60 days of the first positive culture; that death was not attributed to *M. abscessus* infection.

Laboratory Testing

Among culture samples from 11 patients, 6 (55%) were from sputum samples, 4 (36%) from blood samples, and 1 (9%) from an abdominal abscess. Before initiation of mitigation strategies, the IP team collected 47 environmental samples from 19 locations throughout the hospital. Nineteen were bulk water samples, and 28 were swab specimens from faucet and sink drains, including ice machines. Testing revealed *M. abscessus* in the water system at different levels throughout the hospital building, including in ice machines. Among all samples, 18 (38%) grew *M. abscessus* and 15 (32%) had acid-fast bacilli but not *M. abscessus*. For samples that grew *M. abscessus*, density varied: 10–48,000 CFU/swab, or <1–39 CFU/mL for bulk water samples. The sample from the CardioQuip heater-cooler machine did not yield any bacteria. An investigation into various uses of tap water and ice within the hospital did not identify any obvious source of specimen contamination from tap water or ice during specimen collection or processing. However, investigation of case 11, which was identified after mitigation efforts began, revealed ice from restricted ice machines was used to store saline syringes that were used during bronchoalveolar lavage.

After review of clinical and epidemiologic data, we determined that 6 patients had clinical infections and 5 represented likely colonization or specimen contamination. All 5 of those cases involved respiratory tract cultures (Table), thought to be colonization or the result of specimen contamination either because the specimen collection was completed in the emergency department before admission and patients had no previous exposure to the facility or because they had respiratory illness at admission.

The hospital installed point-of-use filters in several locations, guided by the epidemiologic investigation, including high-risk patient areas, ORs, and intensive care units. Water sampling after installation of point-of-use filters showed no bacterial growth. Repeat sampling of sink and faucet sites after flushing and increasing point of entry supplemental disinfectant revealed optimal residual disinfectant but continued detection of *M. abscessus* to different degrees.

WGS

All 18 environmental samples that grew *M. abscessus* and 10 available clinical isolates from 10 distinct patients were sent to the Wadsworth Laboratory for WGS. Sequences reported in this article were submitted to the National Center for Biotechnology Information BioProject Database (BioProject accession no. PRJNA1403517). Among the 28 samples sequenced, we identified 5 subclusters, consisting of 10 patient isolates and 17 environmental isolates. Maximum whole-genome single-nucleotide polymorphism (SNP) distance of the core genome across the 28 isolates was 98,252. Within each subcluster, associated subcluster isolates were within 0–24 SNPs, indicating a high degree of relatedness (*12*–*13*). Four subclusters each included both patient isolates and environmental isolates (0–15 SNPs), and 1 included only isolates from patients (20–24 SNPs). One patient isolate identically matched an environmental sample from the postanesthesia care unit (PACU) ice machine (0 SNP difference). The patient had been in the PACU after a procedure for <24 hours. Two other patient isolates showed close association with PACU environmental samples. One showed close association (5 SNPs) to a PACU sink water sample; that patient had 3 operations during hospital admission. The other patient,

Table. Summary of patient characteristics, including pertinent investigation results, from *Mycobacterium abscessus* cluster in hospital, Maryland, USA, 2024*

Patient ID	Age, y/sex	Risk factors or underlying conditions	Patient unit	Specimen type	Culture date	OR procedure	OR	Matched to ENV isolate	Type
A	30/F	Gastronomy tube	1	Blood	2023 Mar 28	Laminectomy	B	Y	Clinical case
B	38/F	No significant risk factors/conditions	1	Abdominal abscess	2023 Mar 30	Cholecystectomy	B	Y	Clinical case
C	34/F	Endocarditis, hepatitis C	2†	Sputum	2023 Aug 22	None	NA	Y	Contaminant/ colonization
D	74/F	Tuberculosis, diabetes mellitus, coronary artery disease	3	Sputum	2023 Sep 9	None	NA	Y	Contaminant/ colonization
E	32/F	Sickle cell disease	3, 5	Blood	2023 Sep 13	None	NA	Y	Clinical case
F	24/M	Pericarditis	2,‡ 4	Sputum	2023 Nov 27	Creation pericardial window	A	N§	Contaminant/ colonization
G	76/M	Coronary artery disease	2†	Blood	2024 Feb 8	CABG	A	Y	Clinical case
H	74/F	Tracheostomy, gastronomy tube, endocarditis, lung cancer, sarcoidosis	1, 2,‡ 3	Blood	2024 Apr 2	Bilateral aortogram, iliac stents, brachial artery repair, femoral angioplasties	C, D, E	Y	Clinical case
I	42/M	No significant risk factors/conditions	6	Sputum	2024 Apr 2	None	NA	Y	Contaminant/ colonization
J	72/F	Necrotizing pancreatitis, kidney and breast cancer, diabetes mellitus	4	Blood	2024 Jun 5	None	NA	NA	Clinical case
K	53/F	HIV, tuberculosis, diabetes mellitus	3	Sputum	2024 Sep 18	None	NA	N§	Contaminant/ colonization

*Unit names are deidentified; placeholder numbers have been assigned to maintain anonymity. ENV, environmental; NA, not applicable; OR, operating room.
†Patients shared the same room on unit 2 but did not overlap in admission dates.
‡Patients shared the same room on unit 2 but did not overlap in admission dates.
§Only matched to other patient isolates.

whose isolate was closely associated (11 SNPs) with a PACU sink faucet swab, had not spent any time in the PACU and was ultimately determined to be a likely specimen contamination because the sample was collected in the emergency department before admission. Two patient isolates were not found to be closely associated with any of the environmental samples but did cluster closely (20–24 SNPs) with a patient isolate from the facility in 2021. However, we could not determine any additional epidemiologic link between the 2 isolates from this cluster and the 2021 isolate. One environmental isolate was not closely related (≥80 SNPs) to any other environmental or patient isolates.

Discussion

The infectious source in hospital outbreaks of NTM can be hard to identify (*5*). Water sampling and subsequent sequencing of clinical and environmental isolates was instrumental to confirm colonization of the water system in this hospital and implicate ice machines as the probable source of infection on the basis of the close associations (low SNP differences) observed between clinical and environmental samples. The use of genetic sequencing and epidemiologic investigation in outbreaks like this one enables investigators to identify current and potential future sources of pathogen exposure, target interventions, and efficiently allocate resources. Ice machines have been identified as a potential source of NTM infection in other outbreaks, and investigators should consider possible contamination or colonization in future outbreaks (*7*,*14*).

M. abscessus is challenging to remove from a water system after a biofilm has developed (*9*). After *M. abscessus* is identified within a water system, immediate mitigation measures are needed because the persistent organisms can cause serious and difficult to treat infections. Swift action by hospital staff to remove potential sources of infection from patient areas was likely key to preventing additional infections in this cluster. Point-of-use filters are effective; however, they are expensive and must be inspected and replaced regularly. Building flushing and increasing supplemental water disinfectant levels showed a temporary decrease in *M. abscessus* levels. Continued detection could indicate biofilm formation or organism resistance to disinfection practices or agents (e.g., monochloramine), making water system eradication a challenge.

Infections with *M. abscessus* at this facility first occurred within a few months of initial occupancy of a new building, designed to be Leadership in Energy and Environmental Design–certified. New hospital buildings, particularly those with lower water flow and recirculation inherent to energy-efficient design, have been associated with NTM outbreaks (*6*,*15*). Adherence to a robust water management plan and sink safety education are vital practices to prevent outbreaks from *M. abscessus* and other opportunistic premise-plumbing pathogens.

About the Author

Ms. Ludmer is an epidemiologist and consultant at the Maryland Department of Health. Her research interests include domestic and international outbreak response, healthcare-associated infection prevention, surveillance system design, and applied epidemiology and data-driven response initiatives for improving patient safety and public health preparedness.

References

1. Cristancho-Rojas C, Varley CD, Lara SC, Kherabi Y, Henkle E, Winthrop KL. Epidemiology of *Mycobacterium abscessus.* Clin Microbiol Infect. 2024;30:712–7. https://doi.org/10.1016/j.cmi.2023.08.035
2. Johansen MD, Herrmann JL, Kremer L. Non-tuberculous mycobacteria and the rise of *Mycobacterium abscessus*. Nat Rev Microbiol. 2020;18:392–407. https://doi.org/10.1038/s41579-020-0331-1
3. Adjemian J, Olivier KN, Seitz AE, Holland SM, Prevots DR. Prevalence of nontuberculous mycobacterial lung disease in U.S. Medicare beneficiaries. Am J Respir Crit Care Med. 2012;185:881–6. https://doi.org/10.1164/rccm.201111-2016OC
4. Lee MR, Sheng WH, Hung CC, Yu CJ, Lee LN, Hsueh PR. *Mycobacterium abscessus* complex infections in humans. Emerg Infect Dis. 2015;21:1638–46. https://doi.org/10.3201/2109.141634
5. Desai AN, Hurtado RM. Infections and outbreaks of nontuberculous mycobacteria in hospital settings. Curr Treat Options Infect Dis. 2018;10:169–81. https://doi.org/10.1007/s40506-018-0165-9
6. Baker AW, Lewis SS, Alexander BD, Chen LF, Wallace RJ Jr, Brown-Elliott BA, et al. Two-phase hospital-associated outbreak of *Mycobacterium abscessus*: investigation and mitigation. Clin Infect Dis. 2017;64:902–11. https://doi.org/10.1093/cid/ciw877
7. Klompas M, Akusobi C, Boyer J, Woolley A, Wolf ID, Tucker R, et al. *Mycobacterium abscessus* cluster in cardiac surgery patients potentially attributable to a commercial water purification system. Ann Intern Med. 2023;176:333–9. https://doi.org/10.7326/M22-3306
8. Allen KB, Yuh DD, Schwartz SB, Lange RA, Hopkins R, Bauer K, et al. Nontuberculous mycobacterium infections associated with heater-cooler devices. Ann Thorac Surg. 2017;104:1237–42. https://doi.org/10.1016/j.athoracsur.2017.04.067
9. Svensson E, Jensen ET, Rasmussen EM, Folkvardsen DB, Norman A, Lillebaek T. *Mycobacterium chimaera* in heater-cooler units in Denmark related to isolates from the United States and United Kingdom. Emerg Infect Dis. 2017;23:507–9. https://doi.org/10.3201/eid2303.161941

10. Shea J, Halse TA, Lapierre P, Shudt M, Kohlerschmidt D, Van Roey P, et al. Comprehensive whole-genome sequencing and reporting of drug resistance profiles on clinical cases of *Mycobacterium tuberculosis* in New York state. J Clin Microbiol. 2017;55:1871–82. https://doi.org/10.1128/JCM.00298-17
11. Dickinson MC, Wirth SE, Baker D, Kidney AM, Mitchell KK, Nazarian EJ, et al. Implementation of a high-throughput whole genome sequencing approach with the goal of maximizing efficiency and cost effectiveness to improve public health. Microbiol Spectr. 2024;12:e0388523. https://doi.org/10.1128/spectrum.03885-23
12. Davidson RM, Hasan NA, Epperson LE, Benoit JB, Kammlade SM, Levin AR, et al. Population genomics of *Mycobacterium abscessus* from U.S. cystic fibrosis care centers. Ann Am Thorac Soc. 2021;18:1960–9. https://doi.org/10.1513/AnnalsATS.202009-1214OC
13. Olawoye IB, Waglechner N, McIntosh F, Akochy PM, Cloutier N, Grandjean Lapierre S, et al. Genomic epidemiology of *Mycobacterium abscessus* on the Island of Montréal is not suggestive of health care-associated person-to-person transmission. J Infect Dis. 2025;231:e396–406. https://doi.org/10.1093/infdis/jiae407
14. Labombardi VJ, O'brien AM, Kislak JW. Pseudo-outbreak of *Mycobacterium fortuitum* due to contaminated ice machines. Am J Infect Control. 2002;30:184–6. https://doi.org/10.1067/mic.2002.118407
15. Ankrum AL, Caceres SM, Torsell M, Epperson E, Calado Nogueira de Moura V, Gilick JJ, et al. *Mycobacterium chelonae* outbreak investigation at a quaternary pediatric hospital following the opening of a LEED-certified critical care tower: where does water sustainability intersect with infection control? Infect Control Hosp Epidemiol. 2026;47:161–9. https://doi.org/10.1017/ice.2025.10344

Address for correspondence: Sarah Ludmer, Maryland Department of Health, 201 W Preston St, Baltimore, MD 21201, USA; email: sludmer2@gmail.com

Epidemiology of and Risk Factors for Amebic Meningoencephalitis, Kerala, India, 2025

Harikumar Sivanandan,[1] Jeromie Wesley Vivian Thangaraj,[1] Ala Saritha,[2] Anitha Bhaskar,[2] Aravind Reghukumar,[2] Asuma A. Rahim,[2] Bindu Vadakkayil,[2] Chintha Sujatha,[2] Karthika Meenakshy Amma,[2] Manoj Arayakandy Thali,[2] Prathibha M. Thankamoni Amma,[2] Priya Chandran,[2] Rekha Melathuparambil Ravindran,[2] Remya Prakash,[2] Sabitha Rose Jacob,[2] Shameer Vadekkandiyil,[2] Shubin Chenayil,[2] Unnikrishnan Bhaskarannair,[2] Abhishek Gopalakrishnan Saraswthy,[3] Anitha Puduvail Moorkoth,[3] Bhagyalakshmi Mahavan Kanchana,[3] Biju George,[3] Dinesh Gopal,[3] Heera Hassan,[3] Jincy Johnson,[3] Kiran Raj Divakaran,[3] M.C. Sathya Bhama,[3] Megha Shaju,[3] Minu Abraham,[3] Neetha T. Ramankutty,[3] Pressy Sankar,[3] Priyanka Sajeev,[3] Saritha Narayanankutty,[3] O. Sasikumari,[3] Sujina Cheraparambil Muthukutty,[3] Thekkumkara Surendran Anish,[3] Vishnunath Kadavath,[3] Aruna Raman,[4] Bindu Gopalakrishnan Santhakumari,[4] Gayathri Ramakrishnan,[4] Geetha Panarkandy,[4] Jayakrishnan Machinery Puthanpurayil,[4] Mohandas Nair Karippoth,[4] Shameem Anathan Mohammed,[4] Sheeja Sugunan,[4] Sindhu Thekkile Gangadharan,[4] Anuja Ushakumari,[5] Chandni Radhakrishnan,[5] Easwaran Sreekumar,[5] Naveen Anaswara,[5] Pillaveetil Sathyadas Indu,[5] Reetha Kakkarakandiyil Pareri,[5] Sahadevan Sunija,[5] Sajeeth Kumar Keeriyatt Govindan,[5] Jaichand Johnson, Ajan Maheswaran Jaya, Abey Sushan, Raman Swathy Vaman, Lakshmi Geetha Gopalakrishnan, Arun P. Vijayalekshmi, Dinesh Kumar Harikrishnan, Sabarinathan Ramasamy, Navaneeth S. Krishna, Viswanathan V. Kollengode, Reena K. Joseph, Vinay Goyal, Rajan Khobragade, Manoj V. Murhekar; AME Study Group

Amebic meningoencephalitis (AME) is a highly fatal central nervous system infection caused by various free-living amebae. We describe epidemiology of AME cases from Kerala, India, during January 1–November 11, 2025, and identify behavioral risk factors associated with real-time PCR–confirmed *Acanthamoeba* spp. infection through a matched case–control study. We identified 159 AME case-patients, of which 67 (42.1%) tested positive for *Acanthamoeba* spp. amebae. Most AME cases were reported from 4 districts, peaking during the monsoon and postmonsoon periods. Exposure to natural water bodies for swimming or bathing and using nonchlorinated water for domestic purposes were associated with AME. History of maxillofacial injury or nasal surgery with subsequent exposure to natural water bodies and washing ulcers or skin lesions in natural water bodies were associated with higher odds of disease. Targeted risk communication about safe water practices and routine chlorination of domestic water sources could help reduce AME risk in affected communities.

Author affiliations: Government of Kerala Directorate of Health Services, Thiruvananthapuram, India (H. Sivanandan, M.A. Thali, R.M. Ravindran, S. Chenayil, U. Bhaskarannair, A.G. Saraswthy, K.R. Divakaran, M. Abraham, P. Sajeev, R.K. Pareri, A.M. Jaya, A. Sushan, R. Vaman, L.G. Gopalakrishnan, A.P. Vijayalekshmi, R.K. Joseph); Indian Council of Medical Research National Institute of Epidemiology, Chennai, India (J.W.V. Thangraj, A. Saritha, D. Gopal, M. Shaju, V. Kadavath, D.K. Harikrishnan, S. Ramasamy, N.S. Krishna, M.V. Murhekar); Government Medical College, Thiruvananthapuram (A. Bhaskar, A. Reghukumar, K.M. Amma, R. Prakash, B.M. Kanchana, H. Hassan, J. Johnson, M.C.S. Bhama, N.T. Ramankutty, S. Narayanankutty, O. Sasikumari, A. Raman, B.G. Santhakumari, S. Sugunan); Government Medical College, Kozhikode, India (A.A. Rahim, B. Vadakkayil, S. Vadekkandiyil, A.P. Moorkoth, P. Sankar, G. Ramakrishnan, G. Panarkandy, J.M. Puthanpurayil, M.N. Karippoth, S.A. Mohammed, S.K.K. Govindan); Government Medical College, Kollam, India (C. Sujatha, P.M. Thankamoni Amma); Government Medical College, Manjeri, India (P. Chandran, S.R. Jacob, B. George, S.C. Muthukutty); Kerala One Health Centre for Nipah Research and Resilience, Kozhikode (T.S. Anish); Government Medical College, Kasaragod, India (S.T. Gangadharan); Directorate of Medical Education, Kerala, India (A. Ushakumar, V.V. Kollengode); Government Medical College, Wayanad, India (C. Radhakrishnan); Institute of Advanced Virology, Thiruvananthapuram (E. Sreekumar); Kerala Centre for Disease Control and Prevention, Thiruvananthapuram (N. Anaswara); Government Medical College, Thrissur, India (P.S. Indu); State Public Health and Clinical Lab, Thiruvananthapuram (S. Sahadevan); National Health Mission, Government of Kerala, Thiruvananthapuram (V. Goyal); Health & Family Welfare, Government of Kerala, Thiruvananthapuram (R. Khobragade)

DOI: https://doi.org/10.3201/eid3209.260492

[1]These authors contributed equally to this article.
[2]These authors contributed equally to this article.
[3]These authors contributed equally to this article.
[4]These authors contributed equally to this article.
[5]These authors contributed equally to this article.

Amebic meningoencephalitis (AME) is a collection of rare but frequently fatal infections of the central nervous system caused by various free-living amebae (FLA). Such infections include primary amebic meningoencephalitis (PAM), caused by *Naegleria fowleri* amebae, and granulomatous amoebic encephalitis (GAE), caused by different species of *Acanthamoeba*, *Balamuthia mandrillaris*, and *Sappinia* spp. amebae (*1*,*2*). PAM typically manifests as an acute, rapidly progressive meningoencephalitis, whereas GAE usually manifests as a subacute or chronic encephalitic illness. The clinical manifestations of PAM are indistinguishable from those of bacterial meningitis, whereas GAE can mimic brain abscess, encephalitis, or meningitis. PAM and GAE are associated with high mortality rates; case-fatality rates >90% have been reported globally (*3*,*4*).

N. fowleri amebae infect susceptible persons when contaminated water enters the nasal cavity; trophozoites can penetrate the olfactory mucosa, cross the cribriform plate, and invade the olfactory bulb, leading to parenchymal inflammation and tissue damage (*5*,*6*). The trophozoites of *Acanthamoeba* spp. amebae can enter the body through the eyes, nasal passages, or ulcerated or broken skin (*7*,*8*). Ocular exposure can cause severe keratitis (*9*); entry through the respiratory tract or broken skin can cause hematogenous spread to the central nervous system (*10*,*11*). Swimming or diving in warm fresh water like hot springs, lakes, rivers, and ponds are the primary risk factors for *N. fowleri* infection, although other water sources, including tap water, have been implicated (*12*). Environmental risk factors for *Acanthamoeba* GAE include exposure to contaminated soil, dust, freshwater sources, and untreated water systems. Because *Acanthamoeba* is ubiquitous in natural and manmade environments, inhalation of airborne cysts or contamination of skin lesions can result in infection, particularly in susceptible persons (*13*–*15*).

In the state of Kerala, India, 45 cases of AME were reported during 2016–2024, including 15 deaths (33% case-fatality rate). *N. fowleri* accounted for 5 of 7 cases reported during 2016–2023, whereas 38 cases and 8 deaths were reported in 2024, most of which were caused by *Acanthamoeba.* In response to the increasing number of AME cases, the Department of Health and Family Welfare, Government of Kerala, formulated a multipronged action plan in 2025 to improve the diagnosis and management of AME cases (*16*).

Descriptive epidemiology of AME in Kerala has not been documented in published literature. In this context, we aimed to describe the AME cases reported in 2025 in Kerala by time, place, person, and laboratory diagnosis. In addition, we conducted a case–control study to identify behavioral risk factors associated with real-time PCR (rPCR)–confirmed cases of amebic meningoencephalitis caused by *Acanthamoeba* spp. amebae.

Methods

Descriptive Epidemiology

We defined a case as a patient experiencing clinical features suggestive of acute meningoencephalitis, including fever, headache, vomiting, neck stiffness, altered sensorium, seizures, or other neurologic symptoms, diagnosed during January 1–November 11, 2025, and with laboratory evidence of infection with FLA. We defined laboratory evidence as either demonstration of motile trophozoites in cerebrospinal fluid (CSF) by wet-mount microscopy or detection of FLA DNA in CSF by rPCR targeting species-specific 18S rRNA genes for *N. fowleri*, *Acanthamoeba* spp., *Balamuthia mandrillaris*, *Paravahlkampfia* spp., or *Vermamoeba vermiformis.* Molecular assays included conventional pangenus FLA and genus-specific PCR for *Acanthamoeba*, *Naegleria*, and *Balamuthia* and rPCR (*17*,*18*) (Appendix, https://wwwnc.cdc.gov/EID/article/32/9/26-0492-App1.pdf).

Case Search

We identified cases among patients with suspected AME admitted to the Government Medical College, Thiruvananthapuram and Kozhikode, India. We collected information on demographic characteristics, area of residence, clinical manifestation, underlying conditions, date of admission, and outcome status from patients, family members, and hospital admission records.

Data Analysis

We plotted the geographic locations of cases and constructed an epidemic curve to describe the spatial and temporal distribution of cases. We summarized age using median and interquartile range (IQR) and categorical variables using frequencies and percentages. We calculated median durations from date of illness onset to admission and from admission to death. We analyzed all characteristics separately for rPCR-confirmed *Acanthamoeba* spp. cases, rPCR-confirmed *N. fowleri* cases, and cases diagnosed by wet-mount microscopy.

Analytical Epidemiology

We conducted a matched case–control study in the Kollam, Kozhikode, Malappuram, and Thiruvananthapuram districts of Kerala during October–

November 2025. We defined a case-patient as a resident of Kollam, Kozhikode, Malappuram, or Thiruvananthapuram district who experienced clinical features suggestive of AME and received a diagnosis during July–November 2025 that was confirmed by detection of FLA DNA for *Acanthamoeba* spp. in CSF by rPCR. We restricted the analytical study to rPCR-confirmed *Acanthamoeba* spp. cases because wet-mount microscopy does not identify the amebic species and because transmission pathways and risk factors may differ by species. Controls were apparently healthy persons without a history of AME or meningoencephalitis, matched to case-patients by age (±3 years), sex, and place of residence. We sought to include all cases diagnosed during July–November in the study.

Selection of Cases and Controls

The study hospitals prepared a linelist of patients with rPCR-confirmed *Acanthamoeba* spp. AME diagnosed during July–November 2025 residing in the 4 study districts. Trained field investigators visited each case household to obtain consent and collect data. For each case-patient, we prepared a list, with the assistance of a local health worker, of apparently healthy persons who had no history of AME or meningoencephalitis and met the matching criteria. We randomly selected 3 controls from this list for each case-patient.

Human Participant Protection

Institutional Human Ethics Committee of the Indian Council of Medical Research—National Institute of Epidemiology and participating institutions approved the study protocol (NIE/IHEC/202509-01). We obtained written informed consent from adult participants ≥18 years of age and from the parents or guardians of minors <18 years of age. We acquired assent from children 7–17 years of age.

Data Collection

We collected data during October–November 2025. Trained investigators interviewed case-patients and controls at their homes using a structured questionnaire created with Open Data Kit (https://getodk.org). The questionnaire collected information on demographic and socioeconomic characteristics, water sources used for domestic purposes, water-related activities, nasal rinsing practices, chlorination of well water, and underlying conditions suggestive of immunocompromised status, including diabetes, chronic kidney disease, malignancy, or HIV infection. We defined domestic water use as water used for activities involving direct contact with the face, head, nose, or body, such as bathing or washing the face or hair; it did not include washing clothes or utensils. For case-patients, we assessed exposures during the 3 months before illness onset. For controls, we assessed exposures during the corresponding 3-month reference period before illness onset of the matched case-patient. Water-related activities included swimming or bathing in ponds, lakes, rivers, canals, streams, or swimming pools; entry into natural water bodies; domestic or occupational contact with pond, river, canal, stream, or well water other than swimming; nasal irrigation; and nasal ablution as part of ritual cleansing. For case-patients who died, we obtained information from a reliable family member.

Statistical Analysis

We summarized sociodemographic characteristics of cases and controls using frequencies and percentages. We performed univariable conditional logistic regression analysis to estimate the unadjusted matched odds ratios (MOR) along with 95% CIs. We used multivariable conditional logistic regression to estimate adjusted matched odds ratios (aMOR) and 95% CIs. We constructed directed acyclic graphs using DAGitty software (http://www.dagitty.net) to represent hypothesized causal pathways between exposures and AME (Appendix Figure 1). We estimated population attributable fractions (PAF) along with 95% CIs for selected modifiable exposures. We applied the backdoor criterion to identify the minimal sufficient adjustment set for each risk factor. We performed all statistical data analysis using Stata version 17 (StataCorp LLC, https://www.stata.com).

Results

Descriptive Epidemiology

We identified 159 AME case-patients during January 1–November 11, 2025. Of those, 76 (47.8%) were confirmed by rPCR and 83 (52.2%) by wet-mount microscopy. Among the 76 PCR-confirmed case-patients, 67 (88.2%) were positive for *Acanthamoeba* spp. and 9 (11.8%) for *N. fowleri* amebae. The median age was 43 (IQR 29–58) years among rPCR-confirmed *Acanthamoeba* spp. case-patients, 34 (IQR 18–38) years among rPCR-confirmed *N. fowleri* case-patients, and 39 (IQR 14–55) years among case-patients who tested positive by wet-mount microscopy. Male patients accounted for 58.2% and female patients 41.8% of rPCR-confirmed *Acanthamoeba* spp. case-patients; 60.2% of case-patients positive by wet microscopy were male and 39.8% female (Table 1).

Among the 159 case-patients, 41 (25.8%) died. Seventeen (25.4%) deaths were among rPCR-confirmed *Acanthamoeba* spp. case-patients, 4 (44.4%) were among rPCR-confirmed *N. fowleri* case-patients, and 20 (24.1%) were among wet-mount microscopy case-patients. The median duration from illness onset to hospitalization was 4 (IQR 1–13.5) days and broadly similar across the 3 groups. Among the case-patients who died, the median duration from hospital admission to death was 31 (IQR 19–42) days. Overall, 62 (39.0%) case-patients had ≥1 underlying condition. Among rPCR-confirmed *Acanthamoeba* spp. case-patients, 15 (22.4%) had a condition suggestive of an immunocompromising condition or a history of immunosuppressive therapy (Table 1).

Most AME cases were reported from Thiruvanathapuram, Kollam, Kozhikode, and Malappuram districts (Figure 1). The epidemic curve showed a peak in cases during August–October, corresponding to the monsoon and postmonsoon period in Kerala (Figure 2).

The most common clinical signs and symptoms were fever (n = 86 [58.1%]), headache (n = 83 [56.1%]), vomiting (n = 54 [36.5%]), seizures (n = 29 [19.6%]), altered sensorium (n = 27 [18.2%]), neck stiffness (n = 21 [14.2%]), and loss of consciousness (n = 9 [6.1%]). Some patients also experienced less typical symptoms, such as diplopia, blurred vision, sensory disturbances, and cranial nerve palsies (Table 1). A total of 103 (81.7%) patients had CSF pleocytosis; 90 (70.3%) had lymphocytic predominance (Appendix Table 1).

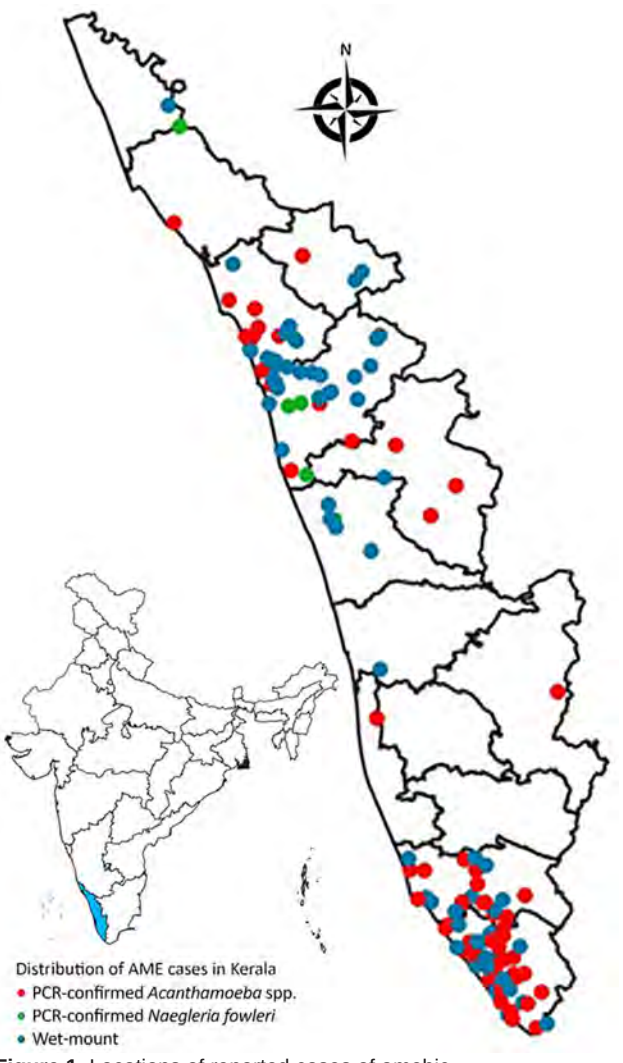

Figure 1. Locations of reported cases of amebic meningoencephalitis in Kerala state, India, 2025. Cases were confirmed by real-time PCR as caused by *Acanthamoeba* spp. or *Naegleria fowleri* amebae or confirmed via wet-mount microscopy of cerebrospinal fluid. Inset map shows location of Kerala in India.

Analytic Epidemiology

During July–November 2025, we identified a total of 46 rPCR-positive *Acanthamoeba* spp. AME case-patients from the 4 study districts. We enrolled 43 of those case-patients and 129 controls in the study. Among the 43 case-patients, 5 (11.6%) were <18 years of age and 23 (53.5%) were >45 years of age; 24 (55.8%) were male and 19 (44.2%) female. Most case-patients resided in rural areas (n = 35 [81.4%]). Almost all participants (97.7% case-patients and 100% controls) lived in pucca or semi-pucca houses. A higher percentage of case-patients (74.4%) than controls (48.8%) belonged to a low socioeconomic group, as indicated by yellow or pink ration card status (Table 2).

In univariable conditional logistic regression analysis, case-patients had higher odds than controls of belonging to a low socioeconomic background (MOR = 2.8 [95% CI 1.3–5.9]) and using nonchlorinated water for domestic purposes, defined as water from unchlorinated household or public wells (MOR = 2.9 [95% CI 1.1–7.8]). Case-patients also had higher odds of exposure to natural water bodies, including ponds, lakes, rivers, canals, and streams, for swimming or bathing or entry into natural water bodies during the preceding 3 months (MOR = 3.6 [95% CI 1.6–8.5]) (Table 3).

Other exposures more frequently reported among case-patients included reaching the bottom of a lake, pond, canal, river, or stream while swimming, bathing, or diving or experiencing Tharipu (a local term for water forcefully entering the nose). Case-patients were also more likely than controls to report a history of maxillofacial injury or nasal surgery followed by exposure to natural water bodies. A higher percentage of case-patients also reported washing ulcers or skin lesions in the natural water bodies (Table 3).

In multivariable conditional logistic regression analysis, exposure to natural water bodies for swimming, bathing, or any entry into such water bodies during the preceding 3 months was associated with AME (aMOR 4.7 [95% CI 1.8–12.1]; PAF 32.9% [95% CI 24.0%–40.8%]). Use of nonchlorinated water for domestic purposes was also independently associated with AME (aMOR 2.9 [95% CI 1.1–8.2]; PAF 34.2% [95% CI 13.5%–49.9%]). Case-patients had higher odds of having washed ulcers or skin lesions in the natural water bodies, although the CI was wide (aMOR 25.4 [95% CI 3.1–210.3; PAF 20.1% [95% CI 18.3%–21.8%]). A history of maxillofacial injury or nasal surgery followed by exposure to ponds, lakes, canals, rivers, or streams was also associated with AME (aMOR 4.8 [95% CI 1.3–16.7]; PAF 12.8% [95% CI 8.5%–17.1%]). Tharipu during swimming, bathing, or diving was associated with AME (aMOR 4.8 [95% CI 1.5–15.4]; PAF 14.7% [95% CI 10.1%–19.1%]) (Table 4).

Discussion

In 2025, Kerala reported an increased number of laboratory-supported AME cases; *Acanthamoeba* spp. amebae accounted for most rPCR-confirmed cases. Case-patients were reported from several districts, peaking during monsoon and postmonsoon months. The substantial case-fatality rates among rPCR-confirmed cases underscored the severity of AME. *Acanthamoeba* GAE accounted for most rPCR-confirmed AME cases in Kerala during 2025. Increased clinical suspicion, wider availability of molecular diagnostics, and improved surveillance could have contributed to the higher number of detected cases; temporal clustering also suggested water-related environmental exposures.

In the matched case–control study restricted to rPCR-confirmed *Acanthamoeba* spp. cases, we identified several exposures associated with the illness. Those included washing ulcers or skin lesions in natural water bodies, exposure to natural water bodies among persons with history of maxillofacial injury or nasal surgery, use of nonchlorinated well water for domestic activities, exposure to natural water bodies for swimming or bathing, and Tharipu. Those findings suggest that both environmental exposures and potential portals of entry affect infection risk. The association between washing ulcers or skin lesions in natural water bodies and AME observed in our study is consistent with the known ability of *Acanthamoeba* spp. amebae to enter through breaks in the skin and subsequently disseminate to the CNS (*13*). Similarly, exposure to natural water bodies after maxillofacial injury or nasal surgery was associated with AME. Although the CIs around some of our estimates were wide, those associations are biologically plausible; such conditions could increase the opportunity for environmental organisms to enter tissue or the respiratory tract. Hence, public health communication should specifically advise persons with open wounds, chronic ulcers, or recent history of maxillofacial surgery to avoid exposure to natural water bodies.

Acanthamoeba spp. amebae are widely distributed in the environment and have been isolated from soil, freshwater, wells, swimming pools, domestic water systems, and tap water (*1*,*19*). An environmental survey in 51 villages that reported cases found that, in 43 (84.3%) villages, ≥1 environmental water sources, including wells, ponds, drinking water sources, and water tanks, tested positive for FLAs (data not shown). Those environmental findings should be interpreted as supportive ecologic evidence only,

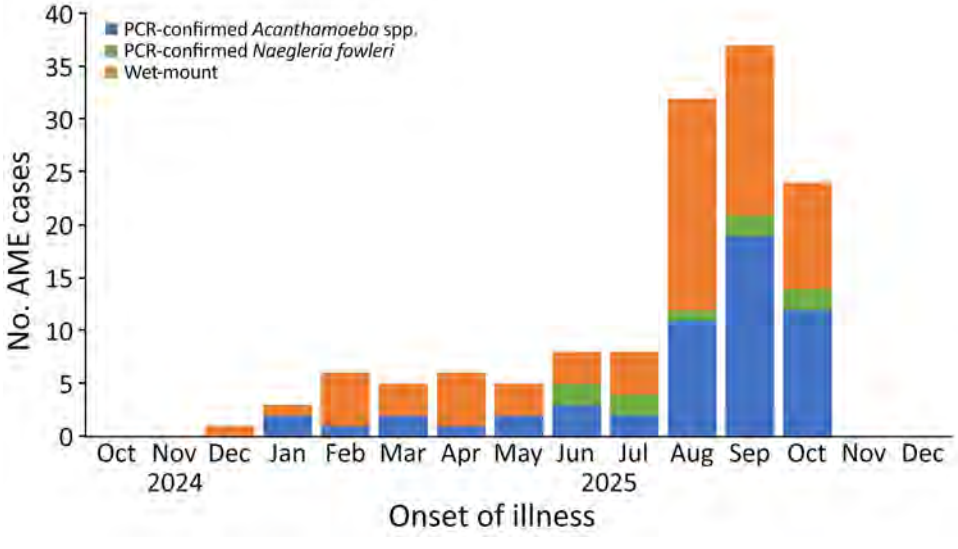

Figure 2. Epidemic curve of AME cases by onset of illness, Kerala state, India, 2025. Cases were confirmed by real-time PCR as caused by *Acanthamoeba* spp. or *Naegleria fowleri* amebae or confirmed via wet-mount microscopy of cerebrospinal fluid. The case shown in Decmber was not confirmed until 2025. AME, amebic meningoencephalitis.

Table 1. Demographic distribution and clinical characteristics of all case-patients in study of amebic meningoencephalitis, Kerala state, India, 2025*

Characteristic	rPCR		CSF wet-mount microscopy, n = 83	Total, N = 159
	Acanthamoeba, n = 67	*Naegleria*, n = 9		
Sex				
F	28 (41.8)	5 (55.6)	33 (39.8)	66 (41.5)
M	39 (58.2)	4 (44.4)	50 (60.2)	93 (58.5)
Age, y				
0–5	2 (3.0)	1 (11.1)	2 (2.4)	5 (3.1)
6–17	9 (13.4)	1 (11.1)	26 (31.3)	36 (22.7)
18–45	27 (40.3)	5 (55.6)	24 (28.9)	56 (35.2)
>45	29 (43.3)	2 (22.2)	31 (37.4)	62 (39.0)
Mean (±SD)	41.9 (20.7)	32.1 (20.4)	36.3 (21.7)	38.4 (21.3)
Median (IQR)	43 (29–58)	34 (18–38)	39 (14–55)	40 (17–56)
Underlying condition				
Y	28 (41.8)	3 (33.3)	31 (37.3)	62 (39.0)
N	39 (58.2)	6 (66.7)	52 (62.7)	97 (61.0)
Underlying condition suggestive of immunocompromise				
Y	15 (22.4)	3 (33.3)	23 (27.7)	41 (25.8)
N	52 (77.6)	6 (66.7)	60 (72.3)	118 (74.2)
Clinical outcome				
Died	17 (25.4)	4 (44.4)	20 (24.1)	41 (25.8)
Survived	50 (74.6)	5 (55.6)	63 (75.9)	118 (74.2)
Days from hospital admission to death	n = 17	n = 4	n = 20	n = 41
Median (IQR)	34 (25–45)	28 (19.5–30)	27.5 (14.2–37)	31 (19−42)
Days from illness onset to hospital admission	n = 52	n = 9	n = 64	n = 125
Median (IQR)	3 (0–13)	4 (2–26)	4 (1–11)	4 (1–13.5)
Clinical manifestations	n = 64	n = 8	n = 76	n = 148
Fever	32 (50.0)	6 (75.0)	48 (63.2)	86 (58.1)
Headache	34 (53.1)	5 (62.5)	44 (57.9)	83 (56.1)
Vomiting	18 (28.1)	5 (62.5)	31 (40.8)	54 (36.5)
Seizures	11 (17.2)	4 (50.0)	14 (18.4)	29 (19.6)
Altered sensorium	11 (17.2)	1 (12.5)	15 (19.7)	27 (18.2)
Weakness in the upper limb/lower limb	13 (20.3)	3 (37.5)	8 (10.5)	24 (16.2)
Neck stiffness/meningeal signs	5 (7.8)	1 (12.5)	15 (19.7)	21 (14.2)
Myalgia/fatigue	7 (10.9)	0	13 (17.1)	20 (13.5)
Diplopia	6 (9.4)	0	5 (6.6)	11 (7.4)
Blurred vision	6 (9.4)	0	3 (3.9)	9 (6.1)
Dizziness/vertigo	6 (9.4)	1 (12.5)	2 (2.6)	9 (6.1)
Loss of consciousness	4 (6.3)	0	5 (6.6)	9 (6.1)
Slurred speech	4 (6.3)	1 (12.5)	3 (3.9)	8 (5.4)
Sensory disturbance	7 (10.9)	0	0	7 (4.7)
Chills/rigors	3 (4.7)	0	2 (2.6)	5 (3.4)
Photophobia	3 (4.7)	0	2 (2.6)	5 (3.4)
6th cranial nerve palsy/upper motor neuron/ lower motor neuron facial palsy	1 (1.6)	0	2 (2.6)	3 (2.0)
Ptosis	2 (3.1)	0	0	2 (1.4)
Involuntary movement	2 (3.1)	0	0	2 (1.4)

*Values are no. (%) except as indicated. CSF, cerebrospinal fluid; IQR, interquartile range; rPCR, real-time PCR.

because sampling was not designed to establish source attribution.

For *N. fowleri* infection, entry of contaminated water through the nose during swimming and bathing, as well through Tharipu, is a definitive route of transmission (*12*). However, those are not well-established routes of transmission for *Acanthamoeba* GAE (*13*–*15*). In a case series of 173 nonkeratitis *Acanthamoeba* infections in the United States during 1956–2020, 10% had exposure to natural water bodies (*19*). Similarly, a review article from India identified 42 case reports, of which 2 had documented exposure to natural water bodies (*11*). A few case reports of *Acanthamoeba* spp. CNS infection among persons with near-drowning events have been documented (*20*,*21*). The associations between *Acanthamoeba* spp. AME and exposure to natural water bodies, use of nonchlorinated well water, and Tharipu observed in our study are epidemiologic associations and do not prove that water exposure led directly to neuroinvasion. Those findings might indicate contact with environmental sources where *Acanthamoeba* spp. amebae are present and possible entry into body by inhalation or respiratory route, water entering the nose during swimming or bathing, or other behaviors associated with untreated water use that we did not measure. Further environmental, clinical, and microbiological studies are needed to determine whether that association reflects a route of acquisition or an epidemiologic marker of exposure to contaminated water.

In Kerala, ≈40% of the landscape is water, featuring an abundance of water bodies, including lakes, ponds, and reservoirs (*22*). Hence, opportunities for exposure to natural water bodies are common during routine bathing, swimming, recreational, and occupational activities. Chlorination of such a large number of natural water bodies is neither feasible nor practical. Hence, prevention strategies need to focus on reducing high-risk exposures, particularly during monsoon and postmonsoon months. Risk communication should advise persons with skin lesions, ulcers, recent facial trauma, or recent nasal surgery to avoid exposure to natural water bodies.

Use of nonchlorinated water from household or public wells for domestic purposes was also associated with *Acanthamoeba* spp. AME and accounted for a substantial PAF. In our study, domestic water use referred to activities involving direct contact with the face, head, skin, or body, such as bathing or washing the face or hair, and did not refer to ingestion. Many households in Kerala depend on individual or public wells. Heavy rainfall, flooding, sewage contamination, organic matter, and algal growth might contribute to contamination or proliferation of FLAs in poorly maintained wells. Periodic chlorination and maintenance of wells, especially wells used for bathing, face washing, hair washing, and wound care, are practical interventions that can be promoted through local administrative systems.

Acanthamoeba infections have frequently been reported among immunocompromised persons (*19*), although studies from India have reported *Acanthamoeba* infection in persons without documented immunocompromising conditions (*23*–*28*). In our study, most rPCR-confirmed *Acanthamoeba* spp. case-patients did not have documented immunocompromising conditions in available records. Although immunocompromised status was associated with moderate increase in odds of illness in our analysis, the CIs were imprecise (MOR 1.9 [95% CI 0.8–4.7]). Therefore, the role of host susceptibility cannot be excluded. In addition, immune status might not have been completely ascertained, which could have resulted in exposure misclassification. Further studies are needed to better understand the host, pathogen, and environmental determinants of *Acanthamoeba* spp. AME in Kerala.

In our study, nasal rinsing and nasal ablution were not associated with rPCR-confirmed *Acanthamoeba* spp. illness. Previous studies have suggested that the use of nonsterile water may increase the risk for FLA infection (*29*). In Kerala, nasal ablution is widely practiced, especially among certain religious

Table 2. Sociodemographic profile of rPCR-confirmed *Acanthamoeba* spp. case-patients and controls in study of amebic meningoencephalitis, Kerala state, India, 2025*

Characteristic	Case-patients, n = 43	Controls, n = 129	p value
Age group, y			0.581
≤5	0	4 (3.1)	
6–10	4 (9.3)	5 (3.9)	
11–17	1 (2.3)	6 (4.7)	
18–45	15 (34.9)	47 (36.4)	
>45	23 (53.5)	67 (51.9)	
Mean age (±SD)	46.2 (3.1)	46.1 (1.8)	
Sex			
M	24 (55.8)	72 (55.8)	NA
F	19 (44.2)	57 (44.2)	
District			
Kollam	12 (27.9)	36 (27.9)	NA
Kozhikode	7 (16.3)	21 (16.3)	
Malappuram	3 (7.0)	9 (7.0)	
Trivandrum	21 (48.8)	63 (48.8)	
Residence			NA
Rural	35 (81.4)	105 (81.4)	
Urban	8 (18.6)	24 (18.6)	
Type of house			1.000
Pucca/semi-pucca	42 (97.7)	129 (100)	
Kutcha	1 (2.3)	0	
Color of ration card			0.007
Yellow/pink	32 (74.4)	63 (48.8)	
Others	11 (25.6)	66 (51.2)	
Education level			0.577
Degree/above	5 (11.6)	15 (11.6)	
High school/higher secondary	20 (46.5)	71 (55.0)	
Primary/middle	15 (34.9)	33 (25.6)	
Illiterate/read-write	2 (4.7)	4 (3.1)	
Not applicable	1 (2.3)	6 (4.7)	

*Values are no. (%) except as indicated. NA, not applicable because cases and controls were matched for this variable; rPCR, real-time PCR.

Table 3. Risk factors associated with *Acanthamoeba*-caused cases by univariate conditional logistic regression analysis in study of amebic meningoencephalitis, Kerala state, India, 2025*

Risk factor	No. (%) cases, n = 43	No. (%) controls, n = 129	Matched odds ratio (95% CI)	p value
Occupation, painter/construction worker/farmer	5 (11.6)	13 (10.1)	1.2 (0.4–3.7)	0.768
Persons living below the poverty line	32 (74.4)	63 (48.8)	2.8 (1.3–5.9)	0.007
Use of nonchlorinated water for domestic use, household/public well, not chlorinated†	14 (50.0)	30 (32.6)	2.9 (1.1– 7.8)	0.029
Presence of fish in well†	1 (3.6)	6 (6.5)	2.9 (0.3– 31.5)	0.374
Cleaned well in previous 3 mo†	2 (7.1)	15 (16.3)	0.3 (0.0- 2.2)	0.223
Cleaned the overhead tank in previous 3 mo	16 (37.2)	60 (46.5)	0.7 (0.3–1.4)	0.275
Observed turbidity or a change in taste/smell in the water	10 (23.3)	21 (16.3)	1.7 (0.7–4.5)	0.253
Exposure to water bodies such as ponds/lakes/rivers/canals/streams for swimming or bathing or entered water body in previous 3 mo	18 (41.9)	25 (19.4)	3.6 (1.6–8.5)	0.003
History of swimming in swimming pool in previous 3 mo	1 (2.3)	0	NA	NA
Reached the bottom of lakes/ponds/canals/rivers/streams during swimming/bathing/diving or experienced Tharipu	8 (18.6)	7 (5.4)	3.7 (1.3–10.8)	0.015
Practised nasal rinsing in previous 3 mo	15 (34.9)	37 (28.7)	1.4 (0.6–3.2)	0.401
Smoking‡	8 (18.6)	21 (16.3)	1.2 (0.4–3.6)	0.686
Consumption of alcohol‡	9 (20.9)	34 (26.4)	0.6 (0.2–1.7)	0.349
Use of nasal snuff‡	0	4 (3.1)	NA	NA
Immunocompromised person§	15 (34.9)	33 (25.6)	1.9 (0.8–4.7)	0.173
Use of steroids in previous 3 mo	6 (13.9)	12 (9.3)	1.6 (0.6–4.6)	0.390
Experienced recurrent sinusitis in previous 3 mo	6 (13.9)	10 (7.8)	2.1 (0.7–6.7)	0.214
Had maxillofacial injury or nasal surgery and exposure to ponds/lakes/canals/rivers/streams	7 (16.3)	6 (4.7)	3.9 (1.2–12.4)	0.022
Hospitalization for severe COVID-19	2 (4.7)	11 (8.5)	0.5 (0.1–2.4)	0.392
Soil/dirt contact during farming/gardening in previous 3 mo	25 (58.1)	75 (58.1)	1 (0.5–2.1)	1.000
Cleaned the air conditioner in previous 3 mo	1 (2.3)	8 (6.2)	0.4 (0.0–2.9)	0.337
Used sprinklers/hose to water plants/wash vehicles in previous 3 mo	17 (39.5)	51 (39.5)	1 (0.5–2.1)	1.000
Had any ulcers/skin lesions in previous 3 mo	17 (39.5)	15 (11.6)	4.7 (2.1–10.8)	0.001
Washed ulcers/skin lesions in ponds/lakes/rivers/canals/streams	9 (20.9)	1 (0.8)	27 (3.4–213.1)	0.002

*NA, not applicable; Tharipu, water forcefully entering the nose.
†Cases, n = 28; controls, n = 92.
‡Current or past.
§Diabetes, HIV, chronic kidney disease, malignancy, or immunosuppressive therapy.

communities, so the high background prevalence of that exposure might have limited our ability to detect the association.

Lower socioeconomic status was associated with AME in univariable analysis and might influence behavioral exposures identified in our study. We included socioeconomic status in the directed acyclic graphs as a potential confounder because it could influence access to safe domestic water, reliance on nonchlorinated wells, and use of natural water bodies for bathing or other routine activities. We therefore adjusted socioeconomic status in the multivariable conditional logistic regression model. Risk communication strategies should prioritize socioeconomically vulnerable communities through improved access to safe water and routine maintenance and chlorination of wells.

A limitation of our study was including case-patients whose diagnosis was by wet-mount microscopy

Table 4. Risk factors associated with *Acanthamoeba*-caused cases by multivariable conditional logistic regression analysis in study of amebic meningoencephalitis, Kerala, India, 2025*

Risk factors	Univariate MOR (95% CI)	Adjusted MOR (95% CI)	PAF, % (95% CI)
Exposure to water bodies such as ponds/lakes/rivers/canals/streams for either swimming or bathing or entered a water body in previous 3 mo	3.6 (1.6–8.5)	4.7 (1.8–12.1)†	32.9 (24.0–40.8)
Use of nonchlorinated water for domestic use, household/public well, not chlorinated	2.9 (1.1–7.8)	2.9 (1.1–8.2)†	34.2 (13.5–49.9)
Washed ulcers/skin lesions in ponds/lakes/rivers/canals/streams	27 (3.4–213.1)	25.4 (3.1–210.3)†	20.1 (18.3–21.8)
Had a maxillofacial injury or undergone nasal surgery in the past, and exposure to ponds/lakes/canals/rivers/streams	3.9 (1.2–12.4)	4.8 (1.3–16.7)†	12.8 (8.5–17.1)
Reached the bottom of lakes/ponds/canals/rivers/streams during swimming/bathing/diving, or experienced Tharipu	3.7 (1.3–10.8)	4.8 (1.5–15.4)‡	14.7 (10.1–19.1)

*MOR, matched odds ratio; PAF, population attributable fraction; Tharipu, water forcefully entering the nose.
†Adjusted for socioeconomic status
‡Adjusted for socioeconomic status and immunocompromised status.

in our descriptive epidemiology. Wet-mount microscopy provides rapid laboratory evidence of motile trophozoites; however, it is less specific than rPCR and does not reliably identify the species of FLA. Although wet-mount examinations were performed independently by 2 trained microbiologists, some misclassification is possible. Second, we restricted the case–control study to rPCR-confirmed *Acanthamoeba* spp. cases from 4 districts, which might not represent all AME cases in Kerala or AME caused by other FLA. We did not compare rPCR-confirmed *Acanthamoeba* spp. case-patients with immunocompromised controls, and the immune status among case-patients may have been incompletely ascertained. Third, the analytical study had a small sample size, resulting in wide CIs for some exposures. Fourth, the incubation period for *Acanthamoeba* spp. GAE can range from days to several weeks (*13*). We used a 3-month referent exposure period in accordance with expert consultation; we did not capture any behavior or practices beyond the 3-month period. Nevertheless, we expected that study participants would perform routine behaviors such as swimming or bathing frequently, and a 3-month referent exposure might be sufficient to capture such activities. Fifth, after the surge of AME cases in the state, Kerala public health authorities issued regular messages discouraging swimming or bathing in natural water bodies and launched widespread campaigns to chlorinate wells (*16*). Those actions might have led case-patients or their relatives to recall behaviors related to swimming or bathing in natural water bodies more readily than controls, resulting in differential recall bias. We attempted to minimize that difference by using a standardized questionnaire and identical reference periods for cases and controls but could not exclude differential recall. Further studies combining pathogen-specific surveillance, molecular testing, environmental sampling, and immune-status assessment are needed to better understand *Acanthamoeba* spp. CNS infection in Kerala.

In conclusion, Kerala reported an increase in laboratory-supported AME cases in 2025. A*canthamoeba* spp. amebae accounted for most rPCR-confirmed infections. Cases increased during monsoon and postmonsoon months, and the overall case-fatality rate was 25.8%. In our analytical study, AME was associated with washing ulcers or skin lesions in natural water bodies, exposure to natural water bodies after maxillofacial injury or nasal surgery, use of nonchlorinated well water for domestic purposes, and exposure to natural water bodies and forceful entry of water into the nose. Public health interventions should focus on maintenance and chlorination of domestic wells and limiting exposure to natural water bodies for persons with wounds or recent facial or nasal procedures.

AME Study Group: Adisha Bhaskaran Reeja, Amaljith Asokan Beenapriya, Amritha Thannikkaparambil Raveendran, Angeline Elsa Koshy, Anima Raj, Anjaly Nattuvathukkal Thulaseedharan, Anju Lekshmi Pradeep, Arun Kinatteri Parambil, Bhagiaswari Kodapally, Harikrishnan Bhuvanendranpillai Rema, Iswarya Sreeja, Jayasankar Jayaprakash, Jeevan Jose Madakkathra, Jessy Prabhakar, Jinsy Edathumthazha Kuny, Khadeeja Nasreen Vadakkepeediyakkal, Meghna P. Dinesh, Muhammed Shifan Tharekandy, Neeraj Ramachandran, Nisamudeen Akkaparamban, Safareena Cherikkal Kunhithayyil, Shanmugam Varadarajan, Shringa Sivanand, Shruti Sarika, Soumya Thulaseedharan Remadevi Pillai, Sreedhish Kunniyullaparambil Sreedharan, Sreenath Manjula Radhakrishnan, Sreeshma Narayanan Pulicka Parambil, Sreeshma Vadakkethodiyil, Sujith Babu Mundakkal Suresh, Sumitha Thulaseedharan Soya, Thottasseri Haseena, Thripthi Tambi, Uwais Nazar, Vipin Thampi, and Vismaya Shajahan (Directorate of Health Services, Government of Kerala, Thiruvananthapuram, India); and Aishwarya Suevia Sudheer (Government Medical College, Kollam, India).

Acknowledgments

We thank Tarun Bhatnagar, Rizwan Suliankatchi Abdulkader, and Saravanakumar for their guidance in the analysis. We thank Suganya Ekambaram for the support provided for the study. We acknowledge the support of local health staff and community health volunteers in implementing the study.

All key anonymized individual participant data pertaining to the results reported in the article, along with a data dictionary and study proposal, are available upon request to the corresponding author after approval of a proposal and a signed data access agreement.

The study did not receive any external funding. The fieldwork was done through the intramural funds of Indian Council of Medical Research -National Institute of Epidemiology, Chennai. The funder of the study had no role in study design, data collection, data analysis, data interpretation, or writing of the report.

Author contributions: M.V.M., J.W.V.T., and A.S. did the literature search. H.S., M.V.M., J.W.V.T., A.S., A.B., A.R.K., A.A.R., and T.S.A. did the study design. J.W.V.T., A.S., A.B., A.R.K., A.A.R., B.V., C.S., K.M.A., M.A.T., P.M.T., P.C.,

R.M.R., R.P., S.R.J., S.V., S.C., U.K.B., A.G.S., A.P.M., B.L.K., D.G., H.H., J.J., K.R.D., M.S., M.A., M.C.S.B., P.S., T.S.A., P.K.S., N.T.R., S.N., S.K.O., V.K., Ar.R., B.G.S., G.R., G.P., J.M.P., M.N.K., S.A.M., S.S., S.T.G., A.B.R., A.A.B., A.T.R., A.E.K., An.R., A.N.T., A.L.P., A.K.P., B.K., H.B.R., I.S., J.S.J., J.J.M., J.P., J.E.K., K.N.V.P., M.P.D., M.S.T.K., N.R., N.A.P., S.C.K., Sh.V., Sh.S., S.Sa., S.T.R.P., S.K.S., S.M.R., S.N.P., S.V., S.B.M.S., S.T.S., T.H., T.T., U.N., V.T., and V.S. did the data collection. M.V.M., J.W.V.T. and A.S. did the data analysis. H.S., M.V.M., J.W.V.T., A.S., A.B., A.R.K., A.A.R., B.V., C.S., K.M.A., M.A.T., P.M.T., P.C., R.M.R., R.P., S.R.J., S.V., S.C., U.K.B., A.G.S., A.P.M., B.L.K., D.G., H.H., J.J., K.R.D., M.S., M.A., M.C.S.B., P.S., T.S.A., P.K.S., N.T.R., S.N., S.K.O., V.K., A.U., C.R., E.S., N.A., P.S.I., R.K.P., S.K.K.G., Su.S., Ja.J., A.M.J., Ab.S., R.S.V., L.G.G., A.P.V., D.K.H., S.R., N.S.K., V.K.V., R.K.J., V.G., and R.K. did the project management. H.S., M.V.M., J.W.V.T., A.S., and A.R.K. did the data interpretation. M.V.M. and J.W.V.T. accessed and verified the data. H.S., M.V.M., J.W.V.T., A.S., and A.R.K. wrote the first draft of the manuscript. All authors approved the final draft of the manuscript.

About the Author

Dr. Thangaraj is a scientist with the Indian Council of Medical Research–National Institute of Epidemiology in Chennai, India. His primary research interests include the vaccine-preventable disease epidemiology and outbreak investigations of acute encephalitis syndrome.

References

1. Visvesvara GS, Moura H, Schuster FL. Pathogenic and opportunistic free-living amoebae: *Acanthamoeba* spp., *Balamuthia mandrillaris*, *Naegleria fowleri*, and *Sappinia diploidea*. FEMS Immunol Med Microbiol. 2007;50:1–26. https://doi.org/10.1111/j.1574-695X.2007.00232.x
2. Marciano-Cabral F, Cabral GA. The immune response to *Naegleria fowleri* amebae and pathogenesis of infection. FEMS Immunol Med Microbiol. 2007;51:243–59. https://doi.org/10.1111/j.1574-695X.2007.00332.x
3. Centers for Disease Control and Prevention. *Naegleria fowleri* infections. 2025 [cited 2026 Jun 10]. https://www.cdc.gov/naegleria/about/index.html
4. Centers for Disease Control and Prevention. DPDx—free living amebic infections. 2024 [cited 2026 Jun 10]. https://www.cdc.gov/dpdx/freelivingamebic/index.html
5. Carter RF. Description of a *Naegleria* sp. isolated from two cases of primary amoebic meningo-encephalitis, and of the experimental pathological changes induced by it. J Pathol. 1970;100:217–44. https://doi.org/10.1002/path.1711000402
6. Barnett NDP, Kaplan AM, Hopkin RJ, Saubolle MA, Rudinsky MF. Primary amoebic meningoencephalitis with *Naegleria fowleri*: clinical review. Pediatr Neurol. 1996;15:230–4. https://doi.org/10.1016/S0887-8994(96)00173-7
7. Vijayan V, Tristram D, Anilkumar AC. Infections caused by free-living amebas. In: StatPearls. Treasure Island (FL): StatPearls Publishing; 2026 [cited 2026 Jun 10]. http://www.ncbi.nlm.nih.gov/books/NBK430754
8. Cherian A, R J, A study on *Acanthamoeba* keratitis in a tertiary eye care centre, South Kerala, India. Indian J Microbiol Res. 2020;5:66–70. https://doi.org/10.18231/2394-5478.2018.0013
9. Lorenzo-Morales J, Khan NA, Walochnik J. An update on *Acanthamoeba* keratitis: diagnosis, pathogenesis and treatment. Parasite. 2015;22:10. https://doi.org/10.1051/parasite/2015010
10. Khan NA. *Acanthamoeba* invasion of the central nervous system. Int J Parasitol. 2007;37:131–8. https://doi.org/10.1016/j.ijpara.2006.11.010
11. Raju R, Khurana S, Mahadevan A, John DV. Central nervous system infections caused by pathogenic free-living amoebae: an Indian perspective. Trop Biomed. 2022;39:265–80. https://doi.org/10.47665/tb.39.2.017
12. Centers for Disease Control and Prevention. How people get *Naegleria fowleri* infection. 2025 [cited 2026 Jun 10]. https://www.cdc.gov/naegleria/causes/index.html
13. Marciano-Cabral F, Cabral G. *Acanthamoeba* spp. as agents of disease in humans. Clin Microbiol Rev. 2003;16:273–307. https://doi.org/10.1128/CMR.16.2.273-307.2003
14. Siddiqui R, Khan NA. Biology and pathogenesis of *Acanthamoeba*. Parasit Vectors. 2012;5:6. https://doi.org/10.1186/1756-3305-5-6
15. Schuster FL, Visvesvara GS. Free-living amoebae as opportunistic and non-opportunistic pathogens of humans and animals. Int J Parasitol. 2004;34:1001–27. https://doi.org/10.1016/j.ijpara.2004.06.004
16. Government of Kerala Director of Health Services. Amoebic encephalitis: One Health–based action plan and revised technical guidelines. 2024 [cited 2026 Jun 10]. https://dhs.kerala.gov.in/wp-content/uploads/2025/11/Amoebic-Encephalitis_One-Health-based-Action-plan-and-Revised-Technical-Guidelines_November-2024-1.pdf
17. Sankar P, Moorkoth AP, Khurana S, Mohan A, Vadekkandyil S, M SA, et al. Microbiological profile of meningoencephalitis due to pathogenic free-living amoebae: a case series from Kerala, India. Cureus. 2026;18:e103922. https://doi.org/10.7759/cureus.103922
18. Qvarnstrom Y, Visvesvara GS, Sriram R, da Silva AJ. Multiplex real-time PCR assay for simultaneous detection of *Acanthamoeba* spp., *Balamuthia mandrillaris*, and *Naegleria fowleri*. J Clin Microbiol. 2006;44:3589–95. https://doi.org/10.1128/JCM.00875-06
19. Haston JC, O'Laughlin K, Matteson K, Roy S, Qvarnstrom Y, Ali IKM, et al. The epidemiology and clinical features of non-keratitis *Acanthamoeba* infections in the United States, 1956–2020. Open Forum Infect Dis. 2023;10:ofac682. https://doi.org/10.1093/ofid/ofac682
20. Gunawan PI, Idarto A, Saharso D. *Acanthamoeba* infection in a drowning child. Ethiop J Health Sci. 2016;26:289–92. https://doi.org/10.4314/ejhs.v26i3.12
21. Das D, Biswas K, Banerjee K, Bhattacharya B, Roy A, Khurana S, et al. Unfurling a case of encephalitis with *Acanthamoeba* after a near-drowning event. Rare. 2024;2:100035. https://doi.org/10.1016/j.rare.2024.100035
22. Chackacherry G, Jayakumar KV. Conservation and management of Vembanad-Kol Wetland, Kerala. Presented at: National Workshop on Ramsar Designated Wetlands of India; January 21, 2011; Kolkata, India.
23. Islam SKT, Siddhanta S, Mandal A, Ghosh S, Mandal M, Chatterjee SK. *Acanthamoeba* meningoencephalitis: an emerging catastrophe—a case series from a tertiary care hospital in Kolkata, eastern India. Bengal Physician J. 2025; 12:90–5. https://doi.org/10.5005/jp-journals-10070-8086

24. Pramanik S, Dasgupta S, Samui S, Chandra A, Kattady FJ, Makhal M. Acute meningoencephalitis with subdural empyema associated with *Acanthamoeba* in an immunocompetent individual. J R Coll Physicians Edinb. 2025;55:184–7. https://doi.org/10.1177/14782715251342120
25. Haldar SN, Banerjee K, Modak D, Mondal A, Sharma C, Vasireddy T, et al. Case report: a series of three meningoencephalitis cases caused by *Acanthamoeba* spp. from eastern India. Am J Trop Med Hyg. 2024;110:246–9. https://doi.org/10.4269/ajtmh.23-0396
26. Mishra J, Paul D, Chatterjee C, Ray R. Granulomatous amoebic encephalitis in an immunocompetent young female: a rare case with microbiological confirmation and survival. Indian J Case Rep. 2025;11:503–6. https://doi.org/10.32677/ijcr.v11i10.7754
27. Prakash R, Reghukumar A, K R, Johnson J, Nath SR, Narayanankutty S, et al. Acanthamoeba myelopathy mimicking tropical spastic paraparesis in immunocompetent hosts: a case series. Neurol Sci. 2026;47:307. https://doi.org/10.1007/s10072-026-08889-6
28. Das D, Banerjee K, Ghosh S, Datta A, Kattady F, Ray Y, et al. Free living amoeba associated meningoencephalitis: case series from eastern India (P9–10.002). Neurology. 2025;104(Supplement_1):3580. https://doi.org/10.1212/WNL.0000000000211096
29. Haston JC, Serra C, Imada E, Martin E, Ali IKM, Cope JR. *Acanthamoeba* infection and nasal rinsing, United States, 1994–2022. Emerg Infect Dis. 2024;30:783–5. https://doi.org/10.3201/eid3004.231076

Address for correspondence: Manoj Murhekar, ICMR National Institute of Epidemiology, R-127, TNHB, Ayapakkam, Chennai 600077, India; email: mmurhekar@nieicmr.org.in

Improved Case Detection of Fleaborne Typhus by PCR Testing, Los Angeles County, California, USA, 2022–2024

Armine Sanosyan, Zuelma A. Contreras, Van Ngo, Michael K. Brown, Nicole M. Green, Lee A. Borenstein, Jill K. Hacker, Will S. Probert, Alexa C. Quintana, Monica P. Haw, Umme-Aiman Halai

Fleaborne typhus (FBT) is reemerging as a significant cause of febrile illness in Southern California, USA. We performed enhanced testing on low-titer *Rickettsia typhi* antibody–positive specimens from patients with FBT-compatible illness reported in Los Angeles County, California, during 2022–2024. We tested 114 specimens by repeat serology and 113 by real-time PCR; 81 (71%) were PCR-positive, and 95 (83%) had higher antibody titers by repeat serology. Most PCR-positive specimens were collected 8–10 days after illness onset, but some were collected up to 15 days after illness onset. All PCR-positive specimens were *R. typhi*–specific. After additional testing, 113 (99%) suspected cases were reclassified as probable or confirmed FBT cases. Our findings indicate that many low-titer seropositive results represent true infections and that use of minimum serology thresholds for public health investigation underestimates surveillance case counts. Expanding commercial molecular testing capacity will improve clinical FBT diagnosis and enhance surveillance accuracy.

Fleaborne typhus (FBT), also referred to as murine or endemic typhus, is a febrile illness spread by fleas infected with the bacterium *Rickettsia typhi*. Infected fleas are often found on mammalian hosts, including rodents, opossums , dogs, and free-roaming cats (*1*,*2*). FBT became a major public health threat in the United States from the 1930s through the early 1940s; thousands of cases were reported annually. Improvements in sanitation, alongside the use of novel rodenticides and synthetic insecticides like DDT, led to a sharp decline in cases by the 1950s (*3*,*4*). Today, most cases are reported in Hawaii, Texas, and Southern California; in Southern California, the disease is reemerging as a major cause of febrile illness (*5*–*7*). In Los Angeles County (LAC), FBT has increased since 2010; an average of 169 cases were documented per year during 2021–2025, and an all-time high of 220 cases were reported in 2025.

FBT ranges from a mild, self-limited infection to severe or fatal illness. Cases typically manifest with nonspecific symptoms such as fever, myalgia, headache, nausea, vomiting, and, less frequently, a rash (*8*). Severe clinical manifestations are rare but might include complications such as meningoencephalitis, myocarditis, and hemophagocytic lymphohistiocytosis (*9*). Doxycycline is the treatment of choice for FBT and is highly effective (*5*,*10*). Although the overall case-fatality rate for FBT is low (<1% with appropriate doxycycline treatment), fatal outcomes can still occur, especially in patients with delayed care or underlying health conditions (*11*,*12*). In 2022, LAC recorded 3 FBT-associated deaths involving hemophagocytic lymphohistiocytosis, myocarditis, and septic shock in patients with underlying conditions (*11*).

Because FBT manifests with undifferentiated influenza-like symptoms that resemble other illnesses, cases are often overlooked or misdiagnosed by healthcare providers (*13*). Delayed or incorrect diagnosis might postpone necessary treatment, which can increase the risk for complications, prolonged illness, or, in severe cases, death (5). Such diagnostic challenges can also affect public health disease surveillance and understanding of disease effects.

Serologic testing for *R. typhi* by using indirect immunofluorescence antibody (IFA) assay is typical

Author affiliations: Los Angeles County Department of Public Health, Los Angeles, California, USA (A. Sanosyan, Z.A. Contreras, V. Ngo, M.K. Brown, N.M. Green, L.A. Borenstein, U.-A. Halai); California Department of Public Health Center for Laboratory Sciences Viral and Rickettsial Disease Laboratory, Richmond, California, USA (J.K. Hacker, W.S. Probert, A.C. Quintana, M.P. Haw).

DOI: https://doi.org/10.3201/eid3209.260554

for diagnosis (*5*). Serologic testing performed on specimens collected within the first week of symptom onset can be falsely negative because detectable antibodies might not yet be present (*14*). Serologic confirmation of *R. typhi* infection requires paired testing of acute and convalescent specimens (drawn within 2–10 weeks) demonstrating a 4-fold increase in IgG titers. However, most patients do not return for second specimen collection. Real-time PCR testing can provide diagnostic confirmation earlier in the disease, when serologic testing might yield nonreactive or low-titer positive results. PCR is most sensitive when conducted on specimens collected within the first week of symptom onset and before the initiation of doxycycline, especially on whole blood or tissue specimens (*15*). Unfortunately, commercial PCR tests are not widely available for provider use to aid in the clinical diagnosis of FBT (*16*). Newer technologies for FBT diagnosis, such as Karius microbial cell-free DNA testing, provide additional alternatives for early detection, but their use is limited by accessibility and expense (*17*).

In California, FBT is a mandated reportable disease under Title 17, California Code of Regulations, §2500. LAC Department of Public Health (LACDPH) receives all positive *R. typhi* test results for LAC residents through electronic laboratory reporting or direct provider reports. LACDPH uses California Department of Public Health (CDPH) surveillance case definitions to determine if the report should be included in surveillance data to monitor disease burden and trends in LAC (Appendix Table, http://wwwnc.cdc.gov/EID/article/32/9/26-0554-App1.pdf).

Because FBT continues to increase locally, LACDPH implemented an enhanced protocol for additional testing of commercial laboratory low-titer positive *R. typhi* specimens from clinically compatible case reports. Those reports with low-titer positive serologic testing are not routinely investigated because they fall below the minimum laboratory criteria required for probable or confirmed CDPH case classification and are instead classified as suspected cases for internal tracking only. The goal of the enhanced protocol we describe in this article was to assess the extent to which routine investigative procedures missed true FBT cases among suspected cases and to determine the utility of molecular testing in supporting FBT clinical diagnosis and public health surveillance.

Methods

In April 2022, LACDPH initiated an expanded testing protocol of patient specimens with low-titer positive *R. typhi* serology results reported from commercial laboratories. Inclusion criteria for this protocol were patients with low titer results of *R. typhi* IgG (1:64) or IgM (1:64 or 1:128) and symptoms consistent with the CDPH clinical criteria for FBT (Appendix Table). Patients who meet those criteria are considered suspected cases according to the CDPH surveillance definition because they have clinically compatible illness but insufficient laboratory evidence with serum titers below the required threshold values (IgG $\geq$1:128, IgM $\geq$1:256). We excluded low-titer positive specimens from this analysis if patients had a secondary specimen reported to LACDPH that met laboratory criteria for a probable or confirmed case. We requested and reviewed medical records for all patients to ensure that clinical criteria were met. Our study included patients with symptom onset dates during April 2022–December 2024.

LACDPH obtained serum specimens from patients meeting the study inclusion criteria and forwarded them to its public health laboratory (LACPHL) for repeat *Rickettsia* sp. IgG and IgM IFA serologic testing and to the CDPH Viral and Rickettsial Disease Laboratory for *Rickettsia* sp. nucleic acid detection by real-time PCR. During the study period, 3 real-time PCRs were used to test serum specimens because of changes in laboratory testing availability and procedures. We tested 13 specimens received through September 2022 by using a DNA-based pan-*Rickettsia* assay (*18*). During October 2022–April 2023, we tested 30 specimens by using a DNA-based (duplex) assay that targeted a 119-bp repeat region within the gene for surface cell antigen 2 (an autotransporter protein) (*11*). During May 2023–December 2024, we tested 70 specimens by using a triplex real-time reverse transcription PCR targeting regions of the 23S rRNA specific to *R. typhi*, *R. rickettsii*, and the *Rickettsia* genus (*19*). There was 1 sample we could not test. We entered and managed patient clinical and laboratory data by using REDCap (https://project-redcap.org) electronic data capture tools hosted at LACDPH (*20*,*21*). We collected data through medical records abstraction and patient interviews, and we included demographics, hospitalization, pertinent symptoms, blood chemistry results, FBT diagnostic testing, and doxycycline treatment. We conducted descriptive analyses of the study population and testing results by using SAS version 9.4 (SAS Institute Inc., https://www.sas.com). We also compared the study population with cases with high-titer positive specimens that met the CDPH criteria of probable or confirmed cases to assess for any major differences. We conducted significance analysis by using Fisher exact test for group comparisons of categorical variables and Wilcoxon rank sum test for group comparisons of continuous

variables; we considered p≤0.05 significant. Of note, we retrospectively tested all specimens originally tested by the pan-*Rickettsia* DNA assay and the duplex DNA assay with the newer rRNA assay by the CDPH Viral and Rickettsial Disease Laboratory to compare with prior results.

Results

Study Population Characteristics

LACDPH received 157 reports of patients with FBT low-titer positive test results; patients had symptom onset during April 2022–December 2024. We included 114 low-titer positive serum specimens in our study and retested the specimens for laboratory evidence of *R. typhi* infection. We did not include 43 low-titer positive serum specimens because those patients had high-titer positive convalescent serum specimens tested commercially (n = 23) or because specimens could not be obtained (n = 20). During the same period, high-titer positive results from 289 patients were reported to LACDPH (Table 1). We did not find significant demographic differences between low-titer and high-titer positive patients. For patients with low-titer positive results, the median age at diagnosis was 39 years (range 1–81 years). Fifty-three percent of the patients were male (n = 60) and 47% were female (n = 54). Most patients were ethnically Hispanic (61%, n = 69). Most patients were hospitalized (85%, n = 97) with a median stay of 5 days (range 1–23 days). After fever (required criteria), nausea or vomiting (69%, n = 79) and headache (67%, n = 76) were the most reported clinically compatible symptoms. Most patients (91%, n = 104), were treated with doxycycline; 66 patients (63%) were treated before or on the same day of specimen collection. More than half of the low-titer positive specimens in our study were collected 8–10 days after symptom onset (51%, n = 58); median time

Table 1. Demographic and clinical characteristics of patients with possible fleaborne typhus, comparing 114 patients with initial low-titer positive serologic results with 289 patients with initial high-titer positive serologic results, Los Angeles County, California, USA, 2022–2024

Characteristics	Low-titer positive	High-titer positive
Age categories, y		
0–17	18 (16)	37 (13)
18–34	31 (27)	56 (19)
35–44	19 (17)	53 (18)
45–54	18 (16)	53 (18)
≥55	28 (25)	90 (31)
Median age, y (range)	39 (1–81)	44 (2–87)
Sex		
M	60 (53)	177 (61)
F	54 (47)	110 (38)
Other/unknown	0 (0)	2 (0.7)
Race/ethnicity		
Hispanic/Latino	69 (61)	178 (62)
White	24 (21)	59 (21)
Asian	6 (5)	22 (8)
Other/unknown	15 (13)	22 (8)
Hospitalized	97 (85)	253 (88)
No. nights hospitalized, median (range)	5 (1–23)	5 (1–83)
Clinical characteristics		
Fever	114 (100)	289 (100)
Headache	76 (67)	195 (68)
Muscle pain/myalgia	69 (61)	155 (54)
Nausea/vomiting†	79 (69)	158 (55)
Rash†	57 (50)	93 (32)
Hematology results		
Thrombocytopenia, <150,000 platelets/μL†	87 (76)	177 (61)
Elevated ALT or AST, >40 IU/L	105 (96)	280 (98)
Treatment	104 (91)	244 (84)
No. days from specimen collection date to doxycycline treatment initiation, median (range)	0 (–3 to 31)	0 (–15 to 28)
Treated before or on same day of collection date	66 (63)	163 (67)
Treated ≥1 days after collection date	38 (37)	81 (33)
No. days from symptom onset date to specimen collection date†		
≤7	41 (36)	50 (17)
8–10	58 (51)	101 (35)
>10	15 (13)	138 (48)
Median (range)†	8 (0–44)	10 (2–65)

*Values are no. (%) except as indicated.
†p value <0.05 for this variable indicating significance.

from symptom onset to date of specimen collection was 8 days (range 0–44 days). Low-titer positive patients were more likely to exhibit nausea or vomiting, rash, and thrombocytopenia than high-titer positive patients. Patients with low-titer positive results were more likely to be tested within the first week of illness onset than patients with high-titer positive results.

Additional Testing Results

Of the 114 retested specimens, repeat serologic testing on the same specimen at LACPHL resulted in a higher IgM or IgG titer in 106 (93%) of the specimens. Furthermore, 95 (83%) specimens resulted in IgG or IgM titers high enough to meet CDPH laboratory surveillance criteria for a probable case. Of the 113 specimens tested by PCR, 81 (71%) were PCR-positive, 22 (19%) were PCR-negative, and 10 (9%) had a PCR result of unsatisfactory or indeterminate. Specimens are considered inadequate for testing and reported as unsatisfactory if they did not meet required collection, shipping, or storage conditions upon arrival. An indeterminate result is reported when replicate results do not agree, which can occur when the gene target is near the limit of detection for the assay. All PCR-positive results were positive for *R. typhi*; no other *Rickettsia* species were detected. Of the 114 specimens, 113 (99%) came back with serologic testing or PCR results that changed their case classification from suspected to probable (28%, n = 32) or confirmed (71%, n = 81) (Table 2).

PCR Results by Timing of Specimen Collection and Serologic Findings

Among the 81 PCR-positive specimens, 34 (42%) were collected within 7 days of illness onset, 40 (49%) were collected at 8–10 days, and 7 (9%) were collected >10 days after onset. In contrast, among the 22 PCR-negative specimens, 4 (18%) were collected within 7 days of onset, 11 (50%) at 8–10 days, and 7 (32%) >10 days after onset. PCR-positive cases had a median of 8 days (range 1–15 days) and PCR-negative cases a median of 9 days (range 0–44 days) from illness onset to specimen collection. PCR-positive specimens were more likely than PCR-negative specimens to have IgM detected and no IgG detected (59%, n = 48) in the initial laboratory draw, whereas the opposite was observed for PCR-negative specimens (IgM not detected and IgG detected, 55%, n = 12) (Table 3).

Retrospective Testing Results

Forty-three samples were initially tested by using DNA assays. We retested those samples by using the rRNA assay; 40 (93%) samples had concordant results, and 3 (7%) changed from unsatisfactory or indeterminate (n = 2) or negative (n = 1) to *R. typhi* positive.

Discussion

In our study, most (71%) of the initial low-titer positive serology specimens obtained from patients with illness consistent with FBT were PCR-positive for *R. typhi*. That finding highlights the effectiveness of using PCR testing for clinical diagnosis and case detection of FBT. Unfortunately, *Rickettsia* sp. PCR testing has not been widely implemented because of the resources and laboratory expertise required (*14*). In the United States, rickettsial PCR testing remains largely limited to specialized public health laboratories and surveillance activities rather than routine clinical use (*22*).

Of note, most (91%) PCR-positive specimens were collected within 10 days after illness onset, with some positive up to 15 days. Those results suggest that the previously recommended 1-week window for FBT PCR testing might be too restrictive (*15*). Furthermore, our results suggest that rickettsial nucleic acids might persist in the bloodstream for longer than previously recognized, thereby extending the diagnostic window for molecular testing. Expanding the testing window beyond the first week could improve case detection and provide a more accurate understanding of the timing of rickettsial nucleic acid persistence in patients.

All 81 PCR-positive specimens in this study tested positive for *R. typhi* and none for *R. felis*. That finding reinforces a previous conclusion that *R. typhi* is the primary etiologic agent of FBT in California (*6*). Historically, both *R. typhi* and *R. felis* have been considered potential causes of FBT (*3*), including in urban Los Angeles, where both pathogens have been demonstrated to circulate in rat populations and associated fleas (*23*). The absence of *R. felis* in our PCR-positive specimens challenges previous assumptions about the involvement of different rickettsial species in FBT infection (*24*). Recognizing *R. typhi* as the principal agent is critical for interpreting the changing epidemiology of FBT, including increases in case numbers, geographic expansion, and evolving risk factors. Our results demonstrated variability in serologic testing results between commercial and public health laboratories. About 93% of the low-titer positive specimens obtained from commercial laboratories for repeat serologic testing had higher titers at the LACPHL. That result is a known major weakness of serologic testing, and our results align with existing evidence that the reading of IFA slides is prone to subjectivity (*14*). In addition, the

lack of standardized IFA reagents, protocols, and criteria for test interpretation might account for titer variability between laboratories (*25*). In practice, it is not feasible for public health laboratories to repeat serologic testing of all commercial low-titer positive specimens. Obtaining confirmatory convalescent serology specimens is also not practical because many patients will have recovered by the recommended 10–14-day return window and no longer need medical care (*14*) or might face financial barriers preventing them from seeking further care. *Rickettsia* sp. serologic testing is also subject to high cross-reactivity between *Rickettsia* species (*16*). Because FBT manifests as a nonspecific illness, making PCR testing commercially available would enable rapid and accurate diagnosis of FBT and confirmation of *Rickettsia* species.

Nearly all (99%) specimens that were submitted for additional testing returned with results that met CDPH surveillance criteria for a probable or confirmed FBT case. Because of this testing protocol result, LACDPH has added 113 probable or confirmed cases of FBT from April 2022–December 2024 to overall case counts. Suspected cases are typically excluded from surveillance case counts publicly reported by public health jurisdictions. Public health jurisdictions that use a minimum titer to initiate case investigations might overlook those low-titer positive cases, resulting in underreporting of FBT case counts.

Our study demonstrates the importance of keeping IgM test results as part of the laboratory criteria in the FBT surveillance case definition. Studies suggest that *Rickettsia* IgM titers are less reliable and have limited utility compared with IgG titers because they have lower specificity and do not rise much earlier than IgG titers (*14*). Those studies prompted the exclusion of IgM test results from the CDPH and national FBT case definition laboratory criteria in 2025 (*26*). In our study, 48 (87%) of 55 patient specimens that had only IgM and no IgG detected in the initial testing by a commercial laboratory were found to be PCR-positive through public health testing. Those specimens were likely collected earlier in the disease

Table 2. Results of additional testing for initial 114 *Rickettsia typhi* low-titer positive serum specimens, Los Angeles County, California, USA, 2022–2024*

Category	No. (%) specimens
Initial commercial laboratory IFA *R.typhi* IgG titer	
<1:64	58 (51)
1:64	56 (49)
Initial commercial laboratory IFA *R. typhi* IgM titer	
<1:64	21 (18)
1:64	65 (57)
1:128	28 (25)
Repeat *R. typhi* IFA IgG titer	
<1:64	14 (12)
1:64	20 (18)
1:128	35 (31)
1:256	18 (16)
≥1:512	25 (22)
Not done or unspecified	2 (2)
Total with IgG that met laboratory criteria (≥1:128)	78 (68)
Repeat *R. typhi* IFA IgM titer	
<1:64	18 (16)
1:64	6 (5)
1:128	24 (21)
1:256	24 (21)
≥1:512	38 (33)
Not done or unspecified	4 (4)
Total with IgM that met laboratory criteria (≥1:256)	62 (54)
IFA serologic testing results higher upon repeat testing	106 (93)
IFA serologic testing results met laboratory criteria† upon repeat testing	95 (83)
PCR results	
Positive	81 (71)
Negative	22 (19)
Unsatisfactory or indeterminate	10 (9)
Not tested	1 (0.9)
Case classification change	
CDPH suspected to probable	32 (28)
CDPH suspected to confirmed	81 (71)
No change	1 (0.9)

*CDPH, California Department of Public Health; IFA, immunofluorescence assay.
†IgG titer ≥1:128 or IgM titer ≥1:256.

Table 3. PCR results by timing of specimen collection and serologic findings of 103 specimens from patients with suspected *Rickettsia typhi* infection, Los Angeles County, California, USA, 2022–2024*

Characteristics	PCR positive, n = 81	PCR negative, n = 22
No. days from symptom onset date to specimen collection date†		
≤7	34 (42)	4 (18)
8–10	40 (49)	11 (50)
>10	7 (9)	7 (32)
Median (range)†	8 (1–15)	9 (0–44)
Time from specimen collection date to doxycycline treatment start		
Treated before or on same day of collection	49 (64)	11 (65)
Treated ≥1 days after collection date	28 (36)	6 (35)
Initial commercial laboratory *R. typhi* IgG titer†		
<1:64	48 (59)	7 (32)
1:64	33 (41)	15 (68)
Initial commercial laboratory *R. typhi* IgM titer†		
<1:64	6 (7)	12 (55)
1:64	51 (63)	8 (36)
1:128	24 (30)	2 (9)
Initial commercial laboratory *R. typhi* results†		
IgM detected at 1:64 or 1:128 titer, IgG not detected	48 (59)	7 (32)
IgM not detected, IgG detected at 1:64 titer	6 (7)	12 (55)
IgM and IgG detected	27 (33)	3 (14)

*Values are no. (%) except as indicated.
†p value <0.05 for this variable indicating significance.

course before a measurable rise in IgG titers occurred and when PCR testing is most sensitive. Those cases (n = 48) would have been misclassified if IgM testing results were not included in our protocol.

Most (91%) cases in this study were appropriately treated with doxycycline, demonstrating that clinicians are correctly suspecting FBT at the time of treatment initiation and ordering diagnostic testing. Furthermore, 63% of patients received doxycycline before or on the same day of specimen collection, indicating that patients with FBT in the differential diagnosis are being treated empirically before serology results are reported. That treatment pattern is encouraging because of the variability of rickettsial serology testing and aligns with public health messaging on the importance of early doxycycline initiation.

Our study population is representative of our overall FBT cases. The case demographics did not differ from those of high-titer positive cases. However, low-titer positive cases manifested with nausea or vomiting, rash, and thrombocytopenia more often than high-titer positive cases did. Low-titer positive cases were also more likely to be seen earlier in their illness, which might explain the differences in symptoms observed. The presence of those symptoms could lead persons to seek care earlier in the course of illness or clinicians to more readily consider FBT in the differential diagnosis.

Retrospective testing of specimens by using rRNA did not change our conclusion that most low-titer specimens were PCR-positive. The rRNA assay did detect 3 additional PCR-positive specimens that had previously returned unsatisfactory, indeterminate, or negative results by the DNA-based assays. Those results would have changed the classification of 3 cases from probable to confirmed. Those cases could not be reclassified in surveillance data because case investigations are finalized after the completion of each calendar year.

The first limitation of our study was the use of residual serum specimens for PCR testing, rather than whole blood or plasma, which are better suited for molecular detection of *Rickettsia*. Because *Rickettsia* are obligate intracellular organisms, their nucleic acids are more concentrated in cellular components and plasma compared with serum, where clot formation removes most cells and might reduce detectable DNA (*14*,*27*). Although only a small percentage of our specimens tested negative for *Rickettsia* nucleic acids by PCR, some of those results might represent false negatives attributable to the use of serum specimens. Of note, 1 case had both serum and plasma from the same collection date available for testing; in that case, *R. typhi* nucleic acids were detected in the plasma but not the serum, underscoring the effect of specimen type on PCR sensitivity. Second, the true effect of FBT in LAC is likely underestimated, and our findings might not fully represent the extent of disease transmission in the community. The reporting of FBT test results to LACDPH by laboratories and healthcare providers could be incomplete, resulting in possible missed cases. Patients with mild FBT symptoms who might not have sought care, were not tested, or were tested very early in their disease course, when antibody titers were undetectable, were not captured in this analysis. Because

the study was geographically restricted to LAC, the findings might not be representative of the general population of the United States. Third, although LACDPH attempted to obtain all medical records relevant to the patients' illness with FBT, it is possible that some follow-up visits were not captured, resulting in incomplete information on doxycycline treatment. Nonetheless, a high percentage of patients received doxycycline treatment in our study. Fourth, the sample size for subgroup comparisons was relatively small. Some statistical analyses, particularly those comparing PCR-positive and PCR-negative patients, had smaller subgroup sizes, reducing statistical power and increasing the likelihood of random error. Last, not all specimens could be obtained for analysis. Commercial laboratories generally retain specimens for a limited time, and retention times vary across laboratories. Delays in obtaining medical records to confirm that patients met clinical criteria meant that some specimens were discarded before they could be retrieved for study purposes, ultimately reducing the total number of specimens available for this analysis.

In conclusion, we demonstrate that many low-titer seropositive results from patients with clinically compatible illness represent true *R. typhi* infections and highlight the utility of molecular testing in supporting both clinical diagnosis and public health surveillance of FBT. PCR testing identified infections beyond the traditionally recognized 1-week window of PCR positivity and up to 15 days after symptom onset, demonstrating that molecular techniques can help confirm infection even into the second week of illness. Enhanced public health laboratory testing, like that conducted in our study, is effective for accurately classifying cases for comprehensive case surveillance. However, that approach is not sustainable as routine practice and further strains limited public health resources. Wider commercial availability of *Rickettsia* PCR testing and other new technologies could substantially enhance both clinical diagnostic capacity and our understanding of true disease effects. The resurgence of FBT in Los Angeles County and other areas of the United States highlights the importance of reexamining the current diagnostic protocols being used in clinical settings and public health surveillance.

The authors used artificial intelligence tools to assist with some language editing of this manuscript. All content was reviewed and verified by the authors, who take full responsibility for the final manuscript.

About the Author

Ms. Sanosyan is an epidemiologist with the Los Angeles County Department of Public Health specializing in fleaborne typhus and Rocky Mountain spotted fever surveillance. Her work focuses on collecting data, monitoring disease trends, and coordinating public health responses and interventions.

References

1. Azad AF, Radulovic S, Higgins JA, Noden BH, Troyer JM. Flea-borne rickettsioses: ecologic considerations. Emerg Infect Dis. 1997;3:319–27. https://doi.org/10.3201/eid0303.970308
2. Snellgrove AN, Goddard J. Murine typhus: a re-emerging rickettsial zoonotic disease. J Vector Ecol. 2024;50:1–13. https://doi.org/10.52707/1081-1710-50.1-1
3. Anstead GM. History, rats, fleas, and opossums: the ascendency of flea-borne typhus in the United States, 1910–1944. Trop Med Infect Dis. 2020;5:37. https://doi.org/10.3390/tropicalmed5010037
4. Centers for Disease Control and Prevention. Murine typhus historical trends [cited 2026 Mar 26]. https://www.cdc.gov/typhus/data-research/facts-stats
5. Blanton LS. Murine typhus: a review of a reemerging flea-borne rickettsiosis with potential for neurologic manifestations and sequelae. Infect Dis Rep. 2023;15:700–16. https://doi.org/10.3390/idr15060063
6. Probert WS, Quintana AC, Kjemtrup AM, Hacker JK. Duplex reverse-transcription real-time PCR assay for detection of flea-borne rickettsioses. Am J Trop Med Hyg. 2024;111:569–74. https://doi.org/10.4269/ajtmh.23-0884
7. Yomogida K, Kjemtrup A, Martínez-López B, Ibrahim M, Contreras Z, Ngo V, et al. Surveillance of flea-borne typhus in California, 2011–2019. Am J Trop Med Hyg. 2023;110:142–9. https://doi.org/10.4269/ajtmh.23-0272
8. Centers for Disease Control and Prevention. About murine typhus [cited 2026 Mar 26]. https://www.cdc.gov/typhus/about/murine
9. Centers for Disease Control and Prevention. Murine typhus: clinical presentation, diagnosis, and treatment [cited 2026 Mar 26]. https://www.cdc.gov/coca/hcp/trainings/murine-typhus
10. Caravedo Martinez MA, Ramírez-Hernández A, Blanton LS. Manifestations and management of flea-borne rickettsioses. Res Rep Trop Med. 2021;12:1–14. https://doi.org/10.2147/RRTM.S274724
11. Alarcón J, Sanosyan A, Contreras ZA, Ngo VP, Carpenter A, Hacker JK, et al. Fleaborne typhus–associated deaths—Los Angeles County, California, 2022. MMWR Morb Mortal Wkly Rep. 2023;72:838–43. https://doi.org/10.15585/mmwr.mm7231a1
12. Pieracci EG, Evert N, Drexler NA, Mayes B, Vilcins I, Huang P, et al. Fatal flea-borne typhus in Texas: a retrospective case series, 1985–2015. Am J Trop Med Hyg. 2017;96:1088–93. https://doi.org/10.4269/ajtmh.16-0465
13. Blanton LS, Paddock CD. Murine typhus—a horse in zebra's clothing. Am J Med. 2025;138:1487–9. https://doi.org/10.1016/j.amjmed.2025.06.005
14. Stewart AG, Stewart AGA. An update on the laboratory diagnosis of *Rickettsia* spp. infection. Pathogens. 2021;10:1319. https://doi.org/10.3390/pathogens10101319
15. Centers for Disease Control and Prevention. Clinical overview of murine typhus [cited 2026 Mar 26].

https://www.cdc.gov/typhus/hcp/clinical-overview/clinical-overview-of-murine-typhus
16. Theunissen C, Cnops L, Van Esbroeck M, Huits R, Bottieau E. Acute-phase diagnosis of murine and scrub typhus by PCR: a case report. BMC Infect Dis. 2017;17:273. https://doi.org/10.1186/s12879-017-2385-x
17. Jung S, Torriani F, Abeles S, Kline A. A cell-free DNA plasma next-generation sequencing test—is it worth the cost? Pathogens. 2025;14:811. https://doi.org/10.3390/pathogens14080811
18. Kato CY, Chung IH, Robinson LK, Austin AL, Dasch GA, Massung RF. Assessment of real-time PCR assay for detection of *Rickettsia* spp. and *Rickettsia rickettsii* in banked clinical samples. J Clin Microbiol. 2013;51:314–7. https://doi.org/10.1128/JCM.01723-12
19. Probert WS, Haw MP, Nichol AC, Glaser CA, Park SY, Campbell LE, et al. Newly recognized spotted fever group *Rickettsia* as cause of severe Rocky Mountain spotted fever–like illness, northern California, USA. Emerg Infect Dis. 2024;30:1344–51. https://doi.org/10.3201/eid3007.231771
20. Harris PA, Taylor R, Thielke R, Payne J, Gonzalez N, Conde JG. Research electronic data capture (REDCap)—a metadata-driven methodology and workflow process for providing translational research informatics support. J Biomed Inform. 2009;42:377–81. https://doi.org/10.1016/j.jbi.2008.08.010
21. Harris PA, Taylor R, Minor BL, Elliott V, Fernandez M, O'Neal L, et al.; The REDCap consortium. building an international community of software partners. J Biomed Inform. 2019;95:103208. https://doi.org/10.1016/j.jbi.2019.103208
22. Chapman AS, Bakken JS, Folk SM, Paddock CD, Bloch KC, Krusell A, et al.; Tickborne Rickettsial Diseases Working Group; CDC. Diagnosis and management of tickborne rickettsial diseases: Rocky Mountain spotted fever, ehrlichioses, and anaplasmosis—United States: a practical guide for physicians and other health-care and public health professionals. MMWR Recomm Rep. 2006;55(RR-4):1–27.
23. Abramowicz KF, Rood MP, Krueger L, Eremeeva ME. Urban focus of *Rickettsia typhi* and *Rickettsia felis* in Los Angeles, California. Vector Borne Zoonotic Dis. 2011;11:979–84. https://doi.org/10.1089/vbz.2010.0117
24. Eremeeva ME, Karpathy SE, Krueger L, Hayes EK, Williams AM, Zaldivar Y, et al. Two pathogens and one disease: detection and identification of flea-borne rickettsiae in areas endemic for murine typhus in California. J Med Entomol. 2012;49:1485–94. https://doi.org/10.1603/ME11291
25. Dhawan S, Robinson MT, Stenos J, Graves SR, Wangrangsimakul T, Newton PN, et al. Selection of diagnostic cutoffs for murine typhus IgM and IgG immunofluorescence assay: a systematic review. Am J Trop Med Hyg. 2020;103:55–63. https://doi.org/10.4269/ajtmh.19-0818
26. Council of State and Territorial Epidemiologists. Standardized surveillance case definition for flea-borne typhus [cited 2026 Mar 26]. https:// www.cste.org/resource/resmgr/position_statements_files_2023/ps_updates/25-ID-05_Flea-borne_Typhus.pdf
27. Eremeeva ME, Dasch GA. Challenges of rickettsial diagnosis: PCR-based detection in blood and tissue samples. In: Rickettsiales: biology, molecular biology, epidemiology, and vaccine development. New York: Springer; 2015. p. 239–66.

Address for correspondence: Zuelma Contreras, Los Angeles County Department of Public Health, 313 N Figueroa St, Rm 222, Los Angeles, CA 90012, USA; email: zcontreras@ph.lacounty.gov

Posttuberculosis Consequences on Tuberculosis Prevention Effectiveness and Cost-effectiveness among New Immigrants, Canada

Aotikuer Ainiwaer, Aashna Uppal, Kevin Schwartzman, Kamila Romanowski, Sarah K. Brode, James C. Johnston, Jonathon R. Campbell

Cost-effectiveness analyses of tuberculosis (TB) preventive treatment rarely consider long-term TB consequences. We examined how long-term TB consequences influence the effectiveness and cost-effectiveness of TB prevention among persons who immigrate to Canada. By using a Markov microsimulation model of 400,000 persons immigrating to Canada in 2025, we compared current postarrival TB infection screening levels (0.5%) with a screening level of 68% among new immigrants. Modelling scenarios included acute TB consequences and long-term TB-related death, illness, and healthcare costs (25-year horizon, 1.5% discount rate). Including long-term TB-related consequences increased the estimated TB-related quality-adjusted life years (QALYs) lost by 2.1-fold (95% uncertainty range 1.7–2.5-fold). When long-term TB-related consequences were included, estimated QALYs gained from expanded screening increased 2.4-fold (95% uncertainty range 1.6–4.4-fold), reducing the cost per QALY from $235,088 to $100,742 CAD. Ignoring long-term TB consequences substantially underestimates the effectiveness and cost-effectiveness of preventive interventions; such consequences should be incorporated into future evaluations.

Tuberculosis (TB) is the world's leading cause of death from a single infectious agent, killing an estimated 1.23 million persons worldwide in 2024 (*1*). Shifts in global migration patterns have changed the epidemiologic landscape for TB in low-incidence regions, and migrant populations bear disproportionately high TB effects (*2*). In migrant populations, most TB disease occurs from the progression of TB infection acquired before immigration (*3*). Therefore, providing TB preventive treatment (TPT) to persons who recently immigrated should be considered among other TB elimination strategies (*4*). However, results of cost-effectiveness analyses evaluating systematic screening and treatment for TB infection among persons who recently immigrated to low-incidence settings have been mixed (*5*,*6*), and the implementation of such programs is rare (*7*). Also, there is substantial variability in how existing studies consider the risks and consequences of TB disease and TPT (*8*). Nearly all studies only consider the acute consequences (disease and death) of TB during the treatment period, omitting the long-term illness and death associated with post-TB consequences (*9*). However, emerging research has highlighted that healthcare utilization spikes in the years after TB treatment (*10*), and TB survivors are at substantially higher risk for illness and death compared with those who never had TB (*11*,*12*).

Failure to account for the long-term consequences of TB disease might underestimate the quality-adjusted life years (QALYs) gained and cost-effectiveness of TB infection screening and TPT. A global analysis of disability-adjusted life years associated with TB suggests post-TB consequences account for half of the total TB-related health issues (*9*). Similarly, an analysis of a hypothetical preventive intervention in high-incidence, low-middle-income settings found considering

Author affiliations: McGill University, Montreal, Quebec, Canada (A. Ainiwaer, K. Schwartzman, J.R. Campbell); University of Oxford, Oxford, UK (A. Uppal); Research Institute of the McGill University Health Centre, Montreal (K. Schwartzman, J.R. Campbell); McGill International TB Centre, Montreal (K. Schwartzman, J.R. Campbell); University of British Columbia, Vancouver, British Columbia, Canada (K. Romanowski, J.C. Johnston); British Columbia Centre for Disease Control, Vancouver (K. Romanowski, J.C. Johnston); University of Toronto, Toronto, Ontario, Canada (S.K. Brode); University Health Network, Toronto (S.K. Brode)

DOI: https://doi.org/10.3201/eid3209.260473

post-TB consequences substantially reduced estimated incremental cost-effectiveness ratios (ICERs) (*13*). However, those analyses were only illustrative and focused primarily on low-middle-income settings. Understanding how post-TB consequences might inform public health decisions in a low-incidence, high-income setting would be useful.

We conducted a modeling analysis to evaluate how post-TB consequences might affect effectiveness and cost-effectiveness of TB prevention among persons who recently immigrated to Canada. We model how incorporating post-TB health consequences affects QALYs lost because of TB and the cost-effectiveness of TB prevention programs under different assumptions.

Methods

Setting and Model Overview

Canada is a low TB incidence country, reporting 2,508 persons with TB disease in 2024, corresponding to an incidence of 6.1/100,000 population (*14*). Overall, 83% of all persons with TB in Canada were born outside the country; most of those persons are now permanent residents and citizens of Canada (*15*). Currently, the Canada immigration medical exam focuses on detection of TB disease before entry into Canada. No provincial or territorial programs provide systematic screening and treatment for TB infection for all recently immigrated persons (*16*), and only 0.5% of persons with clinical risk factors for TB receive screening (*17*).

Because of that context, we developed a microsimulation model to evaluate the costs, effectiveness, and cost-effectiveness of a systematic postarrival TB infection screening program in persons who recently and permanently migrated to Canada. We adapted a Markov microsimulation model by using TreeAge Pro Healthcare 2025 (TreeAge Software, LLC, https://www.treeage.com) (A. Uppal et al., unpub. data). Canada immigration targets for 2025 were 395,000 persons (*18*). We rounded that target to 400,000 persons and simulated a hypothetical cohort structured according to the age and country of origin of new permanent residents of Canada in 2024 (*19*). We used a previous modeling study to estimate the prevalence of TB infection among persons who recently immigrated to Canada, according to age and TB incidence in country of origin (Appendix Table 1, http://wwwnc.cdc.gov/EID/article/32/9/26-0473-App1.pdf). We estimated the risk for progression to TB disease by using the Public Health Agency of Canada data detailing time to development of TB disease after immigration (Appendix) (*15*).

The model compares the existing level of TB infection screening and treatment among persons who recently immigrated to Canada (status quo) with a scaled-up TB infection screening and treatment program (intervention). In the intervention strategy, all new permanent residents whose country of origin has an annual TB incidence of ≥50/100,000 persons would be asked to participate in TB infection screening after arrival in Canada. If the person tested positive for TB infection, they would be given TPT. We assumed 68% of persons would comply with the request on the basis of adherence evidence from other postarrival follow-up activities among immigrants (*20*). In both status quo and intervention strategies, the tuberculin skin test is used for screening, and 4 months of daily rifampin is the TPT regimen (*21*). A simplified model structure, including health states, is provided (Appendix Figure 1).

The primary outcomes were QALYs, TB episodes, TB deaths, and TB-related costs accrued over the 25-year time horizon for both strategies. We took a TB services perspective for this analysis. All outcomes were discounted at a rate of 1.5% per annum, in line with recommendations from Canada (*22*).

Model Parameters

Whenever possible, we used systematic reviews and, if unavailable, high quality randomized trials and data from Canada to source all model parameters and set their distributions for probabilistic analysis (Table 1; Appendix Table 2). Most costs associated with TB came from a pan-Canada costing study (*23*). All cost parameters are expressed in 2023 Canadian dollars; we used consumer price indices to inflate costs to this year.

We parameterized QALYs lost during acute TB consequences by using an estimated annualized loss of 0.057 (excluding death) (*24*) and age-specific risk for death during acute TB by using surveillance data from Canada (*15*). We categorized post-TB consequences as increased risk for death after successful TB treatment, persistent illness because of long-term disability, and excess healthcare costs after TB (*11*). We assumed the risk for death after TB treatment was 69% (95% CI 50%–91%) higher than among age-matched persons without a history of TB disease (*25*) and that the increased risk persisted for life. We parameterized background risk of death from TB according to lifetables from Canada (*26*). In addition, we permanently reduced all TB survivors' health utility by 1.8% (95% CI 0%–4.4%) (*28*). Finally, we estimated TB

survivors would have excess healthcare costs of $3,383 (95% CI $1,934–$5,231) over 5 years after successful TB treatment (*10*), evenly distributed across each of the 5 years. We modeled each of those 3 post-TB consequences separately and together.

Analysis

Our Markov microsimulation model sampled from the associated distribution of each parameter 2,000 times to generate 2,000 parameter sets. For each parameter set, we simulated 400,000 persons and then

Table 1. Key model inputs for immigration TB infection screening and treatment of permanent residents in study of post-TB consequences on TB prevention and cost-effectiveness among new immigrants, Canada*

Parameter	Base-case estimate	PSA distribution (range)
Health utilities		
Health utility: healthy or TB infection	0.81	Beta (0.69–0.91)
Annual absolute QALY loss because of TB adverse event†	0.0077	PERT (0.000–0.0096)
Annual absolute QALY loss associated with TB disease‡	0.057	PERT (0.033–0.100)
Annual relative utility decrement because of post-TB illness	0.018	PERT (0.000–0.044)§
Costs, 2023 CAD		
TST screening	$38	Gamma ($22–$59)
Medical evaluation before TPT	$237	Gamma ($136–$367)
Complete TPT, 4R	$515	Gamma ($163–$1,066)
Incomplete TPT, 4R	$234	Gamma ($21–$687)
Contact investigation¶	$5,429	Gamma ($3,147–$8,266)
Complete TB disease treatment	$21,897	Gamma ($3,260–$57,909)
Incomplete TB disease treatment	$18,495	Gamma ($13,815–$31,810)
TB-related death	$30,562	Gamma ($8,432–$66,681)
Post-TB healthcare, 5 years	$3,383	Gamma ($1,934–$5,231)
Model probabilities and transition parameters		
TST sensitivity	0.78	Beta (0.74–0.82)
TST specificity	0.94	Beta (0.80–1.00)
Proportion of population with TB infection	Country- and age-specific#	PERT
TB infection screening uptake, status quo	0.005	Beta (0.003–0.010)
TB infection screening uptake, intervention	0.68	Beta (0.64–0.72)
Returning for TST reading	0.94	Beta (0.90–0.98)
Initiating TPT	0.88	Beta (0.80–0.94)
Completing TPT, 4R	0.73	Beta (0.65–0.81)
Effectiveness of complete TPT	0.90	Beta (0.63–1.00)
Annual progression from TB infection to active TB per 1,000 person-years	0.85	lognormal (0.75–1.0)
Serious adverse event with TPT, 4R, <50 y	0.0068	PERT (0.0039–0.0097)
Serious adverse event with TPT, 4R, ≥50 y	0.013	PERT (0.005–0.021)
Death during TPT, 4R	0.00002	Beta (0.00000–0.000074)
Recurrence after TB treatment, annual probability during first 2 y	0.015	Triangular (0.0075–0.025)
Death hazard ratio after TB treatment	1.69	PERT (1.50–1.91)
TB-related case fatality probability, age group, y		
0–14	0.009	Fixed
15–24	0.004	Fixed
25–64	0.014	Fixed
≥65	0.056	Fixed
Proportions of persons who immigrate to Canada**		
Age group, y**		
0–14	0.288	Fixed
15–34	0.385	Fixed
35–54	0.291	Fixed
55–74	0.036	Fixed
≥75	0.001	Fixed
TB incidence in country of origin, cases/100,000 persons		
0–9	0.151	Fixed
10–49	0.186	Fixed
50–99	0.215	Fixed
100–199	0.241	Fixed
≥200	0.208	Fixed

*4R, 4 mo of rifampin; PERT, project evaluation and review technique; PSA, probabilistic sensitivity analysis; QALY, quality-adjusted life years; TB, tuberculosis; TPT, TB preventive treatment; TST, tuberculin skin test; UR, uncertainty range.
†Utility decrement of 0.2 for 2 weeks.
‡Health utility decrement of 0.17 for 4 mo.
§From Nicolas Menzies (see Acknowledgments); in the communication the post-TB disability weight used for Canada was 0.018 (0.005–0.044). We further reduced the lower bound of the uncertainty interval from 0.005 to 0 to enable evaluation of no disease occurrence.
¶Cost includes nurse time for a contact investigation involving 4 contacts ($3,630) plus costs of evaluation, diagnosis, and treatment for TB infection and disease among contacts, under the assumption all were evaluated for TB disease and infection with 3% having disease and 33% having infection.
#Appendix Table 1, https://wwwnc.cdc.gov/EID/article/32/9/26-0473-App1.pdf.
**Numbers might not sum to 1 because of rounding.

estimated mean outcomes and 95% uncertainty ranges by using the 2.5th and 97.5th percentiles.

We projected outcomes for 5 scenarios. Each scenario included acute TB consequences: no post-TB consequences, post-TB death only, post-TB illness only, excess post-TB healthcare costs only, and all 3 post-TB consequences.

To estimate the effect of post-TB consequences on the estimated QALYs lost because of TB, we quantified QALYs lost because of TB under the status quo for each post-TB scenario. Next, we calculated incremental costs, QALYs, TB episodes, and TB deaths for the intervention strategy compared with the status quo for each scenario. We calculated the incremental cost per QALY gained and estimated the proportion of simulations where ICERs fell below several willingness-to-pay thresholds (WTP) per QALY, including $50,000, $100,000, and $150,000.

To further understand the relative importance of post-TB consequences to outcomes of cost-effectiveness, we performed a partial rank correlation coefficient (PRCC) analysis examining the different model parameters. For that analysis, the outcome was the incremental net monetary benefit (iNMB) of the intervention compared with the status quo for the scenario where all 3 post-TB consequences are considered, calculated by using a WTP threshold of $100,000 per QALY. We calculated the iNMB by multiplying the incremental QALYs by the WTP and subtracting the incremental intervention costs.

To assess sensitivity of results to post-TB consequence parameters, we selected the 200 simulations with the lowest (0–10th percentile) and highest (90th–100th percentile) values for each parameter (increased disease, death, and healthcare costs). For each of those simulation sets, we estimated incremental outcomes, the ICER, and the proportion with ICERs below a WTP of $100,000 per QALY.

We performed 5 sets of scenario analyses. First, we increased our estimates of the QALYs lost because of the acute consequences of TB to 0.11 (parameterized with a minimum value of 0.03 and maximum of 0.2) (*27*). Second, in place of a tuberculin skin test, we modeled the use of an interferon-γ release assay, which had identical sensitivity but improved specificity (*28*), 100% test completion, and higher cost ($59) (*23*). We parameterized specificity by using a β distribution ($\alpha = 90$ and $\beta = 4$) and the cost with a gamma distribution (shape = 60 and scale = 0.98). Third, we changed the annual discount rate to 0% and 3% (*22*). Fourth, we made our post-TB death parameter more conservative (9% increase, 95% uncertainty range [UR] 2%–17%), which we approximated on the basis of excess death expected from reduced lung function after TB (*9*). Fifth, we evaluated the effect of a lower rate of TB progression (0.75 [95% UR 0.6–0.9]/1,000 person years) on outcomes (*29*).

Results

Under the status quo and considering only acute TB consequences, we projected 927 (95% UR 764–1,123) persons to develop TB and 30 (95% UR 24–36) to die from TB; we projected 312 (95% UR 241–386) QALYs lost. We projected TB-related health system expenditures to total $25.3 million (95% UR $7.6–$61.9 million) over the 25-year time horizon (Table 2; Appendix Table 3). Inclusion of post-TB death increased the estimated number of QALYs lost because of TB 1.6-fold (95% UR 1.4–1.7-fold), representing a 60% increase compared with acute TB consequences only. Similarly, inclusion of post-TB illness increased the estimated number of QALYs lost because of TB by 1.5-fold (95% UR 1.2–2.0-fold). Although including excess healthcare costs post-TB did not affect QALYs lost, it increased estimated TB-related health system expenditures to $27.6 million (95% UR $9.7–$64.5 million). When all post-TB consequences were included, TB was projected to result in 657 (95% UR 479–876) QALYs lost, a 2.1-fold (95% UR 1.7–2.5-fold) increase compared with estimates excluding post-TB consequences (Table 2; Appendix Table 3). This result suggests post-TB consequences accounted for 52% (95% UR 41%–60%) of QALYs lost because of TB.

Across all scenarios, a postarrival TB infection screening intervention was estimated to result in QALY gains, increased costs, and reduced TB episodes and deaths (Table 3). Compared with a scenario including only acute TB consequences, including post-TB death resulted in a slightly greater increase in estimated incremental QALYs gained by the intervention than including post-TB illness. When all 3 post-TB consequences were incorporated, estimated QALY gains increased by 2.4-fold (95% UR 1.6–4.4-fold), estimated TB deaths averted increased by 2.2-fold (95% UR 1.6–3.0-fold), and incremental costs were projected to be 4% (95% UR 1%–13%) lower compared with the exclusion of post-TB consequences.

When only acute consequences of TB were included, the estimated ICER of a postarrival TB infection screening intervention was $235,088 per QALY gained, compared with the status quo. When all 3 post-TB consequences were included, the ICER was reduced to $100,742. In that scenario, 53% of simulations had an ICER below a WTP threshold of $100,000,

Table 2. Total quality adjusted life years lost because of TB when considering acute and long-term consequences in the status quo scenario in study of post-TB consequences on TB prevention and cost-effectiveness among new immigrants, Canada*

QALY loss	Acute TB consequences only, referent	Post-TB elevated risk for death	Post-TB persistent disease	Elevated risk for death and persistent disease
Absolute QALY loss because of TB	312 (241–386)	491 (375–619)	482 (338–665)	657 (479–876)
Relative QALY loss because of TB compared with no post-TB consequences	1.0	1.6 (1.4–1.7)	1.5 (1.2–2.0)	2.1 (1.7–2.5)

*Values are no. (95% uncertainty range). TB, tuberculosis; QALY, quality adjusted life year.

compared with only 8% when only acute consequences were included (Table 3; Appendix Figure 2).

When all post-TB consequences are included, the PRCC analysis showed that post-TB illness and death were positively correlated with iNMB, although excess post-TB healthcare costs were not (Figure). TB infection test specificity, cost of TB disease treatment, TPT effectiveness, annual TB progression rates, and health disutility from post-TB illness were the 5 parameters most positively correlated with iNMB. Post-TB death was the 11th most positively correlated parameter with iNMB. Similarly, we found estimates of effectiveness and cost-effectiveness of postarrival TB infection screening were most sensitive to the disutility associated with post-TB illness and minimally sensitive to post-TB death and excess post-TB healthcare costs (Appendix Table 4).

Estimates of the relative contribution of post-TB consequences to QALYs lost because of TB disease were inversely correlated to the acute consequences of TB (Appendix Table 5), but overall ICERs were more favorable when post-TB consequences were included (Appendix Table 6). Substitution of an interferon-γ release assay for the tuberculin skin test did not substantially affect estimated ICERs (Appendix Table 7) because specificity gains were offset by increased costs. Relative increases in QALYs gained after incorporating post-TB consequences and PRCC estimates were largely unchanged across discount rates (Appendix Tables 8, 9, Figures 3, 4). Unsurprisingly, ICERs were more favorable with no discounting and more unfavorable with 3% discounting. When all post-TB consequences were included, the estimated ICER was $71,714 per QALY gained, and 76% of simulations were <$100,000 per QALY gained with no discounting, whereas the corresponding outcomes with 3% discounting were $137,407 and 27%.

A more conservative parameterization of post-TB death substantially reduced the effect on QALYs lost because of TB and QALYs gained by a screening program. With a more conservative parameterization (9% vs. 69%), including post-TB death only increased the number of QALYs lost because of TB by 5% (95% UR 2%–9%). As a result, overall post-TB consequences accounted for a smaller proportion of QALYs lost because of TB than our base analysis at 44% (95% UR 23%–64%). In addition, the more conservative post-TB death risk reduced its influence on QALYs gained through the screening program and on the ICER (Appendix Tables 10, 11). Reducing the TB progression rate did not affect long-term TB consequence effect on QALYs gained through a screening program, but it

Table 3. Effects of post-TB consequences on incremental outcomes between intervention and status quo in study of post-TB consequences on TB prevention and cost-effectiveness among new immigrants, Canada*

Incremental outcomes between status quo and intervention	Acute TB consequences only, referent	Post-TB elevated risk for death	Post-TB persistent disease	Post-TB healthcare costs	All post-TB consequences
Absolute incremental cost, millions, 2023 CAD	19.4 (4.1–38.0)	19.4 (4.1–38.0)	19.4 (4.1–38.0)	18.7 (3.3–37.3)	18.7 (3.3–37.3)
Relative incremental cost compared with no post-TB consequences	1.0	1.0	1.0	0.96 (0.87–0.99)	0.96 (0.87–0.99)
Absolute incremental QALY	82 (28–124)	138 (76–198)	131 (65–200)	82 (28–124)	186 (109–267)
Relative incremental QALY ratio compared with no post-TB consequences	1.0	1.7 (1.3–3.0)	1.7 (1.2–2.7)	1.0	2.4 (1.6–4.4)
Absolute incremental TB-related deaths	−12 (−15 to −7)	−25 (−33 to −18)	−12 (−15 to −7)	−12 (−15 to −7)	−25 (−33 to −18)
Relative incremental TB deaths ratio compared with no post-TB consequences	1.0	2.2 (1.6–3.0)	1.0	1.0	2.2 (1.6–3.0)
ICER	$235,088	$140,146	$147,595	$227,340	$100,742
<$50,000, %	3	5	5	3	11
<$100,000, %	8	27	25	9	53
<$150,000, %	21	59	54	24	81

*Incremental outcomes refer to the difference between intervention and status quo per 400,000 persons. Values are (95% uncertainty range). ICER, incremental cost-effectiveness ratios; QALY, quality adjusted life year; TB, tuberculosis.

did reduce the estimated cost-effectiveness (Appendix Tables 12, 13).

Discussion

We found excluding post-TB consequences of illness, death, and excess healthcare costs can lead to substantially undervaluing TB prevention strategies in a low-incidence, high-income setting like Canada. Post-TB consequences account for a large fraction of QALYs lost because of TB. Including post-TB consequences in our analysis of a post-arrival TB infection screening and preventive treatment intervention among persons immigrating to Canada more than doubled the estimated QALYs gained and reduced the estimated ICER by >50%.

One of the most studied use cases for TB infection screening and preventive treatment in low-incidence countries is among persons who recently immigrated (*4*,*30*,*31*). Yet, the literature on that topic is largely divided when it comes to cost-effectiveness (*8*). Most of the literature evaluating cost-effectiveness has not incorporated post-TB consequences. A recent systematic review (*8*) found only 3 (*32*–*34*) of 14 included studies evaluating postarrival TB infection screening in immigrants considered post-TB consequences. None of those 3 studies considered increased healthcare cost, and only 1 study (*34*) considered elevated risk for death after TB. Although all 3 studies considered persistent illness after TB, its inclusion was highly variable across studies, which is unsurprising because of the paucity of prospective cohort data estimating health utility decrements associated with post-TB illness. Improving our understanding of the long-term effect of TB on health utility should be a priority, considering our finding that the cost-effectiveness estimates for TB prevention were sensitive to post-TB illness parameterization.

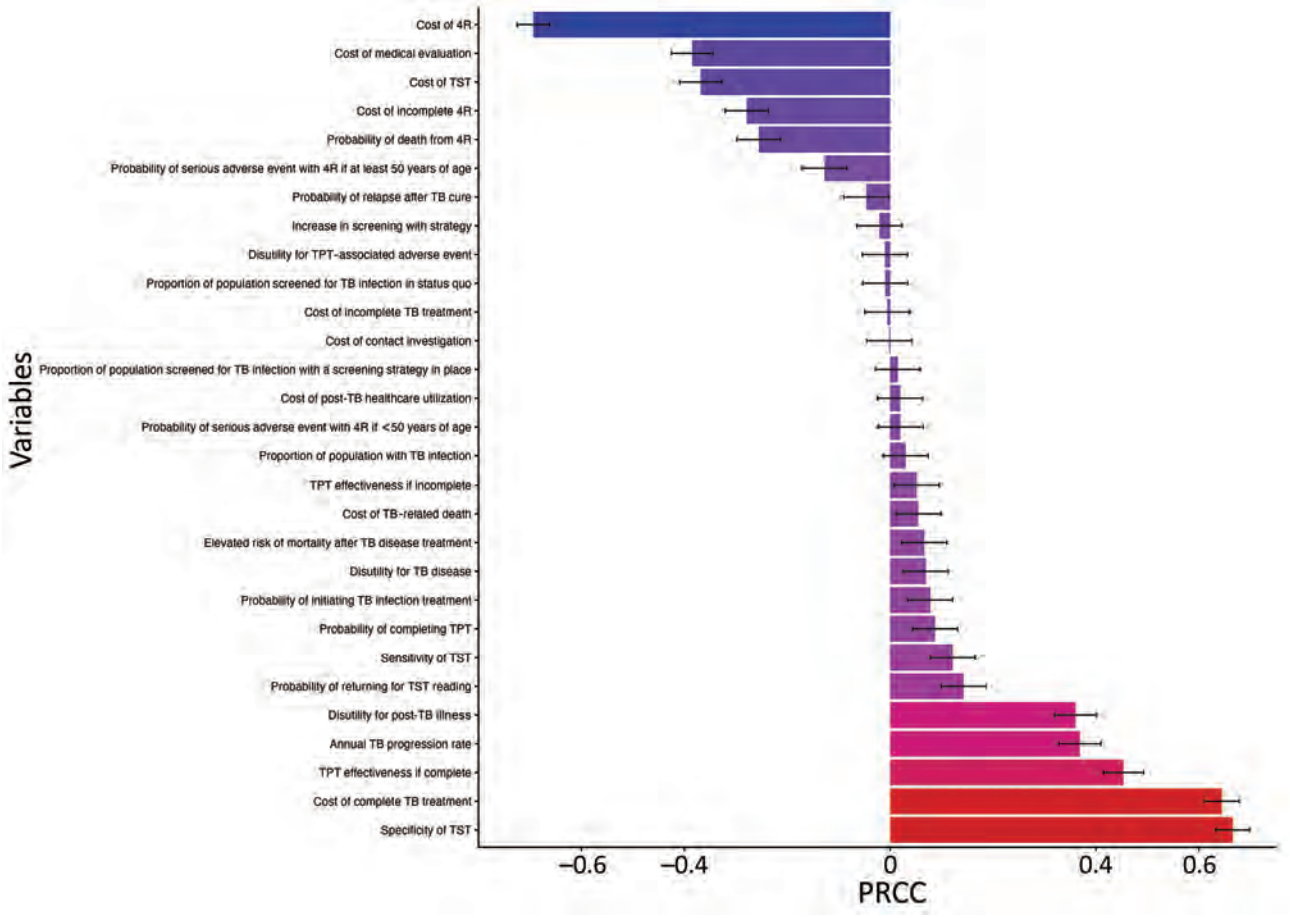

Figure. PRCC for incremental net monetary benefit as drivers of cost-effectiveness of tuberculosis prevention among immigrants, Canada. Incremental net monetary benefit refers to the difference in net monetary benefit between the intervention and the status quo. In this analysis, parameters with more extreme positive PRCC estimates improve the incremental net monetary benefit as they increase. Parameters with more extreme negative PRCC estimates worsen the incremental net monetary benefit as they increase. Error bars indicate 95% uncertainty range. 4R, 4 months of rifampin treatment; PRCC, partial rank correlation coefficient; TB, tuberculosis; TPT, tuberculosis preventive treatment; TST, tuberculin skin test.

A global analysis of the health burden of incident TB estimated that 47% (95% UR 37%–57%) of TB-related disability-adjusted life years were attributed to post-TB illness and death (*9*). In our study, post-TB consequences accounted for 52% (95% UR 41%–60%) of TB-related QALYs lost. Our higher estimate might reflect a lower number of deaths and lower health disutility during the acute phase of TB in Canada but higher estimated post-TB death. When we used a conservative estimate of post-TB death, like the previous global study, our estimated contribution was only 44% (95% UR 23%–64%).

By neglecting the contribution of post-TB consequences on health disutility, most literature to date has likely undervalued the potential benefits of TB prevention strategies. Because ICERs for TB prevention among recent immigrants are typically above common WTP thresholds (*30*,*31*), reductions in the ICER might have meaningful policy implications. Also, ensuring that cost-effectiveness is accurately and comprehensively measured is necessary for policymakers seeking to prioritize scarce healthcare funds.

The first major strength of our study is that we parameterized post-TB consequences in our analysis by using high-quality data from Canada or from other published literature, with appropriate consideration of uncertainty. Second, we leveraged a common use case for our analysis, with our model structured to capture necessary elements of the care cascade and TB natural history. Finally, we also evaluated several implications of ignoring post-TB consequences relevant to both researchers and decision-makers.

The first limitation of our study is that we did not model secondary TB transmission beyond the cost of routine contact investigations. Including future TB cases resulting from secondary transmission would likely improve the estimated cost-effectiveness of the intervention. Second, we assumed that the observed increases in death, disease, and healthcare costs after TB were attributable to TB only and therefore preventable through TPT. Although we carefully adjusted the analyses of our underlying parameterization of those estimates, it is not possible to determine if TB was the only cause of those outcomes (*35*), and there might have been residual confounding factors. Third, we parameterized the elevated risk for illness and death post-TB to be lifelong. Our estimate of post-TB death risk was derived from a population-based study of permanent residents of British Columbia with a mean follow-up of 13 years. The elevated death risk persisted throughout the study period, suggesting it might be long-term. However, data on post-TB illness are less certain. Post-TB respiratory disease is heterogeneous (*35*), and some data suggest that the increase in post-TB respiratory disease might dissipate over time (*36*). However, post-TB illness is not limited to the respiratory system, and nonrespiratory disease might be substantial (*37*,*38*). Those 2 considerations might lead to inaccurately assessing the effect of post-TB illness. Finally, we only considered health system costs related to TB. We did not include costs incurred by patients and caregivers during or after treatment. No comprehensive data on those costs are available in Canada (*39*). It is unclear how including patient-incurred costs would affect cost-effectiveness because patients incur costs during both TB disease and TPT (*40*,*41*).

In summary, neglecting post-TB consequences underestimated the effectiveness of a postarrival infection screening and treatment intervention among persons who recently immigrated to Canada by more than 2-fold. Including all post-TB consequences reduced the estimated ICERs from $235,088 to $100,742 per QALY gained. Our findings suggest the long-term health and economic burden of TB substantially affects how TB prevention is valued. Those findings should motivate TB preventive efforts and prompt the continued collection of relevant cohort data to fill critical knowledge gaps. We encourage the consistent inclusion of post-TB consequences in analyses of TB prevention to guide policy in low-incidence settings moving forward.

Acknowledgments

We thank Nicolas Menzies for providing us with Canada-specific estimates of post-TB morbidity and mortality from their previous analysis.

All data informing the model are included in the manuscript. Access to model files (TreeAge) and code is available upon request to the corresponding author.

This work was funded by the National Sanitarium Association and the Canadian Institutes of Health Research (grant no. PJT-190227). J.R.C. receives salary support from the McGill University Health Centre Foundation and the McGill University Department of Medicine and holds a Chercheur-boursier award from the Fonds de recherche du Québec—Santé (grant no. 330287; https://doi.org/10.69777/330287).

About the Author

Mr. Ainiwaer is a master's degree student in public health at McGill University. His work examines the long-term

impacts of infectious disease on health and economic outcomes, with the aim of supporting more informed and equitable public health decisions.

References

1. World Health Organization. Global Tuberculosis Report, 2025 [cited 2025 Nov 28] https://www.who.int/teams/global-programme-on-tuberculosis-and-lung-health/tb-reports/global-tuberculosis-report-2025
2. Pareek M, Greenaway C, Noori T, Munoz J, Zenner D. The impact of migration on tuberculosis epidemiology and control in high-income countries: a review. BMC Med. 2016;14:48. https://doi.org/10.1186/s12916-016-0595-5
3. Shea KM, Kammerer JS, Winston CA, Navin TR, Horsburgh CR Jr. Estimated rate of reactivation of latent tuberculosis infection in the United States, overall and by population subgroup. Am J Epidemiol. 2014;179:216–25. https://doi.org/10.1093/aje/kwt246
4. Wahedi K, Zenner D, Flores S, Bozorgmehr K. Mandatory, voluntary, repetitive, or one-off post-migration follow-up for tuberculosis prevention and control: a systematic review. PLoS Med. 2023;20:e1004030. https://doi.org/10.1371/journal.pmed.1004030
5. Gogichadze N, Sagrera A, Vicente JÁ, Millet JP, López-Seguí F, Vilaplana C. Cost-effectiveness of active tuberculosis screening among high-risk populations in low tuberculosis incidence countries: a systematic review, 2008 to 2023. Euro Surveill. 2024;29:2300614. https://doi.org/10.2807/1560-7917.ES.2024.29.12.2300614
6. Pinheiro M, Valente C, Cruz M, Nascimento Moreira D, Aguiar A, Duarte R. European guidelines for the management of tuberculosis screening procedures in migrants: a systematic review. Pulmonology. 2025;31:2482855. https://doi.org/10.1080/25310429.2025.2482855
7. Pareek M, Baussano I, Abubakar I, Dye C, Lalvani A. Evaluation of immigrant tuberculosis screening in industrialized countries. Emerg Infect Dis. 2012;18:1422–9. https://doi.org/10.3201/eid1809.120128
8. Robayo SD, Tansey CM, Romanowski K, Campbell JR. Risks and consequences of TB and its prevention in cost-utility analyses among immigrants: a systematic review. IJTLD Open. 2025;2:555–62. https://doi.org/10.5588/ijtldopen.25.0355
9. Menzies NA, Quaife M, Allwood BW, Byrne AL, Coussens AK, Harries AD, et al. Lifetime burden of disease due to incident tuberculosis: a global reappraisal including post-tuberculosis sequelae. Lancet Glob Health. 2021; 9:e1679–87. https://doi.org/10.1016/S2214-109X(21)00367-3
10. Romanowski K, Law MR, Karim ME, Campbell JR, Hossain MB, Gilbert M, et al. Healthcare utilization after respiratory tuberculosis: a controlled interrupted time series analysis. Clin Infect Dis. 2023;77:883–91. https://doi.org/10.1093/cid/ciad290
11. Romanowski K, Baumann B, Basham CA, Ahmad Khan F, Fox GJ, Johnston JC. Long-term all-cause mortality in people treated for tuberculosis: a systematic review and meta-analysis. Lancet Infect Dis. 2019;19:1129–37. https://doi.org/10.1016/S1473-3099(19)30309-3
12. Taylor J, Bastos ML, Lachapelle-Chisholm S, Mayo NE, Johnston J, Menzies D. Residual respiratory disability after successful treatment of pulmonary tuberculosis: a systematic review and meta-analysis. EClinicalMedicine. 2023;59:101979. https://doi.org/10.1016/j.eclinm.2023.101979
13. Tomeny EM, Tran PB, Kazibwe J, Rosu L, Nikolaidis GF, Nightingale R, et al. A broader lens on tuberculosis cost-effectiveness analysis: how patient-incurred costs and post-tuberculosis outcomes reshape estimates in a multi-country study. PLOS Glob Public Health. 2025;5:e0005062. https://doi.org/10.1371/journal.pgph.0005062
14. Public Health Agency of Canada. Tuberculosis disease surveillance. 2025 [cited 2026 Feb 9]. https://health-infobase.canada.ca/tuberculosis
15. Public Health Agency of Canada. Tuberculosis in Canada: 2012–2021 expanded report. Ottawa (ON): The Agency; 2024.
16. Immigration Refugees and Citizenship Canada. Medical examination for permanent residence applicants. 2025 [cited 2025 Nov 28]. https://www.canada.ca/en/immigration-refugees-citizenship/services/application/medical-police/medical-exams/requirements-permanent-residents
17. Heffernan C, Jamro A, Egedahl ML, Long R. Evaluating Canada's initiative of enhanced screening for tuberculosis infection in migrants: implementation lessons from Alberta. Can Commun Dis Rep. 2025;51:381–8. https://doi.org/10.14745/ccdr.v51i101112a02
18. Immigration Refugees Citizenship Canada. Immigration, refugees and citizenship Canada 2025–26 departmental plan, 2025 [cited 2025 Nov 28]. https://www.canada.ca/en/immigration-refugees-citizenship/corporate/publications-manuals/departmental-plans/2025-26-departmental-plan/departmental-plan-2025-2026-full.html
19. Immigration Refugees and Citizenship Canada. Permanent residents—monthly IRCC updates. Open Government Portal. 2025 [cited 2025 Nov 28]. https://open.canada.ca/data/en/dataset/f7e5498e-0ad8-4417-85c9-9b8aff9b9eda
20. Campbell JR, Johnston JC, Cook VJ, Sadatsafavi M, Elwood RK, Marra F. Cost-effectiveness of latent tuberculosis infection screening before immigration to low-incidence countries. Emerg Infect Dis. 2019;25:661–71. https://doi.org/10.3201/eid2504.171630
21. Alvarez G, Pease C, Menzies D. Chapter 6: tuberculosis preventive treatment in adults. In: Canadian tuberculosis standards, 8th edition. Can J Respir Crit Care Sleep Med. 2022;6:77–86. https://doi.org/10.1080/24745332.2022.2039498
22. Canadian Agency for Drugs and Technologies in Health. Guidelines for the economic evaluation of health technologies, 2017 [cited 2025 Nov 28]. https://www.cda-amc.ca/guidelines-economic-evaluation-health-technologies-canada-4th-edition
23. Campbell JR, Nsengiyumva P, Chiang LY, Jamieson F, Khadawardi H, Mah HK, et al. Costs of tuberculosis at 3 treatment centers, Canada, 2010–2016. Emerg Infect Dis. 2022;28:1814–23. https://doi.org/10.3201/eid2809.220092
24. Bauer M, Ahmed S, Benedetti A, Greenaway C, Lalli M, Leavens A, et al. Health-related quality of life and tuberculosis: a longitudinal cohort study. Health Qual Life Outcomes. 2015;13:65. https://doi.org/10.1186/s12955-015-0250-4
25. Basham CA, Karim ME, Cook VJ, Patrick DM, Johnston JC. Post-tuberculosis mortality risk among immigrants to British Columbia, Canada, 1985–2015: a time-dependent Cox regression analysis of linked immigration, public health, and vital statistics data. Can J Public Health. 2021;112:132–41. https://doi.org/10.17269/s41997-020-00345-y
26. Statistics Canada. Life tables, Canada, provinces and territories, 2026 [cited 2026 Feb 9]. https://www150.statcan.gc.ca/n1/en/catalogue/84-537-X
27. Menzies NA, Marks SM, Hsieh YL, Swartwood NA, Beeler Asay GR, Skarbinski J, et al. Contribution of posttuberculosis sequelae to life-years lost from tuberculosis disease in the United States, 2015-2019.

Am J Respir Crit Care Med. 2025;211:1059–68. https://doi.org/10.1164/rccm.202411-2213OC
28. Campbell JR, Pease C, Daley P, Pai M, Menzies D. Chapter 4: diagnosis of tuberculosis infection. In: Canadian tuberculosis standards, 8th edition. Can J Respir Crit Care Sleep Med. 2022;6(S1):49–65. https://doi.org/10.1080/24745332.2022.2036503
29. Ekramnia M, Li Y, Haddad MB, Marks SM, Kammerer JS, Swartwood NA, et al. Estimated rates of progression to tuberculosis disease for persons infected with *Mycobacterium tuberculosis* in the United States. Epidemiology. 2024;35:164–73. https://doi.org/10.1097/EDE.0000000000001707
30. Greenaway C, Pareek M, Abou Chakra CN, Walji M, Makarenko I, Alabdulkarim B, et al. The effectiveness and cost-effectiveness of screening for latent tuberculosis among migrants in the EU/EEA: a systematic review. Euro Surveill. 2018;23:17–00543. https://doi.org/10.2807/1560-7917.ES.2018.23.14.17-00543
31. Petersen E, Al-Abri S, Al-Jardani A, Memish ZA, Aklillu E, Ntoumi F, et al. Screening for latent tuberculosis in migrants—*status quo* and future challenges. Int J Infect Dis. 2024;141:107002. https://doi.org/10.1016/j.ijid.2024.107002
32. Goodell AJ, Shete PB, Vreman R, McCabe D, Porco TC, Barry PM, et al. Outlook for tuberculosis elimination in California: an individual-based stochastic model. PLoS One. 2019;14:e0214532. https://doi.org/10.1371/journal.pone.0214532
33. Ilaiwy G, Dowdy DW. Cost effectiveness of three months of rifapentine and isoniazid for latent tuberculosis in Syrian refugees. J Clin Tuberc Other Mycobact Dis. 2021;24:100262. https://doi.org/10.1016/j.jctube.2021.100262
34. Hsieh YL, Horsburgh CR Jr, Cohen T, Miller JW, Salomon JA, Menzies NA. Cost-effectiveness of screening with transcriptional signatures for incipient TB among U.S. migrants. PLoS Med. 2025;22:e1004603. https://doi.org/10.1371/journal.pmed.1004603
35. Meghji J, Auld SC, Bisson GP, Khosa C, Masekela R, Navuluri N, et al. Post-tuberculosis lung disease: towards prevention, diagnosis, and care. Lancet Respir Med. 2025; 13:460–72. https://doi.org/10.1016/S2213-2600(24)00429-6
36. Nightingale R, Chinoko B, Lesosky M, Rylance SJ, Mnesa B, Banda NPK, et al. Respiratory symptoms and lung function in patients treated for pulmonary tuberculosis in Malawi: a prospective cohort study. Thorax. 2022;77:1131–9. https://doi.org/10.1136/thoraxjnl-2021-217190
37. Akalu TY, Clements ACA, Liyew AM, Gilmour B, Murray MB, Alene KA. Risk factors associated with post-tuberculosis sequelae: a systematic review and meta-analysis. EClinicalMedicine. 2024;77:102898. https://doi.org/10.1016/j.eclinm.2024.102898
38. Auld SC, Bisson GP. Post-tuberculosis sequelae and the burden of "long TB": continuing TB care after treatment completion. Am J Respir Crit Care Med. 2025;211:912–3. https://doi.org/10.1164/rccm.202502-0442ED
39. Portnoy A, Yamanaka T, Nguhiu P, Nishikiori N, Garcia Baena I, Floyd K, et al. Costs incurred by people receiving tuberculosis treatment in low-income and middle-income countries: a meta-regression analysis. Lancet Glob Health. 2023;11:e1640–7. https://doi.org/10.1016/S2214-109X(23)00369-8
40. Vesga JF, Mohamed MS, Shandal M, Jabbour E, Lomtadze N, Kubjane M, et al. The effectiveness, cost-effectiveness, budget impact, and return on investment of scaling up tuberculosis screening and preventive treatment in Brazil, Georgia, Kenya, and South Africa: a modelling study. Lancet Glob Health. 2025;13:e1857–68. https://doi.org/10.1016/S2214-109X(25)00321-3
41. Shepardson D, Marks SM, Chesson H, Kerrigan A, Holland DP, Scott N, et al. Cost-effectiveness of a 12-dose regimen for treating latent tuberculous infection in the United States. Int J Tuberc Lung Dis. 2013;17:1531–7. https://doi.org/10.5588/ijtld.13.0423

Address for correspondence: Jonathon R. Campbell, McGill University, Office 3D.55, 5252 Boulevard de Maisonneuve O, Montreal, QC H4A 3S5, Canada; email: jonathon.campbell@mcgill.ca

Clustering and Source Association of Clinical and Nonclinical *Listeria monocytogenes* Isolates, New York, USA, 2000–2021[1]

Hilal Samut, Damaris V. Mendez-Vallellanes, Hannah Hoyt, Samantha E. Wirth, Lisa Mingle, Brian D. Sauders, Gregory A. Deiulio, Alyssa W. Dickey, Maria L. Ishida, William J. Wolfgang, Kimberlee A. Musser, Martin Wiedmann, Renato H. Orsi

We analyzed whole-genome sequencing data for 1,046 human clinical and 1,332 nonclinical *Listeria monocytogenes* isolates collected across New York, USA, during 2000–2021. Several hypervirulent clonal complexes (CCs) were significantly associated with clinical isolates, and several hypovirulent CCs were associated with nonclinical isolates. Specific CCs also showed association with specific food categories (e.g., processed meat); specific genetic markers (e.g., *inlA* premature stop codons) were also significantly associated with processed meat isolates. Analysis of clusters that contained food isolates, as well as subsequently identified clinical isolates, showed that time of isolation between food isolates and clinical isolates was significantly shorter for produce isolates than for isolates from meat, dairy, or fish. This finding suggests unique transmission pathways for produce, which might reflect short shelf life or limited *L. monocytogenes* persistence (e.g., in agricultural environments). This study highlights new opportunities for use of whole-genome sequencing to improve outbreak investigations and source attribution.

Listeria monocytogenes is a leading cause of foodborne illness–related deaths in the United States; an estimated 1,250 human illnesses and 172 deaths occurred annually during 2016–2019 (*1*). *L. monocytogenes* is frequently isolated from dairy, ready-to-eat meats, seafood, fruits, and vegetables, and it can persist in food processing environments (*2*), leading to recurrent contamination of finished products. Hence, robust surveillance is critical for protecting vulnerable populations and rapid detection of contamination sources.

Multilocus sequence typing (MLST) is widely used to classify *L. monocytogenes* into clonal complexes (CCs), and certain CCs are suggested as presenting higher and lower virulence (*3*). CC1, CC4, and CC6 are considered hypervirulent and are frequently associated with human listeriosis cases (*4*). Conversely, CC9 and CC121 are frequently isolated from food or food-processing environments and are considered hypovirulent CCs (*4*,*5*). Hypovirulent CCs often carry adaptations that promote environmental persistence (e.g., stress tolerance genes) but might have reduced ability to cause invasive disease (*6*). Characterizing the distribution of CCs across clinical and nonclinical isolates is key for identifying contamination reservoirs and understanding the public health relevance of isolates found in foods. Distinguishing hypervirulent strains from those mainly associated with the environment can help prioritize risk management and improve listeriosis prevention strategies (*7*). In this study, we analyzed 2,371 clinical and nonclinical *L. monocytogenes* isolates collected across the state of New York (NY), USA, during 2000–2021 to compare the CC distributions among clinical and nonclinical isolates, examine associations between CCs and food categories, and evaluate the time between food isolate collection and subsequent detection of a genetically-related clinical isolate using single-nucleotide polymorphism (SNP)–based thresholds. The Wadsworth Center and Cornell University Institutional Review Boards reviewed this study and determined

Author affiliations: Cornell University, Ithaca, New York, USA (H. Samut, M. Wiedmann, R.H. Orsi); New York State Department of Health, Wadsworth Center, Albany, New York, USA (D.V. Mendez-Vallellanes, H. Hoyt, S.E. Wirth, L. Mingle, W.J. Wolfgang, K.A. Musser); New York State Department of Agriculture and Markets, Albany (B.D. Sauders, G.A. Deiulio, A.W. Dickey, M.L. Ishida)

DOI: https://doi.org/10.3201/eid3209.260289

[1]Preliminary results from this study were presented at the 2025 International Association for Food Protection Conference; July 27–30, 2025; Cleveland, Ohio, USA.

it to be exempt from human research (submission no. 03-037 and IRB0150826).

Materials and Methods

Detailed materials and methods are provided in the Appendix (https://wwwnc.cdc.gov/EID/article/32/9/26-0289-App1.pdf). In brief, we performed whole-genome sequencing (WGS) on clinical (n = 1,046) and nonclinical (n = 1,332) *L. monocytogenes* isolates collected across NY, as previously described (*8*). We deduplicated clinical isolates from the same patient or mother–infant pairs, resulting in 1,006 clinical isolates. Likewise, we deduplicated multiple nonclinical isolates from the same sampling event, resulting in 1,089 nonclinical isolates.

We used whole-genome SNP distances to assess the genetic relatedness among isolates, as previously described (*8*). We used genetic relatedness of clinical and nonclinical isolates to define 3 types of isolate grouping. When only clinical isolates were involved, we used the term clustered, and when clinical and nonclinical isolates were involved, we used the term linked. Hence, the term linked was used to describe genomic similarity between clinical and nonclinical isolates on the basis of SNP thresholds, rather than confirmed epidemiologic associations. Therefore, NY clinical isolates were considered clustered if clustered with ≥1 other NY clinical isolate by ≤20 SNPs (*9*–*11*), NY nonclinical isolates were considered cluster-linked if linked by ≤50 SNPs with ≥1 clustered NY clinical isolate (*12*), and NY clinical and nonclinical isolates were considered sporadic-linked if a NY clinical isolate was not clustered with any other NY clinical isolate by ≤20 SNPs but was linked with ≥1 NY nonclinical isolate by ≤50 SNPs. The terms clustered, cluster-linked, and sporadic-linked refer only to genetic relatedness on the basis of SNP thresholds, without interpretation of epidemiologic data. Isolates not meeting those criteria were considered unclustered NY clinical isolates and unlinked NY nonclinical isolates.

Results

CC Distributions among Clinical and Nonclinical Isolates

Among clinical isolates, CC1 (n = 138), CC6 (n = 77), CC5 (n = 63), and CC4 (n = 53) were the most prevalent CCs (Figure 1, panel A). Among nonclinical isolates, CC5 (n = 205), CC321 (n = 80), CC6 (n = 80), and CC2 (n = 69) were the most prevalent CCs (Figure 1, panel B). CC1, CC4, CC217, CC388, CC389, and CC554 were significantly overrepresented among clinical isolates, whereas CC5, CC9, CC121, CC199, CC288, and CC321 were significantly overrepresented among nonclinical isolates (Table 1; Figure 2).

On the basis of their grouping patterns within NY isolates, 318 (31.6%) clinical isolates were clustered, 79 (7.9%) were sporadic-linked, and 609 (60.5%) were unclustered (Figure 1, panel A). Among nonclinical isolates, 236 (21.7%) were classified as cluster-linked, 107 (9.8%) were sporadic-linked, and 746 (68.5%) were unlinked (Figure 1, panel B). Most CC321 nonclinical isolates were cluster-linked, whereas CC6, CC2, CC9, and CC121 nonclinical isolates were predominantly unlinked (e.g., 59 out of 61 CC9 nonclinical isolates were unlinked).

Association of CCs with Food Categories in NY

The 313 food isolates (28.7% of nonclinical isolates) came from processed meat (n = 93), processed fish (n = 72), raw dairy (n = 47), raw fish (n = 22), processed dairy (n = 21), raw meat (n = 21), produce (n = 15), sandwiches (n = 9), salad (n = 8), pasta (n = 4), and nuts (n = 1). The most prevalent CCs among food isolates were CC5 (n = 36), CC9 (n = 36), and CC321 (n = 33) (Figure 3). Of the 313 food isolates, 69 were cluster-linked, 25 were sporadic-linked, and 219 were unlinked. Some CCs (e.g., CC5, CC9, CC121) included exclusively or predominantly unlinked food isolates. In contrast, most CC321 and CC155 food isolates were cluster-linked.

Some CCs were significantly associated with certain food categories (Table 2; Figure 4), including raw or processed forms of the same type (e.g., raw or processed dairy). For example, CC9 was significantly associated with processed meat, CC5 with raw meat, and CC121 with processed fish. Other CCs were not statistically associated with certain food categories after correction for multiple testing (false discovery rate–adjusted p value>0.05) but tended to be more commonly found in a specific category. For example, CC6 was ≈11 times more likely to be isolated from processed dairy and 2 times more likely to be isolated from raw dairy compared with all other food categories (Appendix Table 1).

We also performed further comparison for CCs with ≥10 food isolates (Appendix Table 2) to assess whether those CCs were specifically associated with the processed or raw forms of those key food categories (i.e., meat, fish, dairy). CC9 was more frequently observed among processed meat isolates and CC121 was more frequently observed among processed fish isolates than in raw meat (odds ratio [OR] 15.74 [95% CI 0.90–276.54]) and raw fish (OR 1.40 [95% CI 0.31–6.40]) isolates; however, those associations were not statistically significant after correction for multiple testing. Conversely, CC5 isolates were significantly overrepresented among raw meat compared with processed meat isolates (OR 20 [95% CI 4.17–100]), even after false discovery rate correction.

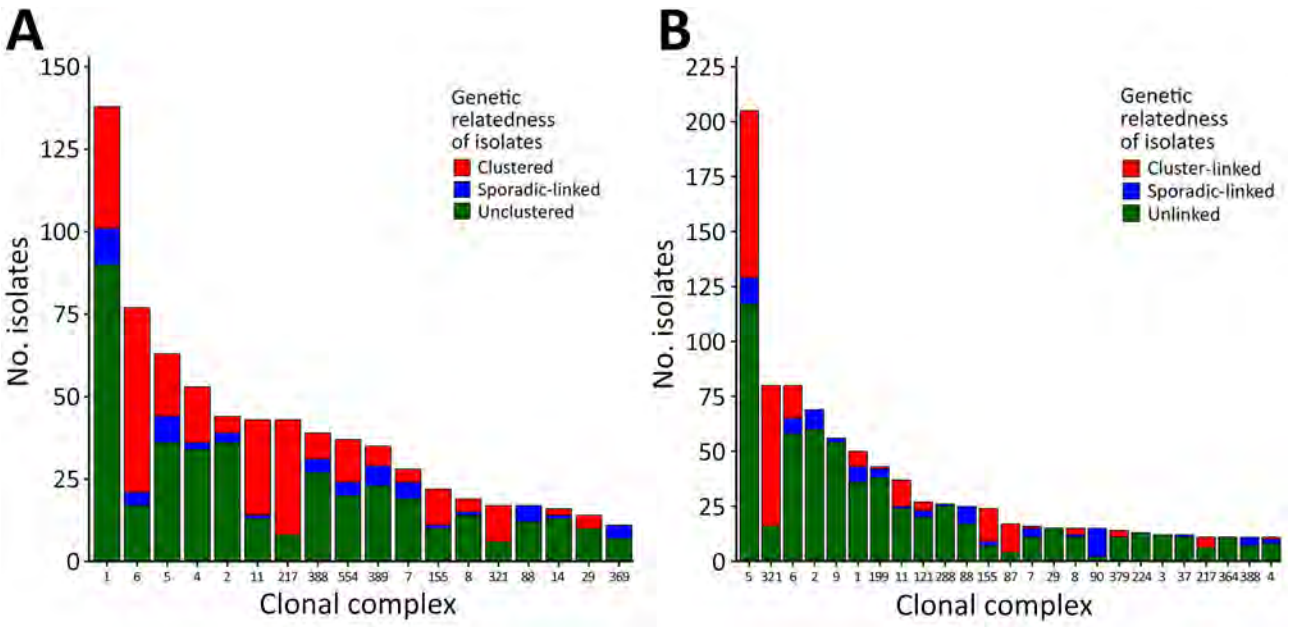

Figure 1. Distribution of *Listeria monocytogenes* CCs by grouping status in terms of genetical relatedness by single-nucleotide polymorphism (SNP) distances in study of clustering and source association of clinical and nonclinical *L. monocytogenes* isolates, New York, USA, 2000–2021. Distribution is shown for clinical (A) and nonclinical (B) isolates. Clinical isolates were considered clustered if they clustered with ≥1 other clinical isolate by ≤20 SNPs and nonclinical isolates were considered cluster-linked if they were linked with ≥1 clustered clinical isolate by ≤50 SNPs; both clinical and nonclinical isolates were considered sporadic-linked if the clinical isolate was not clustered with any other clinical isolate by ≤20 SNPs but linked with ≥1 nonclinical isolate by ≤50 SNPs. The terms clustered, cluster-linked, and sporadic-linked refer only to genetic relatedness based on SNP thresholds, without interpretation of epidemiologic data. Clinical isolates not meeting those criteria were considered unclustered, while nonclinical isolates were considered unlinked. CCs representing <1% of total isolates within each isolate type were grouped as other and excluded from this figure. CC, clonal complex.

Virulence and Sanitizer-Tolerance Genes

We screened clinical and nonclinical isolates for virulence and sanitizer tolerance genes (Appendix Figures 1, 2). The *Listeria* pathogenicity island (LIPI) 1, *inlA*, and *inlB* were nearly ubiquitous across both clinical and nonclinical isolates (≥98%), whereas LIPI-3 and LIPI-4 showed higher prevalence among clinical isolates (43.64% for LIPI-3 and 19.48% for LIPI-4). We detected *inlA* premature stop codons (PMSCs) in 32 (3.18%) clinical and 217 (19.92%) nonclinical isolates; frequency was high among nonclinical-associated CCs such as CC9 (91%), CC199 (93%), and CC321 (97.50%). Among clinical isolates with *inlA* PMSC, 17 (53.12%) carried PMSC type 3 (truncated to 699 aa vs. the full-length 800 aa) and only 2 (6.25%) carried PMSC type 4 (8 aa). Among nonclinical isolates with *inlA* PMSC, PMSCs type 4 (79 [36.40%]) and type 3 (78 [35.94%]) predominated. PMSC type

Table 1. *Listeria monocytogenes* clonal complexes significantly associated with either clinical or nonclinical isolates in study of clustering and source association of clinical and nonclinical *Listeria monocytogenes* isolates, New York, USA, 2000–2021*

CC	No. clinical isolates	No. nonclinical isolates	OR (95% CI)†	FDR-adjusted p value‡
CCs overrepresented among clinical isolates				
CC1	138	50	3.30 (2.34–4.72)	<0.001
CC4	53	11	5.45 (2.79–11.63)	<0.001
CC217	43	11	4.37 (2.20–9.46)	<0.001
CC388	39	11	3.95 (1.97–8.60)	<0.001
CC389	35	7	5.57 (2.42–14.93)	<0.001
CC554	37	9	4.58 (2.16–10.85)	<0.001
CCs overrepresented among nonclinical isolates				
CC5	63	205	0.29 (0.21–0.39)	<0.001
CC9	5	56	0.09 (0.03–0.23)	<0.001
CC121	6	27	0.24 (0.08–0.59)	<0.001
CC199	3	43	0.07 (0.01–0.23)	<0.001
CC288	5	26	0.20 (0.06–0.54)	<0.001
CC321	17	80	0.22 (0.12–0.37)	<0.001

*Only CCs with an FDR-adjusted p value <0.05 are shown. CC, clonal complex; FDR, false discovery rate; OR, odds ratio.
†ORs >1 indicate overrepresentation in clinical isolates, whereas ORs <1 indicate overrepresentation in nonclinical isolates.
‡Statistical significance was assessed using 2-sided Fisher exact test followed by FDR correction for multiple comparisons.

4 was rarer among clinical isolates (n = 3 [0.30% of clinical isolates]) than in nonclinical isolates (n = 79 [7.25% of nonclinical isolates]). The remaining PMSCs spanned 14 other PMSC types, resulting in InlA proteins of varying lengths (Table 3). Sanitizer tolerance genes (*bcrABC, Tn6188_qac,* or *LGI1_LM5578_1862*) were detected in 354 nonclinical isolates (32.51% of nonclinical isolates; OR 5.81 [95% CI 4.44–7.67]). We noted significant overrepresentation of *inlA* PMSCs among processed meat isolates (Table 4). In contrast, *inlA* PMSCs were rare or absent among dairy product isolates (0 of 47 raw dairy isolates; 1 of 21 processed dairy isolates) (Table 4). Sanitizer tolerance genes were significantly overrepresented among isolates from processed fish (OR 3.00 [95% CI 1.74–5.16]) and underrepresented among raw dairy isolates (OR 0.02 [95% CI 0–0.30]) (Appendix Table 3).

Influence of Food Category on Time between Isolate Collection and Detection of Genetically Related Clinical Isolate

We used a Cox proportional hazards model to evaluate the time between food isolate collection and subsequent detection of a genetically related clinical isolate (≤50 SNPs) for food categories with ≥10 isolates (Appendix). Overall, we identified 205 food–clinical isolate pairs; 43 distinct food isolates (13 processed meat, 12 processed fish, 6 raw dairy, 4 processed dairy, 4 produce, 3 salad, and 1 raw meat) were linked with 107 distinct clinical isolates, 1 of which was linked with multiple food sources (processed meat and processed fish) at the same SNP distance. Processed meat (n = 126 pairs) and processed fish (n = 23 pairs) isolates had the highest number of links to clinical isolates (Table 5). The 205 food–clinical pairs were observed in 24 distinct SNP clusters and represented 17 distinct CCs (Table 5). Among the 43 food isolates, 10 of 13 processed meat isolates and 9 of 12 processed fish isolates had *inlA* PMSC. Out of 205 food–clinical isolate pairs, only 48 (23%) pairs with 16 distinct clinical isolates were involved in 4 different formal outbreak investigations. Among those, only 2 outbreak investigations had implicated food sources (processed meat in both outbreaks) for 13 clinical isolates; for those 2 outbreaks, the implicated food sources were consistent with the food category (i.e., processed meat) identified in our analysis.

Food category, but not the presence of *inlA* PMSC, was a significant predictor of the time between food isolate collection and subsequent detection of a genetically related clinical isolate. In particular, produce isolates exhibited the shortest time for subsequent detection of a genetically related clinical isolate. For example, the hazard ratio for produce compared with processed dairy was 9.72 (95% CI 2.46–38.39), indicating a shorter time between produce isolate collection and subsequent detection of a genetically related clinical isolate than for processed dairy isolates (Appendix Table 4). Survival curves revealed that 75% of produce isolates were detected as genetically related with subsequently detected clinical isolates within 2.2 years; in contrast, some raw meat isolate pairs took up to 17 years to be genetically linked with a clinical isolate (Figure 5, panel A).

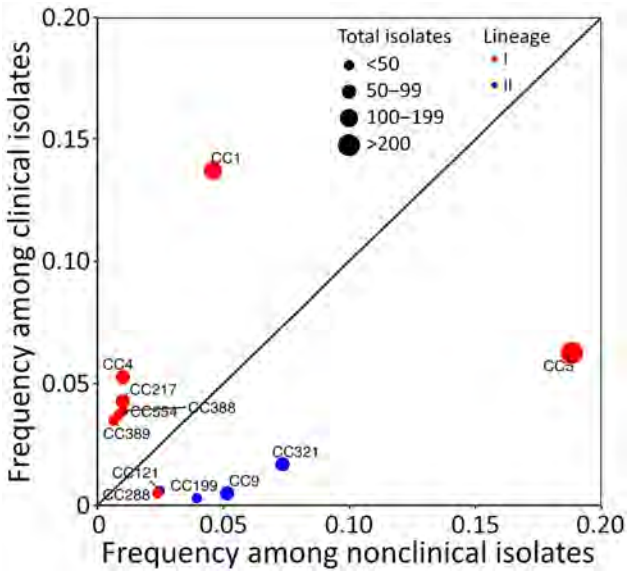

Figure 2. Comparison of the relative frequency of *Listeria monocytogenes* CCs among clinical and nonclinical isolates in study of clustering and source association of clinical and nonclinical *L. monocytogenes* isolates, New York, USA, 2000–2021. Each bubble represents CCs that were found to be significantly overrepresented among either clinical or nonclinical isolates (Table 1). Diagonal reference line indicates equal frequency in clinical and nonclinical isolates; CCs above the line were common in clinical isolates, whereas CCs below were common in nonclinical isolates. CC, clonal complex.

Discussion

Our analysis of *L. monocytogenes* isolates in NY during 2000–2021 reveals clear differences in CC distributions between clinical and nonclinical isolates. Six CCs were significantly overrepresented among clinical isolates. Of those, 2 CCs (CC1 and CC4) have previously been identified as hypervirulent CCs on the basis of experimental evidence showing that they exhibit enhanced gut colonization, intestinal invasion, and infection of internal organs in a humanized mouse model (*4*). CC1, a well-established hypervirulent CC associated with invasive listeriosis (*14*,*15*), was the most frequently isolated CC among clinical isolates in our study, similar to a previous analysis of NY clinical isolates from

2000–2020 (*16*). The other CCs significantly overrepresented among clinical isolates in our study (i.e., CC217, CC388, CC389, and CC554) have not been phenotypically classified in terms of their virulence potential but might represent candidates for additional hypervirulent clones, as supported by studies suggesting that the virulence of *L. monocytogenes* CCs is positively associated with their epidemiologic association with human clinical cases (*3*). CC6 was the second most frequently isolated CC among clinical isolates but was not among the CCs significantly overrepresented among clinical isolates. That CC has previously been classified as hypervirulent and has been implicated in multiple large listeriosis outbreaks, including outbreaks linked to turkey deli meats, hot dogs, and French-style cheese (*17*). Previous studies in France and the Netherlands also identified CC1, CC2, CC4, and CC6 as frequently isolated CCs among clinical isolates (*3*,*18*). Overall, our data support that certain CCs are more likely to cause human disease.

We also identified 6 CCs (CC5, CC9, CC121, CC199, CC288, and CC321) that were significantly overrepresented among nonclinical isolates. CC9, CC121, CC199, and CC321 were the CCs with the highest proportion of isolates carrying *inlA* PMSC, a frequent hallmark of hypovirulent *L. monocytogenes* strains (*13*,*19*,*20*). CC9 and CC121 have previously been described as hypovirulent and environmentally adapted (*4*); those CCs were also reported to show increased tolerance to benzalkonium chloride, a commonly used sanitizer (*4*). Two CCs (CC5 and CC288) were overrepresented among nonclinical isolates but exhibited low frequencies of *inlA* PMSCs. Although CC5 was overrepresented among nonclinical isolates, it was the third most common CC among clinical isolates, suggesting that CC5 isolates are unlikely to be hypovirulent. The observed frequency of CCs among nonclinical isolates differs from observations in Europe. For example, CC121 was the most isolated CC among food and food processing environment–related isolates in France and Norway (*3*,*22*), as was CC9 in the Netherlands (*18*); CC121 and CC9 were the ninth and fifth most common CCs among nonclinical isolates characterized in this study. In contrast, CC5 was the most common CC among nonclinical isolates, but that CC was infrequently found among clinical and nonclinical isolates in France and the Netherlands (*3*,*18*). That discrepancy suggests a geographic difference in the distribution of this CC, which could be driven by possible differences in production systems, food preferences, or regional dynamics in *L. monocytogenes* transmission between NY and those countries in Europe. Despite likely regional differences in prevalence of different CCs, our data further support frequent global occurrence of certain clinically associated CCs (i.e., CC1 and CC4), whereas the occurrence of nonclinically associated CCs seems to show larger regional differences.

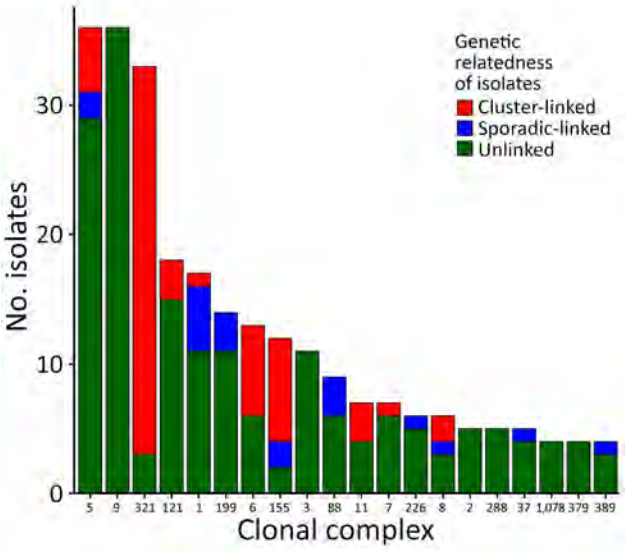

Figure 3. Distribution of *Listeria monocytogenes* clonal complexes (CCs) by grouping status in terms of genetical relatedness by single-nucleotide polymorphism (SNP) distances among food isolates in study of clustering and source association of clinical and nonclinical *L. monocytogenes* isolates, New York, USA, 2000–2021. Nonclinical isolates were considered cluster-linked if they were linked with ≥1 clustered clinical isolate by ≤50 SNPs, and nonclinical isolates were considered sporadic-linked if a clinical isolate was not clustered with any other clinical isolate by ≤20 SNPs but linked with ≥1 nonclinical isolate by ≤50 SNPs. Nonclinical isolates not meeting those criteria were considered unlinked. CCs representing <1% of total isolates within each isolate type were grouped as other and excluded from this figure.

Overall, we found 7 statistically significant associations between CCs and food categories. For example, CC9 was significantly overrepresented among processed meat isolates and CC121 was significantly overrepresented among processed fish isolates. Those findings are consistent with previous reports indicating frequent recovery of those CCs from ready-to-eat meat and fish products and infrequent occurrence in dairy products (*4*,*22*–*24*). In addition, CC5 showed overrepresentation among raw meat isolates compared with processed meat isolates. That finding might suggest that different CCs could be introduced at distinct points along the food production chain; some CCs might be more closely linked to primary production or raw materials and others could be more likely to persist in food processing facilities. For the other 5 CCs associated with specific food categories, associations were based on smaller numbers (<10 isolates for the associated food category) and represented associations that had not been previously reported. Thus, those associations are possibly driven

Table 2. Associations between *Listeria monocytogenes* clonal complexes and food categories in study of clustering and source association of clinical and nonclinical *Listeria monocytogenes* isolates, New York, USA, 2000–2021*

CC†	Food category‡	OR (95% CI)§	FDR-adjusted p value¶
CC5, n = 36	Raw meat, n = 9	7.34 (2.89–18.60)	0.019
CC9, n = 36	Processed meat, n = 32	25.42 (9.12–70.91)	<0.001
CC121, n = 18	Processed fish, n = 12	7.49 (2.78–20.12)	0.015
CC369, n = 3	Produce, n = 3	167.16 (8.18–3414.14)	0.015
CC389, n = 4	Raw dairy, n = 4	55.14 (2.92–1042.22)	0.043
CC573, n = 3	Produce, n = 3	167.16 (8.18–3414.14)	0.015
CC1078, n = 4	Raw dairy, n = 4	55.14 (2.92–1042.22)	0.043

*Only CC-food category pairs with an FDR-adjusted p value <0.05 are shown (7 out of 660 CC-food category pairs). CC, clonal complex; FDR, false discovery rate; OR, odds ratio.
†n value indicates number of food isolates with respective CC.
‡n value indicates number of food isolates with respective food category and with corresponding CC.
§A continuity correction of 0.5 was applied to all cells to allow for OR calculation and ensure comparability across categories. ORs >1 indicate overrepresentation of the CC in the corresponding food category.
¶Associations were assessed using 2-sided Fisher exact test followed by FDR correction for multiple comparisons.

by specific sources (rather than general associations with a product type). Overall, our findings support that some CCs might be associated with certain food categories or with raw versus processed foods in a given category, which highlights opportunities to use WGS data to improve outbreak investigations and enable more rapid identification of a likely food source. However, although some CCs showed overrepresentation within specific food categories (e.g., CC9 with processed meat), others (e.g., CC321) were observed across multiple food sources with no overrepresentation in specific food categories. That finding suggests that certain CCs might not be specific to a single reservoir, and their presence should be interpreted cautiously in the context of source attribution.

Overall, *inlA* PMSCs were significantly overrepresented among isolates from processed meat and overrepresented, but they were not significantly

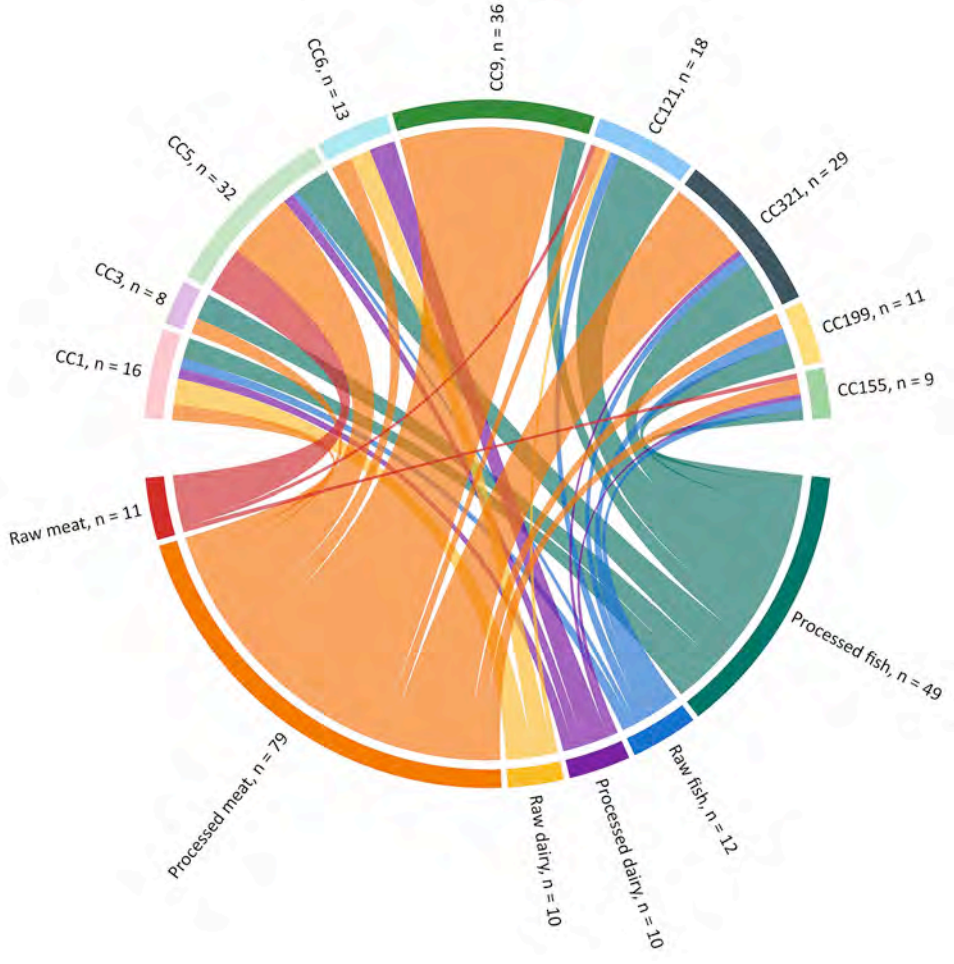

Figure 4. Sankey diagram showing the distribution of *Listeria monocytogenes* CCs across major food categories in study of clustering and source association of clinical and nonclinical *L. monocytogenes* isolates, New York, USA, 2000–2021. Only CCs with ≥10 food isolates are shown. Food categories with <20 isolates (e.g., produce, salad, pasta, nuts, and sandwiches) were excluded for clarity. The width of each flow is proportional to the number of isolates linked with a specific food category (bottom) and a CC (top). CC, clonal complex.

Table 3. Summary of detected *inlA* premature stop codons in study of clustering and source association of clinical and nonclinical *Listeria monocytogenes* isolates, New York, USA, 2000–2021*

CCs with respective *inlA* allele	*inlA* allele IDs with detected PMSCs†	PMSC type (length of truncated protein)‡	No. observed clinical and nonclinical isolates with respective *inlA* allele	Sources of nonclinical isolates with respective *inlA* allele
CC5	138	1 (605 aa)	6 clinical isolates and 18 nonclinical isolates	Raw meat, n = 6; processed meat, n = 4; sandwich, n = 1; salad, n = 1; retail, n = 6
CC9	43	8 (459 aa)	5 nonclinical isolates	Processed meat, n = 3; retail, n = 2
CC9	44	11 (684 aa)	1 nonclinical isolate	Processed fish, n = 1
CC9	47	12 (576 aa)	5 nonclinical isolates	Processed meat, n = 1; retail, n = 4
CC9	48	4 (8 aa)	2 clinical isolates and 39 nonclinical isolates	Processed meat, n = 26; processed fish, n = 1; retail, n = 10; farm, n = 2
CC9	69	19 (326 aa)	1 nonclinical isolate	Processed meat, n = 1
CC121	49	6 (491 aa)	3 clinical isolates and 17 nonclinical isolates	Processed fish, n = 12; processed meat, n = 1; processing environment, n = 4
CC121	438	5 (188 aa)	2 clinical isolates and 6 nonclinical isolates	Raw meat, n = 1; processed meat, n = 1; raw fish, n = 1; retail, n = 1
CC193	41	25 (25 aa)	1 nonclinical isolate	Processed fish, n = 1
CC199	28	4 (8 aa)	1 clinical isolate and 40 nonclinical isolates	Processed fish, n = 5; raw fish, n = 3; processed meat, n = 3; produce, n = 1; nuts, n = 1; retail, n = 26; processing environment, n = 1
CC224	125	2 (655 aa)	1 clinical isolate and 2 nonclinical isolates	Processed fish, n = 1; salad, n = 1
CC321	91	3 (699 aa)	17 clinical isolates and 78 nonclinical isolates	Processed meat, n = 16; processed fish, n = 10; sandwiches, n = 3; processed dairy, n = 1; raw fish, n = 1; salad, n = 1; processing environment, n = 20; retail, n = 26
CC635	439	7 (561 aa)	5 nonclinical isolates	Processing environment, n = 5
ST13	35	15 (76 aa)	1 nonclinical isolate	Processed meat, n = 1

*CC, clonal complex; ID, identification number; PMSC, premature stop codon.
†These allele IDs refer to IDs listed at https://bigsdb.pasteur.fr.
‡The classification of *inlA* PMSC types is based on Maury et al. (*4*) and Van Stelten et al. (*13*).

overrepresented among processed fish isolates. Although our findings are consistent with previous studies that have reported frequent occurrence of *inlA* PMSC in isolates from processing plant environments and ready-to-eat foods (*13*,*19*,*21*,*25*), our analysis further highlights significant differences between processed and raw food isolates in the frequency of *inlA* PMSCs. Of note, a previous study in France also reported that hypovirulent CCs were associated with meat products in general (without clear indications on raw vs. processed sources) and proposed that hypovirulent CCs might be adapted to the processing environment, whereas hypervirulent isolates might be adapted to hosts (*4*). In contrast, we found that intact *inlA* were overrepresented among dairy isolates, which is also consistent with previous studies, such as a study in France that reported hypervirulent CCs to be strongly associated with dairy products (*13*). Finally, we found that intact *inlA* was borderline overrepresented among produce isolates (14 of 15 produce

Table 4. Association between food category and presence of *inlA* premature stop codon among 313 *Listeria monocytogenes* food isolates in study of clustering and source association of clinical and nonclinical *L. monocytogenes* isolates, New York, USA, 2000–2021*

Food category	OR (95% CI)†	FDR-adjusted p value
Raw dairy	0.01 (0.00–0.24)	<0.001
Processed dairy	0.12 (0.02–0.65)	0.006
Produce	0.18 (0.03–0.98)	0.064
Pasta	0.20 (0.01–3.76)	0.474
Raw fish	0.56 (0.20–1.49)	0.462
Raw meat	0.95 (0.38–2.36)	1.000
Salad	1.18 (0.30–4.58)	1.000
Sandwich	1.52 (0.43–5.42)	0.886
Processed fish	1.55 (0.91–2.65)	0.270
Processed meat	4.93 (2.94–8.27)	<0.001
Nuts	5.58 (0.22–138.02)	0.483

*FDR, false discovery rate; OR, odds ratio.
†OR >1 indicates overrepresentation of *inlA* premature stop codon presence in the corresponding food category. Associations were assessed using 2-sided Fisher exact test followed by FDR correction for multiple comparisons. A continuity correction of 0.5 was applied to all cells to allow for OR calculation and ensure comparability across categories.

Table 5. Characteristics of food-clinical *Listeria monocytogenes* isolate pairs used in the analysis of time between food isolate collection and subsequent detection of a genetically related clinical isolate by SNP cluster in study of clustering and source association of clinical and nonclinical *L. monocytogenes* isolates, New York, USA, 2000–2021*

CC	SNP cluster	Food category	No. food–clinical isolate pairs†	No. distinct food isolates	No. distinct clinical isolates linked with food isolates by ≤50 SNPs	*inlA* PMSC types in food and clinical isolates‡
CC1	PDS000003335§	Processed dairy	1	1	1	None
	PDS000025547	Processed meat	3	1	3	None
	PDS000082531	Processed dairy	1	1	1	None
	PDS000091530	Raw dairy	1	1	1	None
CC5	PDS000024625	Processed dairy	1	1	1	None
	PDS000024647	Salad	7	1	7	None
CC6	PDS000025014	Processed dairy	5	1	5	None
	PDS000025078§	Processed meat	23	1	23	None
CC7	PDS000003277	Processed meat	3	1	3	None
CC8	PDS000025311	Raw dairy	2	1	2	None
		Processed fish	1	1	1	None
CC88	PDS000003204	Processed fish	3	1	3	None
CC121	PDS000024645	Processed fish	2	2	1	Type 6
CC155	PDS000024385	Salad¶	1	1	1	None
	PDS000024989§	Raw meat¶	13	1	13	None
CC199	PDS000083553#	Processed fish	2	2	1	Type 4
		Processed meat	1	1	1	Type 4
CC204	PDS000003073	Salad¶	2	1	2	None
CC226	PDS000025453	Raw dairy	1	1	1	None
CC321	PDS000000366§	Processed fish	7	5	3	Type 3
		Processed meat¶	96	9	12	Type 3
CC369	PDS000090530	Produce	1	1	1	None
CC388	PDS000043055	Raw dairy	1	1	1	None
CC389	PDS000024852	Raw dairy	1	1	1	None
CC554	PDS000003170	Processed fish	8	1	8	None
	PDS000003173	Raw dairy	6	1	6	None
CC573	PDS000000308	Produce	12	3	5	None

*CC, clonal complex; PMSC, premature stop codon; SNP, single-nucleotide polymorphism.
†Not all food–clinical isolate pairs met the ≤50 SNP threshold and, therefore, the number of food–clinical isolate pairs is not necessarily equal the number of food isolates times the number of clinical isolates in each SNP cluster.
‡When detected, *inlA* PMSC was present in all food and clinical isolates used in this analysis within the corresponding SNP cluster. When *inlA* PMSC was not detected, it was indicated as none.
§Indicates SNP clusters that had formal outbreak investigations. In our analysis, PDS000003335 had 1 clinical isolate that was linked with 1 processed dairy isolate (by 2 SNPs); PDS000025078 had 9 clinical isolates that were linked with 1 processed meat isolate (3–9 SNPs); PDS000024989 had 2 clinical isolates that were linked with 1 raw meat isolate (0–2 SNPs), and PDS000000366 had 4r clinical isolates that were linked with 9 processed meat isolates (2–50 SNPs). Among those, 2 outbreak investigations (for the isolates in PDS000025078 and PDS000000366) had processed meat as the implicated food source, whereas the remaining investigations did not have a confirmed source.
¶These SNP clusters had other food categories matching to the clinical isolates by ≤50 SNPs. For clinical isolates associated with multiple food categories, only the clinical–food isolate pairs with the lowest pairwise SNP distance were retained.
#For this SNP cluster, 2 food isolates from different food categories had the same minimum SNP distance to the same clinical isolate, and both food-clinical isolate pairs were retained.

isolates showed intact *inlA*). That pattern is consistent with produce- and mushroom-focused surveys in the United States (*5*,*26*), United Kingdom (*27*), and China (*28*), which consistently reported low frequencies of *inlA* PMSCs in produce-associated isolates (*5*). In addition, we also found that sanitizer tolerance genes were significantly overrepresented in processed fish isolates and underrepresented in raw dairy isolates, consistent with a previous study that sanitizer tolerance genes were frequent among processed fish isolates (*5*). Overall, our findings suggest that food categories might differ in their likelihood of carrying virulence-attenuated *L. monocytogenes* and indicate that using WGS data to identify genetic markers (e.g., *inlA* PMSCs, sanitizer tolerance genes) could help with source attribution of raw versus finished products for some specific food categories.

We hypothesized that food category and presence of *inlA* PMSC were associated with the time between a food isolate collection and subsequent detection of a genetically related clinical isolate. Of note, we found that food category, but not the presence of *inlA* PMSC, was a significant predictor of that time; differences in time interval were observed across food categories. Specifically, isolates from produce had a shorter time for subsequent detection of a genetically related clinical isolate than did isolates from all other food categories.

Several factors likely contribute to the early detection of clinical isolates that are genetically related to produce isolates. Fresh produce typically has a shorter shelf life than other ready-to-eat products (e.g., cheese), possibly creating a narrow window in which contamination can directly lead to human exposure and illness. Contaminated produce typically would be consumed

<20 days after processing, whereas cheese could be consumed >6 months after processing. However, the observed difference is unlikely to be explained solely by the short shelf life of fresh produce, because the time scale observed extends well beyond typical produce shelf life. Differences in consumer storage practices across different food categories (e.g., persons would more likely freeze raw meat than fresh produce) might extend the exposure window for certain food categories. In addition, *L. monocytogenes* contamination might be more frequently driven by repeated reintroduction rather than long-term persistence in packing and fresh-cut facilities (*29*–*31*). Persistent *L. monocytogenes* strains have also been detected less frequently in produce packinghouses (*31*–*33*) than in other food-associated facilities, although persistence over multiple seasons in some produce packing houses has been reported (*34*). Further research is needed to elucidate the persistence of *L. monocytogenes* in produce environments (*29*), but our findings suggest somewhat unique *L. monocytogenes* transmission pathways for produce. Of note, our data also showed that the time between the first food isolate and last subsequent detection of genetically linked clinical isolate is shorter for produce than for other food categories. That finding suggests that produce-linked clusters and outbreaks might often cover relatively short time frames, although long-term multistate outbreaks linked to produce have been reported (*35*). Even extremely small outbreaks putatively linked to produce might need to be further prioritized for outbreak investigations.

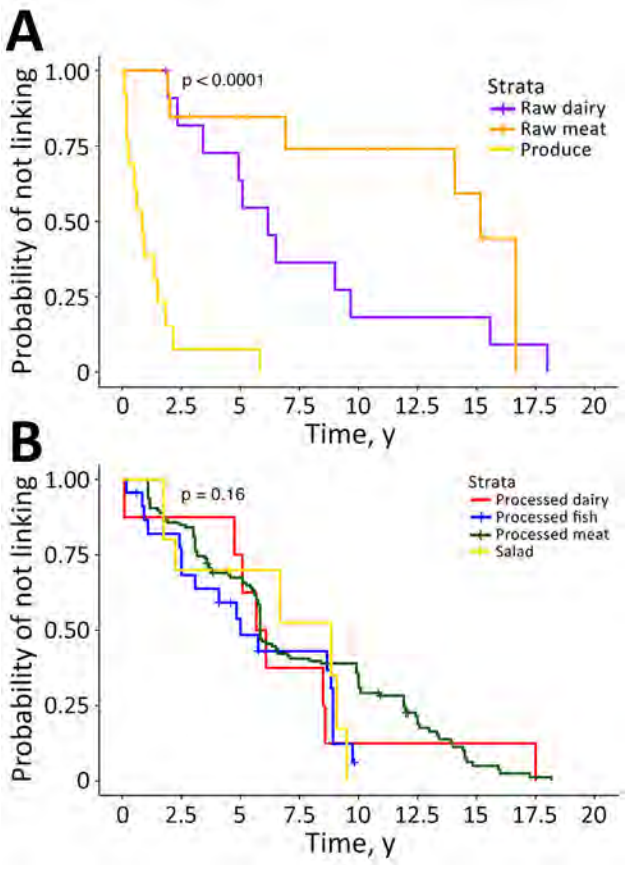

Figure 5. Kaplan-Meier survival curves for the time between food isolate collection and subsequent detection of a genetically related clinical *Listeria monocytogenes* isolate (single-nucleotide polymorphisms ≤50) by food category in study of clustering and source association of clinical and nonclinical *L. monocytogenes* isolates, New York, USA, 2000–2021. p<0.0001 indicates a significant difference in time between food isolate collection and subsequent detection of genetically related clinical isolate by single-nucleotide polymorphism cluster across food categories. A) Raw food categories (produce, raw meat and raw dairy); B) processed food categories (processed dairy, processed fish, processed meat, and salad). Salad refers to ready-to-eat mixed products that might involve additional handling steps and potential contamination during preparation or in retail establishments.

The first limitation of our study is that our dataset only included isolates obtained in NY during 2000–2021. Therefore, the proportion of unclustered and unlinked isolates might be overestimated because some clinical and nonclinical isolates could be clustered or linked with isolates from outside NY. Second, the SNP thresholds used to define clustering and linkage (i.e., ≤20 SNPs for clinical–clinical isolates and ≤50 SNPs for clinical–nonclinical isolates) are supported by previous studies as useful initial cut-offs for screening of potential clusters and sources but might need adjustment based on available epidemiologic data, particularly during outbreak investigations. Consequently, genetic relatedness inferred using those thresholds should be interpreted with caution. Third, genetic similarity alone does not establish epidemiologic linkage. Isolates with low SNP distances might reflect persistence in food production environments or widespread dissemination rather than direct transmission events. This study did not incorporate epidemiologic data (e.g., exposure histories), which limits the ability to confirm specific food sources for clinical cases. Similarly, a limitation of the cluster analysis is that some observed intervals between food isolate collection and subsequent detection of a genetically related clinical isolate were long. Those long intervals reduce confidence in interpreting the food as a continuous source of human exposure. Instead, such associations might reflect repeated reintroduction or cross-contamination across different reservoirs or food commodities. That interpretation is further supported by the observation that some SNP clusters included isolates from multiple food categories (Table 5). Therefore, the time intervals should be interpreted as reflecting temporal patterns of genomic relatedness rather than

direct evidence of long-term source attribution to a single reservoir or commodity. Fourth, the dataset might be subject to biases, including uneven representation across food categories and time periods. In particular, the dataset includes isolates collected through targeted surveillance and research activities, which might result in overrepresentation of certain food categories or production environments. In addition, although thought to be rare, underdiagnosis or underreporting of listeriosis cases might lead to incomplete capture of clinical isolates. Finally, this study relied solely on SNP-based analyses. Incorporating approaches such as core-genome/whole-genome MLST could further strengthen the robustness of the findings, which highlights the need for more comprehensive integration of clinical and nonclinical isolates into unified databases to enable consistent genomic analyses, clustering, and outbreak investigations. In the future, advances in artificial intelligence and machine learning might further enhance the interpretation of surveillance datasets by identifying potential source attribution that are not easily analyzed through conventional approaches.

Acknowledgments

We thank the staff of the Advanced Genomic Technologies Cluster at the Wadsworth Center where library preparation and sequencing were carried out.

For New York State Department of Agriculture and Markets, the whole-genome sequencing was supported by the Food and Drug Administration (FDA) of the US Department of Health and Human Services (HHS) as part of a financial assistance award (5U19FD007122), with 100% funded by FDA/HHS. The contents are those of the authors and do not necessarily represent the official views of, nor an endorsement, by FDA/HHS or the US government. For New York State Department of Health, this work was supported by New York State, the Centers for Disease Control and Prevention Epidemiology and Laboratory Capacity Grant (cooperative agreement no. NU50CK000423), and the Food and Drug Administration's LFFM Grant (cooperative agreement no. 1U19FD007089). For Cornell University, this work was supported by an ELC Foodborne Illness Centers of Excellence grant (no. 5NU50CK000516-05-00) awarded by Health Research Inc.

About the Author

Ms. Samut is a PhD student in food science at Cornell University with a research focus on foodborne bacterial pathogens. Her research interests include molecular epidemiology and evolutionary dynamics of *Salmonella enterica* and *Listeria monocytogenes*.

References

1. Scallan Walter EJ, Cui Z, Tierney R, Griffin PM, Hoekstra RM, Payne DC, et al. Foodborne illness acquired in the United States—major pathogens, 2019. Emerg Infect Dis. 2025;31:669–77.
2. Ferreira V, Wiedmann M, Teixeira P, Stasiewicz MJ. *Listeria monocytogenes* persistence in food-associated environments: epidemiology, strain characteristics, and implications for public health. J Food Prot. 2014;77:150–70. https://doi.org/10.4315/0362-028X.JFP-13-150
3. Maury MM, Tsai YH, Charlier C, Touchon M, Chenal-Francisque V, Leclercq A, et al. Uncovering *Listeria monocytogenes* hypervirulence by harnessing its biodiversity. Nat Genet. 2016;48:308–13. https://doi.org/10.1038/ng.3501
4. Maury MM, Bracq-Dieye H, Huang L, Vales G, Lavina M, Thouvenot P, et al. Hypervirulent *Listeria monocytogenes* clones' adaption to mammalian gut accounts for their association with dairy products. Nat Commun. 2019;10:2488. https://doi.org/10.1038/s41467-019-10380-0
5. Daeschel D, Pettengill JB, Wang Y, Chen Y, Allard M, Snyder AB. Genomic analysis of *Listeria monocytogenes* from US food processing environments reveals a high prevalence of QAC efflux genes but limited evidence of their contribution to environmental persistence. BMC Genomics. 2022;23:488. https://doi.org/10.1186/s12864-022-08695-2
6. He Y, Xu T, Li S, Mann DA, Britton B, Oliver HF, et al. Integrative assessment of reduced *Listeria monocytogenes* susceptibility to benzalkonium chloride in produce processing environments. Appl Environ Microbiol. 2022;88:e0126922. https://doi.org/10.1128/aem.01269-22
7. Stout A, Van Stelten-Carlson A, Marquis H, Ballou M, Reilly B, Loneragan GH, et al. Public health impact of foodborne exposure to naturally occurring virulence-attenuated *Listeria monocytogenes:* inference from mouse and mathematical models. Interface Focus. 2020;10:20190046. https://doi.org/10.1098/rsfs.2019.0046
8. Samut H, Mendez-Vallellanes DV, Hoyt H, Wirth SE, Mingle L, Sauders BD, et al. Retrospective analysis of historical *Listeria monocytogenes* clinical isolates, New York, USA, 2000–2021. Emerg Infect Dis. 2025;31:1883–92. https://doi.org/10.3201/eid3110.241876
9. Pightling AW, Pettengill JB, Luo Y, Baugher JD, Rand H, Strain E. Interpreting whole-genome sequence analyses of foodborne bacteria for regulatory applications and outbreak investigations. Front Microbiol. 2018;9:1482. https://doi.org/10.3389/fmicb.2018.01482
10. Jackson KA, Gould LH, Hunter JC, Kucerova Z, Jackson B. Listeriosis outbreaks associated with soft cheeses, United States, 1998–2014. Emerg Infect Dis. 2018;24:1116–8. https://doi.org/10.3201/eid2406.171051
11. Chen Y, Gonzalez-Escalona N, Hammack TS, Allard MW, Strain EA, Brown EW. Core genome multilocus sequence typing for identification of globally distributed clonal groups and differentiation of outbreak strains of *Listeria monocytogenes*. Appl Environ Microbiol. 2016;82:6258–72. https://doi.org/10.1128/AEM.01532-16
12. Pettengill JB, Rand H, Wang SS, Kautter D, Pightling A, Wang Y. Transient and resident pathogens: intra-facility genetic diversity of *Listeria monocytogenes* and *Salmonella* from food production environments. PLoS One. 2022; 17:e0268470.
13. Van Stelten A, Simpson JM, Ward TJ, Nightingale KK. Revelation by single-nucleotide polymorphism genotyping that mutations leading to a premature stop codon in *inlA* are common among *Listeria monocytogenes* isolates from ready-to-eat foods but not human listeriosis cases. Appl

Environ Microbiol. 2010;76:2783–90. https://doi.org/10.1128/AEM.02651-09
14. Moura A, Lefrancq N, Wirth T, Leclercq A, Borges V, Gilpin B, et al.; Listeria CC1 Study Group. Emergence and global spread of *Listeria monocytogenes* main clinical clonal complex. Sci Adv. 2021;7:eabj9805. https://doi.org/10.1126/sciadv.abj9805
15. Fotopoulou ET, Jenkins C, Barker CR, Painset A, Didelot X, Simbo A, et al. Genomic epidemiology of the clinically dominant clonal complex 1 in the *Listeria monocytogenes* population in the UK. Microb Genom. 2024;10:001155. https://doi.org/10.1099/mgen.0.001155
16. Ikhimiukor OO, Mingle L, Wirth SE, Mendez-Vallellanes DV, Hoyt H, Musser KA, et al. Long-term persistence of diverse clones shapes the transmission landscape of invasive *Listeria monocytogenes*. Genome Med. 2024;16:109. https://doi.org/10.1186/s13073-024-01379-4
17. Chen Y, Gonzalez-Escalona N, Hammack TS, Allard MW, Strain EA, Brown EW. Core genome multilocus sequence typing for identification of globally distributed clonal groups and differentiation of outbreak strains of *Listeria monocytogenes*. Appl Environ Microbiol. 2016;82:6258–72. https://doi.org/10.1128/AEM.01532-16
18. Coipan CE, Friesema IHM, van Hoek AHAM, van den Bosch T, van den Beld M, Kuiling S, et al. New insights into the epidemiology of *Listeria monocytogenes*—a cross-sectoral retrospective genomic analysis in the Netherlands (2010–2020). Front Microbiol. 2023;14:1147137. https://doi.org/10.3389/fmicb.2023.1147137
19. Nightingale KK, Windham K, Martin KE, Yeung M, Wiedmann M. Select *Listeria monocytogenes* subtypes commonly found in foods carry distinct nonsense mutations in *inlA*, leading to expression of truncated and secreted internalin A, and are associated with a reduced invasion phenotype for human intestinal epithelial cells. Appl Environ Microbiol. 2005;71:8764–72. https://doi.org/10.1128/AEM.71.12.8764-8772.2005
20. Magagna G, Gori M, Russini V, De Angelis V, Spinelli E, Filipello V, et al. Evaluation of the virulence potential of *Listeria monocytogenes* through the characterization of the truncated forms of Internalin A. Int J Mol Sci. 2023;24:10141. https://doi.org/10.3390/ijms241210141
21. Manuel CS, Van Stelten A, Wiedmann M, Nightingale KK, Orsi RH. Prevalence and distribution of *Listeria monocytogenes inlA* alleles prone to phase variation and *inlA* alleles with premature stop codon mutations among human, food, animal, and environmental isolates. Appl Environ Microbiol. 2015;81:8339–45. https://doi.org/10.1128/AEM.02752-15
22. Fagerlund A, Wagner E, Møretrø T, Heir E, Moen B, Rychli K, et al. Pervasive *Listeria monocytogenes* is common in the Norwegian food system and is associated with increased prevalence of stress survival and resistance determinants. Appl Environ Microbiol. 2022;88:e0086122. https://doi.org/10.1128/aem.00861-22
23. Wu J, NicAogáin K, McAuliffe O, Jordan K, O'Byrne C. NicAogáin K, McAuliffe O, Jordan K, O'Byrne C. Phylogenetic and phenotypic analyses of a collection of food and clinical *Listeria monocytogenes* isolates reveal loss of function of sigma B from several clonal complexes. Appl Environ Microbiol. 2022;88:e00051-22. https://doi.org/10.1128/aem.00051-22
24. Pérez-Baltar A, Pérez-Boto D, Medina M, Montiel R. Genomic diversity and characterization of *Listeria monocytogenes* from dry-cured ham processing plants. Food Microbiol. 2021;99:103779. https://doi.org/10.1016/j.fm.2021.103779
25. Wagner E, Fagerlund A, Thalguter S, Jensen MR, Heir E, Møretrø T, et al. Deciphering the virulence potential of *Listeria monocytogenes* in the Norwegian meat and salmon processing industry by combining whole genome sequencing and in vitro data. Int J Food Microbiol. 2022;383:109962. https://doi.org/10.1016/j.ijfoodmicro.2022.109962
26. Amarasekara NR, Swamy AS, Paudel SK, Jiang W, Li K, Shen C, et al. Hypervirulent clonal complex (CC) of *Listeria monocytogenes* in fresh produce from urban communities. Front Microbiol. 2024;15:1307610. https://doi.org/10.3389/fmicb.2024.1307610
27. Smith A, Hearn J, Taylor C, Wheelhouse N, Kaczmarek M, Moorhouse E, et al. *Listeria monocytogenes* isolates from ready to eat plant produce are diverse and have virulence potential. Int J Food Microbiol. 2019;299:23–32. https://doi.org/10.1016/j.ijfoodmicro.2019.03.013
28. Chen M, Cheng J, Wu Q, Zhang J, Chen Y, Zeng H, et al. Prevalence, potential virulence, and genetic diversity of *Listeria monocytogenes* isolates from edible mushrooms in Chinese markets. Front Microbiol. 2018;9:1711. https://doi.org/10.3389/fmicb.2018.01711
29. Belias A, Sullivan G, Wiedmann M, Ivanek R. Factors that contribute to persistent *Listeria* in food processing facilities and relevant interventions: a rapid review. Food Control. 2022;133:133. https://doi.org/10.1016/j.foodcont.2021.108579
30. Sullivan G, Orsi RH, Estrada E, Strawn L, Wiedmann M. Whole-genome sequencing-based characterization of *Listeria* isolates from produce packinghouses and fresh-cut facilities suggests both persistence and reintroduction of fully virulent *L. monocytogenes*. Appl Environ Microbiol. 2022;88:e0117722. https://doi.org/10.1128/aem.01177-22
31. Estrada EM, Hamilton AM, Sullivan GB, Wiedmann M, Critzer FJ, Strawn LK. Prevalence, persistence, and diversity of *Listeria monocytogenes* and *Listeria* species in produce packinghouses in three U.S. states. J Food Prot. 2020;83:277–86. https://doi.org/10.4315/0362-028X.JFP-19-411
32. Murugesan L, Kucerova Z, Knabel SJ, LaBorde LF. Predominance and distribution of a persistent *Listeria monocytogenes* clone in a commercial fresh mushroom processing environment. J Food Prot. 2015;78:1988–98. https://doi.org/10.4315/0362-028X.JFP-15-195
33. Chen Y, Simonetti T, Peter K, Jin Q, Brown E, LaBorde LF, et al. Genetic diversity of *Listeria monocytogenes* isolated from three commercial tree fruit packinghouses and evidence of persistent and transient contamination. Front Microbiol. 2022;12:756688. https://doi.org/10.3389/fmicb.2021.756688
34. Simonetti T, Peter K, Chen Y, Jin Q, Zhang G, LaBorde LF, et al. Prevalence and distribution of *Listeria monocytogenes* in three commercial tree fruit packinghouses. Front Microbiol. 2021;12:652708. https://doi.org/10.3389/fmicb.2021.652708
35. Palacios A, Vasser M, Madad A, Ivory S, Edwards L, Donovan D, et al. Two concurrent outbreaks of *Listeria monocytogenes* infections linked to packaged salads, United States, 2014–2022. Emerg Infect Dis. 2025;31:2216–24. https://doi.org/10.3201/eid3112.250989

Address for correspondence: Renato H. Orsi, Department of Food Science, Cornell University, 326 Stocking Hall, Ithaca, NY 14853, USA; email: rho2@cornell.edu

Dual PCR–Sanger Sequencing Assay for Simultaneous *sqle*-Based Identification and Resistance Detection in *Trichophyton* Species

Nissrine Abou-Chakra, Karin M. Jørgensen, Karen Marie Thyssen Astvad, Maiken Cavling Arendrup

Trichophyton fungal infections are common and increasingly complicated by terbinafine resistance. To support accurate molecular identification and resistance profiling, we provide a validated dataset of full-length squalene epoxidase (*sqle*) gene sequences from 493 *Trichophyton* isolates representing 18 species, addressing limited availability and misannotation of *sqle* sequences in public databases, particularly within the *T. mentagrophytes* complex. On the basis of that dataset, we designed 2 Sanger sequencing assays for simultaneously identifying species and detecting resistance-associated mutations. One targets the full-length gene, whereas the other amplifies a short region capturing all key resistance hotspots and species-specific single-nucleotide polymorphisms. The partial assay was evaluated on 66 clinical specimens and enabled clinically relevant species identification without internal transcribed spacer sequencing, supporting culture-independent detection. Of note, this approach differentiates *T. indotineae* from closely related species, overcoming a key diagnostic limitation and supporting clinical decision-making, surveillance, and management of resistant infections, despite limited resolution within certain species complexes.

Trichophyton species fungi cause infections of the skin, nails, and hair and are estimated to affect 20%–25% of persons during their lifetimes (*1*). Clinical manifestations include pruritus, erythema, scaling, alopecia, and inflammation (*2*). Although infections are often considered minor, chronic or extensive dermatophytosis can cause considerable illness, involving prolonged treatment, increased healthcare use, and impaired quality of life (*3*). The recent rising prevalence of terbinafine-resistant *Trichophyton* strains is associated with therapeutic failure, underscoring the need for rapid and reliable diagnostics to detect resistance, guide therapy, and thereby limit transmission (*4*–*6*).

Traditional culture-based diagnostics are slow and exhibit suboptimal sensitivity, especially in onychomycosis or after antifungal therapy (*7*). Molecular assays targeting the internal transcribed spacer (ITS) region of ribosomal DNA are widely adopted because of its high copy number and potential for improved identification (*8*). However, limited sequence variation in this region hinders reliable discrimination among closely related *Trichophyton* species, particularly within the *T. mentagrophytes* complex (*9*,*10*). Of note, *T. indotineae*, an emerging and often terbinafine-resistant species within this complex, might be misidentified by certain ITS-based diagnostic kits and commercial platforms such as DermaGenius 2.0 (PathoNostics, https://www.pathonostics.com) (*11*–*16*). Those challenges are further compounded by recent taxonomic revisions and inconsistencies in available reference databases (*9*,*12*).

The *sqle* gene (alternatively, *erg1*) encodes squalene epoxidase (SQLE), the molecular target of terbinafine. Mutations at conserved hotspot positions (e.g., L393, F397, F415, and H440) reduce drug binding while preserving enzymatic function, thereby conferring terbinafine resistance (*17*). Recent studies from India, Europe, and North America document the global increase of resistant SQLE variants, particularly in *T. indotineae* and *T. rubrum* (*18*–*21*). However, the absence of robust, curated, and taxonomically validated *sqle* reference sequences limits the diagnostic and surveillance utility of this gene.

In this study, we generated a curated, taxonomically validated dataset of full-length *sqle* sequences, supported by reliable ITS-based identification, to address limitations in existing databases. We

Author affiliations: Statens Serum Institut, Copenhagen, Denmark (N. Abou-Chakra, K.M. Jørgensen, K.M.T. Astvad, M.C. Arendrup); Rigshospitalet, Copenhagen (M.C. Arendrup); University of Copenhagen, Copenhagen (M.C. Arendrup)

DOI: https://doi.org/10.3201/eid3209.260819

also present a sequencing-based workflow enabling simultaneous species identification and detection of terbinafine resistance-conferring *sqle* mutations in *Trichophyton* directly from clinical specimens or isolates.

Materials and Methods

Strains and Clinical Samples

We included a total of 493 clinical *Trichophyton* isolates (Table 1; Appendix Table 1, https://wwwnc.cdc.gov/

Table 1. MICs determined using the EUCAST E.Def 11.0 reference method for dermatophytes in study of dual PCR–Sanger sequencing assay for simultaneous *sqle*-based identification and resistance detection in *Trichophyton* species†

Species	SQLE amino acid alteration (intrinsic SNPs)	Terbinafine MIC, mg/L		No. isolates
		Modal MIC‡	Range	
T. indotineae, n = 105	WT	ND	0.03–0.06	3
	L393F	ND	>4	1
	L393S	ND	0.5–1	3
	F397L	>4	2–>4	63
	F397L/Y414H	ND	>4	1
	F397L/A448T	ND	>4	6
	Q408L	2	1–4	20
	F415C	ND	1	1
	F415L	ND	0.5	1
	A448T	ND	0.03–0.125	6
T. interdigitale, n = 26	WT	0.008/0.016	≤0.004-0.06	21
	L393F	ND	>4	1
	L393S	ND	0.25–1	3
	F415L	ND	0.25	1
T. mentagrophytes ITS genotype DK-I, n = 1§	WT (SNPs: N276¶, F419 and T454)	ND	0.06	1
T. mentagrophytes ITS genotype DK-II, n = 4§	WT (SNPs: N276¶, F419 and P454)	ND	0.008–0.06	4
T. mentagrophytes ITS genotype III, n = 2§	WT (SNPs: N276¶, F419 and T454)	ND	0.016–0.03	2
T. mentagrophytes ITS genotype III*, n = 9§	WT (SNPs: N276¶, F419 and T454)	ND	0.008–0.03	9
T. mentagrophytes ITS genotype IV, n = 1§	WT (SNPs: K276¶, L419 and T454)	ND	0.03	1
T. mentagrophytes ITS genotype VII, n = 2§	WT (SNPs: N276¶, F419 and T454)	ND	0.016–0.03	2
T. rubrum, n = 285	WT	0.016	≤0.004–0.06	143
	Y110C¶	ND	0.008	1
	I121M¶	ND	0.03	1
	I121M¶/F415S	ND	0.5	1
	L335F¶/F415S	ND	2	1
	L393del	ND	4	2
	L393F	ND	>4	7
	L393F/Y394del	ND	>4	2
	L393S	0.5	0.25–2	15
	S395_I396insS	ND	0.5	3
	F397I	1	0.25–1	11
	F397L	4	1->4	78
	Y414H	ND	0.03–0.06	2
	F415L	ND	0.125	1
	F415S	ND	0.125–1	3
	H440Y	ND	0.016–0.125	9
	A448T	ND	0.03	1
	A448V	ND	0.004	1
	L451P	ND	0.125	1
	C476Y	ND	0.016–0.03	2
T. soudanense, n = 2§	WT	ND	≤0.004–0.008	2
T. tonsurans, n = 16§	WT	0.016	0.008–0.06	16
T. violaceum, n = 24§	WT	0.03	0.004–0.125	24
T. equinum, n = 1§	WT	ND	0.03	1
T. simii, n = 1§	WT	ND	≤0.004	1
T. erinacei, n = 2§#	WT	ND	Not tested	2
T. concentricum, n = 1§#	WT	ND	Not tested	1
T. europaeum, n = 1§	WT	ND	0.03	1
T. benhamiae var. benhamiae/var. luteum, n = 10§	WT	ND	0.004–0.06	10

†EUCAST tentative epidemiological cutoff values for terbinafine (0.125 mg/L for *T. indotineae* and 0.03 mg/L for *T. rubrum*) were used to classify isolates as wild-type or non–wild-type. Underlined SQLE alterations are associated with terbinafine MICs above the corresponding tentative epidemiological cutoff values. An expanded version of this table appears in the Appendix (https://wwwnc.cdc.gov/EID/article/32/9/26-0819-App1.pdf). DK-I, unassigned I; DK-II, unassigned II; EUCAST, European Committee on Antimicrobial Susceptibility Testing; ITS, internal transcribed spacer; ND, not determined; SNP, single-nucleotide polymorphism; SQLE, squalene epoxidase; WT, wild-type.
‡Modal MIC is reported only for distributions comprising >10 isolates. Bimodal distributions are reported as both modal MICs.
§Indicates that all isolates of the indicated species were wild-type. DK-I and DK-II denote novel ITS genotypes identified in this study.
¶Indicates that the codon is not covered by sequencing of the short *sqle* fragment (spanning amino acids H376–V483).
#EUCAST susceptibility testing was not performed.

EID/article/32/9/26-0819-App1.pdf), collected during 2022–2025 and representing 18 species. We confirmed species identification by ITS sequencing, showing 100% identity to reference sequences (*4*,*16*,*22*) (Appendix Table 2). *T. schoenleinii* was unavailable in culture but was included on the basis of its *sqle* sequence, which we retrieved from GenBank (accession no. GCA_018357685.2). We used the *sqle* sequence for *Microsporum canis* as an outgroup for phylogenetic rooting, following the procedures described in the CLC Genomics Workbench manual 24.0.4 (QIAGEN,https://www.qiagen.com). In addition, we included 66 clinical specimens (skin scrapings, nail clippings, scalp, and hair) that previously tested positive for *Trichophyton* spp. using an in-house ITS-based PCR (*23*) that does not distinguish among *T. mentagrophytes*, *T. interdigitale*, and *T. indotineae*.

DNA Extraction

For fungal isolates, we suspended colonies in 400 µL of NUCLISENS Lysis Buffer (bioMérieux, https://www.biomerieux.com), of which we used 200 µL for DNA extraction on the automated eMAG system (bioMérieux) according to protocol B, which includes automated nucleic acid purification to reduce the presence of potential PCR inhibitors. We eluted DNA in 100 µL of NUCLISENS Extraction Buffer 3 (bioMérieux). We incubated clinical samples overnight at 56 °C in 1,000 µL NUCLISENS Lysis Buffer with 50 µL proteinase K (QIAGEN). Subsequently, we added 100 µL of 1 M dithiothreitol (DTT) (Sigma-Aldrich) and incubated samples for 30 minutes before centrifugation at 22,000 × *g* for 5 minutes. We then subjected 1,000 µL of clarified supernatant to extraction on the eMAG system according to protocol B and eluted it in 50 µL of NUCLISENS Extraction Buffer 3. Each run included a negative extraction control. We stored extracted DNA at −20 °C until further analysis.

Antifungal Susceptibility Testing

We determined MICs in RPMI 1640 medium according to the EUCAST E.Def 11.0 reference method (*24*). We prepared terbinafine (final concentration after inoculation 0.004–4 mg/L) from frozen stock solutions. We adopted EUCAST tentative epidemiologic cutoff values (TECOFFs) of terbinafine as 0.125 mg/L for *T. indotineae* and 0.03 mg/L for *T. rubrum* for classification as wild-type or non–wild-type (*25*).

Amplification and Sequencing of *sqle*

Two PCR strategies enabled species identification and detection of resistance-associated mutations: full-length *sqle* amplification and sequencing for cultured isolates and partial *sqle* amplification for clinical specimens. All primers were *Trichophyton*-specific. Each run included a positive fungal DNA control and a no-template control. PCR product purification and sequencing were performed by Macrogen Europe BV (https://www.macrogen-europe.com).

Full-Length *sqle*

We performed amplification using primers TRI-SE-F (5′-GGTGACAGCGACAAGTGCC-3′) and TRI-SE-R (5′-AGTCCAACCRACCCCAGTCA-3′; R = A/G). PCR reactions (25 µL) contained 2 µL genomic DNA, 0.4 µM of each primer, 12.5 µL Extract-N-Amp PCR ReadyMix (Sigma-Aldrich, https://www.sigmaaldrich.com), and 8.5 µL UltraPure DNase/RNase-free water (Thermo Fisher Scientific, https://www.thermofisher.com). Cycling conditions were 95°C for 30 seconds, followed by 35 cycles of 95°C for 30 seconds, 57°C for 45 seconds, and 72°C for 90 seconds. We performed bidirectional sequencing using the amplification primers and internal primers TRI-SE-S1 (5′-GGAATATCTCCCCATACAACCAG-3′) and TRI-SE-S2 (5′-AACGCAGCTTCAAAYGAGGG-3′; Y = C/T).

Partial *sqle*

We amplified a 388-bp fragment spanning positions 1125–1512 of the full-length *sqle* sequence and encompassing clinically relevant terbinafine resistance–associated mutations, as well as species-specific single-nucleotide polymorphisms (SNPs) for species-level identification, using primers F0 (5′-CCACTGGCAACGGAAGTC-3′) and R0 (5′-ATACGAAAGGAAGGATGACCC-3′). PCR reactions (25 µL) contained 5 µL template DNA, 0.4 µM of each primer, 12.5 µL Extract-N-Amp PCR ReadyMix (Sigma-Aldrich), and 5.5 µL UltraPure DNase/RNase-free water. Cycling conditions were 95°C for 30 seconds, followed by 35 cycles of 95°C for 30 seconds, 58°C for 45 seconds, and 72°C for 90 seconds. We performed sequencing using the amplification primers.

Sequence Analysis and Phylogenetics

We quality-checked, trimmed, and assembled raw reads; we aligned full-length sequences using CLC Main Workbench (QIAGEN). Species and genotype assignments were based on sequence alignment and comparison of informative species- and genotype-specific SNP profiles within the analyzed region. We identified terbinafine resistance–associated mutations by evaluation of nucleotide substitutions at previously described SQLE resistance hotspots. We calculated pairwise SNP differences and reconstructed phylogenetic relationships using the neighbor-joining

algorithm with the Kimura 2-parameter (K2P/K80) model. We evaluated node support by 1,000 bootstrap replicates.

Results

Complete Intraspecies Conservation in Wild-Type Isolates

We obtained full-length *sqle* sequences for 493 terbinafine wild-type and non–wild-type isolates (Table 1; Appendix Table 1) representing phylogenetically and epidemiologically relevant taxa and aligned them within each taxon to assess intraspecific conservation. We identified high-frequency wild-type *sqle* alleles in 244 terbinafine-susceptible isolates, including *T. rubrum* (143/285), *T. interdigitale* (21/26), and *T. indotineae* (3/105), all showing complete sequence conservation within each species. The same pattern was also observed for all ITS genotypes of *T. mentagrophytes* (n = 19), *T. violaceum* (n = 24), *T. benhamiae* (n = 10), *T. tonsurans* (n = 16), and other less common *Trichophyton* species.

Only *sqle* sequences from isolates with wild-type MICs and no SQLE amino acid alterations were included in the curated reference dataset. A strict wild-type consensus was defined for each taxon. Those sequences have been deposited in GenBank (accession nos. PZ614143–PZ614159 and PX205352) and, together with the *sqle* sequence of *T. schoenleinii*, constitute the final reference dataset (Appendix Table 2).

We analyzed the spectrum of SQLE amino acid alterations and corresponding MICs in the remaining isolates. We observed low-frequency variants (A448T, A448V, Y110C, C476Y, and I121M) sporadically (n = 12); those variants were confined to *T. rubrum* and *T. indotineae* isolates with MICs within the species-specific wild-type range. The Y414H substitution was detected in 2 *T. rubrum* isolates with MICs around the TECOFF. Those variants were not considered part of the predominant wild-type allele population. The remaining 235 isolates harbored missense mutations affecting hotspot amino acid residues within the catalytic domain of SQLE and were associated with elevated terbinafine MICs (Table 1; Appendix Table 1).

Species-Level Discrimination of *Trichophyton* Using Full-Length *sqle* Sequencing

Pairwise comparisons of full-length *sqle* consensus sequences revealed substantial interspecies SNP variation across *Trichophyton*, enabling discrimination at multiple taxonomic levels (Appendix Table 3, Figure 1). Polymorphisms were distributed throughout the gene, with species-specific and genotype-specific patterns capturing both interspecies and intracomplex diversity. SNP differences ranged from complete sequence identity (0 SNPs) among closely related taxa to 92 SNPs within *Trichophyton* and 341–351 SNPs relative to the outgroup *M. canis*. Phylogenetic analyses showed clear separation between species and major clades (Figure 1).

The *T. rubrum* complex was distinct from the *T. mentagrophytes* complex and other species (≈65–75 SNPs). Of note, *T. indotineae*, within the *T. mentagrophytes* complex, differed from the *T. rubrum* complex

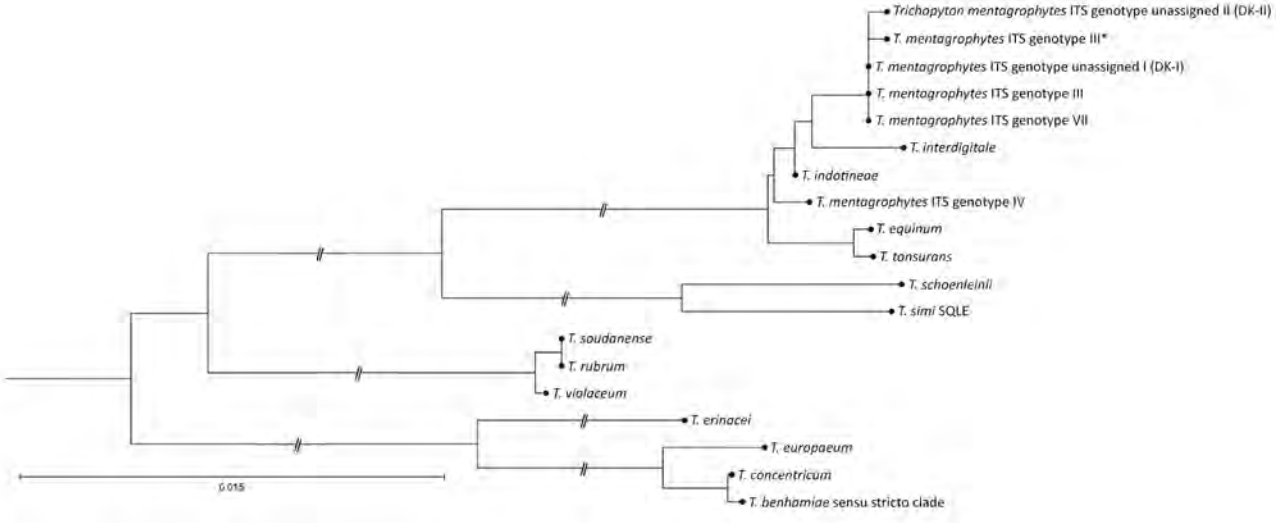

Figure 1. Phylogenetic tree of *Trichophyton* species inferred from sequence variation in the full-length squalene epoxidase (*sqle*) gene in study of dual PCR–Sanger sequencing assay for simultaneous *sqle*-based identification and resistance detection in *Trichophyton* species. Within the *T. mentagrophytes* species complex, isolates identified as *T. mentagrophytes* represented ITS genotypes III, III*, IV, and VII. The remaining *T. mentagrophytes* isolates formed 2 consensus sequences that did not show 100% identity to any sequence in GenBank and were designated DK-I and DK-II. Scale bar indicates number of substitutions per site.

by 65–66 SNPs distributed across the full-length *sqle* gene, including 6 resulting in amino acid substitutions. Within the *T. rubrum* complex, divergence was minimal: *T. rubrum* and *T. soudanense* shared identical sequences, whereas *T. violaceum* differed by 2 SNPs (positions 186 and 522), the latter resulting in a nonsynonymous substitution. *T. tonsurans* and *T. equinum* formed a closely related pair, differing by only 2 SNPs (positions 117 and 1256), but diverged from *T. indotineae* by 7 SNPs, from the *T. mentagrophytes* complex by 8–12 SNPs, and from *T. interdigitale* by 13 SNPs.

More distantly related species showed ≥60 SNP differences relative to both the *T. mentagrophytes* and *T. rubrum* complexes and were individually clearly separable. *T. simii* and *T. schoenleinii* differed by 24 SNPs, 4 of which were nonsynonymous. Within the *T. benhamiae* complex, sequence diversity was notable. *T. concentricum*, the only strictly anthropophilic species within the complex (*26*), differed from *T. benhamiae* by a single SNP, whereas *T. europaeum* differed by 10 SNPs and *T. erinacei* differed by 42 SNPs.

Within closely related taxa of the *T. mentagrophytes* complex, SNP differences were lower but remained structured. *T. interdigitale* showed the greatest divergence, differing from *T. indotineae* by 6 synonymous SNPs (positions 169, 642, 882, 1251, 1457, and 1460) and from other genotypes by 8 to 9 SNPs, comprising both synonymous and nonsynonymous changes.

Similarly, *T. indotineae* differed from other genotypes within the *T. mentagrophytes* complex by 3–5 SNPs, reflecting a structured pattern of variation. It differed from unassigned lineage II and genotype III* by 5 SNPs (3 synonymous: 717, 996, 1251; 2 nonsynonymous: 828, 1317), whereas divergence from unassigned lineage I and genotypes III and VII was limited to 4 SNPs at the same loci; position 717 was conserved across those groups. The closest relationship was observed with genotype IV, from which *T. indotineae* differed by only 3 synonymous SNPs (positions 246, 813, 1391).

Within the *T. mentagrophytes* complex, unassigned lineage I and genotypes III and VII shared identical *sqle* sequences. Those showed limited variation relative to unassigned lineage II, genotype III*, and genotype IV. Genotype IV was the most divergent, differing by 7–8 SNPs from the other genotypes. In contrast, genotype III* and unassigned lineage II each differed from the identical group by a single synonymous SNP at position 717 for genotype III* and position 1422 for unassigned lineage II. Although the number of SNP differences among closely related members of the *T. mentagrophytes* complex was limited, distinct SNP profiles enabled discrimination of *T. indotineae*, *T. interdigitale*, and the investigated lineages/genotypes (Appendix Table 4).

Lineage-Specific Variation Within the *T. mentagrophytes* Complex

Comparative analysis of full-length 489-aa sequences within the *T. mentagrophytes* complex revealed distinct lineage-associated patterns without effects on the susceptibility (MICs 0.008–0.06 mg/L) (Figure 2). A group of isolates consistently harbored N276 and F419, including 13 isolates assigned to ITS genotypes III (n = 2), III* (n = 9), and VII (n = 2), and 5 unassigned isolates (unassigned lineage I, n = 1; unassigned lineage II, n = 4). In addition to the characteristic N276 and F419 residues, all unassigned lineage II isolates harbored a unique alteration at position P454, in contrast with an alteration at position T454 in all other genotypes and species across the genus. In contrast, the *T. mentagrophytes* ITS genotype IV isolate differed from other genotypes in displaying K276 and L419, a pattern shared with *T. interdigitale* and *T. indotineae*.

Species Identification Using 388-bp *sqle* Fragment Sequencing

A second primer set was designed to amplify a 388 bp fragment of the *sqle* gene (≈1531–1534 bp from start to stop codon, depending on species) spanning amino acid residues H376 to V483 within the catalytic domain and including known terbinafine-resistance hotspots (*27*). Despite its short length, this segment exhibited sufficient interspecies SNP variation to enable discrimination of most *Trichophyton* species and to support resistance detection (Appendix Table 5, Figure 2). Phylogenetic reconstruction supported its discriminatory capacity, yielding well-supported clades corresponding to major species complexes (Figure 3). The *T. mentagrophytes* ITS genotypes were clearly delineated from *T. indotineae* and *T. interdigitale*, which were also resolved from each other. The *T. rubrum* complex (*T. rubrum*, *T. violaceum*, and *T. soudanense*) formed a coherent cluster, although species-level resolution was not achieved. Within the *T. benhamiae* clade, *T. erinacei* was clearly differentiated (14 SNPs), whereas *T. europaeum*, *T. benhamiae*, and *T. concentricum* clustered together. Finally, *T. schoenleinii* and *T. simii* formed an independent lineage.

Clinical Validation of the Partial *sqle* PCR

We applied the partial *sqle* PCR directly to DNA from 66 clinical specimens (skin, hair, and nails) previously positive for *Trichophyton* spp. using an in-house ITS-based PCR unable to distinguish among *T. mentagrophytes*, *T. interdigitale* and *T. indotineae*. All samples

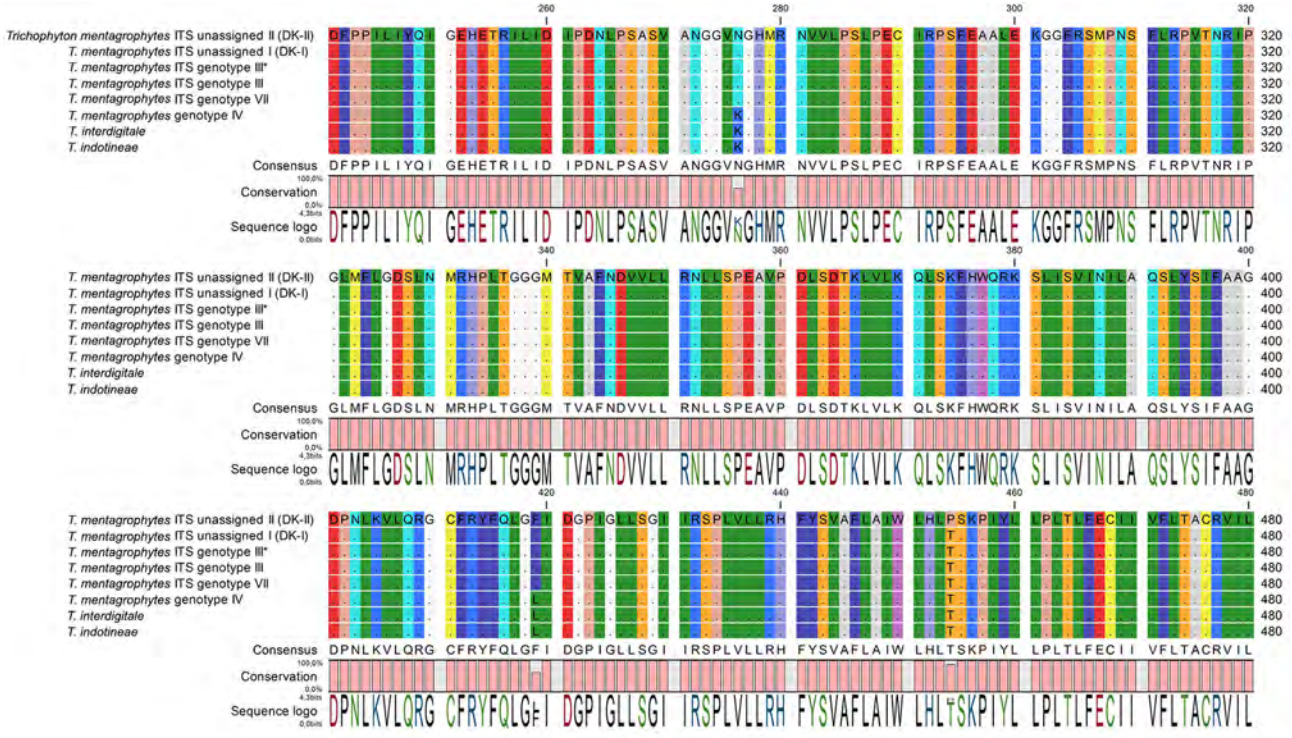

Figure 2. Amino acid polymorphisms in squalene epoxidase within the *T. mentagrophytes* complex in the study of dual PCR-Sanger sequencing assay for simultaneous *sqle*-based identification and resistance detection in *Trichophyton* species. Alignment of SQLE amino acid sequences showing lineage-specific patterns: N276/F419 (ITS genotypes III/III*/VII and unassigned genotypes [DK-I–II]), P454 unique to DK-II, and K276/L419 in ITS genotype IV (shared with *T. interdigitale* and *T. indotineae*).

produced amplicons of the expected size, enabling sequencing-based species identification as well as detection of resistance-associated mutations (Table 2).

The 28 samples previously identified as *T. mentagrophytes* complex were unambiguously resolved by *sqle* sequencing as *T. interdigitale* (n = 16), *T. indotineae* (n = 11), and *T. mentagrophytes* (n = 1). All *T. interdigitale* samples were wild-type, whereas 10 of 11 *T. indotineae* samples harbored ≥1 nonsynonymous alterations, including known terbinafine resistance–associated substitutions: Q408L (n = 4), F397L (n = 3), and F397L/A448T (n = 1). In addition, 24 samples from the *T. rubrum* complex were confirmed, of which 19 were wild-type and 5 harbored nonsynonymous substitutions (L393S, n = 1; F397L, n = 2; F415S, n = 1; L427M, n = 1).

We confirmed 4 scalp and skin samples initially identified as *T. tonsurans/T. equinum* as *T. tonsurans*, all with wild-type *sqle* sequences. Two hair and scalp specimens previously identified as *T. violaceum* and 4 additional scalp specimens previously identified only at the genus level were assigned to the *T. rubrum* complex, all without resistance-associated *sqle* mutations. Four hair and skin scraping specimens initially assigned to the *T. benhamiae* complex were resolved as *T. benhamiae* sensu stricto, all with wild-type sequences and distinct from *T. erinacei*.

Discussion

Early and accurate identification and susceptibility classification of *Trichophyton* isolates are essential for clinical management, source tracing, and epidemiologic surveillance, particularly in the context of terbinafine resistance, highly transmissible anthropophilic lineages, and increased person-to-person transmission, including sexual transmission (*28*–*33*). Morphological differentiation remains challenging because of phenotypic variability and overlap between species (*34*–*36*). Historically, species within the *T. mentagrophytes* complex were grouped broadly, contributing to taxonomic ambiguity. Although molecular approaches improved resolution, taxonomic confusion remained. For example, isolates within the *T. mentagrophytes/interdigitale* complex were often assigned to *T. interdigitale* (*36*), and species from the *T. benhamiae* complex, including *T. erinacei*, were misclassified at *T. mentagrophytes* complex (*26*). The 2017 taxonomy revision by de Hoog et al. (*34*) provided a more structured framework, yet genetic resolution remains challenging. ITS sequencing often lacks discriminatory power

within closely related taxa, including the *T. mentagrophytes* and *T. rubrum* complexes, where limited variation does not reflect clinical or epidemiologic diversity (*37*,*38*). That shortfall is particularly relevant for *T. indotineae* (formerly *T. mentagrophytes* type VIII), now recognized as a distinct species of clinical importance (*9*,*36*,*37*), and for type VII, an emerging anthropophilic genotype associated with genital lesions among men who have sex with men (*30*,*33*).

BLAST-based identification is further limited by inconsistent database annotation, lack of standardized genotype classification, and ongoing taxonomic revisions. Consequently, identical ITS sequences might yield multiple high-scoring (even 100%) matches across closely related species, requiring manual curation and preventing reliable species-level identification. Those issues, combined with outdated database entries and limited ITS variability, reduce the utility of ITS-based diagnostics and highlight the need for curated reference databases and complementary genetic markers.

Alternative genetic targets, including translation elongation factor 1-α, β-tubulin, calmodulin, 28S rDNA and mating-type genes, offer improved resolution (*39*–*42*). However, their routine use is limited by less universal primers, the need for species-specific or optimised PCR protocols, limited reference data, and the increased complexity and cost of multilocus sequencing, limiting their applicability in routine diagnostics.

Against this background, we investigated *sqle* as a combined marker for *Trichophyton* identification and terbinafine-resistance detection. Successful amplification and sequencing across all strains generated a robust reference dataset and demonstrated broad primer applicability. Complete intraspecies conservation supports strong functional constraint, whereas interspecies variation enables discrimination of closely related taxa. Phylogenetically, the *T. rubrum* and *T. benhamiae* complexes were clearly distinct from each other and from the *T. mentagrophytes* complex.

Of note, the full-length *sqle* gene enables reliable discrimination of *T. indotineae* and *T. interdigitale* from other members of the *T. mentagrophytes* complex, including genotype IV. That distinction is clinically critical, because both are anthropophilic rather than zoophilic, and *T. indotineae* is frequently terbinafine-

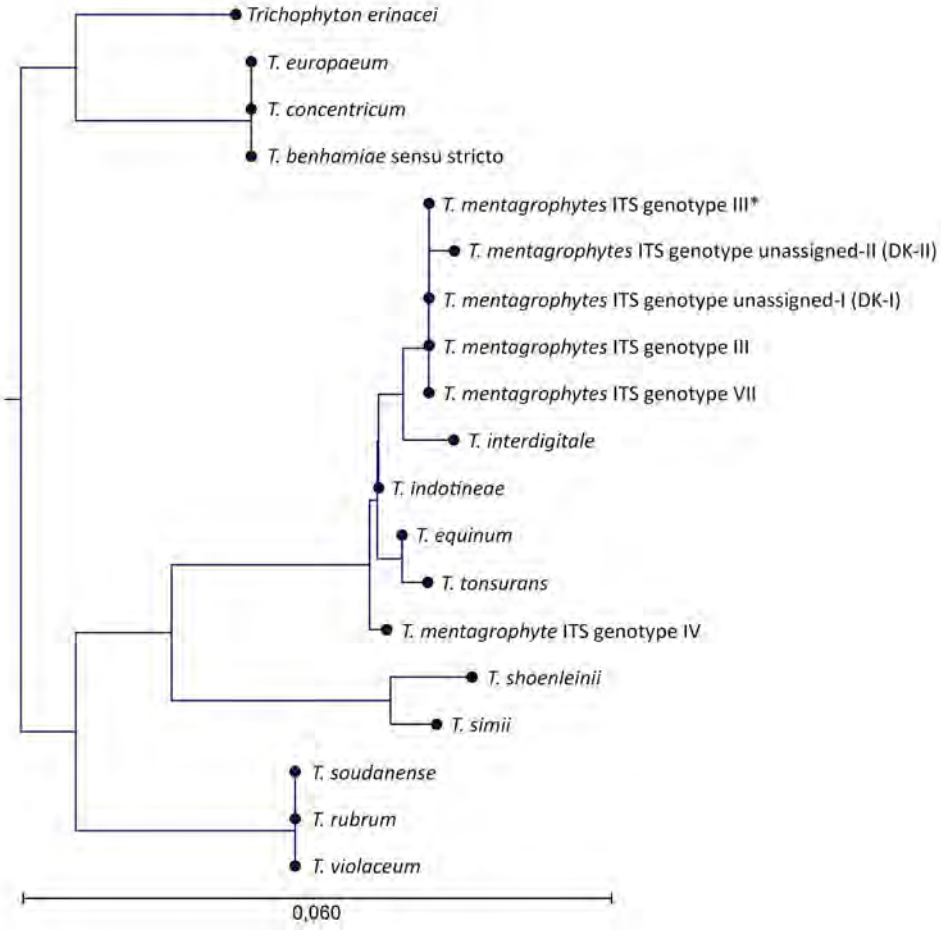

Figure 3. Phylogenetic tree of *Trichophyton* species inferred from sequence differences in the partial 388-bp squalene epoxidase (*sqle*) gene fragment in study of dual PCR–Sanger sequencing assay for simultaneous *sqle*-based identification and resistance detection in *Trichophyton* species. Within the *T. mentagrophytes* species complex, isolates identified as *T. mentagrophytes* represented ITS genotypes III, III*, IV, and VII. The remaining *T. mentagrophytes* isolates formed 2 consensus sequences that did not show 100% identity to any sequence in GenBank and were designated DK-I and DK-II. Scale bar indicates number of substitutions per site.

Table 2. Species identification and *sqle* alterations detected by direct PCR and sequencing of a partial 388-bp *sqle* gene fragment from clinical specimens positive for *Trichophyton* spp. in study of dual PCR–Sanger sequencing assay for simultaneous *sqle*-based identification and resistance detection in *Trichophyton* species*

Initial ITS-based identification	Specimen types	No. clinical samples	Final species identification (*sqle* sequencing)	SQLE variant(s)
T. rubrum	Nail, skin scraping	24	*T. rubrum complex*†	Wild-type, n = 19 L393S, n = 1 F397L, n = 2 F415S, n = 1 L427M, n = 1
T. mentagrophytes complex‡	Nail, skin scraping	28	*T. interdigitale* (n = 16) *T. mentagrophytes* (n = 1) *T. indotineae* (n = 11)	Wild-type, n = 16 Wild-type, n = 1 Q408L, n = 4 F397L, n = 3 A448T, n = 2 F397L/A448T, n = 1 Wild-type, n = 1
T. tonsurans/*T. equinum*	Hair, skin scraping	4	*T. tonsurans*	Wild-type, n = 4
T. violaceum	Hair, scalp	2	*T. rubrum* complex†	Wild-type, n = 2
Trichophyton spp.‡	Scalp	4	*T. rubrum* complex†	Wild-type, n = 4
T. benhamiae complex	Hair, skin scraping	4	*T. benhamiae* sensu stricto clade	Wild-type, n = 4

*Initial species identification was based on ITS analysis, with final identification resolved by *sqle* sequencing. Detected *sqle* variants include both wild-type and amino acid substitutions within the terbinafine resistance hotspot region. ITS, internal transcribed spacer; SQLE, squalene epoxidase.
†Indicates assignment to species complexes where species-level resolution was not achieved.
‡Further identification not possible.

resistant and associated with more persistent and outbreak-prone infections. The remaining isolates within *T. mentagrophytes* complex belonged to established genotypes (III, III*, IV, and VII), which are largely associated with distributions in Europe (*43*). Genotype IV showed greater divergence (7–9 SNPs) but remained closest to *T. indotineae* (3 SNPs). Five isolates formed 2 ITS consensus sequences **(**DK-I and DK-II**)** that could not be assigned to any currently reported ITS genotypes; the closest database matches showed only 99.5%–99.6% sequence identity. In contrast, 3 ITS genotypes (DK-I, III, and VII) shared identical *sqle* gene sequences and differed minimally from others, indicating that additional markers such as ITS are required if fine-scale resolution within this complex is required. Additional *sqle* diversity might exist in unrepresented genotypes. The genetic findings were further reflected at the amino acid level: genotype IV shared K276 and L419 with *T. indotineae* and *T. interdigitale*, whereas other genotypes consistently carried N276 and F419. Reports of N276 alone might therefore reflect incomplete *sqle* reference sequences lacking the region encompassing position 419 (*44*). The DK-II isolates harbored a unique P454 substitution (threonine to proline) not observed in other *Trichophyton* species, suggesting additional lineage-level variation, although confirmation requires larger datasets. Of note, lineage-specific polymorphisms such as N276 and F419 have often been reported as the K276N/L419F substitution because of inappropriate *sqle* reference sequences. On the basis of our findings, those variants should be considered wild-type and intrinsic to certain *T. mentagrophytes* genotypes; reported MIC variation more likely reflects methodological differences or genotype-specific susceptibility rather than acquired resistance (*18*,*45*,*46*).

Within the *T. rubrum* complex, *T. rubrum* and *T. violaceum* could be distinguished, whereas *T. soudanense* shared identical *sqle* sequences with *T. rubrum*, indicating that *sqle* alone is insufficient for discrimination and requires complementary ITS sequencing. That limitation also applies to ITS, because species within the *T. rubrum* complex, including *T. violaceum* and *T. soudanense*, also show minimal genetic variation despite being epidemiologically and phenotypically distinct. In contrast, the *T. benhamiae* complex showed greater genetic heterogeneity with *sqle*, providing improved resolution compared with ITS, particularly among *T. benhamiae*, *T. europaeum*, and *T. erinacei*.

Our analysis confirmed that terbinafine non–wild-type *Trichophyton* isolates harbor nonsynonymous *sqle* mutations within the catalytic domain, clustering at residues critical for terbinafine binding (*27*). Resistance in absence of *sqle* mutations appeared rare; only a single *T. rubrum* isolate had an MIC marginally above the TECOFF, which might reflect technical variation associated with MIC testing. All resistant isolates contained ≥1 alteration within the L393–L451 region.

Targeted amplification of a short *sqle* fragment offers a practical and clinically applicable alternative to full-length sequencing. Despite its reduced size, the 388-bp region retained sufficient phylogenetic

information to delineate major *Trichophyton* species and complexes, while capturing resistance-conferring mutations. The shorter amplicon improves PCR efficiency and sensitivity and can be applied directly to clinical specimens, enabling culture-independent detection of both species and resistance. Its ability to distinguish clinically relevant taxa—such as *T. indotineae*, *T. interdigitale*, and the remaining *T. mentagrophytes* genotypes as a single group, as well as the *T. rubrum* and *T. benhamiae* complexes as distinct entities—supports its diagnostic utility, because resolution at this complex level is often sufficient for clinical decision-making. However, discrimination within certain complexes remains limited. Most *T. mentagrophytes* genotypes (DK-I, III, III*, and VII) cluster with identical *sqle* sequences, whereas DK-II was distinguished by 1 SNP and genotype IV was distinguished by 3 SNPs. Similarly, *T. rubrum* and *T. violaceum* (within the *T. rubrum* complex), and *T. benhamiae* sensu stricto, *T. europaeum*, and *T. concentricum* (within the *T. benhamiae* complex) were not fully resolved within their respective clusters.

The first limitation of this study is that although the assay performed well under routine diagnostic conditions, we did not formally evaluate its analytical sensitivity (limit of detection) and specificity, which should be addressed in future validation studies. Moreover, antifungal susceptibility testing was performed only once per isolate. Consequently, technical variation could explain the elevated MIC observed for terbinafine against 1 *T. rubrum* isolate despite its wild-type *sqle* genotype.

In conclusion, *sqle* sequencing enables simultaneous species identification and resistance detection of *Trichophyton* species, supported by a curated reference dataset for reliable interpretation. A short-amplicon approach enables application to clinical specimens and provides information on resistance-associated mutations and clinically relevant species discrimination, although with limited resolution within some complexes. This approach has the potential to enable early optimization of antifungal therapy even in culture-negative cases.

Acknowledgments

We thank the staff and laboratory technicians of the Unit of Mycology and the PCR Laboratory, Statens Serum Institut, for their technical assistance.

No external funding was received for this study. M.C.A. declares grants or contracts paid to the institution from Cidara/Mundipharma, F2G/Shionogi, Pfizer, Pulmocide, Liophilchem, Basilea, and Scynexis. She has received an honorarium for one talk each from Shionogi and Gilead and for one advisory board meeting at Shionogi. She is the current immediate past-chair of the EUCAST antifungal subcommittee.

ChatGPT SSI enterprise (not used by OpenAI for training) was used for proofreading of the text but was not used to generate text or illustrations.

N.A.-C. conceptualized the study, performed the molecular work, analyzed the data, and drafted the manuscript. K.M.J and K.M.T.A. conducted the EUCAST MIC determinations. M.C.A. revised the manuscript. All authors reviewed, approved, and agreed to the final version of the manuscript.

About the Author

Mrs. Abou-Chakra holds a diploma in chemical and bio engineering responsible for the molecular work at the mycology unit, Statens Serum Institut, Denmark. Her primary research interests include the molecular diagnosis, identification, and antifungal resistance of medically important fungi.

References

1. Havlickova B, Czaika VA, Friedrich M. Epidemiological trends in skin mycoses worldwide. Mycoses. 2008;51(Suppl 4):2–15. https://doi.org/10.1111/j.1439-0507.2008.01606.x
2. Chanyachailert P, Leeyaphan C, Bunyaratavej S. Cutaneous fungal infections caused by dermatophytes and non-dermatophytes: an updated comprehensive review of epidemiology, clinical presentations, and diagnostic testing. J Fungi (Basel). 2023;9:669. https://doi.org/10.3390/jof9060669
3. Khan SS, Saunte DML. Dermatophyte treatment failure: a rapid global response to an emerging global health issue. Acta Derm Venereol. 2025;105:adv42948. https://doi.org/10.2340/actadv.v105.42948
4. Astvad KMT, Hare RK, Jørgensen KM, Saunte DML, Thomsen PK, Arendrup MC. Increasing terbinafine resistance in Danish *Trichophyton* isolates 2019–2020. J Fungi (Basel). 2022;8:150. https://doi.org/10.3390/jof8020150
5. Gupta AK, Susmita, Nguyen HC, Liddy A, Economopoulos V, Wang T. Terbinafine resistance in *Trichophyton rubrum* and *Trichophyton indotineae*: a literature review. Antibiotics (Basel). 2025;14:472. https://doi.org/10.3390/antibiotics14050472
6. Mohseni S, Abou-Chakra N, Oldberg K, Chryssanthou E, Young E. Terbinafine resistant *Trichophyton indotineae* in Sweden. Acta Derm Venereol. 2025;105:adv42089. https://doi.org/10.2340/actadv.v105.42089
7. Gupta AK, Mays RR, Versteeg SG, Shear NH, Piguet V. Update on current approaches to diagnosis and treatment of onychomycosis. Expert Rev Anti Infect Ther. 2018;16:929–38. https://doi.org/10.1080/14787210.2018.1544891
8. Schoch CL, Seifert KA, Huhndorf S, Robert V, Spouge JL, Levesque CA, et al.; Fungal Barcoding Consortium; Fungal Barcoding Consortium Author List. Nuclear ribosomal internal transcribed spacer (ITS) region as a universal DNA barcode marker for fungi. Proc Natl Acad Sci U S A. 2012;109:6241–6. https://doi.org/10.1073/pnas.1117018109

9. Tang C, Ahmed SA, Deng S, Zhang L, Zoll J, Al-Hatmi AMS, et al. Detection of emerging genotypes in *Trichophyton mentagrophytes* species complex: a proposal for handling biodiversity in dermatophytes. Front Microbiol. 2022;13:960190. https://doi.org/10.3389/fmicb.2022.960190
10. Pchelin IM, Zlatogursky VV, Rudneva MV, Chilina GA, Rezaei-Matehkolaei A, Lavnikevich DM, et al. Reconstruction of phylogenetic relationships in dermatomycete genus *Trichophyton* Malmsten 1848 based on ribosomal internal transcribed spacer region, partial 28S rRNA and beta-tubulin genes sequences. Mycoses. 2016;59:566–75. https://doi.org/10.1111/myc.12505
11. Chakraborty P, Lyngdoh V, Gogoi N, Gandhi S, Lyngdoh DL, Lanong S, et al. Molecular characterization of dermatophytes isolated in a tertiary care hospital in the north eastern part of India. Cureus. 2024;16:e74815.
12. Tang C, Kong X, Ahmed SA, Thakur R, Chowdhary A, Nenoff P, et al. Taxonomy of the *Trichophyton mentagrophytes*/*T. interdigitale* species complex harboring the highly virulent, multiresistant genotype T. indotineae. Mycopathologia. 2021;186:315–26. https://doi.org/10.1007/s11046-021-00544-2
13. Baron A, Hamane S, Gits-Muselli M, Legendre L, Benderdouche M, Mingui A, et al. Dual quantitative PCR assays for the rapid detection of *Trichophyton indoti*neae from clinical samples. Med Mycol. 2024;62:myae067. https://doi.org/10.1093/mmy/myae067
14. Singh A, Masih A, Monroy-Nieto J, Singh PK, Bowers J, Travis J, et al. A unique multidrug-resistant clonal *Trichophyton* population distinct from *Trichophyton mentagrophytes*/*Trichophyton interdigitale* complex causing an ongoing alarming dermatophytosis outbreak in India: genomic insights and resistance profile. Fungal Genet Biol. 2019;133:103266. https://doi.org/10.1016/j.fgb.2019.103266
15. Singh A, Singh P, Dingemans G, Meis JF, Chowdhary A. Evaluation of DermaGenius resistance real-time polymerase chain reaction for rapid detection of terbinafine-resistant *Trichophyton* species. Mycoses. 2021;64:721–6. https://doi.org/10.1111/myc.13271
16. Kano R, Kimura U, Kakurai M, Hiruma J, Kamata H, Suga Y, et al. *Trichophyton indotineae* sp. nov.: a new highly terbinafine-resistant anthropophilic dermatophyte species. Mycopathologia. 2020;185:947–58. https://doi.org/10.1007/s11046-020-00455-8
17. Yamada T, Maeda M, Alshahni MM, Tanaka R, Yaguchi T, Bontems O, et al. Terbinafine resistance of *Trichophyton* clinical isolates caused by specific point mutations in the squalene epoxidase gene. Antimicrob Agents Chemother. 2017;61:e00115-17. https://doi.org/10.1128/AAC.00115-17
18. Kong X, Tang C, Singh A, Ahmed SA, Al-Hatmi AMS, Chowdhary A, et al. Antifungal susceptibility and mutations in the squalene epoxidase gene in dermatophytes of the *Trichophyton mentagrophytes* species complex. Antimicrob Agents Chemother. 2021;65:e0005621. https://doi.org/10.1128/AAC.00056-21
19. Blanchard G, Amarov B, Fratti M, Salamin K, Bontems O, Chang YT, et al. Reliable and rapid identification of terbinafine resistance in dermatophytic nail and skin infections. J Eur Acad Dermatol Venereol. 2023;37:2080–9. https://doi.org/10.1111/jdv.19253
20. Singh A, Masih A, Khurana A, Singh PK, Gupta M, Hagen F, et al. High terbinafine resistance in *Trichophyton interdigitale* isolates in Delhi, India harbouring mutations in the squalene epoxidase gene. Mycoses. 2018;61:477–84. https://doi.org/10.1111/myc.12772
21. Gupta AK, Cooper EA, Wang T, Polla Ravi S, Lincoln SA, Piguet V, et al. Detection of squalene epoxidase mutations in United States patients with onychomycosis: implications for management. J Invest Dermatol. 2023;143:2476–2483.e7. https://doi.org/10.1016/j.jid.2023.04.032
22. Gräser Y, El Fari M, Vilgalys R, Kuijpers AF, De Hoog GS, Presber W, et al. Phylogeny and taxonomy of the family Arthrodermataceae (dermatophytes) using sequence analysis of the ribosomal ITS region. Med Mycol. 1999;37:105–14. https://doi.org/10.1080/02681219980000171
23. Brillowska-Dąbrowska A, Saunte DM, Arendrup MC. Five-hour diagnosis of dermatophyte nail infections with specific detection of *Trichophyton rubrum*. J Clin Microbiol. 2007;45:1200–4. https://doi.org/10.1128/JCM.02072-06
24. Arendrup MC, Kahlmeter G, Guinea J, Meletiadis J; Subcommittee on Antifungal Susceptibility Testing (AFST) of the ESCMID European Committee for Antimicrobial Susceptibility Testing (EUCAST). How to perform antifungal susceptibility testing of microconidia-forming dermatophytes following the new reference EUCAST method E.Def 11.0, exemplified by *Trichophyton*. Clin Microbiol Infect. 2021;27:55–60. https://doi.org/10.1016/j.cmi.2020.08.042
25. EUCAST European Committee on Antimicrobial Susceptibility Testing. Clinical breakpoint table (yeasts and moulds) [cited 2026 Apr 16]. https://www.eucast.org/fungi-afst/clinical-breakpoints-and-interpretation/clinical-breakpoint-table
26. Baert F, Lefevere P, D'hooge E, Stubbe D, Packeu A. A polyphasic approach to classification and identification of species within the *Trichophyton benhamiae* complex. J Fungi (Basel). 2021;7:602. https://doi.org/10.3390/jof7080602
27. Padyana AK, Gross S, Jin L, Cianchetta G, Narayanaswamy R, Wang F, et al. Structure and inhibition mechanism of the catalytic domain of human squalene epoxidase. Nat Commun. 2019;10:97. https://doi.org/10.1038/s41467-018-07928-x
28. Ferreira CB, Lisboa C. A systematic review on the emergence of terbinafine-resistant *Trichophyton indotineae* in Europe: time to act? J Eur Acad Dermatol Venereol. 2025;39:364–76. https://doi.org/10.1111/jdv.20270
29. Dos Santos AR, Uhrlaß S, Nenoff P, Gold JAW, Bhuiyan MSI, Goturu S, et al. Global emergence of antifungal-resistant dermatophytosis caused by *Trichophyton indotineae* (formerly *T. mentagrophytes* ITS genotype VIII): a genomic investigation involving 14 countries. Mycoses. 2025;68:e70101. https://doi.org/10.1111/myc.70101
30. Astvad KMT, Saunte DML. Sexual transmission of a new emerging dermatophyte: *T. mentagrophytes* genotype VII. J Eur Acad Dermatol Venereol. 2025;39:245–6. https://doi.org/10.1111/jdv.20402
31. El-Baba M, Hall CW, Armstrong I, Woodward K. Two cases of sexually transmitted *Trichophyton indotineae*. CMAJ. 2026;198:E10–2. https://doi.org/10.1503/cmaj.251088
32. Jabet A, Chiarabini T, Hennequin C, Bouscarat F, Valin N, Cruchet R, et al. Autochthonous transmission of *Trichophyton indotineae* through sexual contact, France, 2024. Euro Surveill. 2025;30:2500416. https://doi.org/10.2807/1560-7917.ES.2025.30.26.2500416
33. Jabet A, Dellière S, Seang S, Chermak A, Schneider L, Chiarabini T, et al. Sexually transmitted *Trichophyton mentagrophytes genotype* VII Infection among men who have sex with men. Emerg Infect Dis. 2023;29:1411–4. https://doi.org/10.3201/eid2907.230025
34. de Hoog GS, Dukik K, Monod M, Packeu A, Stubbe D, Hendrickx M, et al. Toward a novel multilocus

phylogenetic taxonomy for the dermatophytes. Mycopathologia. 2017;182:5–31. https://doi.org/10.1007/s11046-016-0073-9
35. Gräser Y, Scott J, Summerbell R. The new species concept in dermatophytes—a polyphasic approach. Mycopathologia. 2008;166:239–56. https://doi.org/10.1007/s11046-008-9099-y
36. Nenoff P, Uhrlaß S, Verma SB, Panda S. *Trichophyton mentagrophytes* ITS genotype VIII and *Trichophyton indotineae*: a terminological maze, or is it? Indian J Dermatol Venereol Leprol. 2022;88:586–9. https://doi.org/10.25259/IJDVL_112_2022
37. Chowdhary A, Singh A, Kaur A, Khurana A. The emergence and worldwide spread of the species *Trichophyton indotineae* causing difficult-to-treat dermatophytosis: a new challenge in the management of dermatophytosis. PLoS Pathog. 2022;18:e1010795.
38. Su H, Packeu A, Ahmed SA, Al-Hatmi AMS, Blechert O, İlkit M, et al. Species distinction in the *Trichophyton rubrum* complex. J Clin Microbiol. 2019;57:e00352–19.
39. Mirhendi H, Makimura K, de Hoog GS, Rezaei-Matehkolaei A, Najafzadeh MJ, Umeda Y, et al. Translation elongation factor 1-α gene as a potential taxonomic and identification marker in dermatophytes. Med Mycol. 2015;53:215–24.
40. Rezaei-Matehkolaei A, Mirhendi H, Makimura K, de Hoog GS, Satoh K, Najafzadeh MJ, et al. Nucleotide sequence analysis of beta tubulin gene in a wide range of dermatophytes. Med Mycol. 2014;52:674–88. https://doi.org/10.1093/mmy/myu033
41. Ahmadi B, Mirhendi H, Makimura K, de Hoog GS, Shidfar MR, Nouripour-Sisakht S, et al. Phylogenetic analysis of dermatophyte species using DNA sequence polymorphism in calmodulin gene. Med Mycol. 2016;54:500–14. https://doi.org/10.1093/mmy/myw004
42. Rudramurthy SM, Shaw D, Shankarnarayan SA, Abhishek, Dogra S. Comprehensive taxonomical analysis of *Trichophyton mentagrophytes/interdigitale* complex of human and animal origin from India. J Fungi (Basel). 2023;9:577. https://doi.org/10.3390/jof9050577
43. Uhrlaß S, Verma SB, Gräser Y, Rezaei-Matehkolaei A, Hatami M, Schaller M, et al. *Trichophyton indotineae*—an emerging pathogen causing recalcitrant dermatophytoses in India and worldwide—a multidimensional perspective. J Fungi (Basel). 2022;8:757. https://doi.org/10.3390/jof8070757
44. Sacheli R, Egrek S, El Moussaoui K, Kurt B, Machowski E, Harag S, et al. National Belgian study on terbinafine resistance in *Trichophyton interdigitale/mentagrophytes/indotineae* (2022–2023): epidemiology and molecular features. J Fungi (Basel). 2025;11:676. https://doi.org/10.3390/jof11090676
45. Sacheli R, Hayette MP. Antifungal resistance in dermatophytes: genetic considerations, clinical presentations and alternative therapies. J Fungi (Basel). 2021;7:983. https://doi.org/10.3390/jof7110983
46. Kumar P, Ramachandran S, Das S, Bhattacharya SN, Taneja B. Insights into changing dermatophyte spectrum in India through analysis of cumulative 161,245 cases between 1939 and 2021. Mycopathologia. 2023;188:183–202. https://doi.org/10.1007/s11046-023-00720-6

Address for correspondence: Nissrine Abou-Chakra, Unit of Mycology, Statens Serum Institut, Bldg 45/112, Artillerivej 5, DK-2300 Copenhagen S, Denmark; email: nac@ssi.dk

etymologia revisited

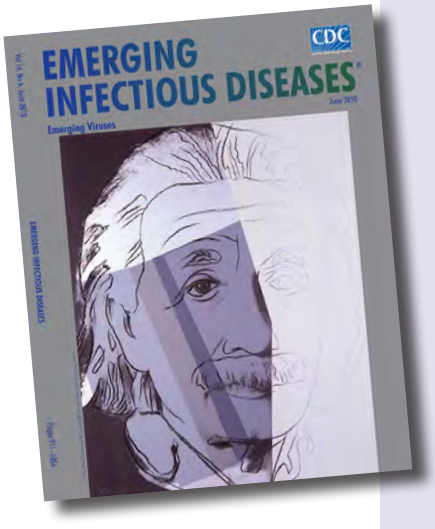

Originally published in June 2010

Lassa Virus
[lah sə] virus

This virus was named after the town of Lassa at the southern end of Lake Chad in northeastern Nigeria, where the first known patient, a nurse in a mission hospital, had lived and worked when she contracted this infection in 1969. The virus was discovered as part of a plan to identify unknown viruses from Africa by collecting serum specimens from patients with fevers of unknown origin. Lassa virus, transmitted by field rats, is endemic in West Africa, where it causes up to 300,000 infections and 5,000 deaths each year.

References:

1 Frame JD, Baldwin JM Jr, Gocke DJ, Troup JM. Lassa fever, a new virus disease of man from West Africa. I. Clinical description and pathological findings. Am J Trop Med Hyg. 1970;19:670–6
2. Mahy BW. The dictionary of virology, 4th ed. Burlington (MA): Elsevier; 2009.

https://wwwnc.cdc.gov/eid/article/16/6/et-1606_article

Invasive *Wickerhamomyces anomalus* Infections among Injecting Drug Users, France, 2012–2024[1]

Maxime Lefranc,[2] Adrien Pain,[2] Fréderic Dalle, Pierre Baudino, Claudio Plaisant, Taieb Chouaki, Josephine Dorin, Anne-Pauline Bellanger, Julie Bonhomme, Maxime Moniot, Celia Rouges, Françoise Botterel, Gregoire Pasquier, Lilia Hasseine, Estelle Perraud-Cateau, Jean-Pierre Gangneux, Laurence Delhaes, Damien Costa, Juliette Guitard, Alexandre Alanio, Valerie Letscher-Bru, Emilie Guemas, Guillaume Desoubeaux, Karine Boukris-Sitbon, Olivier Lortholary, Fanny Lanternier, WAIT-IV Study Group,[3] Marie Desnos-Ollivier, Sebastien Imbert

Wickerhamomyces anomalus is a yeast rarely involved in human invasive fungal diseases (IFD). We retrospectively analyzed 44 episodes of *W. anomalus* IFD in France during 2012–2024. Injecting drug use (IDU) was the main risk factor among 26/35 (74.3%) incident cases. Most infections were community acquired; overall 3-month mortality rate was 1/30 (3.3%). Short tandem repeat (STR) genotyping and whole-genome sequencing analyses revealed substantial genetic diversity among isolates. However, 1 STR genotype was shared by 2 IDU patients, suggesting common exposure. In addition, 1 isolate obtained from a cotton filter used for drug preparation was identical by STR genotyping to the bloodstream isolate from the same patient, indicating direct inoculation via contaminated material or poor injection practices. Our findings highlight the increased risk for *W. anomalus* IFD among IDU patients and emphasize the importance of targeted preventive measures within that population.

Wickerhamomyces anomalus (syn. *Candida pelliculosa*, *Pichia anomala*) is a diploid, ubiquitous yeast species found in diverse environments including soil, fruits, trees, wastewater, marine ecosystems, and the digestive tracts of insects (*1*). It exhibits antimicrobial activity against other yeasts, filamentous fungi, and bacteria and possesses the ability to produce aromatic compounds and exoenzymes (*2*). Those properties make *W. anomalus* of notable interest for various biotechnological applications, including those in the food, environmental, industrial, and medical sectors, as well as in oenological biotechnology (*3*).

W. anomalus is rarely isolated in clinical settings and is responsible for <1% of invasive fungal diseases (IFD) caused by yeasts (*4*–*6*). Nevertheless, hospital outbreaks of *W. anomalus* IFD have been documented,

Author affiliations: CHU Bordeaux, Bordeaux, France (M. Lefranc, P. Baudino, C. Plaisant, L. Delhaes, S. Imbert); Université de Bordeaux, Bordeaux (M. Lefranc, S. Imbert); Institut Pasteur, Paris, France (A. Pain, K. Boukris-Sitbon, O. Lortholary, M. Desnos-Ollivier, F. Lanternier); CHU Dijon, Dijon, France (F. Dalle); CHU Amiens-Picardie, Amiens, France (T. Chouaki); CHU d'Antibes Juan les Pins, Antibes, France (J. Dorin); CHU de Besançon, Besançon, France (A.-P. Bellanger); CHU Caen, Caen, France (J. Bonhomme); CHU Clermont-Ferrand, Clermont-Ferrand, France (M. Moniot); AP-HP Hôpital Cochin, Paris (C. Rouges); CHU Henri Mondor, Créteil, France (F. Botterel); CHU de Montpellier, Montpellier, France (G. Pasquier); CHU Nice, Nice, France (L. Hasseine); CHU Poitiers, Poitiers, France (E. Perraud-Cateau); CHU de Rennes, Rennes, France (J.-P. Gangneux); CHU de Rouen, Rouen, France (D. Costa); Sorbonne Universite, Paris (J. Guitard); Hôpital Saint-Antoine, Paris (J. Guitard); Hôpital Saint-Louis, Paris (A. Alanio); Hôpitaux Universitaires de Strasbourg, Strasbourg, France (V. Letscher-Bru); CHU Toulouse, Toulouse, France (E. Guemas); CHU de Tours, Tours, France (G. Desoubeaux)

DOI: https://doi.org/10.3201/eid3209.251817

[1]Preliminary results from this study were presented at ESCMID Global 2025; April 11–15, 2025; Vienna, Austria; and at the annual congress of the Société Française de Mycologie Médicale; June 18–20, 2025; Amiens, France.

[2]These authors contributed equally to this article.

[3]Additional members of the WAIT-IV Study Group are listed at the end of this article.

particularly in neonatal and pediatric intensive care units (ICUs) (*7*–*12*). In several instances, clonal transmission has been demonstrated, suggesting an exogenous source of contamination (*8*,*13*). Additional outbreaks have also been reported among immunocompromised adult patients (*13*–*17*). Furthermore, a recent nationwide retrospective cross-sectional study on fungemia among injecting drug users (IDUs) in France identified *W. anomalus* as overrepresented in IDU-related cases (*18*), reinforcing the hypothesis of exogenous contamination. However, in both hospital outbreaks and IDU cases, the precise source of infection remains unidentified.

In this study, we aimed to investigate factors associated with *W. anomalus* IFD in France. We conducted a comprehensive analysis of epidemiologic, clinical, and genetic characteristics of all *W. anomalus* IFD cases reported over a 13-year period nationwide, with particular emphasis on IDU-associated infections.

Materials and Methods

Study Design and Network

We analyzed IFDs caused by *W. anomalus* yeast diagnosed during January 2012–December 2024 in France and declared during the 2 consecutive prospective national surveillance programs RESSIF (RESeau de Surveillance des Infections Fongiques invasives; ended December 31, 2022) and SINFONI (Surveillance des Infections FONgiques Invasives; started January 1, 2023). The RESSIF multicentric surveillance program was described previously (*4*). SINFONI is a multicentric prospective program for surveillance of IFD started January 1, 2023, and active as of August 2026 involving 59 hospitals in France and overseas (Appendix Figure 1, https://wwwnc.cdc.gov/EID/article/32/9/25-1817-App1.pdf). Participants report all cases of IFD diagnosed in the hospital using an online secured REDCap questionnaire (https://projectredcap.org) designed and monitored at the National Reference Center for Invasive Mycoses and Antifungals (NRCMA; Institut Pasteur, Paris, France). For both RESSIF and SINFONI surveillance programs, participants completed the questionnaire for each episode of IFD, reporting demographic data (age, sex, hospital), clinical information (risk factor for IFD, underlying conditions, preexposure to antifungals, first treatment for IFD, outcome) and microbiologic findings (species identification).

The Institut Pasteur Institutional Review Board approved NRCMA surveillance activities (no. 2009-34/IRB), as did the Commission Nationale de l'Informatique et des Libertés (déclaration no. 351952). We designed and reported our study in accordance with Strengthening the Reporting of Observational Studies in Epidemiology (STROBE) guidelines (*19*).

W. anomalus IFD Case Definitions

W. anomalus IFD cases included both fungemia and deep-seated infections. We defined fungemia by the isolation of *W. anomalus* yeast from a blood culture specimen. We defined deep-seated infections by the isolation of *W. anomalus* from a normally sterile site, regardless of whether fungemia was also present. We defined community-onset cases as episodes in which a positive blood culture for *W. anomalus* was obtained ≤3 days after hospital admission. We defined recurrent episodes as the reisolation of the same fungal species ≥10 days after the initial episode (*18*).

Strain Identification

We checked all *W. anomalus* isolates sent to the NRCMA on BBL CHROMagar *Candida* medium (https://www.chromagar.com) for purity, then identified them at the species level using a polyphasic approach combining matrix-assisted laser desorption/ionization time-of-flight (MALDI-ToF) mass spectrometry (Bruker Biotyper or Sirius devices; Bruker MBT Library, https://www.bruker.com), sequencing D1D2 and internal transcribed spacer (ITS) regions of the DNA ribosomal loci using panfungal primers NL1/NL4 and V9D/LS266 (*20*). We performed DNA extraction using NucleoMag Plant DNA extraction kit (Macherey Nagel, https://www.mn-net.com) in a Thermo KingFisher extractor (Thermo Fisher Scientific, https://www.thermofisher.com) preceded by 2 bead beating steps using ATL Buffer lysis (QIAGEN, https://www.qiagen.com) in lysing matrix tubes Y (MP Biomedicals, https://flowsciences.com) and a heating step in the presence of RNase A. Sequences of D1D2 and internal transcribed spacer regions of the isolates had a percentage identity >99% with the sequences of the type strain of *W. anomalus* CBS 5759, enabling species identification. We performed antifungal susceptibility testing in accordance with EUCAST broth microdilution reference method (*21*).

Short Tandem Repeat Genotyping

We performed short tandem repeat (STR) genotyping as previously described (22), with slight modifications. In brief, we used a panel of 6 STR markers, 3 trinucleotide and 3 hexanucleotide repeats, resulting in a unique 12-marker profile for each isolate. We amplified the 3 trinucleotide STRs in 1

multiplex PCR reaction and the 3 hexanucleotide STRs in 3 distinct simplex PCR reactions. We used GoTaq DNA polymerase (Promega, https://www.promega.com) for all amplifications. We then diluted PCR products 1:100 in water; we mixed 1 μL of the diluted products with 10.2 μL of formamide and 0.3 μL of MapMarker 1000 DNA size standard (Eurogentec, https://www.eurogentec.com). We incubated the mixtures at 95°C for 3 minutes and subsequently analyzed them using a 3500 XL Dx genetic analyzer (Thermo Fisher). We determined repeat numbers for each STR locus using GeneMapper 5 (Thermo Fisher). We converted the resulting STR profiles into a genetic distance matrix using the bruvo.dist function from the poppr package in R version 4.5 (The R Project for Statistical Computing, https://www.r-project.org) as previously described (*23*). We constructed an UPGMA tree via the bruvo.boot function to visualize genetic relationships among samples; we exported the resulting tree in Newick format and visualized it using the Interactive Tree of Life web interface (*24*).

Whole-Genome Sequencing Analysis

We sequenced whole genomes at the Mutualized Platform for Microbiology (P2M), Institut Pasteur, using an Illumina NextSeq 500 sequencer. We constructed libraries using Nextera DNA Library preparation kit (Illumina) and sequenced them using a 2 × 150 nt paired-end strategy. We also incorporated 11 publicly available isolates reprocessed with the same pipeline (*22*). We assessed raw read quality using FastQC version 0.12.1 (http://www.bioinformatics.babraham.ac.uk/projects/fastqc) and MultiQC version 1.12 (https://github.com/MultiQC/MultiQC) (*25*). We performed read cleaning with AlienTrimmer version 2.0 (ftp://ftp.pasteur.fr/pub/gensoft/projects/AlienTrimmer) (*26*): we considered bases with a Phred score <15 (–q 15) of low confidence, and after trimming, we discarded reads <50 bases (–l 50) or containing >50% low-confidence bases (–p 50). Cleaned reads are available at the European Nucleotide Archive (accession no. PRJEB93917).

Variant Calling and Population Genomic Analyses

We defined methods for variant calling and population genomic analyses (Appendix). In brief, we aligned reads to the *W. anomalus* KG16 reference genome assembly (GenBank no. GCA_019321675.1) and imported variant calls into R version 4.3.2 using the VCFR package as described previously (*27*). We converted the filtered VCF file to a genlight object (vcfR2genlight) and set diploidy. We computed pairwise genetic distances between isolates as the proportion of differing single-nucleotide polymorphisms (SNPs) using bitwise distances (bitwise.dist function in poppr package) (*23*), normalized by the reference genome size (13,671,194 bp; KG16 assembly). We constructed a neighbor-joining phylogenetic tree from the distance matrix using the nj function from the APE package as described (*28*). We assessed node support by bootstrap resampling 1,000 replicates using the aboot function in poppr package. We exported the final tree in Newick format and visualized it using Interactive Tree of Life web interface (*24*).

We assessed genetic diversity by computing Simpson diversity index (λ), Nei unbiased gene diversity (Hexp), and global genetic differentiation between phylogenetic clades (FST). We inferred population structure using ADMIXTURE (https://dalexander.github.io/admixture/index.html).

De Novo Genome Assemblies and Loss of Heterozygosity Map

We performed de novo genome assemblies using the fq2dna pipeline (https://gitlab.pasteur.fr/GIPhy/fq2dna), which performs read deduplication, quality trimming, error correction, digital normalization, and de novo assembly with SPAdes (*29*). We assessed assembly quality using QUAST (*30*). We described methods to identify and visualize regions of Loss of heterozygosity (LOH) (Appendix); in brief, we processed allele depth matrices in R using dplyr (https://dplyr.tidyverse.org), tidyr (https://tidyr.tidyverse.org), and ggplot2 (*31*) as described previously. We stratified analyses and visualizations both globally and by predefined phylogenetic clusters.

Statistical Analysis

We summarized continuous variables as medians with interquartile ranges (IQRs), where appropriate, and categorical variables as counts and percentages. To avoid autocorrelation, we included only incident cases in the description of baseline characteristics. We compared continuous variables using the Wilcoxon rank-sum test and categorical variables using Fisher exact test. All statistical tests were 2-sided, and significance threshold was $p<0.05$. We conducted analysis using the gtsummary package in R version 4.5.

Results

W. anomalus IFD Episodes

During the study period, a total of 47 *W. anomalus* IFD episodes were reported to the NRCMA, 31

during the RESSIF program and 16 during the SINFONI program. We excluded 3 episodes from the study, 2 superficial ocular infections and 1 with inconsistent data, for a total of 44 episodes (40 fungemia and 4 osteoarticular infections) among 35 patients (Table). Episodes originated from 18 centers located across mainland France; each center reported 1–12 episodes. Among centers that participated exhaustively in both RESSIF and SINFONI surveillance programs (n = 15), we have observed an upward trend in the annual incidence of new cases since 2021; during 2012–2020 the mean was 2.2 reported cases per year, and during 2021–2024 the mean was 5.25 reported cases per year (Appendix Figure 2).

Of the 35 patients in our study, 26 (74.2%) were IDUs and 20 had no other risk factor for IFD. Among the other usual risk factors for IFD, the presence of a central vascular catheter (n = 9) and ICU admission at diagnosis (n = 7) were the most frequent. Univariate analysis showed that those risk factors were significantly less frequent in IDU patients (p<0.001 by Fisher exact test). One patient was a premature neonate. We found deep-seated *W. anomalus* infections or secondary localizations with (n = 3) or without (n = 4) fungemia in 7 patients, all of whom were IDUs: 3 spondylodiscitis, 2 septic arthritis (wrist and knee), 1 endocarditis, and 1 endophthalmitis. We identified concurrent bacterial infections in 8 and fungal infection in 7 cases. In contrast to non-IDU cases, most *W. anomalus* infections in the IDU group were community acquired (p = 0.039 by Fisher exact test). Recurrent episodes occurred in 5 IDU patients: 4 experienced 3 episodes each, and 1 had 2 episodes. The overall 3-month mortality rate was low (1/30 deaths, 3.3%); we observed no significant differences between IDU and non-IDU groups.

IDU Characteristics

We collected data on injected products for 23/26 IDU patients. Most (n = 16 [69.6%]) patients were

Table. Demographic and clinical characteristics of invasive *Wickerhamomyces anomalus* infection cases reported through multicentric prospective national surveillance programs, France, 2012–2024*

Characteristic	All patients, N = 35	IDU, n = 26	Non-IDU, n = 9	p value†
Age median (IQR)	42 (36–50)	41 (36–45)	55 (36–68)	0.11
Sex				
M	27/35 (77)	20/26 (77)	7/9 (78)	>0.9
F				
Invasive fungal disease				0.6
Fungemia	31/35 (89)	22/26 (85)	9/9 (100)	
Osteoarticular infection	4/35 (11)	4/26 (15)	0/9 (0)	
IFD risk factor other than IDU‡				
HIV infection	2/31 (6.5)	2/26 (7.7)	0/5 (0)	>0.9
Recent surgery	2/35 (5.7)	0/26 (0)	2/9 (22)	0.061
Central vascular catheter	9/35 (26)	2/26 (7.7)	7/9 (78)	<0.001
Intensive care unit	7/35 (20)	3/26 (12)	4/9 (44)	0.055
Other underlying conditions‡	4/35 (11)	1/26 (4)	4/9 (33)	0.010
≥1 risk factor other than IDU	13/35 (37)	6/26 (23)	8/9 (89)	<0.001
IFD history	8/33 (24)	7/25 (28)	1/8 (13)	0.6
Community onset	17/34 (50)	16/26 (62)	1/8 (13)	0.039
Associated deep-seated IFD				0.8
Spondylodiscitis	3/35 (8.6)	3/26 (12)	0/9 (0)	
Septic arthritis	2/35 (5.7)	2/26 (7.7)	0/9 (0)	
Endocarditis	1/35 (2.9)	1/26 (3.8)	0/9 (0)	
Endophthalmia	1/35 (2.9)	1/26 (3.8)	0/9 (0)	
None	28/35 (80)	19/26 (73)	9/9 (100)	
Bacterial co-infection	8/35 (23)	5/26 (19)	3/9 (33)	0.4
Invasive fungal co-infection	7/35 (20)	4/26 (15)	3/9 (33)	0.3
First-line antifungal treatment				0.5
Echinocandin monotherapy	25/35 (71)	19/26 (73)	6/9 (67)	
Fluconazole monotherapy	3/35 (8.6)	3/26 (12)	0/9 (0)	
Voriconazole monotherapy	2/35 (5.7)	1/26 (3.8)	1/9 (11)	
Combination therapy	2/35 (5.7)	1/26 (3.8)	1/9 (11)	
No antifungals	3/35 (8.6)	2/26 (7.7)	1/9 (11)	
Median length of hospital stay, d (IQR)	15 (7–31)	12 (6–23)	55 (22–64)	0.005
Recurrence	5/30 (17)	5/22 (23)	0/8 (0)	0.3
90-d all-cause mortality	1/30 (3.3)	0/22 (0)	1/8 (13)	0.3

*Values are no. (%) except as indicated. Data reported through Reseau de Surveillance des Infections Fongiques invasives (RESSIF) and Surveillance des Infections Fongiques Invasives (SINFONI). Denominators lower than the N/n value for each category indicate missing data. IDU, injecting drug user; IFD, invasive fungal disease; IQR, interquartile range.
†Determined by Wilcoxon rank-sum test or Fisher exact test.
‡Other underlying conditions were hematologic malignancy (n = 1), solid organ malignancy (n = 1), premature neonate (n = 1), and severe malnutrition (n = 1).

multiple drug injectors. Heroin and cocaine were the most commonly injected substances (n = 13 each), followed by buprenorphine (n = 11), other opioids (n = 7), amphetamines (n = 4), and methylphenidate (n = 4). No single substance was common to all cases. In addition, 14 (60.9%) patients reported a history of alcohol abuse. A total of 21 patients documented their housing status; 13 (61.9%) were either homeless (n = 10) or living in precarious conditions (2 in caravans and 1 in a social hostel), whereas 8 (38.1%) resided in private housing.

W. anomalus Isolates

Among the 47 reported episodes of *W. anomalus* IFD, 36 isolates were available for subsequent analyses. We recovered multiple isolates from recurrent episodes in 5 patients. Of note, 1 isolate had been obtained from the cotton a patient had used to filter injected drugs; it had been collected concurrently with a W. *anomalus* fungemia. All identifications provided by MALDI-ToF mass spectrometry and sequencing methods were concordant. In addition, we included 19 *W. anomalus* isolates collected during 2004–2024, outside the RESSIF and SINFONI surveillance programs (involved or not in IFD), and the NRRL Y3668 reference strain in subsequent genotypic analyses, resulting in a total of 56 isolates.

STR Genotyping

We subjected 49 of the 56 isolates to STR genotyping: 26 originating from IDU patients, 15 from non-IDU patients, and 7 from patients with unknown IDU status or environmental sources, as well as the reference strain. Analysis revealed 41 unique STR profiles identified across both IDU and non-IDU groups (Figure 1). We observed no distinct genetic cluster among all IDU isolates. However, 8 isolates, including 7 from 4 IDU patients across different hospitals, formed a small cluster with limited variations in repeat numbers. Furthermore, 3 genotypes were shared across different patients: 1 was found in 2 IDU patients from the same hospital (isolates CNRMA23.611/CNRMA24.852, hospital H1), and the other 2 in patients who differed in time of infection, geographic location, and IDU status (isolates CNRMA20.747/CNRMA14.503 and CNRMA9.1011/CNRMA15.118). In addition, an IDU patient's blood culture isolate (isolate CNRMA24.858) and the isolate recovered from the cotton used by the same patient to filter drugs, collected concomitantly with the fungemia (isolate CNRMA24.857) shared the same genotype. Finally, regarding recurrent episodes, all isolates were genotypically identical (isolates CNRMA12.528/CNRMA14.76, CNRMA24.850/CPELBDX11, and CNRMA24.853/CNRMA24.852) or showed a minor repeat number variation at a single locus (isolates CNRMA15.118/CNRMA15.277), except for 1 patient who had 2 W. anomalus isolates with distant STR profiles (isolates CNRMA19.199/CNRMA17.645).

Whole-Genome Sequencing Analysis

Whole-genome sequencing (WGS) analysis of 53 of the 56 isolates from this study, together with 11 publicly available genomes (Appendix Table 1), yielded an alignment of 391,733 SNPs and revealed 6 main clades (Figure 2). Across all 64 genomes, pairwise distances were 742–346,637 (mean 208,986) SNPs. Within-patient pair ranges were 742–15,296 SNPs and all clustered together in the phylogeny, including the 2 that appeared distant by STR (isolates CNRMA17.645 and CNRMA19.199). The STR locus implicated in this discordance, namely M3b, lies within an LOH region on chromosome CM033148.1 (positions 1,446,243–1,447,304) (Figure 3) in CNRMA19.199, explaining the discrepancy. Genetic diversity indices computed on 16,935 LD-pruned SNPs across 52 isolates (excluding LOH-affected isolates) confirmed substantial allelic diversity (Simpson $\lambda = 0.98$; Nei unbiased gene diversity Hexp = 0.38 ± 0.08), with moderate differentiation between phylogenetic clades (global FST = 0.16). Population structure using ADMIXTURE revealed 7 genetic clusters broadly concordant with the 6 phylogenetic clades: 2 clades showed exclusive cluster assignment, whereas the remaining 4 displayed admixed profiles (Appendix Figure 3, panel A). Isolates from the same city consistently belonged to distinct clusters, providing no evidence for city-level population structure (Appendix Figure 3, panel B).

De novo assemblies were 12–30 Mb, consistent with results from public datasets for *W. anomalus* from the National Center for Biotechnology Information in which 26 genomes spanned 12.72–26.55 Mb (https://www.ncbi.nlm.nih.gov/datasets/genome/?taxon=4927; accessed 2025 Sep 16). Isolates with the smallest assemblies clustered within a subclade enriched for LOH regions (Figures 2, 3), suggesting that expanded LOH promotes haplotig coalescence and yields more compact assemblies. QUAST (https://quast.sourceforge.net) further showed that assembly size increases with the duplication ratio (Appendix Figure 4), consistent with retention of haplotigs or unpurged duplicated segments, or both. We observed similar patterns in several of the assemblies, indicating that larger assembly sizes often reflect duplicated content rather than intrinsically larger

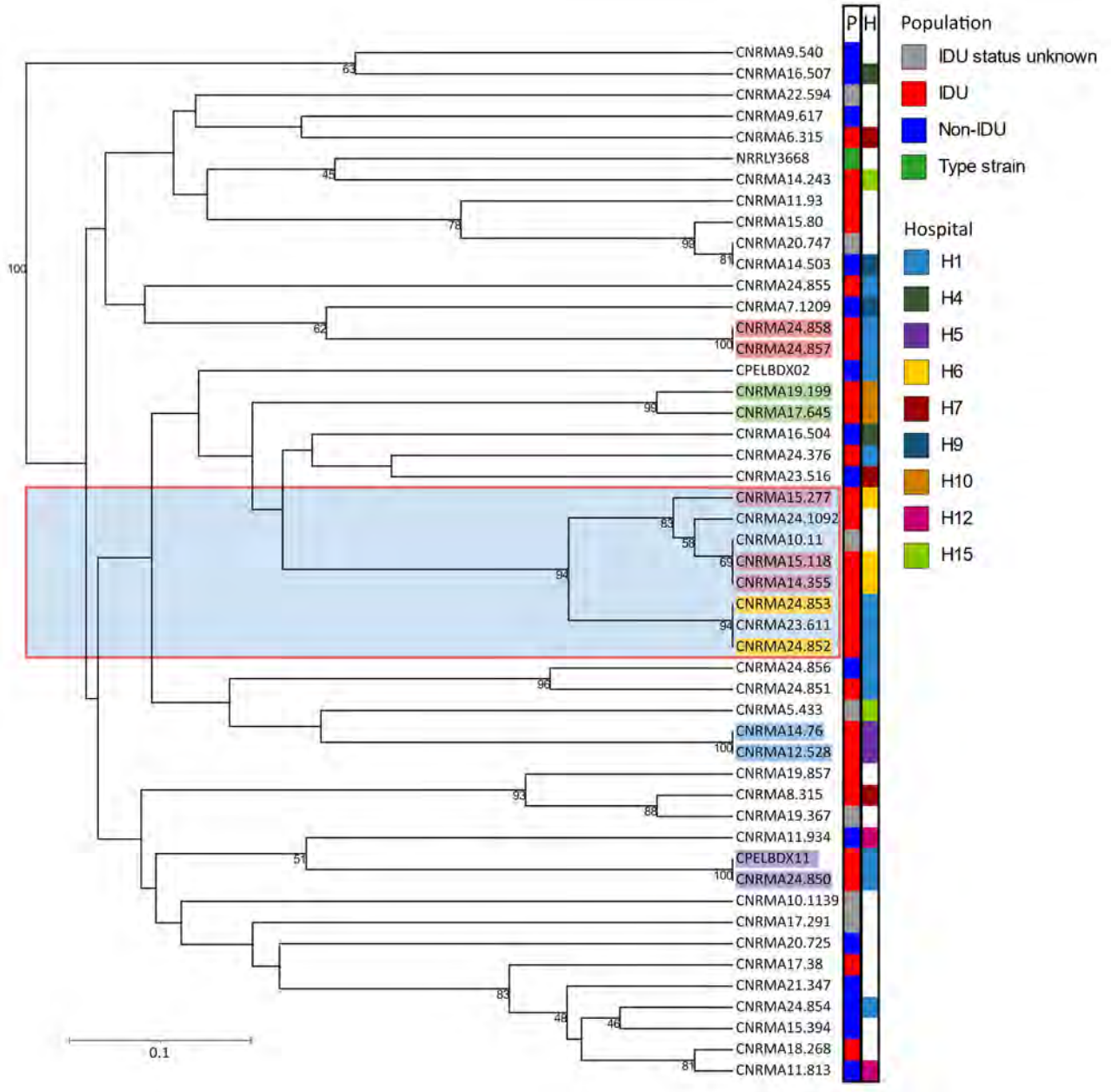

Figure 1. *Wickerhamomyces anomalus* isolates in study of invasive *W. anomalus* infections among injecting drug users, France, 2012–2024. Dendrogram was created by of 49 *W. anomalus* isolates genotyped using a 12-marker short tandem repeat approach. The P column indicates the IDU status of the patient from whom each isolate originated. The H column denotes hospital of origin for hospitals contributing ≥2 isolates. Blue shaded area indicates cluster of 7 IDU-associated isolates. Matching colored shading on isolate names indicates those isolates belong to the same patient. Numbers at nodes indicate bootstrap values. Scale bar represents the Bruvo genetic distance (short tandem repeat differences). IDU, injecting drug use.

genomes. Finally, VAF profiles (Appendix Figure 5) showed shifts compatible with segmental aneuploidy in some genomic regions, although not fully supported by read depth.

Discussion

This retrospective multicentric nationwide study, conducted over a 13-year period, provides new insights on *W. anomalus* IFD. Of note, IDU emerged as a major risk factor, representing the sole underlying condition in 20 (57.1%) of 35 cases (Table). An additional 6 cases occurred in IDU patients with other predisposing factors for IFD. Furthermore, a marked increase in *W. anomalus* IFD has been observed since 2020, primarily driven by IDU-related infections, as 14 (53.8%) of 26 cases occurred after

2020. In contrast to previous reports, we observed no hospital-based outbreaks in ICU or neonatal settings; of note, only 1 case was documented in a premature neonate. All but 1 non-IDU patients had classical risk factors for yeast IFD; that patient was homeless and exhibited behaviors suggestive of IDU, although we could not definitively confirm whether that was correct.

Although IDU is a well-recognized risk factor for invasive candidiasis (*32*,*33*), only 1 case of *W. anomalus* infection in an IDU had been reported in the literature (*34*) before a study published in 2025 that reported 7 cases and demonstrated a notable overrepresentation of *W. anomalus* yeast in IDU-associated infections (*18*). However, a US study on fungemia among IDU patients did not report that association (*35*), suggesting that the emergence of *W. anomalus* infections may reflect local transmission dynamics, potentially linked to specific drug products, injection practices, or environmental exposures. Of interest,

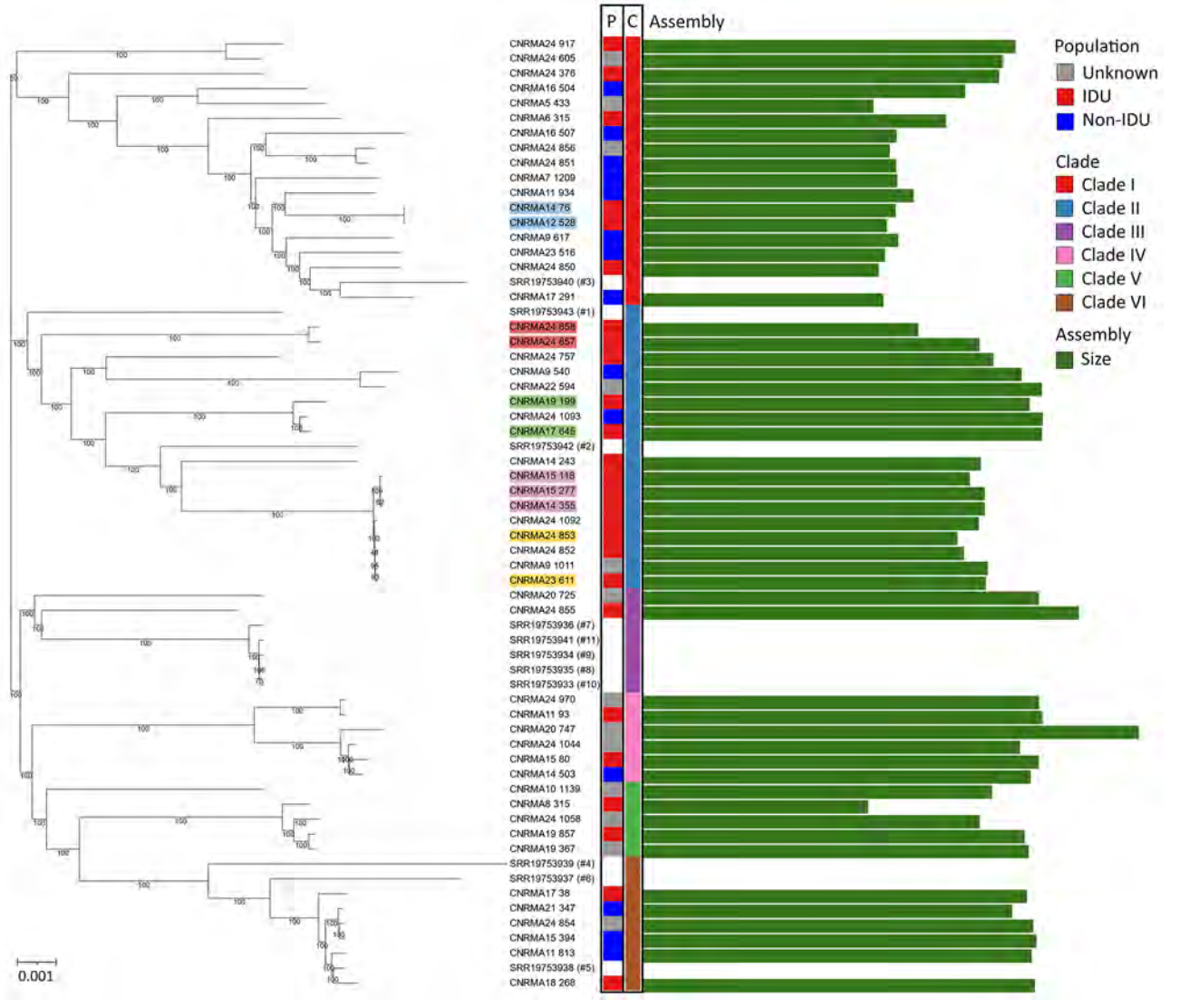

Figure 2. Phylogenetic tree of *Wickerhamomyces anomalus* isolates in study of invasive *W. anomalus* infections among injecting drug users, France, 2012–2024. Tree is based on genomewide SNPs from 53 *W. anomalus* isolates collected in the study and 11 publicly available genomes (isolate names starting with SRR) and was developed by neighbor-joining method. The P column indicates the IDU status of the patient from whom each isolate originated. The C column denotes phylogenetic clade. Matching colored shading on isolate names indicates those isolates belong to the same patient. Green bars represent assembled genome size of 13.9–29.7 Mb. Variation in assembly size reflects levels of genomic heterozygosity: isolates with extensive loss of heterozygosity (clade 1) have smaller assemblies caused by haplotype collapse, whereas highly heterozygous isolates have larger assemblies with uncollapsed haplotypes. Numbers at nodes indicate bootstrap values. Scale bar represents genetic distance (proportion of differing SNPs). IDU, injecting drug use; SNP, single-nucleotide polymorphism.

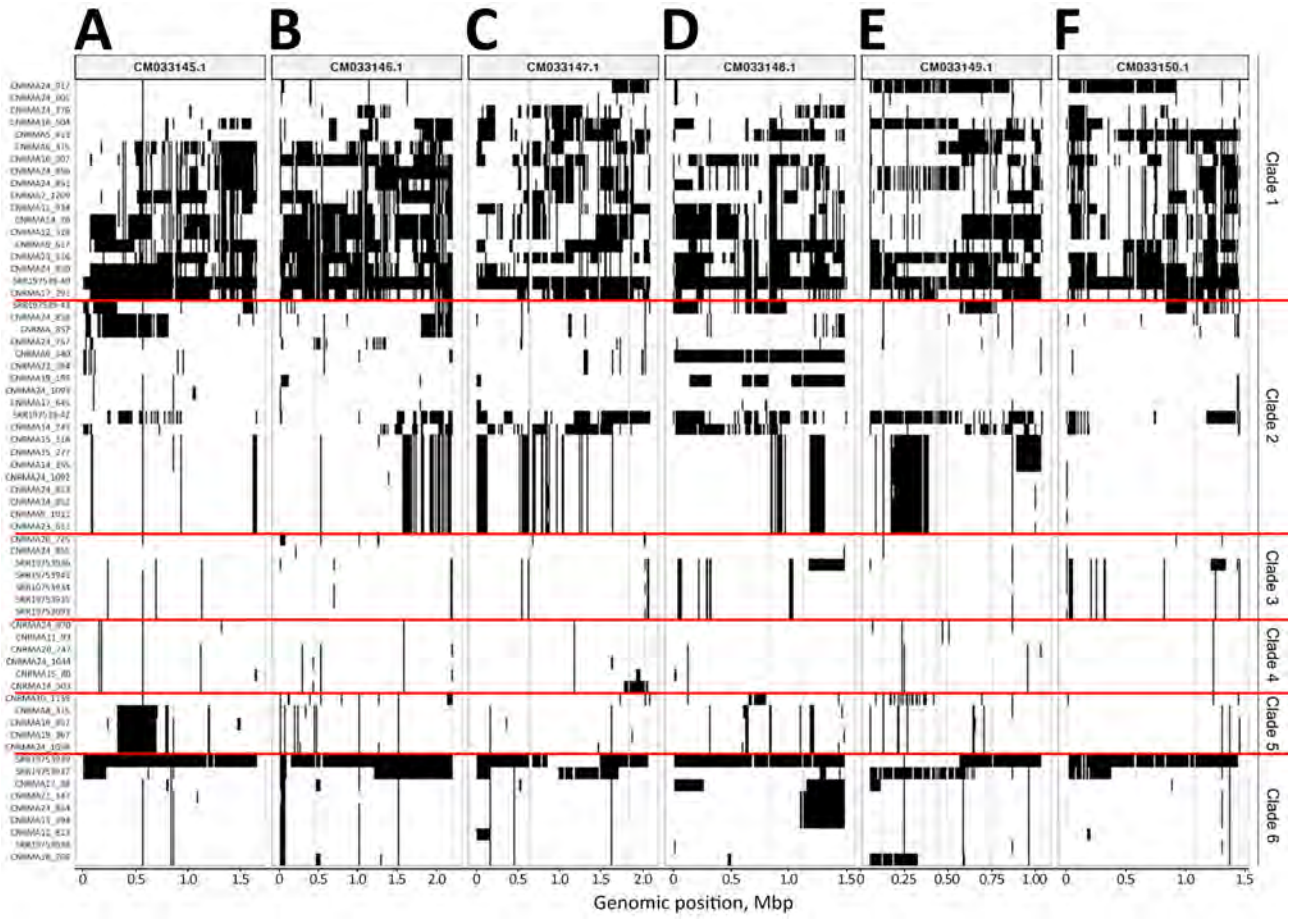

Figure 3. Genomewide loss of heterozygosity distribution across 6 chromosomes of *Wickerhamomyces anomalus* fungi in study of invasive *W. anomalus* infections among injecting drug users, France, 2012–2024. We analyzed 53 *W. anomalus* isolates collected in this study and 11 publicly available genomes, grouped by phylogenetic clade. Chromosomes are CM033145.1 (A), CM033146.1 (B), CM033147.1 (C), CM033148.1 (D), CM033149.1 (E), and CM033150.1 (F). Red lines indicate clades. Black indicates loss of heterozygosity (LOH); gray, insufficient variant coverage; white (no color), heterozygosity. LOH patterns vary extensively within and between clades. Clade 1 (top) exhibits high levels of LOH and substantial variation between isolates. Other clades show more moderate and heterogeneous LOH distributions. Some isolates within a clade share similar patterns; others display distinct profiles.

in the study we report, a *W. anomalus* isolate was recovered from the cotton a patient had used to filter injected drugs, which was collected concurrently with a blood culture that tested positive for *W. anomalus*. Genotyping analysis revealed that both *W. anomalus* isolates shared an identical STR genotype. The patient was otherwise colonized by *Nakaseomyces glabratus* (formerly *Candida glabrata*) yeast. Taken together, those findings strongly suggest direct inoculation via a contaminated drug preparation, rather than skin contamination. However, we identified no specific drug product as associated with the risk for *W. anomalus* IFD in our cohort. In addition, STR genotyping and WGS analyses did not reveal any specific cluster among IDU-associated cases, arguing against contamination from a single source or a unique product over the 13-year study period. We did not identify consistent environmental exposure either; patients had diverse housing situations across 15 cities. Nevertheless, 8 (30.8%) of 26 patients originated from the same city, and 2 patients shared an identical STR genotype within a 6-month interval, suggesting possible local transmission or exposure. Finally, injection practices themselves may contribute to the transmission risk for *W. anomalus*. Previous reports have linked fungemia in IDU populations to the use of contaminated lemon juice for diluting brown heroin (*36*). Given that *W. anomalus* yeast is commonly found in water sources, food products, and fermented beverages such as wine and beer, exposure could plausibly occur through the use of nonsterile diluents. However, further environmental investigations and prospective practices surveys are warranted to substantiate our hypothesis.

Most (n = 25) *W. anomalus* IFD patients were treated with echinocandins either as monotherapy or in combination with other antifungals (n = 2). Remarkably,

the overall 3-month mortality rate remained low (3.3%, n = 1/30) across both IDU and non-IDU groups, even in instances in which antifungal therapy was absent (n = 3) or limited to fluconazole (n = 3), despite elevated minimal inhibitory concentrations to fluconazole (*37*) (Appendix Table 1). That observation may suggest that *W. anomalus* exhibits lower virulence than other yeast species commonly implicated in fungemia.

MALDI-TOF mass spectrometry using commercial databases appears to be an efficient method for accurate species-level identification of *W. anomalus* in clinical practice. In addition, both STR and WGS methods are suitable approaches for *W. anomalus* genotyping, yielding overall concordant results. However, *W. anomalus* is a diploid heterothallic species, and our WGS analysis suggests that LOH events are frequently happening among this species. Genome assemblies of 12–30 Mb in our study match those of public data; smaller assemblies linked to LOH and larger ones to unpurged duplications (Appendix Figure 4). In that context, WGS SNP analysis might have overestimated the number of SNPs, suggesting that STR genotyping is a more reliable approach for assessing isolates' relatedness and explaining the minor discordances observed between the 2 methods. LOH events have been shown to enable rapid adaptation to both host environments and antifungal exposure (*38*); they have also been reported to constitute a major evolutionary mechanism driving divergence within *C. albicans* populations (*39*). LOH can lead to loss-of-function alleles with notable phenotypic variations. An example is in *C. albicans* clade I isolates, which carry a heterozygous LOF mutation in *FUR1* conferring elevated intrinsic resistance to 5-fluorocytosine (*40*); once rendered homozygous by LOH, the mutation results in complete resistance to the drug. Four isolates exhibited resistance to 5-fluorocytosine in vitro (Appendix Table 1), but none showed evidence of LOH affecting the *FUR1* homologue. Nevertheless, we observed an interesting LOH event in 2 isolates recovered from the same patient at different times (isolates CNRMA17.645 in 2017 and CNRMA19.199 in 2019). In such pathogen, LOH might represent a more immediate adaptive response to environmental stress than sexual recombination. Additional analysis could be useful to determine precise chromosomic location of LOH and eventually loss-of-function related.

Data collection issues affected our study. Reported IDU status and drugs injected might not reflect the patient's situation at the time of the IFD episode. Similarly, because neither RESSIF nor SINFONI was specifically designed to capture IDU infections, participating centers might have missed information on injected products. In addition, the relatively limited number of cases and the imbalance between the numbers of IDU and non-IDU patients restrict the possibility of assessing confounding risk factors between the 2 groups through multivariate analysis.

In conclusion, this nationwide study in France highlights the increased risk for *W. anomalus* IFD among persons who use injected drugs; we observed a rise in cases since 2021. Our findings strongly suggest an exogenous source of infection, potentially linked to environmental exposure or unsafe injection practices, and emphasize the importance of targeted preventive measures within IDU populations.

Additional members of the WAIT-IV Study Group: Sophie Brun (Bobigny, France); Charles Soler (Clamart, France); Nicole Desbois-Nogard (Fort de France, France); Muriel Cornet (Grenoble, France); Florent Morio (Nantes, France); Christine Bonnal, Eric Dannaoui (Paris, France); Lucrecia Delarue (Perigueux, France); Céline Tournus (Saint Denis de La Reunion, France); Jacques Sartre (Valence, France); and Elisabeth Chachaty (Villejuif, France).

Acknowledgments

We thank Constance Caroff, Olivier Capdeboscq, and Odin Lussier for their insights into the local context of injected drug use and associated harm-reduction efforts and Frédéric Grenouillet for kindly providing the *Wickerhamomyces anomalus* reference strain.

Cleaned reads from the WGS analysis are available at the European Nucleotide Archive (accession no. PRJEB93917). All R analysis scripts used in this study are available at https://doi.org/10.5281/zenodo.21901725.

This research was supported by a grant from the Société Française de Mycologie Médicale and institutional support by Institut Pasteur and Santé Publique France. The funders had no role in study design, data collection and analysis, decision to publish, or preparation of the manuscript.

Author contributions: writing, original draft: M.L., A.P., M.D.O., S.I.; writing, review & editing: all; methodology: M.L., A.P., C.P., S.I., M.D.O.; data curation: K.B.S., F.D., T.C., A.P.B., J.B., M.M., C.R., F.B., G.P., L.H., E.P.C., J.P.G., D.C., J.G., A.A., V.L.B., E.G., G.D.; conceptualization: M.L., F.D., P.B., O.L., S.I., F.L., M.D.O.

About the Author

Dr. Lefranc is a medical mycologist at Centre Hospitalier Universitaire de Bordeaux, France. His primary research interest is medical diagnosis of fungal diseases and antifungal resistance.

References

1. Kurtzman CP. Phylogeny of the ascomycetous yeasts and the renaming of *Pichia anomala* to *Wickerhamomyces anomalus*. Antonie van Leeuwenhoek. 2011;99:13–23. https://doi.org/10.1007/s10482-010-9505-6
2. Passoth V, Fredlund E, Druvefors UÃ, Schnürer J. Biotechnology, physiology, and genetics of the yeast *Pichia anomala*. FEMS Yeast Res. 2006;6:3–13. https://doi.org/10.1111/j.1567-1364.2005.00004.x
3. López-Enríquez L, Vila-Crespo J, Rodríguez-Nogales JM, Fernández-Fernández E, Ruipérez V. Modulation of the aromatic profile of Verdejo wine through sequential inoculation of *Wickerhamomyces anomalus* and *Saccharomyces cerevisiae*. Fermentation. 2023;9:977. https://doi.org/10.3390/fermentation9110977
4. Bretagne S, Sitbon K, Desnos-Ollivier M, Garcia-Hermoso D, Letscher-Bru V, Cassaing S, et al. Active surveillance program to increase awareness on invasive fungal diseases: the French RESSIF Network (2012 to 2018). mBio. 2022;13:e00920-22. https://doi.org/10.1128/mbio.00920-22
5. Díaz-García J, Mesquida A, Sánchez-Carrillo C, Reigadas E, Muñoz P, Escribano P, et al. Monitoring the epidemiology and antifungal resistance of yeasts causing fungemia in a tertiary care hospital in Madrid, Spain: any relevant changes in the last 13 years? Antimicrob Agents Chemother. 2021;65:e01827–20. https://doi.org/10.1128/AAC.01827-20
6. Song Y, Chen X, Yan Y, Wan Z, Liu W, Li R. Prevalence and antifungal susceptibility of pathogenic yeasts in China: a 10-year retrospective study in a teaching hospital. Front Microbiol. 2020;11:1401. https://doi.org/10.3389/fmicb.2020.01401
7. Lin HC, Lin HY, Su BH, Ho MW, Ho CM, Lee CY, et al. Reporting an outbreak of *Candida pelliculosa* fungemia in a neonatal intensive care unit. J Microbiol Immunol Infect. 2013;46:456–62. https://doi.org/10.1016/j.jmii.2012.07.013
8. Pasqualotto AC, Sukiennik TCT, Severo LC, de Amorim CS, Colombo AL. An outbreak of *Pichia anomala* fungemia in a Brazilian pediatric intensive care unit. Infect Control Hosp Epidemiol. 2005;26:553–8. https://doi.org/10.1086/502583
9. Murphy N, Buchanan CR, Damjanovic V, Whitaker R, Hart CA, Cooke RWI. Infection and colonisation of neonates by *Hansenula anomala*. Lancet. 1986;1:291–3. https://doi.org/10.1016/S0140-6736(86)90827-5
10. Chakrabarti A, Singh K, Narang A, Singhi S, Batra R, Rao KLN, et al. Outbreak of *Pichia anomala* infection in the pediatric service of a tertiary-care center in northern India. J Clin Microbiol. 2001;39:1702–6. https://doi.org/10.1128/JCM.39.5.1702-1706.2001
11. Yang Y, Wu W, Ding L, Yang L, Su J, Wu B. Two different clones of *Candida pelliculosa* bloodstream infection in a tertiary neonatal intensive care unit. J Infect Dev Ctries. 2021;15:870–6. https://doi.org/10.3855/jidc.12103
12. da Silva CM, de Carvalho Parahym AMR, Leão MPC, de Oliveira NT, de Jesus Machado Amorim R, Neves RP. Fungemia by *Candida pelliculosa* (*Pichia anomala*) in a neonatal intensive care unit: a possible clonal origin. Mycopathologia. 2013;175:175–9. https://doi.org/10.1007/s11046-012-9605-0
13. Jung J, Moon YS, Yoo JA, Lim JH, Jeong J, Jun JB. Investigation of a nosocomial outbreak of fungemia caused by *Candida pelliculosa* (*Pichia anomala*) in a Korean tertiary care center. J Microbiol Immunol Infect. 2018;51:794–801. https://doi.org/10.1016/j.jmii.2017.05.005
14. Zhang L, Xiao M, Arastehfar A, Ilkit M, Zou J, Deng Y, et al. Investigation of the emerging nosocomial *Wickerhamomyces anomalus* infections at a Chinese tertiary teaching hospital and a systemic review: clinical manifestations, risk factors, treatment, outcomes, and anti-fungal susceptibility. Front Microbiol. 2021;12:744502. https://doi.org/10.3389/fmicb.2021.744502
15. Thuler LCS, Faivichenco S, Velasco E, Martins CA, Nascimento CRG, Castilho IAMA. Fungaemia caused by *Hansenula anomala*—an outbreak in a cancer hospital. Mycoses. 1997;40:193–6. https://doi.org/10.1111/j.1439-0507.1997.tb00213.x
16. Evren K, Akçay E, Yücel M, Bal AZ, Erdinç FŞ, Dinç B, et al. A case of peritonitis caused by *Wickerhamomyces anomalus* (*Candida pelliculosa*) related to peritoneal dialysis [in Turkish]. Mikrobiyol Bul. 2021;55:665–72. https://doi.org/10.5578/mb.20219718
17. Mehta V, Mohanty A, Meena S, Rahul JS, Uttam Kumar N, Chattopadhyay D, et al. *Wickerhamomyces anomalous*: a rare cause of fungemia causing febrile neutropenia in acute lymphoblastic leukemia. Case Rep Infect Dis. 2020:1–4. https://doi.org/10.1155/2020/8847853
18. Paccoud O, Lortholary O, Imbert S, Letscher-Bru V, Boukris-Sitbon K, Obadia T, et al.; French Mycoses Study Group. Yeast fungaemia among injection drug users in France (2012–2022): a cross-sectional observational study. Lancet Reg Health Eur. 2025;55:101365. https://doi.org/10.1016/j.lanepe.2025.101365
19. Von Elm E, Altman DG, Egger M, Pocock SJ, Gøtzsche PC, Vandenbroucke JP. STROBE Initiative. Strengthening the Reporting of Observational Studies in Epidemiology (STROBE) statement: guidelines for reporting observational studies. BMJ. 2007;335:806–8. https://doi.org/10.1136/bmj.39335.541782.AD
20. Kurtzman CP, Robnett CJ. Identification and phylogeny of ascomycetous yeasts from analysis of nuclear large subunit (26S) ribosomal DNA partial sequences. Antonie van Leeuwenhoek. 1998;73:331–71. https://doi.org/10.1023/A:1001761008817
21. Guinea J, Meletiadis J, Arikan-Akdagli S, Giske C, Muehlethaler K, Arendrup MC. Method for the determination of broth dilution minimum inhibitory concentrations of antifungal agents for yeasts. 2023 [cited 2025 Nov 19]. https://www.eucast.org/fileadmin/eucast/pdf/AFST/methodology/EUCAST_E.Def_7.4_Yeast_definitive_revised_2023.pdf
22. Spruijtenburg B, Rudramurthy SM, Meijer EFJ, van Haren MHI, Kaur H, Chakrabarti A, et al. Application of novel short tandem repeat typing for *Wickerhamomyces anomalus* reveals simultaneous outbreaks within a single hospital. Microorganisms. 2023;11:1525. https://doi.org/10.3390/microorganisms11061525
23. Kamvar ZN, Tabima JF, Grünwald NJ. Poppr: an R package for genetic analysis of populations with clonal, partially clonal, and/or sexual reproduction. PeerJ. 2014;2:e281. https://doi.org/10.7717/peerj.281
24. Letunic I, Bork P. Interactive Tree Of Life (iTOL) v5: an online tool for phylogenetic tree display and annotation. Nucleic Acids Res. 2021;49(W1):W293–6. https://doi.org/10.1093/nar/gkab301
25. Ewels P, Magnusson M, Lundin S, Käller M. MultiQC: summarize analysis results for multiple tools and samples in a single report. Bioinformatics. 2016;32:3047–8. https://doi.org/10.1093/bioinformatics/btw354
26. Criscuolo A, Brisse S. AlienTrimmer: a tool to quickly and accurately trim off multiple short contaminant sequences from high-throughput sequencing reads. Genomics. 2013;102:500–6. https://doi.org/10.1016/j.ygeno.2013.07.011

27. Knaus BJ, Grünwald NJ. VCFR: a package to manipulate and visualize variant call format data in R. Mol Ecol Resour. 2017;17:44–53. https://doi.org/10.1111/1755-0998.12549
28. Paradis E, Claude J, Strimmer K. APE: Analyses of Phylogenetics and Evolution in R language. Bioinformatics. 2004;20:289–90. https://doi.org/10.1093/bioinformatics/btg412
29. Prjibelski A, Antipov D, Meleshko D, Lapidus A, Korobeynikov A. Using SPAdes de novo assembler. Curr Protoc Bioinformatics. 2020;70:e102. https://doi.org/10.1002/cpbi.102
30. Mikheenko A, Saveliev V, Hirsch P, Gurevich A. WebQUAST: online evaluation of genome assemblies. Nucleic Acids Res. 2023;51(W1):W601–6. https://doi.org/10.1093/nar/gkad406
31. Wickham H. Data analysis. In: ggplot2. Use R! 2nd ed. Cham (Switzerland): Springer International Publishing; 2016. p. 189–201.
32. Poowanawittayakom N, Dutta A, Stock S, Touray S, Ellison RT III, Levitz SM. Reemergence of intravenous drug use as risk factor for candidemia, Massachusetts, USA. Emerg Infect Dis. 2018;24:631–7. https://doi.org/10.3201/eid2404.171807
33. Rossow JA, Gharpure R, Brennan J, Relan P, Williams SR, Vallabhaneni S, et al. Injection drug use-associated candidemia: incidence, clinical features, and outcomes, east Tennessee, 2014–2018. J Infect Dis. 2020;222(Suppl 5):S442–50. https://doi.org/10.1093/infdis/jiaa024
34. Nohinek B, Zee-Cheng CS, Barnes WG, Dall L, Gibbs HR. Infective endocarditis of a bicuspid aortic valve caused by *Hansenula anomala.* Am J Med. 1987;82:165–8. https://doi.org/10.1016/0002-9343(87)90400-1
35. Zhang AY, Shrum S, Williams S, Petnic S, Nadle J, Johnston H, et al. The changing epidemiology of candidemia in the United States: injection drug use as an increasingly common risk factor-active surveillance in selected sites, United States, 2014–2017. Clin Infect Dis. 2020;71:1732–7. https://doi.org/10.1093/cid/ciz1061
36. Miró JM, Puig de la Bellacasa J, Odds FC, Gill BK, Bisbe J, Gatell JM, et al. Systemic candidiasis in Spanish heroin addicts: a possible source of infection. J Infect Dis. 1987;156:857–8. https://doi.org/10.1093/infdis/156.5.857
37. Luo Z, Ning Y, Xiao M, Guo D, Xu H, Liu Y, et al. High azole non-wild type rates and nosocomial microsatellite typing aggregation of *Wickerhamomyces anomalus* in China according to a 12-year multicenter surveillance study. J Antimicrob Chemother. 2025;80:1964–71. https://doi.org/10.1093/jac/dkaf156
38. Ford CB, Funt JM, Abbey D, Issi L, Guiducci C, Martinez DA, et al. The evolution of drug resistance in clinical isolates of *Candida albicans*. eLife. 2015;4:e00662. https://doi.org/10.7554/eLife.00662
39. Wang JM, Bennett RJ, Anderson MZ. The genome of the human pathogen *Candida albicans* is shaped by mutation and cryptic sexual recombination. mBio. 2018;9:e01205-18. https://doi.org/10.1128/mBio.01205-18
40. Dodgson AR, Dodgson KJ, Pujol C, Pfaller MA, Soll DR. Clade-specific flucytosine resistance is due to a single nucleotide change in the *FUR1* gene of *Candida albicans.* Antimicrob Agents Chemother. 2004;48:2223–7. https://doi.org/10.1128/AAC.48.6.2223-2227.2004

Address for correspondence: Sebastien Imbert, Service de parasitologie-mycologie, Hôpital Pellegrin, Place Amelie Raba Leon, 33075 Bordeaux CEDEX, France; email: sebastien.imbert@u-bordeaux.fr

Reemergence of Scrub Typhus Associated with *Leptotrombidium akamushi* Mites and Karp-Like *Orientia tsutsugamushi* Genotype Bacteria, Japan, 2024–2025

Motohiko Ogawa, Nobuhiro Takada, Takashi Katayama, Yuki Hashimoto, Kei Nagano, Hirotaka Komine, Yukihiro Akeda

Scrub typhus is a miteborne infectious disease caused by *Orientia tsutsugamushi* bacteria. In Japan, most cases occur in spring and autumn and are transmitted by *Leptotrombidium pallidum* and *L. scutellare* mites; summer scrub typhus, transmitted by *L. akamushi* mites, is rarely reported. In August 2024, a pregnant woman had scrub typhus develop after attending a fireworks event in Niigata Prefecture, Japan, resulting in fetal death. A Vietnam-related Karp-like *O. tsutsugamushi* genotype, distinct from the Kato type usually associated with *L. akamushi* mites, was detected from patient samples. Field investigations at the site of the fireworks event revealed seasonal predominance of *L. akamushi* mites in summer. We detected *O. tsutsugamushi* sequences identical to the patient's strain in 3 *L. akamushi* mite larvae and 1 field mouse, suggesting that *L. akamushi* mites were the source of human infection. Our findings suggest reemergence of summer scrub typhus associated with infected *L. akamushi* mites carrying a locally novel genotype.

Scrub typhus is a miteborne infectious disease caused by *Orientia tsutsugamushi* bacteria and transmitted by larval trombiculid mites of the genus *Leptotrombidium* (*1*). Patients typically have an eschar develop at the site of the mite bite, accompanied by fever, rash, and elevated liver enzyme and C-reactive protein levels (*2*,*3*). Tetracycline-class antimicrobial agents are generally highly effective against scrub typhus, but delayed treatment can lead to severe disease and occasionally death.

In Japan, scrub typhus exhibits a bimodal seasonal distribution, with peaks occurring in spring and autumn (*2*). That seasonal pattern is largely determined by the life cycles of vector mite species. The principal vectors in Japan are *L. pallidum* and *L. scutellare* mites (*1*,*4*). Both species hatch in autumn, and their larvae parasitize vertebrate hosts, contributing to the autumn peak of disease incidence. *L. pallidum* larvae can overwinter and remain active until the following spring, thereby contributing to the spring peak of scrub typhus cases. Historically, summer scrub typhus, transmitted by *L. akamushi* mites, occurred in river basin environments of northern and central Japan, including major river systems in Akita, Yamagata, and Niigata Prefectures, such as the Shinano River Basin (*2*,*5*). However, summer scrub typhus is now rare, and only sporadic cases have been reported in recent decades, including a suspected Kato-type infection reported in Akita Prefecture in 2008 (*6*).

Different *Leptotrombidium* mite species are associated with specific *O. tsutsugamushi* serotypes. For example, *L. akamushi* mites are primarily associated with the Kato serotype, whereas *L. pallidum* and *L. scutellare* mites are associated with other major serotypes, including Gilliam, Karp, Kawasaki, and Kuroki (*2*,*7*,*8*). More recently, *L. palpale* mites have been proposed as a vector candidate for the Shimokoshi type *O. tsutsugamushi* bacteria (*9*). In Japan, reports of infections caused by the Kato serotype are rare, and the *O. tsutsugamushi* bacterial genotypes currently associated with *L. akamushi* mites remain poorly characterized in regions where summer scrub typhus was

Author affiliations: National Institute of Infectious Diseases, Japan Institute for Health Security, Tokyo, Japan (M. Ogawa, Y. Hashimoto, Y. Akeda); University of Fukui, Fukui, Japan (N. Takada); Kanagawa Prefectural Institute of Public Health, Kanagawa, Japan (T. Katayama); Niigata City General Hospital, Niigata, Japan (K. Nagano); Yamagata University, Yamagata, Japan (H. Komine)

DOI: https://doi.org/10.3201/eid3209.260646

historically endemic and where that mite species was the principal vector.

In August 2024, a pregnant woman who had attended a fireworks event on a riverbank in Niigata Prefecture had scrub typhus develop, resulting in fetal death. She had no recent travel history outside Niigata Prefecture before symptom onset. *O. tsutsugamushi* bacteria were detected in the patient's serum and placenta. Sequence analysis of the 56-kDa type-specific antigen (TSA) gene revealed a Karp-like genotype closely related to strains previously reported from Vietnam (*10*). The fireworks event, the suspected exposure site, was held in the Shinano River Basin, a region historically known for summer scrub typhus transmitted by *L. akamushi* mites.

Detection of *O. tsutsugamushi* in larval mites can provide evidence of the direct source of human infection, and infection in rodents can provide indirect evidence of infected mites in the area. Therefore, we conducted a field investigation in the suspected exposure area to capture mites and field mice to determine *O. tsutsugamushi* infection and characterize the local maintenance of *O. tsutsugamushi* in mite vectors and their host species.

Materials and Methods

We conducted a field investigation at the suspected exposure site along a riverbank in Nagaoka City, Niigata Prefecture, Japan (37°27.283′N, 138°50.269′E). We selected 2 sampling sites within ≈200 meters of the suspected exposure site: site A was an area of dense bushy vegetation adjacent to farmland, and site B was an area of dense bushy vegetation immediately adjacent to the river's edge (Figure 1). Both sites provided suitable habitats for trombiculid mites and small mammal hosts, including *Apodemus* spp. field mice.

We conducted field surveys at 1 or both sites during June, July, August, and November 2025; site A was not sampled in August. We used Sherman traps to capture field mice and set ≈50 traps per night across both sites. We anesthetized captured field mice and collected blood by cardiac puncture for serologic testing before humanely euthanizing the mice. We then collected spleen samples for molecular detection. We carefully removed attached larval trombiculid mites from field mice for mite species identification and *O. tsutsugamushi* detection. The Institutional Animal Care and Use Committee of the National Institute of Infectious Diseases approved all animal procedures (approval no. 125159).

Mite Identification

We morphologically identified mites under a stereomicroscope, according to standard taxonomic methods (*11*). Because *L. akamushi* mites have rarely been reported in recent field surveys, we performed molecular identification on selected specimens on the basis of the cytochrome oxidase I (*COX1*) gene (*12*) to verify species identification. We used PrepMan Ultra Sample Preparation Reagent (Thermo Fisher Scientific, https://www.thermofisher.com) to extract DNA from individual mites.

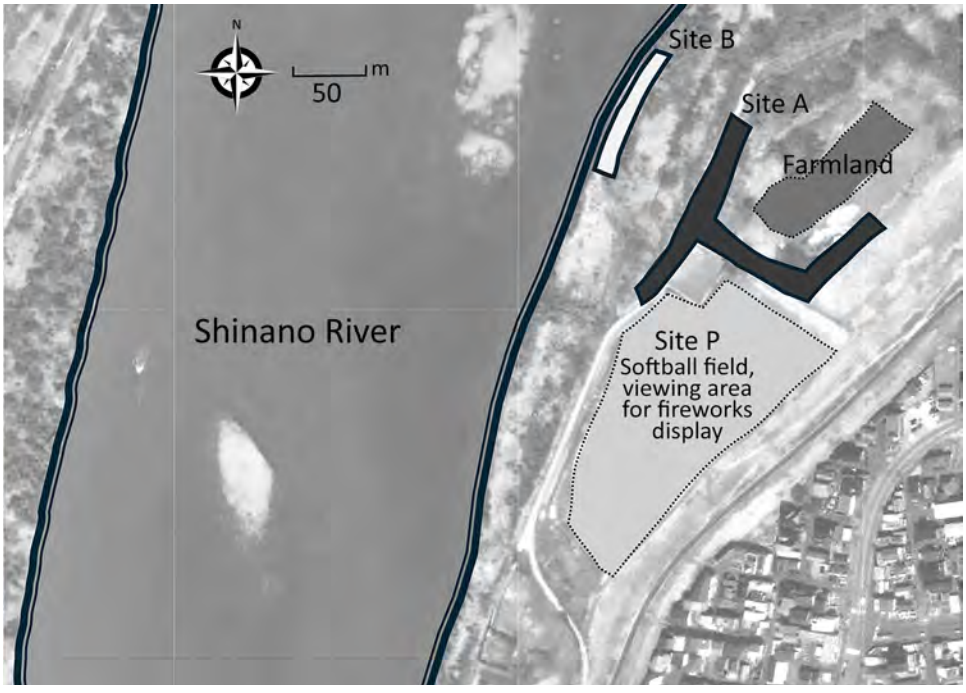

Figure 1. Study sites for investigation of reemergence of scrub typhus associated with *Leptotrombidium akamushi* mites and Karp-like *Orientia tsutsugamushi* genotype bacteria, Japan, 2024–2025. Map shows suspected exposure site along the Shinano River in Niigata Prefecture (P) and 2 sampling sites (A and B). Site A was located adjacent to farmland, and site B was located along the riverbank. Sites A and B are within 200 m of the patient's suspected exposure site.

Detection of *O. tsutsugamushi* in Mice and Mites

We tested mouse serum samples for 6 *O. tsutsugamushi* antibody serotypes by using an indirect immunofluorescence assay (*13*) and considered titers ≥80 positive. We extracted DNA from spleen samples by using a FavorPrep Tissue Genomic DNA Extraction Mini Kit (Favorgen Biotech Corp., https://www.favorgen.com). We used real-time PCR targeting the 16S rRNA gene (*14*) on DNA extracted from field mouse spleens and engorged mites to screen for *O. tsutsugamushi*. For samples that tested positive or equivocal, we conducted further analysis by using nested PCR targeting the 56-kDa TSA gene (*15*). We sequenced amplicons and performed phylogenetic analysis by using the neighbor-joining method in MEGA X version 11.01.3 (https://www.megasoftware.net) with 1,000 bootstrap replicates (*16*).

Results

Detection of *O. tsutsugamushi* in Mice

We captured a total of 54 field mice, all of which were large Japanese field mice (*Apodemus speciosus*). Serum samples suitable for serologic testing were obtained from 45 mice (37 from site A and 8 from site B). From site A, 31 (84%) of 37 tested field mice were *O. tsutsugamushi*–seropositive. In site B, 7 (88%) of 8 tested field mice were *O. tsutsugamushi*–seropositive (Figure 2). From site A, PCR genotyping revealed Japanese Gilliam–type strains of *O. tsutsugamushi* bacteria in field mice collected during June, July, and November, and we detected a Karp-type strain in 1 field mouse collected in June. At site B, we detected Japanese Gilliam–type strains in 1 field mouse in June.

Mite Abundance and Identification

The composition and seasonal abundance of mites collected from field mice differed markedly between the 2 sampling sites. From site A, we detected mites in November (mean 16.3 mites/mouse) and June (mean 6.5 mites/mouse) but not in July (Table). We conducted no sampling at site A in August. All mites collected in June were *L. pallidum*, whereas 57.7% of mites collected in November were *L. pallidum* and 42.3% were *Neotrombicula japonica* (Figure 3). At site B, all mites collected in June and August were *L. pallidum*, whereas *L. akamushi* accounted for 96.3% of mites collected in July (Figure 3).

Representative mite specimens showed the characteristic position of the sensillary setae anterior to the posterolateral setae and 8 dorsal idiosomal setae, consistent with *L. akamushi* mites (Figure 4). Of 52 *L. akamushi* mites analyzed, 24 yielded *COX1* sequences

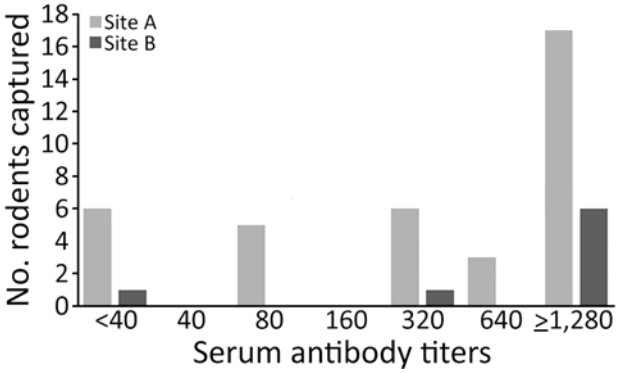

Figure 2. Antibody titers from field mice in a study of reemergence of scrub typhus associated with *Leptotrombidium akamushi* mites and Karp-like *Orientia tsutsugamushi* genotype bacteria, Japan, 2024–2025. We tested serum samples from large Japanese field mice (*Apodemus speciosus*) by indirect immunofluorescence assay against 6 *O. tsutsugamushi* bacterial serotypes. Titers ≥80 were considered positive.

confirming species identification. The other 28 specimens did not yield reliable sequences, likely because of the extremely small body size of larvae and variable DNA quality. However, all specimens exhibited morphologic characteristics consistent with established diagnostic criteria for *L. akamushi* mites under stereomicroscopic examination. Together with the molecular results, those findings indicate the presence of *L. akamushi* mites at the study site.

Phylogenetic Analysis of *O. tsutsugamushi* Strains

We identified Japanese Gilliam–type *O. tsutsugamushi* strains in 5 field mice collected at site A in June, 1 field mouse collected in July, and 2 field mice collected in November. At site B, we identified the same

Table. Number of mice and mites collected per site in an investigation of reemergence of scrub typhus associated with *Leptotrombidium akamushi* mites and Karp-like *Orientia tsutsugamushi* genotype bacteria, Japan, 2024–2025*

Collection site and month collected	Total no. mice captured	No. mites collected†	
		Total no. collected	Mean no./mouse
Site A			
June	20	130	6.5
July	11	0	0
August	NS	NS	NS
November	7	114	16.3
Site B			
June	2	24	12
July	5	54	10.8
August	8	5	0.6
November	1	0	0

*Sampling sites were within ≈200 meters of the suspected exposure site in Nagaoka City, Niigata Prefecture, Japan (37°27.283′N, 138°50.269′E). Site A was dense bushy vegetation adjacent to farmland; and site B was dense bushy vegetation immediately adjacent to the Shinano River. NS, not sampled.
†Mite species included *L. akamushi*, *L. pallidum*, *Neotrombicula japonica*, and other unidentified species.

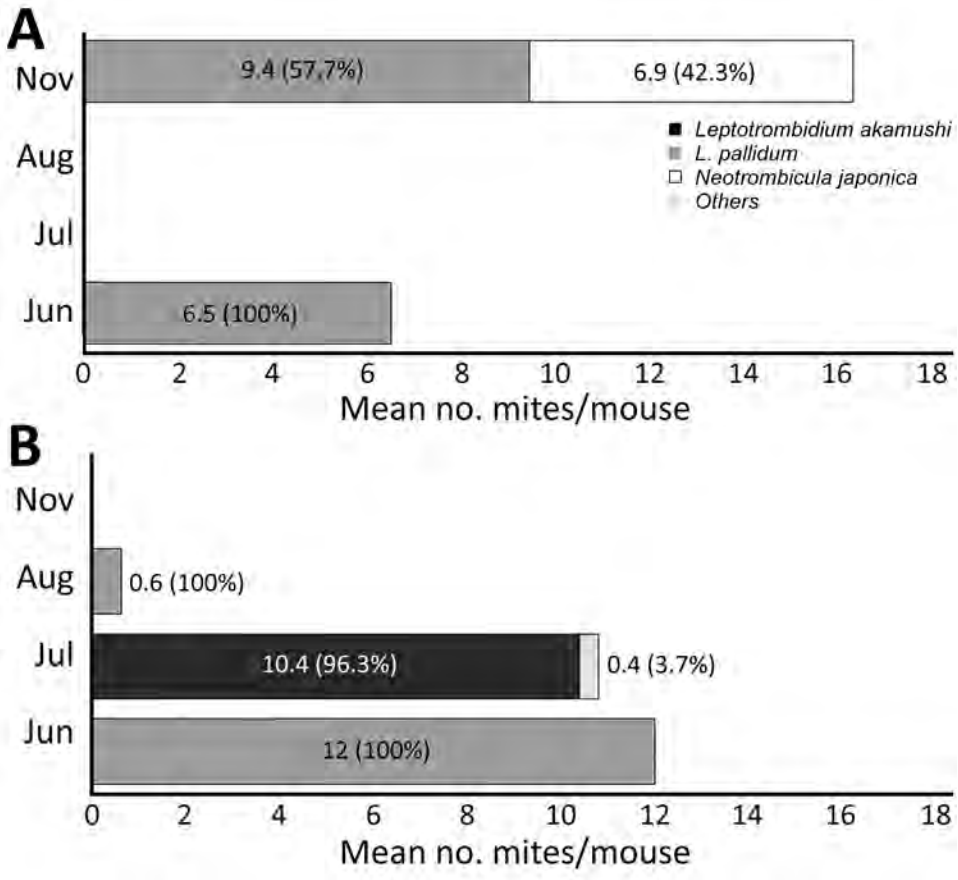

Figure 3. Seasonal abundance and species composition of trombiculid mites collected from field mice in a study of reemergence of scrub typhus associated with *Leptotrombidium akamushi* mites and Karp-like *Orientia tsutsugamushi* genotype bacteria, Japan, 2024–2025. A) Site A, near a tract of farmland; B) site B, near the riverbank. Graphs show mean numbers of mites per mouse and species composition for each sampling period. Mite species composition differed markedly between the sites: *L. pallidum* was predominant at site A in June (early summer) and November (autumn), whereas *L. akamushi* was predominant at site B in July (summer). *Neotrombicula japonica* and other mite species were also detected.

strain in 1 field mouse and 1 mite collected in June. We identified a Karp-like strain of *O. tsutsugamushi* in 1 field mouse and 3 *L. akamushi* larvae collected at site B in July. *COX1* analysis confirmed the larvae as *L. akamushi* species mites.

The Karp-like strain of *O. tsutsugamushi* we detected was more closely related to strains from Vietnam than to the Kato type historically associated with *L. akamushi* mites in Japan. The longest 56-kDa TSA gene sequence (959 bp) we obtained was from the placenta specimen (GenBank accession no. LC912005). That sequence showed the highest nucleotide identity (98.5%) to 2 previously reported strains from Vietnam (GenBank accession nos. HQ718457.1 [945 bp] and HQ718455.1 [959 bp]) (Figure 5). Related Karp-like sequences have been identified elsewhere in Asia, but those 2 strains from Vietnam had the highest sequence similarity to sequence LC912005. In addition, the 959-bp sequence obtained from the placenta specimen was identical to 2 other sequences (GenBank accession nos. LC912009 and LC912010) obtained from 2 *L. akamushi* mite larvae. The nucleotide sequences of an ≈420-bp region were identical among the placenta specimen (GenBank accession no. LC912005), patient serum sample (accession no. LC921007), 1 field mouse spleen sample (accession no. LC912003), and 3 *L. akamushi* larvae (accession nos. LC912007, LC912009, and LC912010). Phylogenetic analysis on the basis of that 420-bp region placed all samples within the same Karp-like cluster (Figure 5).

The *O. tsutsugamushi*–positive larvae were engorged *L. akamushi* larvae attached to field mice at the time of collection. However, the spleens of the field mouse hosts to which those larvae were attached tested negative for *O. tsutsugamushi* by PCR. Because trombiculid larvae feed only once on vertebrate hosts, larvae that acquire *O. tsutsugamushi* from an infected host cannot subsequently transmit the pathogen to another host. Moreover, horizontally acquired infection is not efficiently maintained across generations (*8*,*17*). Therefore, detection of *O. tsutsugamushi* in engorged larvae attached to PCR-negative field mice strongly suggests that those larvae acquired the pathogen before attaching to the mice, likely through vertical transmission; therefore, *L. akamushi* could be the source of human infection in this instance. Furthermore, sequence analysis showed that the nucleotide sequences of the *O. tsutsugamushi* bacterial strain in the larvae were identical to those detected in the patient's serum and placenta, providing strong evidence that human infection was likely caused by bites of in-

fected *L. akamushi* larvae during the fireworks event on the riverbank.

Discussion

Our findings demonstrate marked seasonal differences in mite species abundance and composition within a limited area along a riverbank in Niigata Prefecture and identified *L. akamushi* as the predominant mite species at the time and location where the patient is suspected to have been exposed. Detection of the same genotype of *O. tsutsugamushi* in *L. akamushi* mites, field mice, and the patient suggests that human infection occurred at this site.

The marked predominance of *L. akamushi* in July suggests that this species is strongly associated with the summer occurrence of *O. tsutsugamushi* scrub typhus at this site. Historically, *L. akamushi* mites have been recognized as the principal vector of summer scrub typhus in northern Japan, particularly in river basin environments. The contrasting predominance of *L. pallidum* mites at site A and *L. akamushi* mites at site B might reflect differences in local environmental conditions, although the specific factors responsible remain unclear.

Of note, we identified engorged *O. tsutsugamushi*–positive larvae attached to field mice whose spleens tested *O. tsutsugamushi*–negative by PCR, indicating that the larvae acquired the pathogen before attaching to their hosts. Because trombiculid larvae feed only once on vertebrate hosts and horizontally acquired infection is not efficiently maintained across generations, only larvae that already harbor *O. tsutsugamushi*, presumably through vertical transmission, can serve as the source of human infection. Those findings suggest that *O. tsutsugamushi* is maintained primarily within mite populations and that infected larval mites are the principal source of human infection, rather than vertebrate hosts serving as amplification reservoirs.

The strain we identified was a Vietnam-related Karp-like genotype, distinct from the Kato type historically associated with *L. akamushi* mites, suggesting the presence of a previously unrecognized lineage associated with this vector species in Japan. That finding demonstrates that *L. akamushi* mites are not associated exclusively with the Kato genotype, as previously thought, but can also harbor genetically distinct lineages, including Vietnam-related Karp-like strains.

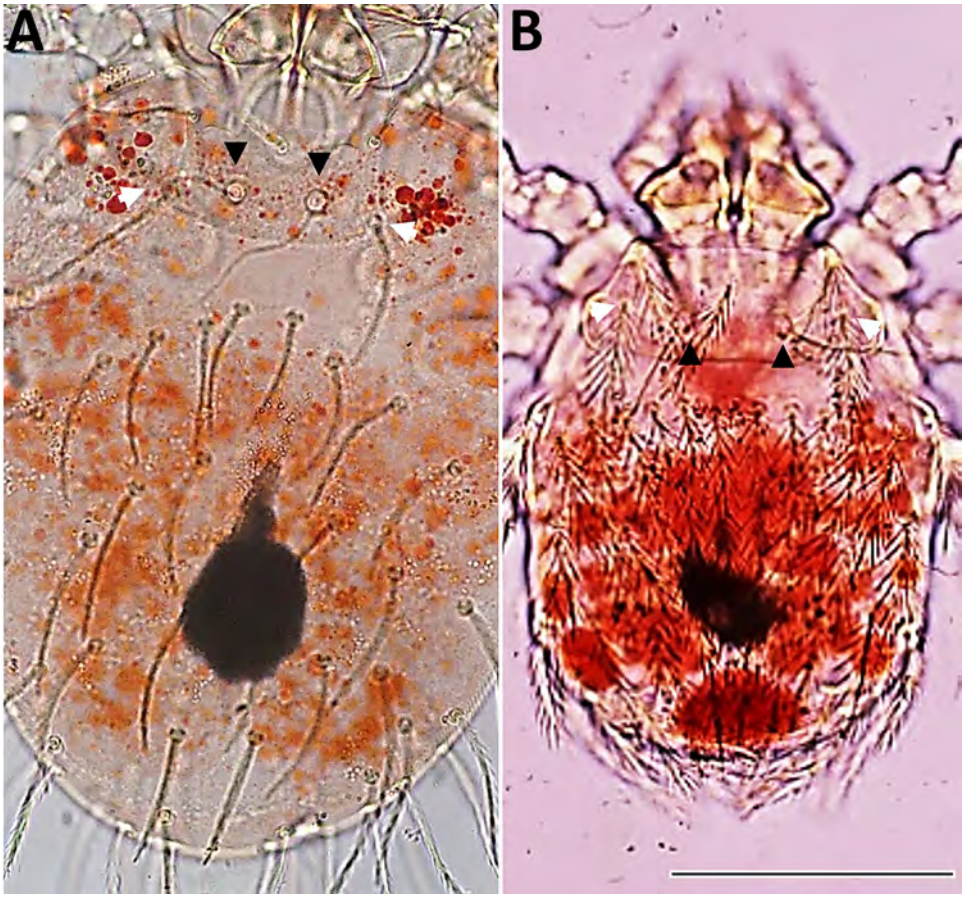

Figure 4. Comparison of engorged larval mites from a study of reemergence of scrub typhus associated with *Leptotrombidium akamushi* mites and Karp-like *Orientia tsutsugamushi* genotype bacteria, Japan, 2024–2025. A) *L. akamushi* larva; B) semi-engorged *L. pallidum* larva. Larvae were collected from field mice in Niigata Prefecture at the site of probable patient *O. tsutsugamushi* infection. *L. akamushi* can be distinguished from *L. pallidum* by the position of the sensillary setae (black arrows), which arise anterior to the posterolateral setae of the scutum, and by the presence of 8 dorsal idiosomal setae in a transverse row (white arrows). Those morphological characteristics were consistent with the molecular identification on the basis of *COX1* sequence analysis. Scale bar indicates 100 μm; both images are at the same magnification.

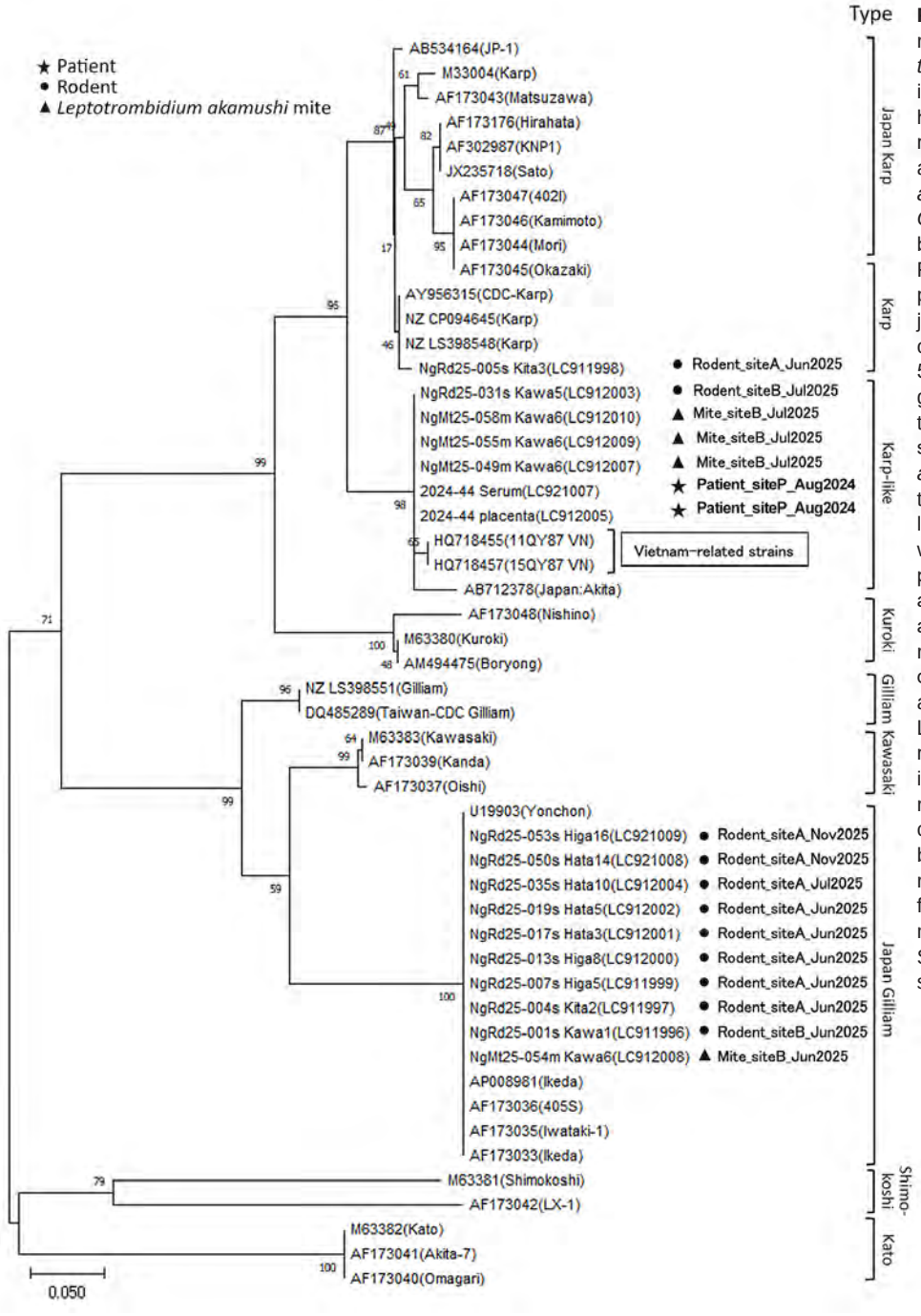

Figure 5. Phylogenetic relationships of *Orientia tsutsugamushi* strains detected in field mice, mites, and a human patient from a study of reemergence of scrub typhus associated with *Leptotrombidium akamushi* mites and Karp-like *O. tsutsugamushi* genotype bacteria, Japan, 2024—2025. Phylogenetic analysis was performed using the neighbor-joining method on the basis of an ≈420-bp region of the 56-kDa type–specific antigen gene. Sequences obtained from the placenta specimen, patient serum, 1 field mouse, and 3 *L. akamushi* mite larvae clustered together within the Karp-like lineage and were identical within the analyzed region. The placenta sequence (GenBank accession no. LC912005) was also identical over a 959-bp region to 2 *L. akamushi* mite–derived sequences (GenBank accession nos. LC912009 and LC912010). Reference strains representing major genotypes, including Kato and Karp-related strains, are included for comparison. *O. tsutsugamushi* bacterial sequences from rodents were all obtained from large Japanese field mice (*Apodemus speciosus*). Scale bar indicates nucleotide substitutions per site.

In summary, the high seroprevalence in field mice at both survey sites suggests widespread circulation of *O. tsutsugamushi* and infected vector mites within the study area. Collectively, our findings provide evidence for the re-emergence of summer scrub typhus associated with infected *L. akamushi* mites and highlight the need for continued vector surveillance and molecular *O. tsutsugamushi* bacterial surveillance to clarify scrub typhus risk in Japan.

Acknowledgments

We thank the Niigata Prefectural Government for granting permission to conduct rodent trapping at the study sites and colleagues at the National Institute of Infectious Diseases for support during field investigations. We are grateful to T. Miura for assistance with laboratory testing, patient information, and coordination with the attending physician. We thank Editage (https://www.editage.jp) for English language editing.

About the Author

Dr. Ogawa is a senior researcher in the Department of Bacteriology I at the National Institute of Infectious Diseases, Tokyo, Japan. His research interests include vector-borne infectious diseases and the molecular epidemiology of rickettsial pathogens.

References

1. Elliott I, Pearson I, Dahal P, Thomas NV, Roberts T, Newton PN. Scrub typhus ecology: a systematic review of *Orientia* in vectors and hosts. Parasit Vectors. 2019;12:513. https://doi.org/10.1186/s13071-019-3751-x
2. Kawamura A, Tanaka H, Tamura A, editors. Tsutsugamushi disease. Tokyo: University of Tokyo Press; 1995.
3. Ogawa M, Hagiwara T, Kishimoto T, Shiga S, Yoshida Y, Furuya Y, et al. Scrub typhus in Japan: epidemiology and clinical features of cases reported in 1998. Am J Trop Med Hyg. 2002;67:162–5. https://doi.org/10.4269/ajtmh.2002.67.162
4. Iwasa M, Kasuya S, Noda N, Hioki A, Ito A, Ohtomo H. Trombiculid mites (Acari: Trombiculidae) and *Rickettsia tsutsugamushi* isolated from wild rodents in a new endemic area of Japan. J Med Entomol. 1990;27:501–8. https://doi.org/10.1093/jmedent/27.4.501
5. Kitaoka M, Asanuma K, Otsuji J. Transmission of *Rickettsia orientalis* to man by *Leptotrombidium akamushi* at a scrub typhus endemic area in Akita Prefecture, Japan. Am J Trop Med Hyg. 1974;23:993–9. https://doi.org/10.4269/ajtmh.1974.23.993
6. Sato H, Kokusho Y, Shibata C, Saito H, Saito S, Fujita H, et al. A case of classical tsutsugamushi disease confirmed after an interval of 15 years in Akita Prefecture, Japan [in Japanese]. Kansenshogaku Zasshi. 2010;84:454–6. https://doi.org/10.11150/kansenshogakuzasshi.84.454
7. Takahashi M, Misumi H, Urakami H, Nakajima S, Furui S, Yamamoto S, et al. Mite vectors (Acari: Trombiculidae) of scrub typhus in a new endemic area in northern Kyoto, Japan. J Med Entomol. 2004;41:107–14. https://doi.org/10.1603/0022-2585-41.1.107
8. Takahashi M, Murata M, Misumi H, Hori E, Kawamura A Jr, Tanaka H. Failed vertical transmission of *Rickettsia tsutsugamushi* (Rickettsiales: Rickettsiaceae) acquired from rickettsemic mice by *Leptotrombidium pallidum* (Acari: trombiculidae). J Med Entomol. 1994;31:212–6. https://doi.org/10.1093/jmedent/31.2.212
9. Seto J, Suzuki Y, Otani K, Qiu Y, Nakao R, Sugimoto C, et al. Proposed vector candidate: *Leptotrombidium palpale* for Shimokoshi type *Orientia tsutsugamushi*. Microbiol Immunol. 2013;57:111–7. https://doi.org/10.1111/1348-0421.12015
10. Duong V, Mai TT, Blasdell K, Lo V, Morvan C, Lay S, et al. Molecular epidemiology of *Orientia tsutsugamushi* in Cambodia and Central Vietnam reveals a broad region-wide genetic diversity. Infect Genet Evol. 2013;15:35–42. https://doi.org/10.1016/j.meegid.2011.01.004
11. Takada N, Takahashi M, Fujita H, Natsuaki M. Medical acarology in Japan [in Japanese]. Tokyo: Hokuryukan; 2019.
12. Ogawa M, Takahashi M, Matsutani M, Takada N, Noda S, Saijo M. Obligate intracellular bacteria diversity in unfed *Leptotrombidium scutellare* larvae highlights novel bacterial endosymbionts of mites. Microbiol Immunol. 2020;64:1–9. https://doi.org/10.1111/1348-0421.12745
13. Ogawa M, Ando S, Saijo M. Evaluation of recombinant type-specific antigens of *Orientia tsutsugamushi* expressed by a baculovirus-insect cell system as antigens for indirect immunofluorescence assay in the serological diagnosis of scrub typhus. Jpn J Infect Dis. 2020;73:330–5. https://doi.org/10.7883/yoken.JJID.2019.334
14. Kawamori F, Shimazu Y, Sato H, Monma N, Ikegaya A, Yamamoto S, et al. Evaluation of diagnostic assay for rickettsioses using duplex real-time PCR in multiple laboratories in Japan. Jpn J Infect Dis. 2018;71:267–73. https://doi.org/10.7883/yoken.JJID.2017.447
15. Furuya Y, Yoshida Y, Katayama T, Kawamori F, Yamamoto S, Ohashi N, et al. Specific amplification of *Rickettsia tsutsugamushi* DNA from clinical specimens by polymerase chain reaction. J Clin Microbiol. 1991;29:2628–30. https://doi.org/10.1128/jcm.29.11.2628-2630.1991
16. Kumar S, Stecher G, Li M, Knyaz C, Tamura K. MEGA X: molecular evolutionary genetics analysis across computing platforms. Mol Biol Evol. 2018;35:1547–9. https://doi.org/10.1093/molbev/msy096
17. Takahashi M, Murata M, Nogami S, Hori E, Kawamura A Jr, Tanaka H. Transovarial transmission of *Rickettsia tsutsugamushi* in *Leptotrombidium pallidum* successively reared in the laboratory. Jpn J Exp Med. 1988;58:213–8.

Address for correspondence: Motohiko Ogawa, Department of Bacteriology I, National Institute of Infectious Diseases, Japan Institute for Health Security, 1-23-1, Toyama, Shinjuku-ku, Tokyo 162-8640, Japan; email: ogawa.mo@jihs.go.jp

Serologic Evidence of Hantavirus Exposure in Humans, Italy, 2004–2018

Giulia Faolotto, Anishia Wasberg, Rommel Iheozor-Ejiofor, Essi M. Korhonen, Rosalba Minisini, Tarja Sironen, Ruut Joensuu, Jiaxin Ling, Åke Lundkvist, Olli Vapalahti, Eili Huhtamo, Paolo Ravanini

Rodentborne hantaviruses and lymphocytic choriomeningitis virus (LCMV) circulate in northern Italy but are rarely diagnosed. We tested samples collected from 371 patients during 2004–2018 and detected LCMV IgG in 2.7% of samples and hantavirus IgG in 7.3%. Puumala virus–neutralizing antibodies were confirmed in 10 cases, indicating unrecognized local hantavirus circulation.

In Europe, endemic rodentborne viruses include Old World hantaviruses (Hantaviridae) and lymphocytic choriomeningitis virus (LCMV; Arenaviridae) (*1*). Puumala virus (PUUV), carried by the bank vole (*Clethrionomys glareolus*), is the most widespread hantavirus in Europe. In southeastern Europe and the Balkans, Dobrava-Belgrade virus (DOBV) in yellow-necked mice (*Apodemus flavicollis*) and Saaremaa virus in striped field mice (*A. agrarius*) are also present (*1*). Those mouse species and other potential reservoir species, such as the *Mus musculus* mouse and *Rattus norvegicus* rat, are common in northern Italy, including the regions discussed in this article (*2*).

DOBV and PUUV cause hemorrhagic fever with renal syndrome (HFRS), and LCMV, transmitted by house mice (*M. musculus*), can cause febrile illness or aseptic meningitis (*1*). Unlike in many neighboring countries, rodentborne infections are not commonly diagnosed in Italy, although evidence of LCMV and DOBV circulation and human exposure exists (*2*–*6*). This study aimed to determine serologic evidence of hantaviruses and LCMV exposure in northwestern Italy, a region where these viruses have not been extensively studied.

Author affiliations: Maggiore della Carità University Hospital, Novara, Italy (G. Faolotto, P. Ravanini); Uppsala University, Uppsala, Sweden (A. Wasberg, J. Ling, Å. Lundkvist); University of Helsinki, Helsinki, Finland (R. Iheozor-Ejiofor, E.M. Korhonen, T. Sironen, R. Joensuu, O. Vapalahti, E. Huhtamo); University of Eastern Piedmont, Novara (R. Minisini); University of Helsinki and Helsinki University Hospital, HUSLAB, Helsinki (O. Vapalahti)

DOI: https://doi.org/10.3201/eid3209.260840

The Study

The study samples (n = 371, average age 59.9 years) were collected during 2004–2018 for other studies in the provinces of Novara, Biella, Vercelli, and Verbano Cusio-Ossola (Figure) and included patients with various chronic diseases, including nephrologic pathologies, alcohol abuse, hepatitis C virus infection, and liver diseases. All patients provided written informed consent, and the study was approved by the local ethics committee. In 2018, we screened patient plasma samples for PUUV, DOBV, and LCMV IgG using immunofluorescence assay (IFA) as previously described (*2*). To further determine hantavirus antibody specificity, we tested neutralizing antibodies in 2024 and 2025 against PUUV and DOBV for samples with IgG titers >1:40 in DOBV or PUUV IgG IFA.

We performed focus reduction neutralization tests (FRNTs) in Vero E6 cells according to previously published protocols (*7*,*8*). In brief, we incubated Vero E6 cells with serially diluted plasma samples and hantavirus (50 focus-forming units/well) in 24-well plates. After adsorption, we overlaid cells with MEM-agarose and incubated for 8–10 days, depending on the virus. We detected foci by immunostaining with a hantavirus-specific monoclonal antibody and horseradish peroxidase–conjugated secondary antibody, visualized with AEC (3-amino-9-ethylcarbazole) substrate. We determined neutralizing titers on the basis of the reduction in foci relative to virus-only controls; we used an 80% reduction relative to the negative control as the cutoff for enhanced specificity.

Of 371 patients, 27 (7.3% [95% Wilson CI 5.0%–10.4%]) were positive for hantavirus IgG by IFA (titers 1:20–1:640) (Table 1). We further tested 11 with titers >1:40 by FRNT and detected PUUV-neutralizing activity in 10/11 of the tested samples (titers 1:80

to ≥1:320). Neutralization of DOBV was generally lower (titers <1:40 to 1:80). Several samples exhibited PUUV-specific neutralization with minimal or absent DOBV-neutralizing activity (Table 2). For LCMV, 10 of 371 patients (2.7% [95% Wilson CI 1.5%–4.9%]) were IgG positive (titers 1:20 to 1:40) (Table 1). Seropositive cases were geographically dispersed (Figure), and antibodies to both viruses were detected only in the region of Novara.

This study detected antibodies against hantaviruses and arenaviruses in patients from a previously unstudied region of northwestern Italy. Hantavirus infections are routinely reported in neighboring countries but are rarely diagnosed in Italy; yearly cases have been reported in France, Austria, and Slovenia (*9*). LCMV seroprevalence (2.7%) matched previous reports from the Trentino area (*2*). Our hantavirus seropositivity (7.3%) was higher than the 0.2% DOBV IgG reported for forestry workers in Trentino in 2002 (*2*) and above the estimated 1.7% average in the general population in Italy (*10*). Higher seroprevalence (up to 8.8%) has been reported in occupationally rodent-exposed risk groups (*5*).

IFA results demonstrated that plasma samples were positive for PUUV or for DOBV IgG; however, FRNT demonstrated predominantly PUUV-specific neutralizing activity, suggesting PUUV as the likely infecting virus. Neutralization against DOBV was absent or detected at low titers, consistent with serologic cross-reactivity rather than an actual DOBV infection. Only 1 sample (S52) showed reactivity to both PUUV and DOBV antigens by IFA and had a

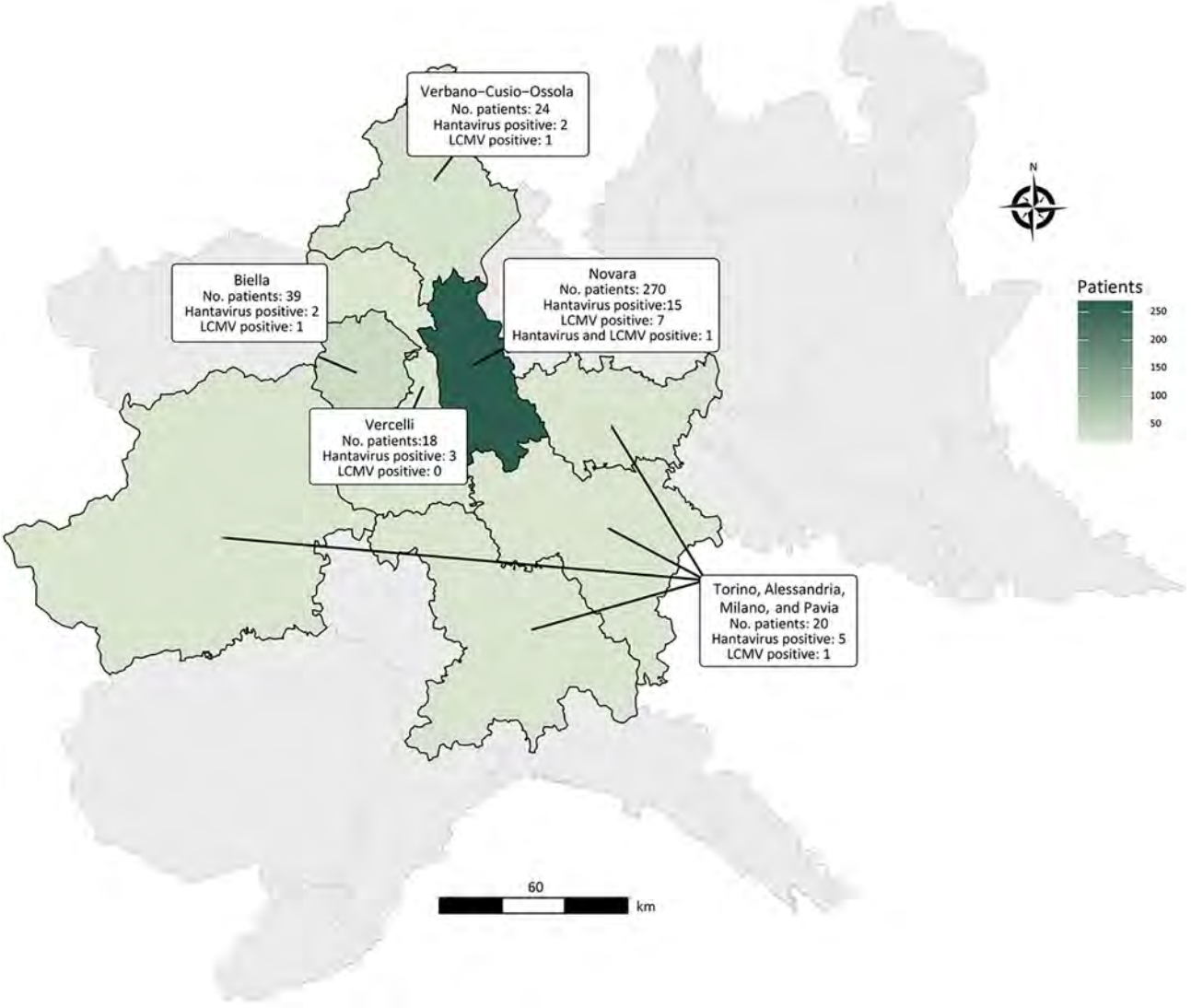

Figure. Geographic distribution of study participants and seropositive cases by region in study of serologic evidence of hantavirus exposure in humans, Italy, 2004–2018.

Table 1. Antibody screening results determined by immunofluorescence assay in study of serologic evidence of hantavirus exposure in humans, Italy, 2004–2018

Classification/patient group description	Sampling year	No. (%) patients				
		Total	Hantavirus IgG positive			LCMV IgG positive
			PUUV	DOBV	Combined	
Alcohol abuse	2013–2016 (mostly 2013)	28 (7.55)	2 (7.14)	1 (3.57)	3 (10.71)	0
Liver diseases	2004, 2009, 2012 (mostly 2012)	177 (47.71)	5 (2.82)	11 (6.21)	16 (9.04)	4 (1.69)
HCV infections	2018	30 (8.09)	0	0	0	1 (3.33)
Renal diseases	2006, 2007, 2018	110 (29.65)	3 (2.72)	3 (2.72)	6 (5.45)	5 (4.55)
Oral anticoagulant treatment	2007	26 (7)	1 (3.85)	1 (3.85)	2 (7.69)	0
Total		371 (100)	11 (2.96)	16 (4.31)	27 (7.28)	10 (2.70)

*DOBV, Dobrava-Belgrade virus; HCV, hepatitis C virus; LCMV, lymphocytic choriomeningitis virus; PUUV, Puumala virus.

mixed neutralization profile. That finding could indicate exposure to an antigenically related hantavirus or the presence of cross-reactive antibodies. Cross-neutralizing antibody responses among hantaviruses have been documented in both acute and late-convalescent patient samples, potentially complicating serologic interpretation. Although dual exposure to both PUUV and DOBV cannot be excluded, the serologic findings do not enable a definite distinction between these possibilities (*7*,*11*)

The first limitation of our study is that single-time-point sampling precluded infection timing and symptom linkage to seropositivity. Because samples were collected from chronically ill persons, the findings might not fully represent the general population, and data on risk factors, residence, and travel history were unavailable. Residence in a large metropolitan area such as Milan could argue against local transmission; however, patients' chronic conditions and regular follow-up at the regional university hospital support predominantly local or regional exposure. Furthermore, geographic representation was uneven; most patients resided in the Novara area, potentially biasing the spatial distribution of seropositive cases.

Overall, we found no clear association between serologic findings and patient group, location, or sampling timing. Most hantavirus-seropositive patients were men 36–88 years of age, consistent with reports of higher incidence of hantavirus infection in men and a predominance in the 45–64–year age group (*9*).

The neutralization profile strongly suggested exposure to PUUV or a closely related hantavirus rather than DOBV, previously reported in Italy (*2*,*4*–*6*). The symptoms of PUUV and DOBV infections can vary from asymptomatic to severe and often include fever, headache, abdominal pain, backache, and nausea, occurring in the absence of respiratory symptoms (*1*). Although both viruses can cause HFRS, disease associated with DOBV is more severe (5%–10% fatality rate), whereas PUUV infection is typically milder (<1% fatality rate) (*1*), which might hinder clinical recognition. PUUV infections have been documented in neighboring countries in the Alpine region and central Europe (*12*–*14*) and, given the continuity of forest ecosystems and the distribution of the bank vole, its presence in northern Italy is plausible. Although the bank vole, the natural host of PUUV, typically inhabits forests, our study area was largely semiurban and agricultural with fragmented woodland. How human exposure occurs in such environments warrants further investigation. Of note, a recent PUUV outbreak in coastal Croatia (*15*) highlights the virus's ability to emerge beyond typical bank vole habitats.

Table 2. Hantavirus IFA and FRNT results among participants in study of serologic evidence of hantavirus exposure in humans, Italy, 2004–2018*

Sampling year	Location (Province)	Sample code	IFA results, titer		FRNT assay results, titer	
			PUUV	DOBV	PUUV	DOBV
2004	Abbiategrasso (Milano)	681	<10	40	160	<40
2005	Novara (Novara)	791	80	80	160	80
2011	Arona (Novara)	S09	40	<10	80	40
2012	Galliate (Novara)	S65	40	<10	80<160	40
2012	Novara (Novara)	S42	80	80	160	40
2012	Castelletto sopra Ticino (Novara)	S22	80	40	80	<40
2012	Novara (Novara)	S52	320	640	ND	80<160
2012	Robecchetto con Induno (Milano)	S18	40	<10	80	40<80
2013	Trecate (Novara)	E19	40	10	80	40<80
2015	Piedimulera (Verbania)	E27	80	<10	160<320	40
2018	Galliate (Novara)	N04	40	<10	160	80

*Average age of participants was 58.9 years; participants were 63.6% male and 36.3% female. DOBV, Dobrava-Belgrade virus; FRNT, focus reduction neutralization test; IFA, immunofluorescence assay; ND, not determined; PUUV, Puumala virus.

Conclusions

Our serologic findings in a cohort of chronically ill patients in northern Italy demonstrated exposure to hantaviruses and LCMV. The rate of hantavirus antibody detection was notably high, suggesting local transmission. Together with previous reports from Italy, our findings highlight that rodentborne viruses, particularly hantaviruses, are likely endemic beyond the currently recognized regions. Because of limited data on human infections, hantaviruses remain largely underdiagnosed and neglected in Italy. Although the most recent samples in this study date from 2018, the detection of antibodies across multiple sampling years suggests sustained exposure in this region. Further studies in both rodents and humans are needed to identify endemic hantavirus species and better estimate associated risks and disease burden. Raising clinician awareness of mild forms of HFRS, such as nephropathia epidemica, and ensuring access to appropriate laboratory diagnostics are crucial for timely detection and confirmation of infections. Public health messaging would be essential to minimize exposure to rodents and their excreta, helping to prevent rodentborne diseases across Italy.

This study was supported by grants from FreeMover of the Università del Piemonte Orientale, Sigrid Jusélius Foundation, Jane and Aatos Erkko Foundation, and the Research Council of Finland.

About the Author

Dr. Faolotto is a physician affiliated with the University Hospital in Novara, Italy, where she combines clinical practice with research. Her work has included contributions to research in infectious diseases and epidemiology, with a focus on advancing clinical knowledge and patient care.

References

1. Kallio-Kokko H, Uzcategui N, Vapalahti O, Vaheri A. Viral zoonoses in Europe. FEMS Microbiol Rev. 2005;29:1051–77. https://doi.org/10.1016/j.femsre.2005.04.012
2. Kallio-Kokko H, Laakkonen J, Rizzoli A, Tagliapietra V, Cattadori I, Perkins SE, et al. Hantavirus and arenavirus antibody prevalence in rodents and humans in Trentino, northern Italy. Epidemiol Infect. 2006;134:830–6. https://doi.org/10.1017/S0950268805005431
3. Tagliapietra V, Rosà R, Hauffe HC, Laakkonen J, Voutilainen L, Vapalahti O, et al. Spatial and temporal dynamics of lymphocytic choriomeningitis virus in wild rodents, northern Italy. Emerg Infect Dis. 2009;15:1019–25. https://doi.org/10.3201/eid1507.01524
4. Tagliapietra V, Rosà R, Rossi C, Rosso F, Hauffe HC, Tommasini M, et al. Emerging rodent-borne viral zoonoses in Trento, Italy. EcoHealth. 2018;15:695–704. https://doi.org/10.1007/s10393-018-1335-4
5. Nuti M, Amaddeo D, Autorino GL, Crovatto M, Crucil C, Ghionni A, et al. Seroprevalence of antibodies to hantaviruses and leptospires in selected Italian population groups. Eur J Epidemiol. 1992;8:98–102. https://doi.org/10.1007/BF03334979
6. Leopardi S, Drzewnioková P, Baggieri M, Marchi A, Bucci P, Bregoli M, et al. Identification of Dobrava-Belgrade virus in *Apodemus flavicollis* from north-eastern Italy during enhanced mortality. Viruses. 2022;14:1241. https://doi.org/10.3390/v14061241
7. Lundkvist A, Hukic M, Hörling J, Gilljam M, Nichol S, Niklasson B. Puumala and Dobrava viruses cause hemorrhagic fever with renal syndrome in Bosnia-Herzegovina: evidence of highly cross-neutralizing antibody responses in early patient sera. J Med Virol. 1997;53:51–9. https://doi.org/10.1002/(SICI)1096-9071(199709)53:1<51::AID-JMV9>3.0.CO;2-P
8. Ye C, Wang D, Liu H, Ma H, Dong Y, Yao M, et al. Corrigendum: an improved enzyme-linked focus formation assay revealed baloxavir acid as a potential antiviral therapeutic against hantavirus infection. Front Pharmacol. 2020;11:201. https://doi.org/10.3389/fphar.2020.00201
9. European Centre for Disease Prevention and Control. Hantavirus infection. Annual epidemiological report for 2020 [cited 2026 Feb 13]. https://www.ecdc.europa.eu/sites/default/files/documents/Hantavirus-AER-2020.pdf
10. Riccò M, Peruzzi S, Ranzieri S, Balzarini F, Valente M, Marchesi F, et al. Hantavirus infections in Italy: not reported doesn't mean inexistent. Acta Biomed. 2021;92:e2021324.
11. Clark JJ, et al. Cross-binding antibodies capable of neutralising diverse hantaviruses are produced in response to Puumala virus infection. EBioMedicine. 2025.
12. Vetter P, L'Huillier AG, Montalbano MF, Pigny F, Eckerle I, Torriani G, et al. Puumala virus infection in a family, Switzerland. Emerg Infect Dis. 2021;27:658–60. https://doi.org/10.3201/eid2702.203770
13. Aberle SW, Lehner P, Ecker M, Aberle JH, Arneitz K, Khanakah G, et al. Nephropathia epidemica and Puumala virus in Austria. Eur J Clin Microbiol Infect Dis. 1999;18:467–72. https://doi.org/10.1007/s100960050325
14. Avsic-Zupanc T, Petrovec M, Duh D, Plyusnina A, Lundkvist A, Plyusnin A. Puumala hantavirus in Slovenia: analyses of S and M segment sequences recovered from patients and rodents. Virus Res. 2007;123:204–10. https://doi.org/10.1016/j.virusres.2006.08.008
15. Tomljenovic M, Lakoseljac D, Knezevic L, Batista M, Vilibic-Cavlek T, Kaic B, et al. Spread of Puumala hantavirus to new areas in a large Croatian outbreak of hemorrhagic fever with renal syndrome, 2021. Vector Borne Zoonotic Dis. 2024;24:773–83. https://doi.org/10.1089/vbz.2024.0032

Address for correspondence: Anishia Wasberg, Department of Medical Biochemistry and Microbiology, Uppsala University, Box 582, 751 23 Uppsala, Sweden; email: anishia.wasberg@imbim.uu.se

Seroprevalence of Influenza A(H5N1) Virus in Domestic Cats at Epicenter of Dairy Cattle Outbreaks, California, USA, 2024–2026

Ian G. Bemis, Ismaila Shittu, Jacob F. Gomez, Esther A. Fadaka, Sofia Perez, Gregory C. Gray, Kristen K. Coleman

We conducted a serologic study of domestic cats near the epicenter of the dairy cattle outbreaks of influenza A(H5N1) in California, USA. Three of the 12 cats sampled within 2 km of farms had neutralizing antibodies against H5N1 virus. Proximity to dairy farms was a statistically significant risk factor for seropositivity.

Highly pathogenic avian influenza A(H5N1) clade 2.3.4.4b is emerging in domestic cats (*Felis catus*), presenting urgent public health and animal welfare implications. Historically, cats have not been widely considered important hosts of influenza viruses. However, sporadic infections and outbreaks of avian influenza viruses in cats have occurred for >20 years (*1*). The emergence of H5N1 clade 2.3.4.4b virus has resulted in widespread mammalian infections (*2*,*3*), including an alarming increase in infections among domestic cats, in which the estimated case-fatality rate is 90% (*1*). Although most of those infections emerged from direct bird-to-cat transmission, several recent outbreaks among US cats have involved infected dairy farms (*4*–*6*) or links to workers in the dairy industry (*7*). Contaminated raw dairy milk (*5*,*8*) and raw meat–based diets (*9*) have been identified as sources of infection in cats.

Author affiliations: University of Maryland School of Public Health, College Park, Maryland, USA (I.G. Bemis, E.A. Fadaka, S. Perez, K.K. Coleman); University of Maryland College of Agriculture and Natural Resources, College Park (I.G. Bemis, K.K. Coleman); University of Texas Medical Branch Division of Infectious Diseases, Galveston, Texas, USA (I. Shittu, G.C. Gray); Cross Street Small Animal Veterinary Hospital, Tulare, California, USA (J.F. Gomez)

DOI: https://doi.org/10.3201/eid3209.260785

Like swine, cats have α-2,6- and α-2,3-linked sialic acid receptors (*10*) and can be co-infected with avian and human influenza viruses. Thus, with widespread H5N1 virus infections, a growing potential exists for influenza virus co-infections in domestic cats that could result in viral reassortment and selection for novel human-adapted viruses. Infections resulting from cat-to-human transmission of avian influenza have been documented 3 times in the United States, including in a veterinarian and an animal shelter worker exposed to shelter cats infected with influenza A(H7N2) virus in New York, New York, in 2016 (*11*,*12*) and in a veterinary professional exposed to a domestic cat infected with H5N1 virus in Los Angeles, California, in 2024 (*13*). Suspected human-to-cat transmission of H5N1 virus also occurred in 2024 in Michigan, resulting in the deaths of 2 house cats (*7*). Ten additional cats died from another H5N1 outbreak in 2024 in South Dakota (*14*) in which cattle-to-bird-to-cat transmission was suspected.

Although several US dairy industry–related outbreaks of H5N1 among cats have been reported, the resulting seroprevalence of H5N1 virus among domestic cats near affected dairy farms is unknown. Therefore, we performed a serosurvey of domestic cats at the epicenter of the 2024–2025 dairy cattle outbreaks in California's Central Valley.

The Study

An animal welfare organization in Tulare County, California, provided serum samples collected from cats during routine blood draws. Because serum samples from routine blood draws were provided, an ethics review was not required. We shipped aliquots to the University of Maryland (College Park, MD, USA) and the University of Texas Medical Branch (Galveston,

TX, USA) and tested them using ELISA and H5 microneutralization assays (Appendix, https://wwwnc.cdc.gov/EID/article/32/9/26-0785-App1.pdf). We compared approximate age, sex, weight, and distance to nearest dairy farm between seropositive and seronegative cats (Appendix).

During December 2024–March 2026, we collected 73 serum samples from indoor and outdoor cats (Figure 1) within 9.7 km (6 miles) of ≥1 dairy farms (mean 4.7 km [2.9 miles]). Among the 73 cats, 3 tested positive for both influenza A virus nucleoprotein antibodies and neutralizing antibodies against H5 clade 2.3.4.4b. One indoor-only and 1 outdoor feral cat had neutralizing antibody titers of 1:160, and 1 indoor-only cat had a titer of 1:640, indicating strong positivity and 100% agreement between the ELISA and microneutralization assay. All negative samples had titers of <1:20.

Three (25%) of the 12 cats sampled within 2 km (1.24 miles) of dairy farms were seropositive for H5N1 virus (Figure 2), yielding an overall seropositivity rate of 4.1% for all surveyed cats. Seropositive cats had a mean distance to the nearest dairy farm of 1.34 km (0.8 miles), compared with 4.83 km (3 miles) for seronegative cats ($p = 0.014$) (Figure 3). Average age of surveyed cats was ≈1.6 years (range ≈3 months–4.9 years); 60% were female and 40% male. Age and sex were not significantly different for seropositive and seronegative cats. Of the 73 cats surveyed, 68 (93%) were in rural areas and 5 (7%) in urban areas. All seropositive cats were in rural areas. No indoor cats were fed raw meat or dairy.

Conclusions

Avian influenza A(H5N1) clade 2.3.4.4b is an emerging threat to domestic cats and public health. We report a 25% seropositivity rate for the virus among domestic cats within 2 km (1.2 miles) of dairy farms in the epicenter of the H5N1 cattle outbreaks in California during 2024–2026. Proximity to dairy farms in counties experiencing outbreaks may be a risk factor for H5N1 spillover to indoor and outdoor domestic cats. Our research provides insight into potential H5N1 virus sources and transmission routes among domestic cats in the United States, for which data are scarce. Our results may help refine public health guidance on the prevention of avian influenza in cats and set the stage for future studies.

Although only 3 seropositive cats were identified in our study, their closer proximity to dairy farms compared with seronegative cats is an important epidemiologic finding. Although we cannot determine the source (or sources) of H5N1 among the seropositive cats in our study, their close proximity to dairy farms suggests that cats may share a source of infection with infected cattle or that dairy herds are directly infecting nearby cat populations. Infections and deaths also have been reported among cats exposed to H5N1 on affected dairy farms in Texas (*4*), New Mexico (*5*), and Minnesota (*6*) and among domestic cats near dairy farms in South Dakota (*14*) and in the households of Michigan dairy industry workers (*7*). Similar to the South Dakota outbreak (*14*), cattle-to-bird-to-cat transmission is one plausible explanation for the seropositive feral cat identified in our study. The feral cat was found within 0.8 km (0.5 miles) of a farm and could have wandered and been exposed directly to cattle or contaminated milk or other sources. Cat movement onto influenza-infected farms should be studied, in addition to cat exposure to infected rodents and other small mammals. Regarding the seropositive indoor-only cats in our study, both were from a household of a dairy industry worker, similar to the infections in Michigan cats (*7*). The route of transmission, including human-to-cat transmission, cannot be confirmed in our study. However, we can rule out raw meat or dairy as a potential source.

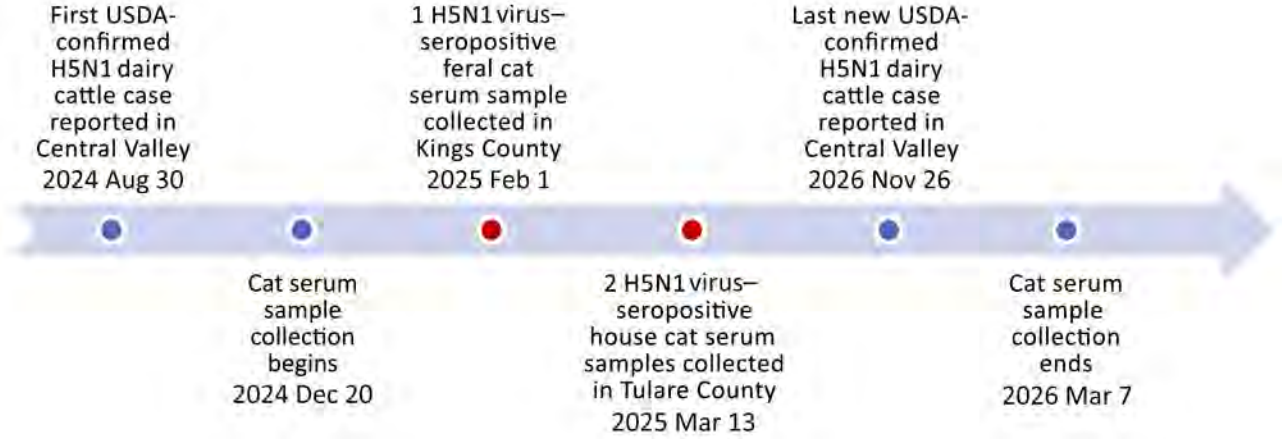

Figure 1. Timeline of highly pathogenic avian influenza A(H5N1) dairy cattle outbreaks and domestic cat (*Felis catus*) serum sample collection, Central Valley, California, USA, 2024–2026. USDA, US Department of Agriculture.

Figure 2. Grouped distance to the nearest dairy farm for domestic cats (*Felis catus*) seropositive and seronegative for highly pathogenic avian influenza A(H5N1) clade 2.3.4.4b virus near epicenter of dairy cattle outbreaks, Central Valley, California, USA, 2024–2026.

Because of the high case-fatality rate in cats with H5N1 virus infection (*1*), the seroprevalence reported in our study probably is an underestimate of the actual prevalence of H5N1 virus infection in cats in this region. In addition, cats infected with H5N1 virus often have onset of acute encephalitis with multifocal necrosis, resulting in paralysis, blindness, ataxia, and other severe long-term sequelae, sometimes requiring ambulatory assistive devices (*8*). Such complications may preclude working cats from escaping predation or effectively hunting or deterring rodents on farms. To help mitigate that animal welfare and farm maintenance issue, vaccinating dairy cattle should be considered (*15*) because it could protect cattle and other at-risk animals on or near farms.

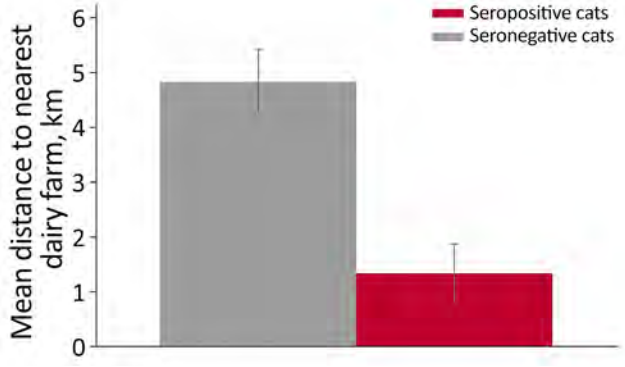

Figure 3. Mean distance to the nearest dairy farm for domestic cats (*Felis catus*) seropositive and seronegative for influenza A(H5N1) clade 2.3.4.4b virus near epicenter of the dairy cattle outbreaks, Central Valley, California, USA, 2024–2026. Error bars represent SEM.

Our study highlights a critical gap in companion animal surveillance and might be helpful to health agencies as they seek approaches to mitigating this emerging infectious disease threat. Proximity to dairy farms was a risk factor for H5N1 spillover to cats in our study. However, cattle-to-cat transmission of H5N1 virus is a relatively new phenomenon, and most cat infections reported in the literature over the past 20 years have been from bird-to-cat transmission (*1*). To assess the in situ risk for human-adapted reassortant influenza viruses emerging in cats, future work is needed to characterize the seroprevalence of human influenza viruses in cats and avian influenza

viruses in cats near outbreaks in poultry and wild birds. Cat surveillance studies also could provide insight into nearby H5N1 outbreaks that have yet to be discovered, fully investigated, or contained.

Acknowledgments

We thank the Valley Oak Society for the Prevention of Cruelty to Animals and Alexandra van der Hoeven. We also thank the University of Maryland Baltimore Institute for Clinical and Translational Research and the University of Maryland Strategic Partnership, MPowering the State. We thank Richard J. Webby for sharing the recombinant H5N1 virus (rg-A/bald eagle/Florida/W22-134-OP/2022) used in the microneutralization assay.

Raw data are available and may be provided by the authors upon reasonable request.

This study was funded in part by the University of Maryland Baltimore Institute for Clinical and Translational Research and the University of Maryland Strategic Partnership, MPowering the State (awarded to K.K.C.). Discretionary funding from the University of Maryland School of Public Health, Department of Global, Environmental, and Occupational Health was awarded to K.K.C. This project also was supported in part by US Department of Agriculture Agricultural Research Service (agreement 58-3022-4-048, awarded to G.C.G.).

Author contributions: I.G.B. and K.K.C drafted the initial version of the manuscript, and I.G.B, K.K.C, I.S., J.F.G., and G.C.G provided revisions; K.K.C, I.S., and G.C.G. conceptualized the study; J.F.G. helped provide serum samples; I.G.B and I.S. performed the laboratory work and provided the laboratory data, with the help of E.A.F. and S.P.

About the Author

Mr. Bemis is a comparative biomedical sciences PhD student at the University of Maryland Department of Veterinary Medicine in College Park, Maryland, USA. His primary research interests include animal virology, respiratory virus transmission, virulence factors, viral zoonosis, and reverse zoonosis.

References

1. Coleman KK, Bemis IG. Avian influenza virus infections in felines: a systematic review of two decades of literature. Open Forum Infect Dis. 2025;12:ofaf261. https://doi.org/10.1093/ofid/ofaf261
2. Peacock TP, Moncla L, Dudas G, VanInsberghe D, Sukhova K, Lloyd-Smith JO, et al. The global H5N1 influenza panzootic in mammals. Nature. 2025;637:304–13. https://doi.org/10.1038/s41586-024-08054-z
3. US Department of Agriculture. Detections of highly pathogenic avian influenza in mammals. 2026 Jun 26 [cited 2026 Apr 24]. https://www.aphis.usda.gov/livestock-poultry-disease/avian/avian-influenza/hpai-detections/mammals
4. Burrough ER, Magstadt DR, Petersen B, Timmermans SJ, Gauger PC, Zhang J, et al. Highly pathogenic avian influenza A(H5N1) clade 2.3.4.4b virus infection in domestic dairy cattle and cats, United States. Emerg Infect Dis. 2024;30:1335–43. https://doi.org/10.3201/eid3007.240508
5. Caserta LC, Frye EA, Butt SL, Laverack M, Nooruzzaman M, Covaleda LM, et al. Spillover of highly pathogenic avian influenza H5N1 virus to dairy cattle. Nature. 2024;634:669–76. https://doi.org/10.1038/s41586-024-07849-4
6. Mainenti M, Siepker C, Magstadt DR, Gauger P, Baum D, Petersen B, et al. Distribution of lesions and detection of influenza A(H5N1) virus, clade 2.3.4.4b, in ante- and postmortem samples from naturally infected domestic cats on U.S. dairy farms. J Vet Diagn Invest. 2025;37:27–35. https://doi.org/10.1177/10406387241300464
7. Naraharisetti R, Weinberg M, Stoddard B, Stobierski MG, Dodd KA, Wineland N, et al. Highly pathogenic avian influenza A(H5N1) virus infection of indoor domestic cats within dairy industry worker households—Michigan, May 2024. MMWR Morb Mortal Wkly Rep. 2025;74:61–5. https://doi.org/10.15585/mmwr.mm7405a2
8. Frye EA, Nooruzzaman M, Cronk B, Laverack M, de Oliveira PSB, Caserta LC, et al. Isolation of highly pathogenic avian influenza A(H5N1) virus from cat urine after raw milk ingestion, United States. Emerg Infect Dis. 2025;31:1636–9. https://doi.org/10.3201/eid3108.250309
9. Kang YM, Heo GB, An SH, Lee H, Park E, Cha RM, et al. Highly pathogenic avian influenza A(H5N1) virus infection in cats, South Korea, 2023. Emerg Infect Dis. 2024;30:2510–20. https://doi.org/10.3201/eid3012.240154
10. Wang H, Wu X, Cheng Y, An Y, Ning Z. Tissue distribution of human and avian type sialic acid influenza virus receptors in domestic cat. Acta Vet Hung. 2013;61537–46.
11. Lee CT, Slavinski S, Schiff C, Merlino M, Daskalakis D, Liu D, et al.; Influenza A(H7N2) Response Team. Outbreak of influenza A(H7N2) among cats in an animal shelter with cat-to-human transmission—New York City, 2016. Clin Infect Dis. 2017;65:1927–9. https://doi.org/10.1093/cid/cix668
12. Poirot E, Levine MZ, Russell K, Stewart RJ, Pompey JM, Chiu S, et al. Detection of avian influenza A(H7N2) virus infection among animal shelter workers using a novel serological approach—New York City, 2016–2017. J Infect Dis. 2019;219:1688–96. https://doi.org/10.1093/infdis/jiy595
13. Vaughan A, Joyce A, Traub E, Jae M, Beeler E, Paiva E, et al. Serologic evidence of highly pathogenic avian influenza A(H5N1) virus infection in a veterinary professional exposed to an infected domestic cat—Los Angeles County, California, December 2024–January 2025. MMWR Morb Mortal Wkly Rep. 2026;75:215–20. https://doi.org/10.15585/mmwr.mm7517a1
14. Chothe SK, Srinivas S, Misra S, Nallipogu NC, Gilbride E, LaBella L, et al. Marked neurotropism and potential adaptation of H5N1 clade 2.3.4.4.b virus in naturally infected domestic cats. Emerg Microbes Infect. 2025;14:2440498. https://doi.org/10.1080/22221751.2024.2440498
15. Gray GC, Warren CJ, Webby RJ, Bowman AS. Why we must vaccinate US dairy cattle against HPAI H5N1. J Infect Dis. 2026;jiag183. https://doi.org/10.1093/infdis/jiag183

Address for correspondence: Kristen K. Coleman, University of Maryland School of Public Health, 4200 Valley Dr, College Park, MD 20742, USA; email: kkcolema@umd.edu

Genomic and Epidemiologic Insights into Ongoing Measles Outbreak, Israel, 2025–2026

Efrat Bucris,[1] Neta S. Zuckerman,[1] Tal Levin, Yara Kanaaneh, Oran Erster, Victoria Indenbaum, Keren Friedman, Danit Sofer, Eli Schwartz, Elena Chernin, Or Kriger, Rana Shibli, Sharon Elroi Prais, Zohar Mor, Nitza Abramson, Michal Savion, Naama Nuss, Ady Cohen Golan, Eva Avramovich, Dror Yakir, Liora Guy David, Efrat Rorman, National Measles Working Group,[2] Yaniv Lustig

An ongoing measles outbreak in Israel, involving ≈3,200 cases and 16 deaths, threatens the country's measles elimination status and reflects declining vaccination rates observed globally and within Israel. Epidemiologic investigations supported by sequencing suggest that a single importation triggered the outbreak, underscoring the critical role of rapid genomic surveillance in outbreak control.

Measles is a highly contagious, vaccine-preventable disease; clinical manifestations typically include high fever, maculopapular rash, cough, and conjunctivitis. Severe complications, including pneumonia and encephalitis, can occur in up to 30% of cases, and the case-fatality rate is ≈1/1,000 cases (*1*). Despite an effective vaccine (measles, mumps, and rubella [MMR]), measles remains a major global health concern; in 2025, Romania, Vietnam, Morocco, and the United States reported outbreaks (*2*–*4*).

In Israel, MMR vaccine coverage has declined in recent years to 83% receiving the first dose at <25 months of age and 87% a second dose at <8 years of age. Corresponding rates are 83% and 85% in Jerusalem and 89% and 93% in the Central District; coverage is lower in Ultra-Orthodox communities (Israel Ministry of Health, unpub. data). Israel achieved measles elimination in 2015, but outbreaks continue, including >4,000 cases in 2018–2019 and smaller outbreaks during 2023–2024 (*5*–*7*). We report on an ongoing measles outbreak that began in Israel in April 2025.

The Outbreak

During April 7, 2025–February 28, 2026, a total of 3,203 measles cases, including 16 deaths, were reported across Israel, the largest outbreak since 2018–2019 (*8*). Epidemiologic investigations found 13 case-patients had a history of travel abroad shortly before illness onset (Table). Among reported case-patients, mean age was 5.58 years (SD 9.35 years; range 1 month–73 years); 82.7% were unvaccinated, 7.1% were partially vaccinated, 2.2% were fully vaccinated, and 8.5% had unknown vaccination status.

As part of routine surveillance, 132 measles virus–positive samples collected during April 2025–February 2026 were selected for sequencing (Appendix Table 1, https://wwwnc.cdc.gov/EID/article/32/9/26-0625-App1.pdf). Samples were sequenced on the basis of the following criteria: all available imported cases, all travel-associated cases, representative samples from newly affected areas, and randomized samples collected in established

Author affiliations: Central Virology Laboratory, Public Health Services, Ministry of Health and Sheba Medical Center, Ramat-Gan, Israel (E. Bucris, N.S. Zuckerman, T. Levin, Y. Kanaaneh, O. Erster, V. Indenbaum, K. Friedman, D. Sofer, Y. Lustig); Gray Faculty of Medicine, Tel-Aviv University, Tel-Aviv, Israel (N.S. Zuckerman, Y. Lustig); The Center for Geographic Medicine and Tropical Diseases, The Chaim Sheba Medical Center, Tel Hashomer, Israel (E. Schwartz); Ministry of Health Division of Epidemiology, Jerusalem, Israel (E. Chernin, O. Kriger, R. Shibli, S.E. Prais); Health Intelligence, Ministry of Health, Jerusalem (S.E. Prais, D. Yakir, L.G. David); Program for Public Health, Ashkelon Academic College, Ashkelon, Israel (Z. Mor); Jerusalem Department of Health, Ministry of Health, Jerusalem (Z. Mor, N. Abramson); Tel Aviv Department of Health, Ministry of Health, Tel-Aviv (M. Savion, N. Nuss); Central District Health Bureau, Ramla, Israel (A.C. Golan, E. Avramovich); Ministry of Health Department of Laboratories, Jerusalem (E. Rorman)

DOI: https://doi.org/10.3201/eid3209.260625

[1]These authors contributed equally to this manuscript.

[2]Group members are listed at the end of the article.

Table. Patient data from investigation of genomic and epidemiologic insights into ongoing measles outbreak, Israel, 2025–2026*

Patient no.	Case ID	Symptom onset date	Date of return	Country of infection	Epidemiologic data	Sequence available	Genotype
1	597/25	2025 Apr 5	2025 Mar 30	Serbia	Transmission chain of 2 cases	Y	D8
2	681/25	2025 Apr 10	2025 Apr 4†	Belgium	Index case	N	NA
3	651/25	2025 Apr 16	2025 Apr 3	Vietnam	Single imported case	Y	B3
4	835/25	2025 Apr 30	2025 Apr 21	Russia	Transmission chain of 2 cases	Y	B3
5	1813/25	2025 Jun 15	2025 Jun 11	Belgium	NA	Y	B3
6	1929/25	2025 Jul 10	2025 Jul 5	Thailand	Transmission chain of 2 cases	Y	D8
7	3067/25	2025 Aug 26	2025 Aug 22	Poland	Virus likely acquired in Israel	Y	B3
8	3425/25	2025 Oct 2	2025 Sep 30	Ukraine	NA	N	NA
9	4319/25	2025 Oct 3	2025 Oct 10	Poland	Single import-associated case	N	NA
10	4130/25	2025 Oct 31	NA	Ethiopia	Virus likely acquired in Israel	Y	B3
11	5745/25	2025 Nov 5	2025 Oct 22	India	Single import-associated case	N	NA
12	4988/25	2025 Nov 27	2025 Nov 30	Germany	Virus likely acquired in Israel	Y	B3
13	833/26	2026 Jan 11	2026 Jan 8	Greece	NA	N	NA

*ID, identification; NA, not available.
†Date of return is estimated; a sample from a close contact was sequenced and determined as B3 genotype.

outbreak locations every 2 weeks throughout the outbreak. Samples were excluded from sequencing when epidemiologic data showed that transmission occurred in established measles-positive locations (i.e., same street or household) (Appendix). Complete measles virus genomes were sequenced (*9*) (Appendix)

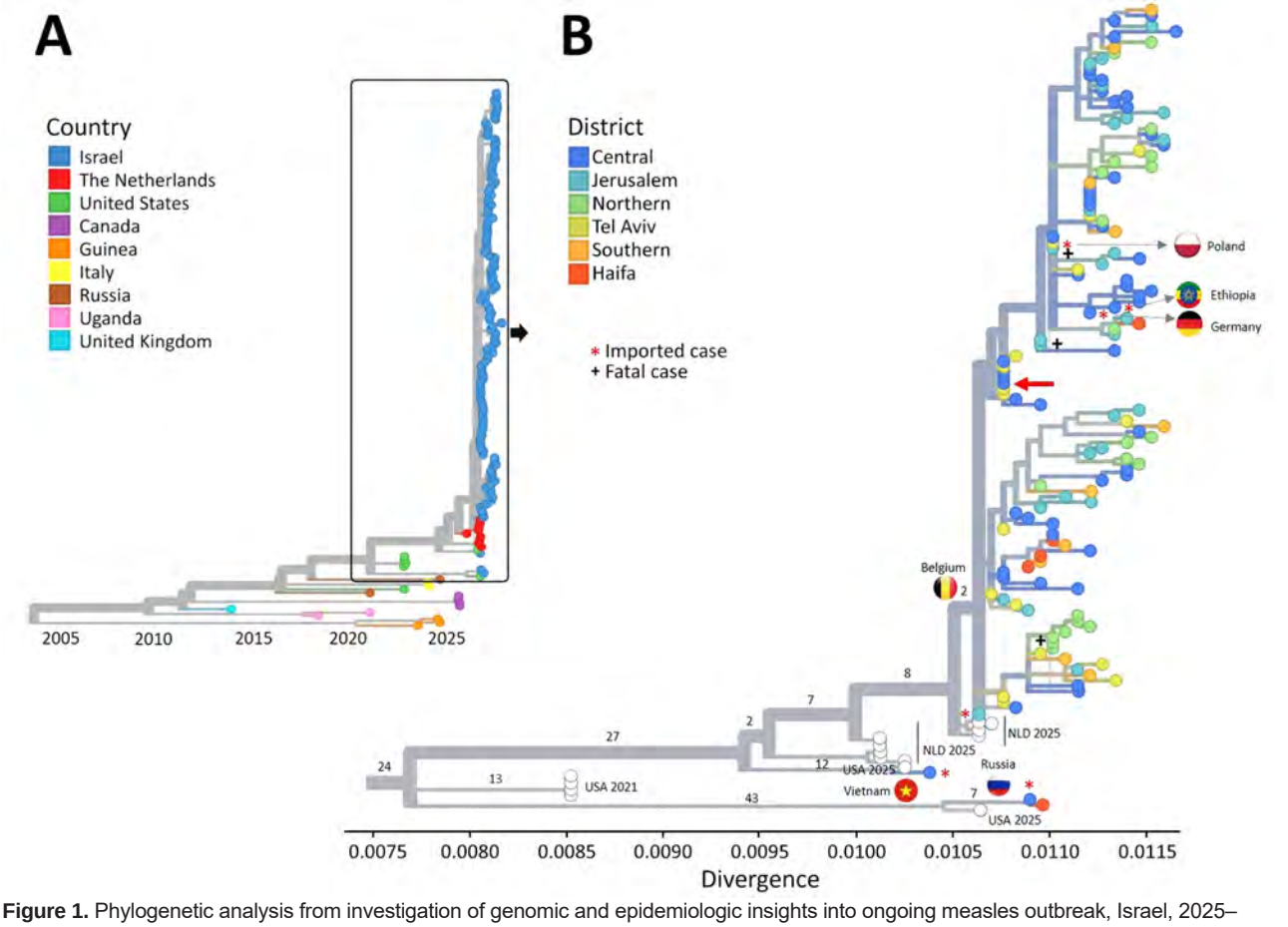

Figure 1. Phylogenetic analysis from investigation of genomic and epidemiologic insights into ongoing measles outbreak, Israel, 2025–2026. Phylogenetic tree including 132 sequences from Israel collected during April 2025–February 2026 and 29 global sequences from 2020–2025 available in the National Center for Biotechnology Information (Appendix Table 3, https://wwwnc.cdc.gov/EID/article/32/9/article/26-0625-App1.pdf). Tree was constructed using the Nextrain Augur pipeline under the generalized time reversible substitution model, and visualized with Auspice (*10*). A) Time-resolved phylogenetic tree including Israel and global sequences. B) Divergence tree highlighting the Israel clusters and indicating the district of origin for each sample; branch lengths and the x-axis represent genetic divergence, whereas numbers along branches indicate inferred nucleotide substitutions relative to the parental node. Asterisks (*) denote cases with documented travel around the time of measles identification; country flags indicate the reported travel destination when known. Plus signs (+) denote fatal cases in children. Red arrow denotes the epidemiologically linked case related to the initial importation from Belgium.

and used for phylogenetic analysis to support transmission chain reconstruction. The N450 region of the measles viral genome confirmed the sequences as genotype B3, matching the reference MVs/Quetta.PAK/44.20 strain from Pakistan.

Phylogenetic analysis showed the Israel sequences clustered most closely with sequences from the Netherlands and the United States collected in 2025 (Figure 1); however, because up-to-date global sequence data in public repositories are limited, intermediate diversity could be missing. The Israel sequences showed 3 likely clusters within the dominant B3 lineage, each derived from a separate documented importation: Belgium, Vietnam, and Russia. We found no spread of D8 lineage sequences imported to Israel. The Russia cluster likely originated from a documented importation from Russia (patient 4; Rehovot, May 2025) and is linked to an additional sample collected in Haifa in June 2025. That cluster is most closely related to a global sequence from California, USA (2025), differing by 7 nucleotides. Transmission in the cluster was limited to only 2 cases because close contacts were fully vaccinated and that location has high overall vaccine coverage. The Vietnam cluster, separated from the nearest ancestor by 12 nt, likely originated from a documented importation from Vietnam (patient 3; Beit-Itzhak, April 2025) and is not linked to additional Israel cases in the phylogeny. No further transmission was documented in the cluster, consistent with sequencing results and similar to the Russia cluster. The main and largest cluster (n = 129) was traced through epidemiologic investigations to a documented importation from Belgium (patient 2; Modi'in Illit, April 2025). That case was diagnosed retrospectively through contact tracing of infected close family members. Although the imported case was confirmed serologically (positive IgM), the available specimen contained insufficient viral RNA, precluding sequencing. However, sequencing was available for an epidemiologically linked close contact of the imported case (Bnei-Brak, April 2025; Figure 1, red arrow), located within the main cluster; epidemiologic data indicated subsequent spread to additional cities in Central District, Jerusalem, and later North District. That cluster also includes an additional sequenced importation from Belgium (case 5; Jerusalem, June 2025), unrelated epidemiologically to the other Belgium cases, located on the ancestral branch. The main cluster is most closely related to global sequences from the Netherlands collected in 2025, differing by 2 mutations. That strain has subsequently spread in Israel and is still circulating, accumulating mutations and giving rise to several sublineages. Most samples in that cluster were from locations with low vaccine coverage and within Ultra-Orthodox communities (Figure 2; Appendix Table 3).

The sequences obtained from deceased children were located within different sublineages in the main outbreak cluster (Figure 1). The first case

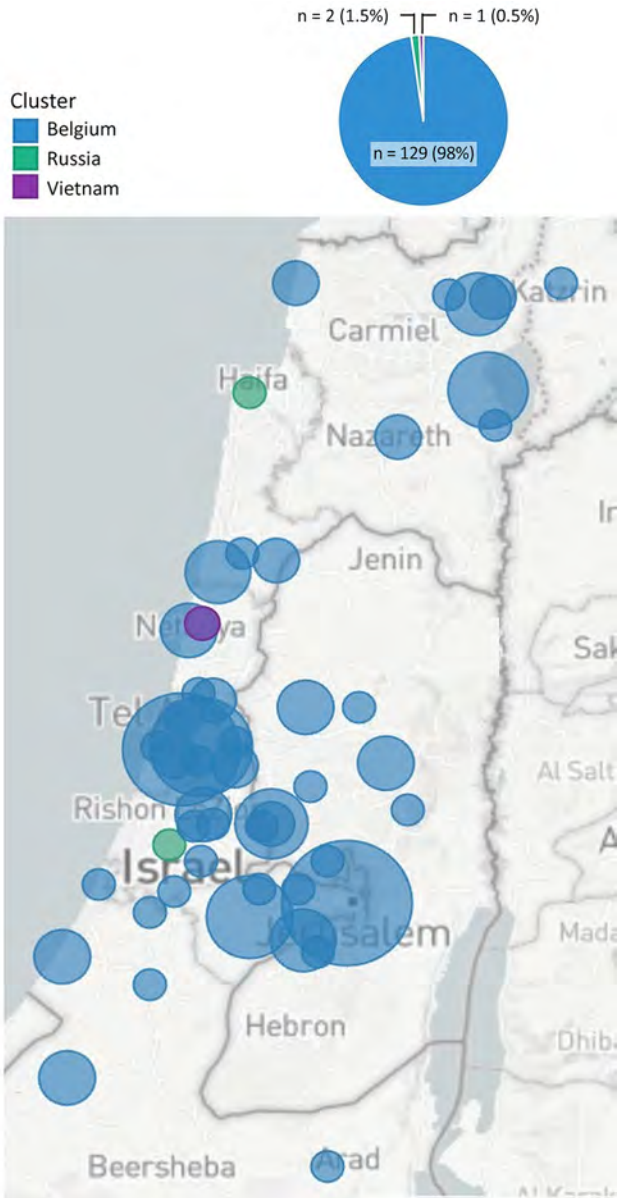

Figure 2. Geographic distribution of sequenced measles cases and importation clusters from genomic and epidemiologic investigation into ongoing measles outbreak, Israel, 2025–2026. Map displays the geographic distribution of sequenced cases by city. Colors denote the 3 major identified importation clusters, and the accompanying pie chart represents the percentage of sequenced samples belonging to each outbreak cluster; number of samples sequenced out of 132 total samples are shown.

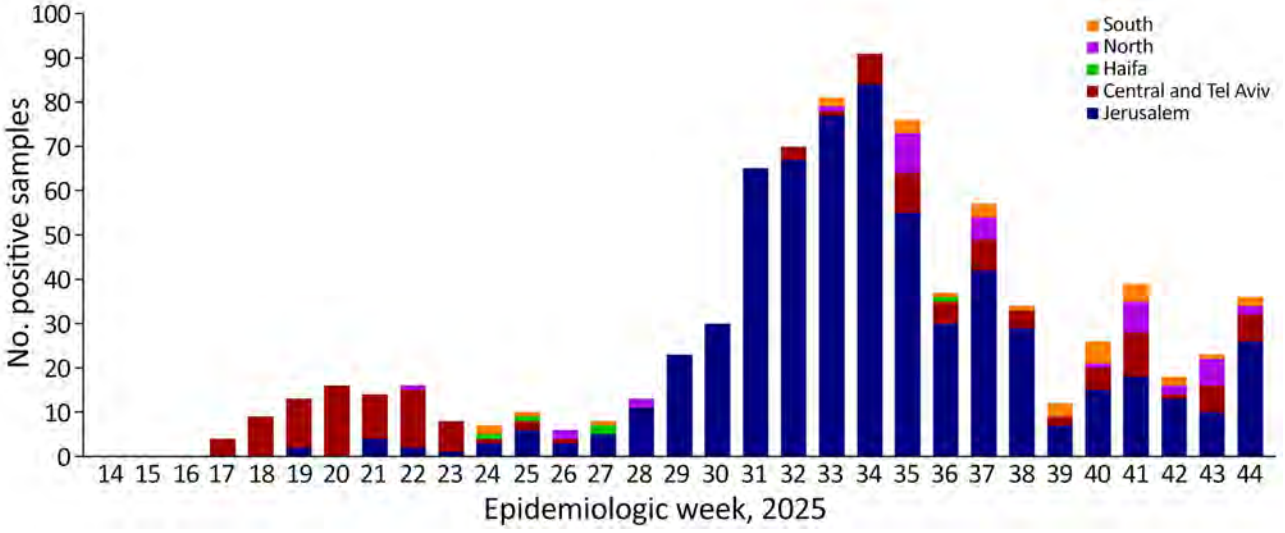

Figure 3. Positivity rates by epidemiologic week during April 1–October 31, 2025, from genomic and epidemiologic investigation into ongoing measles outbreak, Israel, 2025–2026. Weekly number of measles cases by district was confirmed by quantitative reverse transcription PCR.

(Jerusalem, July 2025) was identical to 2 sequences detected elsewhere (Tel Aviv, September 2025; Emmanuel, August 2025). The second case (Jerusalem, July 2025) was identical to another from Jerusalem (June 2025). The third case (Poriya, November 2025) was identical to 2 cases from the North District (Nahariya, November 2025). The identical genomes suggest close epidemiologic linkage and, when detected in different districts, indicate transmission across multiple regions in Israel. That finding suggests the virus in fatal cases was typical of the outbreak strain. Three additional case-patients with documented travel abroad (patient 7, Poland; patient 10, Ethiopia; patient 12, Germany) near the time of measles detection had sequences within the main cluster, suggesting that infection was more likely acquired in Israel, not abroad.

To investigate positivity dynamics from an epidemiologic perspective, we evaluated the weekly ratios of positive and negative samples collected during April–October 2025 (epidemiologic weeks 14–44). When the outbreak began, the positivity rate was low (10%–20%), likely reflecting heightened awareness and broad testing of suspected cases with low pretest probability for measles. As transmission became established in specific districts during weeks 28–38, positivity increased to ≈60%, indicating outbreak persistence and targeted sampling (Appendix Figure). During weeks 39–44, as the outbreak expanded to additional districts, the overall ratio decreased (Figure 3); we observed a similar trend through February 2026 (data not shown).

Conclusions

The ongoing measles outbreak in Israel threatens the country's elimination status, defined by the World Health Organization as absence of endemic transmission for ≥12 months (https://iris.who.int/server/api/core/bitstreams/b0ee4708-ba01-4b40-9003-f6f1aba317da/content). This outbreak highlights the profound risks associated with declining vaccination coverage. Genomic sequencing of targeted measles samples indicated that a single importation event was most likely the primary driver of the outbreak. Phylogenetic analysis showed 3 validated distinct importation events from Russia, Vietnam, and Belgium; outcomes differed drastically based on local immunity. The main Belgium-linked cluster strain, detected in April 2025, likely sparked an extensive national outbreak. The second documented importation case from Belgium might have contributed to the main transmission cluster. The epidemiologic investigation indicated that this case-patient had many contacts and resided in an area experiencing a substantial outbreak. However, the case was detected 2 months after the Belgium index case, so it likely had little impact on outbreak dynamics. Furthermore, its shared mutations with the April 2025 Belgium case suggest a common source.

Additional undetected single cases might exist because of underreporting. However, our strict criteria and direct contact to Ministry of Health epidemiologic data enabled systematic assessment of each focal point, so underreporting is unlikely to have substantially affected the main phylogenetic findings. Positivity rates rose from 10%–20% during

early broad testing to 60% during weeks 28–38, as diagnostics shifted to targeted surveillance during outbreak spread.

In summary, we integrated epidemiologic investigations with molecular surveillance, demonstrating that a single case can spark extensive measles transmission. Our findings highlight the critical role of molecular surveillance in measles outbreak management.

Members of the National Measles Working Group who contributed to providing clinical samples and collecting relevant clinical information: Haim Ben-Zvi (Beilinson Hospital, Petah Tikva, Israel); Yehudit Shindler (Mayanei HaYeshua Medical Center, Beni Brak, Israel); Ola Salach (Carmel Medical Center, Haifa, Israel); Hephzibah Ivgi (Shaare Zedek Medical Center, Jerusalem, Israel); Nadav Sorek (Assuta University Hospital, Ashdod, Israel); Danielle Keidar-Friedman (Assuta University Hospital, Ashdod, Israel); Margalit Zosev (Kaplan Medical Center, Rehovot, Israel); Merav Shtrauss (Emek Medical Center, Migdal HaEmek, Israel); Hila Ben-Amram (Ziv Medical Center, Zefat, Israel); Mona Shehadeh (Galilee Medical Center, Nahariya, Israel); Olga Bunder (Shamir Medical Center, Be'er Ya'akov, Israel); Dana Wolf, Mila Rivkin, and Esther Oiknine-Djian (Hadassah Medical Center, Jerusalem); Ayelet Naus (Soroka University Medical Center, Beer Sheba, Israel); Orna Shwartz (Wolfson, Israel); Moran Szwarcwort (Rambam Health Care Campus, Haifa); Maya Azarad (Tzafon Medical Center, Ramat Poriya, Israel); and Ayman Fadila (Meir Medical Center, Kfar Saba, Israel).

About the Author

Dr. Bucris is the head of the Measles and Rubella national center with Central Virology Laboratory, Public Health Services, Ministry of Health and Sheba Medical Center, Ramat-Gan, Israel. Her research interest is vaccine-preventable viral diseases.

References

1. Do LAH, Mulholland K. Measles 2025. N Engl J Med. 2025;393:2447–58. https://doi.org/10.1056/NEJMra2504516
2. Hewitt GL, Obeid A, Fischer PR. Measles outbreaks in the United States in 2025: practice, policy, and the canary in the coalmine. New Microbes New Infect. 2025;65:101591. https://doi.org/10.1016/j.nmni.2025.101591
3. Ong T, Thuy CT, Tam NH, Nga LH, Uyen NTV, Lan TTT, et al. Detection of immunity gap before measles outbreak, Ho Chi Minh City, Vietnam, 2024. Emerg Infect Dis. 2025;31:2059–62. https://doi.org/10.3201/eid3110.250234
4. Mokhlis FE, Hrimech A, Fourtassi M, El Bairi K. The measles outbreak in Morocco: a failure of scientific communication and training on evidence-based medicine. J Evid Based Med. 2025;18:e70048. https://doi.org/10.1111/jebm.70048
5. Indenbaum V, Bucris E, Friedman K, Kushnir T, Eliyahu H, Azar R, et al. Measles sequencing: lessons learned from a large-scale outbreak. Viruses. 2025;17:913. https://doi.org/10.3390/v17070913
6. Bucris E, Indenbaum V, Levin T, Kanaaneh Y, Friedman K, Kushnir T, et al. Rapid molecular epidemiology investigations into two recent measles outbreaks in Israel detected from October 2023 to January 2024. Euro Surveill. 2024;29:2400202. https://doi.org/10.2807/1560-7917.ES.2024.29.16.2400202
7. Stein-Zamir C, Levine H. The measles outbreak in Israel in 2018–19: lessons for COVID-19 pandemic. Hum Vaccin Immunother. 2021;17:2085–9. https://doi.org/10.1080/21645515.2020.1866918
8. Anis E, Haas EJ, Indenbaum V, Singer SR, Warshavsky B, Rishpon S, et al. A prolonged, nationwide measles outbreak despite very high vaccination coverage in Israel, 2018–19. J Infect. 2021;83:678–85. https://doi.org/10.1016/j.jinf.2021.09.025
9. Penedos AR, Myers R, Hadef B, Aladin F, Brown KE. Assessment of the utility of whole genome sequencing of measles virus in the characterisation of outbreaks. PLoS One. 2015;10:e0143081. https://doi.org/10.1371/journal.pone.0143081
10. Hadfield J, Megill C, Bell SM, Huddleston J, Potter B, Callender C, et al. Nextstrain: real-time tracking of pathogen evolution. Bioinformatics. 2018;34:4121–3. https://doi.org/10.1093/bioinformatics/bty407

Address for correspondence: Yaniv Lustig, The Central Virology Laboratory, Ministry of Health, Ramat Gan, Tel Hashomer 5262000, Israel; email: yaniv.lustig@sheba.health.gov.il

Case Report and Retrospective Review of *Acanthamoeba* Encephalitis and Chronic Lymphocytic Leukemia, United States

Michele Persico, Julia C. Haston, Erin Imada, Jennifer Kasten, Cederic Pimentel, Jeffrey M. Collins

We describe a case of *Acanthamoeba* encephalitis with chronic lymphocytic leukemia (CLL) in the United States and summarize the Free-Living Ameba database to highlight CLL as the most common underlying malignancy for *Acanthamoeba* infections. CLL patients are more likely to have improved survival and nondisseminated cutaneous disease than those with other cancers.

Acanthamoeba is a free-living amoeba (FLA) transmitted via inhalation or direct contact with the eyes or skin (*1*) that can cause keratitis and granulomatous amebic encephalitis (GAE) (*2*). GAE occurs most often in immunocompromised patients; risk factors include hematologic malignancy and immunosuppressive drugs (*2*). Chronic lymphocytic leukemia (CLL), the most common leukemia (*3*), can lead to immune dysfunction from immunosuppressive treatments and hypogammaglobulinemia, as well as impairments in complement activity, cell-mediated immunity, and neutrophil function (*4*). The 5-year risk for severe infections in CLL is as high as 57% when IgG levels are low (*5*). Ibrutinib, a Bruton tyrosine-kinase inhibitor (*6*), is an immunomodulatory drug used for CLL treatment that increases the risk for invasive infections up to 11.4% during the first year of treatment through innate immune system impairment (*7*–*9*). We report a case of *Acanthamoeba* GAE in a patient with CLL managed with ibrutinib. Using a retrospective analysis of data from the Centers for Disease Control and Prevention (CDC) Free-Living Ameba database (Appendix, https://wwwnc.cdc.gov/EID/article/32/9/26-0790-App1.pdf), we sought to determine the frequency of *Acanthamoeba* infections among patients with CLL and to compare clinical characteristics with those of patients without CLL.

Author affiliations: Emory University, Atlanta, Georgia, USA (M. Persico, C. Pimentel, J.M. Collins); Centers for Disease Control and Prevention, Atlanta (J.C. Haston, E. Imada, J. Kasten)

DOI: https://doi.org/10.3201/eid3209.260790

The Study

A 71-year-old man with CLL who was receiving ibrutinib sought care for fever, encephalopathy, and focal right-sided weakness. Neuroimaging showed a rapidly enlarging left frontal lesion with surrounding edema; test results for bacterial, viral, and parasitic pathogens were unremarkable (Appendix Table). Brain biopsy demonstrated necrosis, inflammation, and rare Periodic acid-Schiff–positive organisms (Figure). CDC testing confirmed *Acanthamoeba* infection. Despite initiation of azithromycin, sulfadiazine, flucytosine, fluconazole, and miltefosine, the patient died 23 days after symptom onset.

To further investigate the possible role of CLL in this patient's course, we examined all US cases of *Acanthamoeba* infection reported to the CDC FLA database during 1956–2023 (Appendix). This activity was reviewed by CDC, deemed not research, and was conducted consistent with applicable federal law and CDC policy (see e.g., 45 C.F.R. part 46, 21 C.F.R. part 56; 42 U.S.C. §241(d); 5 U.S.C. §552a; 44 U.S.C. §3501 et seq.).

The mean age of diagnosis was 48 years for all case-patients with *Acanthamoeba* infection and 68 years in the CLL subgroup (Table). Among the 16 *Acanthamoeba* cases in CLL patients with known sex, 14 occurred in male patients and 2 in female patients, compared with 118 male patients and 173 female patients in cases without CLL. Fifty-six patients had ≥1

malignancy at the time of *Acanthamoeba* diagnosis: 16 had CLL alone, 1 had CLL and non-Hodgkin lymphoma, and 30 had ≥1 non-CLL hematologic malignancy (5 with acute lymphoblastic leukemia, 7 with acute myeloid leukemia, 2 with chronic myeloid leukemia, and 13 with lymphoma). Twelve had ≥1 nonhematologic malignancy.

Of 17 patients with CLL, 8 had central nervous system (CNS) involvement, including 3 with GAE alone and 5 with GAE and disseminated disease. In comparison, CNS involvement was seen among 24 of 31 with non-CLL hematologic malignancies and 11 out of 12 of those with non-hematologic malignancies. Nine of 17 CLL patients had non-CNS *Acanthamoeba* infections: 5 with cutaneous disease, 1 with rhinosinusitis, and 3 with non-CNS disseminated disease.

Of the 17 CLL cases, 8 survived, 3 died, and 6 had an unknown survival status. The 3 patients with CLL who died all had GAE, whereas 1 of 8 survivors had GAE. Among patients with a non-CLL malignancy and known survival outcome (n = 33), 2 patients survived and 31 died. Neither of the 2 non-CLL survivors had GAE; GAE was present in 28 of 31 non-CLL patients who died. *Acanthamoeba* infection in patients with CLL was associated with lower odds for death than non-CLL malignancies (odds ratio [OR] 0.03 [95% CI 0.003–0.18]; p<0.0001); that OR was likely a result of the lower frequency of GAE among CLL patients. GAE was associated with markedly greater odds of death in patients with any type of cancer (OR 68.6 [95% CI 9.0–2,075.9]; p<0.0001).

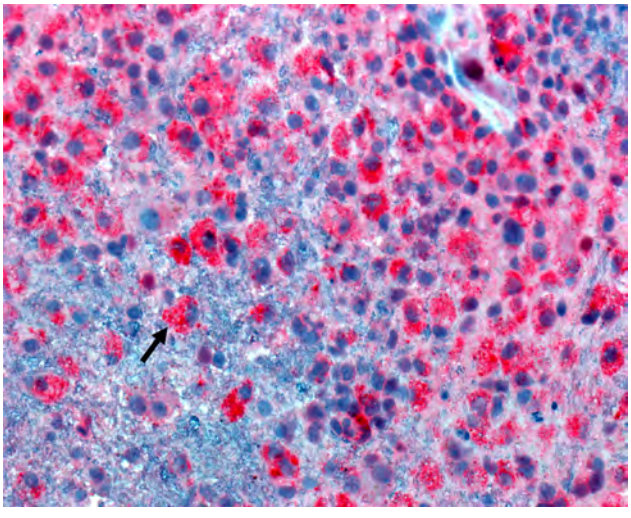

Figure. *Acanthamoeba* immunoassay from study of *Acanthamoeba* encephalitis and chronic lymphocytic leukemia, United States. Arrow indicates free-living amebic trophozoites of small to medium size that have rare double-walled cysts and show immunoreactivity to an *Acanthamoeba* spp. immunoassay.

Conclusions

We investigated the frequency of CLL among patients with *Acanthamoeba* infection and its effect on survival. CLL was the most prevalent malignancy among patients with *Acanthamoeba* infection. Of note, a lower number of *Acanthamoeba* cases occurred in persons with hematologic malignancies that are generally associated with a higher risk for opportunistic infections, including acute myeloid leukemia and acute lymphoblastic leukemia. Those findings suggest that unique immune impairments in CLL might predispose to disease from *Acanthamoeba*. Potential mechanisms include hypogammaglobulinemia and neutropenia (*10*), which could potentially be mitigated by immunoglobulin replacement. Our case study demonstrated that, although GAE most often has a subacute clinical course, it can have a rapid onset and progression. In addition, we showed that CLL and ibrutinib exposure could be important risk factors for disease caused by *Acanthamoeba*.

The clinical course and mortality rate of non-keratitis *Acanthamoeba* infections depend on the organ system involved. GAE has the highest mortality rate, exceeding 90%, whereas death from cutaneous *Acanthamoeba* infection or rhinosinusitis is less common (*11*). We found that patients with CLL had significantly higher odds of survival compared with patients who had other hematologic malignancies or solid tumors; that result was partially explained by the relatively high proportion of *Acanthamoeba* infections in CLL patients without CNS involvement. In our study, 53% of patients with CLL had non-CNS *Acanthamoeba* infections, whereas 30% of the overall cohort of patients had non-CNS *Acanthamoeba* infections (Table). Previous studies have reported lower mortality rates among those who did not have CNS involvement (*2*). The older age in the CLL group likely reflected the higher median age, 64 years, at CLL diagnosis (*12*). Patients with CLL are predominantly male (66%–69%) (*12*), which is similar to the overall sex distribution among *Acanthamoeba* cases in the FLA database.

Including the patient in our report, of the 18 reported patients with CLL, ≥4 patients have been treated with ibrutinib since it was introduced to the US market in 2012. Similar to our case, 2 other cases describe a more acute course, in which death occurred 4–14 days after the patients initially sought care at the hospital (*13*,*14*). That finding was unusual because GAE is typically considered a subacute to chronic form of encephalitis (*2*). Given the small number of cases reported, it is unclear whether the more acute clinical course can be attributed to CLL

Table. Clinical and demographic characteristics of *Acanthamoeba* cases in the United States during 1956–2023*

Characteristic	Total no. patients	No. (%) patients				
		Any cancer, n = 56	No cancer, n = 137	CLL, n = 17	Other hematologic malignancy, n = 31	Nonhematologic malignancy, n = 12
Age group, y						
0–17	11	2 (3.6)	9 (6.6)	0	2 (6.5)	0
18–34	36	5 (8.9)	31 (22.6)	0	5 (16.1)	1 (8.3)
35–64	105	25 (44.6)	80 (58.4)	6 (35.3)	16 (51.6)	4 (33.3)
≥65	36	23 (41.1)	13 (9.5)	11 (64.7)	7 (22.6)	7 (58.3)
Unknown	5	1 (1.8)	4 (2.9)	0	1 (3.2)	0
Sex						
M	132	37 (66.1)	95 (69.3)	14 (82.4)	17 (54.8)	9 (75)
F	57	17 (30.4)	40 (29.2)	2 (11.8)	13 (41.9)	3 (25)
Unknown	4	2 (3.6)	2 (1.5)	1 (5.9)	1 (3.2)	0
Ethnicity/race						
Hispanic	21	5 (8.9)	16 (11.7)	0	4 (12.9)	1 (8.3)
NH White	24	13 (23.2)	11 (8)	9 (53)	3 (9.7)	2 (16.7)
NH Asian	3	0	3 (2.2)	0	0	0
NH Black	6	0	6 (4.4)	0	0	0
NH American Indian or Alaskan Native	1	0	1 (0.7)	0	0	0
Other	51	8 (14.3)	43 (31.4)	2 (11.8)	5 (16.1)	2 (16.7)
Unknown	87	30 (53.6)	57 (41.6)	6 (35.3)	19 (61.3)	7 (58.3)
Survived						
Y	32	11 (19.6)	21 (15.3)	8 (47.1)	2 (6.5)	1 (8.3)
N	133	34 (60.7)	99 (72.3)	3 (17.6)	25 (80.6)	10 (83.3)
Unknown	28	11 (19.6)	17 (12.4)	6 (35.3)	4 (12.9)	1 (8.3)
Disease manifestation						
GAE only	78	20 (35.7)	58 (42.3)	3 (17.6)	12 (38.7)	7 (58.3)
Cutaneous only	19	8 (14.3)	11 (8)	5 (29.4)	3 (9.7)	0
Rhinosinusitis only	8	1 (1.8)	7 (5.1)	1 (5.9)	0	0
Disseminated with GAE	58	19 (33.9)	39 (28.5)	5 (29.4)	12 (38.7)	4 (33.3)
Disseminated without GAE	30	8 (14.3)	22 (16.1)	3 (17.6)	4 (12.9)	1 (8.3)

*The total number of patients with cancer was 56. The sum of patients represented in the CLL, other hematologic malignancy, and nonhematologic malignancy categories is 60; several patients had >1 malignancy and are represented in multiple categories. CLL, chronic lymphocytic leukemia; GAE, granulomatous amebic encephalitis; NH, non-Hispanic.

or immunosuppressive treatment. Further monitoring could determine whether ibrutinib may increase the risk for *Acanthamoeba* infection or death.

Our cross-sectional analysis of US disease surveillance data had limitations. For patients with a cancer diagnosis, detailed clinical and laboratory data, as well as treatment history and survival time, were not routinely collected in the CDC FLA database. In addition, information on the method of *Acanthamoeba* diagnosis, treatment, and time to death after diagnosis was not generally available. Last, the CDC FLA database includes *Acanthamoeba* cases from the United States only, which limited generalizability of our results.

Since 1956, a total of 18 *Acanthamoeba* infections have been identified in patients with CLL, including the case we reported here. CLL is the most common malignancy among patients with invasive *Acanthamoeba* infections. CLL patients with *Acanthamoeba* infections had lower rates than patients with other malignancies, which could be attributed to a greater likelihood of cutaneous disease and lower rates of CNS involvement. Further monitoring can elucidate the clinical factors and treatments mediating the association between CLL and *Acanthamoeba* infection.

Acknowledgments

We express our gratitude to the patient's family for their willingness to consent to share their medical case.

The authors received no financial support for the research, authorship, or publication of this article.

About the Author

Dr. Persico is a fourth-year neurology resident at Emory University School of Medicine and part of the editorial board for the journal *Neurology*: Resident and Fellow Section. His primary research interests include drug discovery and targeted therapies in neuro-oncology and complications of cancer and cancer therapies.

References

1. Visvesvara GS, Moura H, Schuster FL. Pathogenic and opportunistic free-living amoebae: *Acanthamoeba* spp., *Balamuthia mandrillaris*, *Naegleria fowleri*, and *Sappinia diploidea*. FEMS Immunol Med Microbiol. 2007;50:1–26. https://doi.org/10.1111/j.1574-695X.2007.00232.x
2. Haston JC, O'Laughlin K, Matteson K, Roy S, Qvarnstrom Y, Ali IKM, et al. The epidemiology and clinical features of non-keratitis *Acanthamoeba* infections in the United States, 1956–2020. Open Forum Infect Dis. 2023;10:ofac682. https://doi.org/10.1093/ofid/ofac682

3. Fedele PL, Opat S. Chronic lymphocytic leukemia: time to care for the survivors. J Clin Oncol. 2024;42:2005–11. https://doi.org/10.1200/JCO.23.02738
4. Morrison VA. Management of infectious complications in patients with chronic lymphocytic leukemia. Hematology (Am Soc Hematol Educ Program). 2007;2007:332–8. https://doi.org/10.1182/asheducation-2007.1.332
5. Molica S, Levato D, Levato L. Infections in chronic lymphocytic leukemia. Analysis of incidence as a function of length of follow-up. Haematologica. 1993;78:374–7.
6. Cameron F, Sanford M. Ibrutinib: first global approval. Drugs. 2014;74:263–71. https://doi.org/10.1007/s40265-014-0178-8
7. Fiorcari S, Maffei R, Vallerini D, Scarfò L, Barozzi P, Maccaferri M, et al. BTK inhibition impairs the innate response against fungal infection in patients with chronic lymphocytic leukemia. Front Immunol. 2020;11:2158. https://doi.org/10.3389/fimmu.2020.02158
8. Stephens DM, Byrd JC. How I manage ibrutinib intolerance and complications in patients with chronic lymphocytic leukemia. Blood. 2019;133:1298–307. https://doi.org/10.1182/blood-2018-11-846808
9. Varughese T, Taur Y, Cohen N, Palomba ML, Seo SK, Hohl TM, et al. Serious infections in patients receiving ibrutinib for treatment of lymphoid cancer. Clin Infect Dis. 2018;67:687–92. https://doi.org/10.1093/cid/ciy175
10. Bloch KC, Schuster FL. Inability to make a premortem diagnosis of *Acanthamoeba* species infection in a patient with fatal granulomatous amebic encephalitis. J Clin Microbiol. 2005;43:3003–6. https://doi.org/10.1128/JCM.43.6.3003-3006.2005
11. Siddiqui R, Khan NA. Biology and pathogenesis of *Acanthamoeba*. Parasit Vectors. 2012;5:6. https://doi.org/10.1186/1756-3305-5-6
12. Shanafelt TD, Rabe KG, Kay NE, Zent CS, Jelinek DF, Reinalda MS, et al. Age at diagnosis and the utility of prognostic testing in patients with chronic lymphocytic leukemia. Cancer. 2010;116:4777–87. https://doi.org/10.1002/cncr.25292
13. Crothers JW, Hsu L, Marty FM. Fulminant *Acanthamoeba castellanii* encephalitis in an ibrutinib-treated patient. Open Forum Infect Dis. 2020;7:ofaa025. https://doi.org/10.1093/ofid/ofaa025
14. Voshtina E, Huang H, Raj R, Atallah E. Amebic encephalitis in a patient with chronic lymphocytic leukemia on ibrutinib therapy. Case Rep Hematol. 2018;2018:6514604. https://doi.org/10.1155/2018/6514604

Address for correspondence: Michele Persico, Emory University, 12 Executive Park Dr NE, 5th Fl, Atlanta, GA, 30329, USA; email: mpersi2@emory.edu

Global Spread of *Trichophyton indotineae* Tracked by Mass Spectrometry Identification Network, 2022–2025

Arnaud Jabet, Anne-Cécile Normand, Karin Amilon, Christine Schuttler, Lionel Fontao, Douglas Chan, Alicia Moreno-Sabater, Lise Kristensen, Sophie Brun, Aina Myhre, Damien Dupont, Ann Packeu, Mohammed Jami, Renaud Piarroux, MIND Study Group,[1] Arnaud Fekkar

Trichophyton indotineae is an emerging dermatophyte that is often resistant to terbinafine. We analyzed data produced by the Mass Spectrometry Identification global network. Those data revealed a 3-fold increase in *T. indotineae* identification during 2022–2025, demonstrating that this application is an effective tool for monitoring global spread of this pathogen.

Infections caused by the dermatophyte *Trichophyton indotineae* have recently emerged as a global public health concern (*1*). Although the first cases of infection by *T. indotineae* were retrospectively identified as early as 2008, beginning in 2016 dermatologists in India began to report a sharp increase in cases of extensive and difficult-to-treat dermatophytosis in their country. Those cases were later attributed to strains belonging to the *T. mentagrophytes* complex, which were frequently resistant to terbinafine (*1*). In 2020, the designation *T. indotineae* was proposed to denote these strains, although debate is ongoing about whether this clade should be considered a distinct species or merely a variety within *T. mentagrophytes* (*2*). Current alternative denominations include *T. mentagrophytes* internal transcribed spacer (ITS) genotype VIII and *T. mentagrophytes* variant. *indotineae*. *T. indotineae* infections are now being reported in many countries, mostly as individual case reports or small single-center series, illustrating the rapid international spread of this species through migration and travel. Only a few publications provide data at broader (regional or national) scales and over longer periods (*3*–*5*).

Macro-microscopic–based identification of *T. indotineae* remains challenging because of its close similarity with *T. interdigitale* and *T. mentagrophytes*. Reference identification relies on sequencing of the ITS1–5.8s–ITS2 region. Matrix-assisted laser desorption/ionization time-of-flight mass spectrometry has become established in recent years as a highly effective method for identifying fungal pathogens. The Mass Spectrometry Identification (MSI) application (https://msi.happy-dev.fr) is a free tool developed and hosted by the Parasitology-Mycology Laboratory of Hôpital Universitaire Pitié Salpêtrière (Paris, France) that enables accurate and fast identification of large numbers of fungal pathogens on the basis of their mass spectra (*6*). It includes a large number of reference spectra (17,563 spectra corresponding to 1,700 fungal species) and enables the identification of rare species. In March 2022, MSI was upgraded to identify

Author affiliations: Hôpital Universitaire Pitié Salpêtrière, Paris, France (A. Jabet, A.-C. Normand, M. Jami, R. Piarroux, A. Fekkar); Karolinska University Hospital, Stockholm, Sweden (K. Amilon); Laboratoire Bio Paris Ouest, Levallois-Perret, France (C. Schuttler); Hopitaux Universitaires de Genève, Geneva, Switzerland (L. Fontao); NG Teng Fong General Hospital & Jurong Community Hospital, Singapore (D. Chan); Sorbonne Université, CIMI-Paris, AP-HP, Service de Parasitologie-Mycologie, Hôpital Saint-Antoine, Paris (A. Moreno-Sabater, A. Fekkar); Aarhus University Hospital, Aarhus, Denmark (L. Kristensen); Service de Parasitologie-Mycologie, Hôpital Avicenne, AP-HP, Université Sorbonne Paris Nord, INSERM UMR1137 IAME, Bobigny, France (S. Brun); Oslo University Hospital, Oslo, Norway (A. Myhre); Hospices Civils de Lyon, Institut des Agents infectieux, Parasitologie Mycologie Médicale, Hôpital de la Croix-Rousse, Lyon, France (D. Dupont); Sciensano, Brussels, Belgium (A. Packeu)

DOI: https://doi.org/10.3201/eid3209.260463

[1]Members of the MIND (MSI INuSuAle Network Database) Study Group are listed at the end of this article.

T. indotineae with excellent sensitivity and specificity (>95% for both parameters) (*7*,*8*). The ability to produce a reliable identification relies on the presence of 2 pairs of peaks, the presence or absence of which enables *T. interdigitale* and *T. mentagrophytes* to be effectively distinguished (*8*). Furthermore, the widespread use of this free online application has enabled the creation of an extensive international network of laboratories with ≈450 regular users in 27 countries. In this study, we analyzed identification data generated by MSI to describe the spatial and temporal dynamics of *T. indotineae* infections.

The Study

We analyzed all spectra identified as *T. indotineae* during March 2022–December 2025 by MSI users. We considered only first-intention identifications with a score of ≥20 (i.e., above the threshold used for the application for correct species identification as previously described [*9*]). When the same spectrum was uploaded multiple times, only 1 entry was retained. We addressed the bias caused by the increase in the number of users over time by normalizing the number of *T. indotineae* identifications relative to the number of identifications for the genus *Trichophyton* spp.

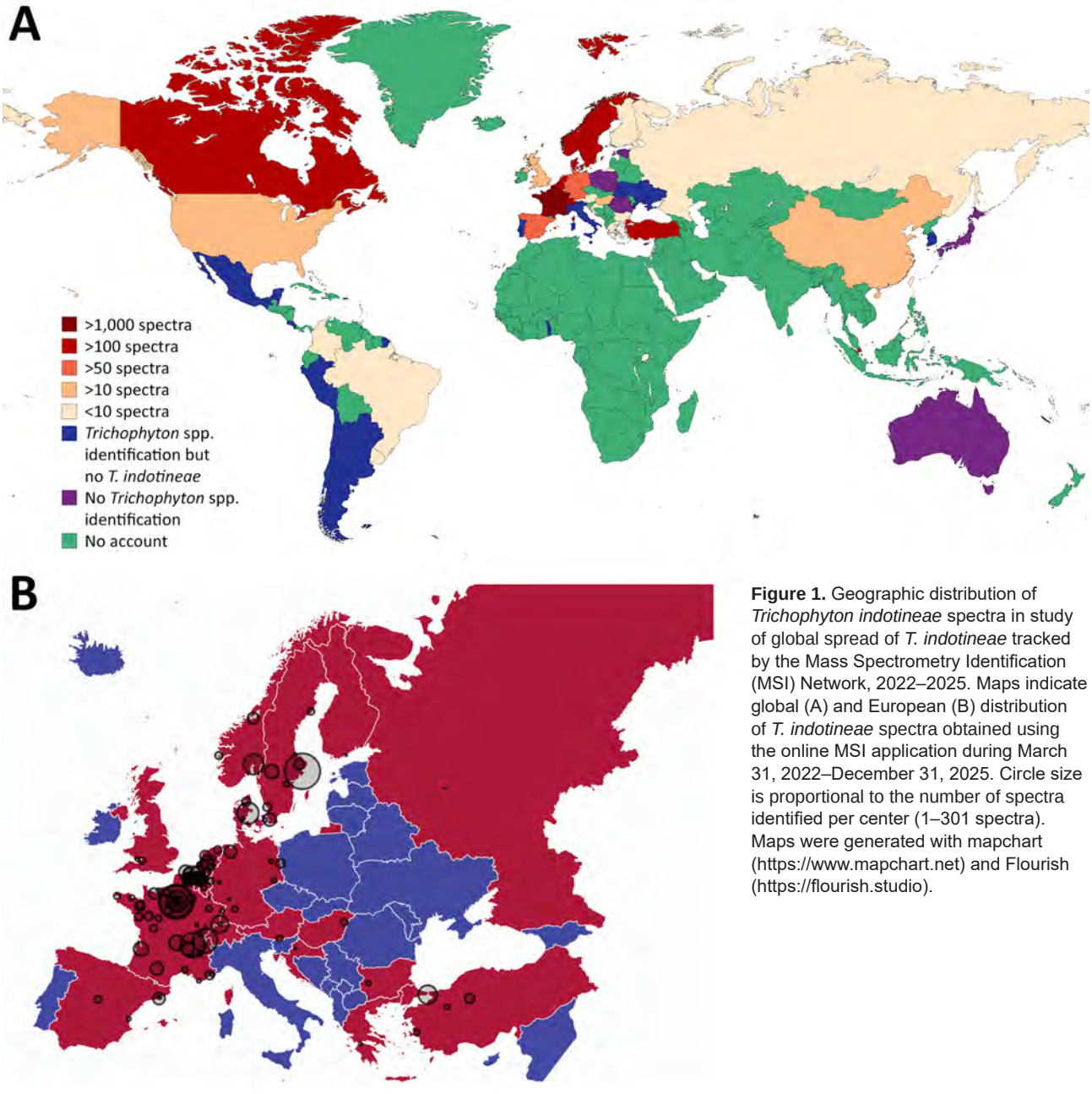

Figure 1. Geographic distribution of *Trichophyton indotineae* spectra in study of global spread of *T. indotineae* tracked by the Mass Spectrometry Identification (MSI) Network, 2022–2025. Maps indicate global (A) and European (B) distribution of *T. indotineae* spectra obtained using the online MSI application during March 31, 2022–December 31, 2025. Circle size is proportional to the number of spectra identified per center (1–301 spectra). Maps were generated with mapchart (https://www.mapchart.net) and Flourish (https://flourish.studio).

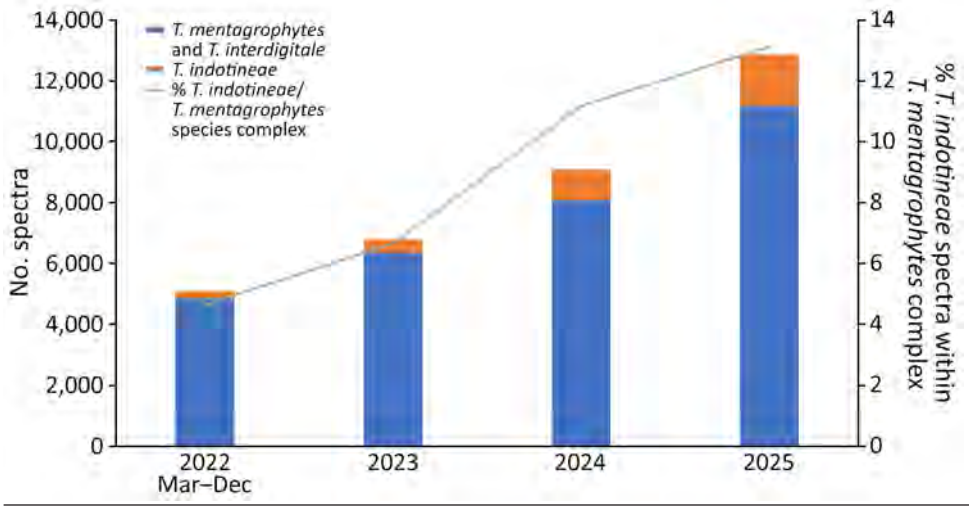

Figure 2. Temporal evolution of *Trichophyton indotineae* spectra identified in study of global spread of *T. indotineae* tracked by the Mass Spectrometry Identification Network, 2022–2025. Spectra were identified during March 31, 2022–December 31, 2025, and normalized to the total number of spectra within the *T. mentagrophytes* species complex (i.e., *T. mentagrophytes*, *T. interdigitale*, and *T. indotineae*).

and for the *T. mentagrophytes* complex (i.e., *T. mentagrophytes*, *T. interdigitale*, and *T. indotineae*).

During the study period, 566 users from 54 countries submitted 1,657,334 spectra that led to the identification of fungal agents. Those identifications included 123,025 (7.7%) that were identified as *Trichophyton* spp. (by 316 users in 44 countries) and 3,399 (0.2%) that were identified as *T. indotineae* (by 183 users in 29 countries) (Figure 1, panel A). The number of *T. indotineae* identifications per user ranged from 1 to 299 spectra. Europe accounted for 63.8% of users, ahead of Asia (16.8%), Latin America (15.7%), North America (1.6%), Oceania (1.6%), and Africa (0.5%). As a consequence, most *T. indotineae* spectra were identified in Europe (3,040 [89.4%]). In western and northern Europe, which had the highest number of MSI users, detections were not limited to major urban centers.

Over the study period, the number of *T. indotineae* spectra increased continuously: from 237 in 2022 to 454 in 2023, then to 1,016 in 2024, and finally to 1,692 in 2025. At the same time, the percentage of spectra identified as *T. indotineae* within the *Trichophyton* genus increased from 1.2% to 3.6% and within the *T. mentagrophytes* complex from 4.6% to 13.1% (Figure 2). Among centers identifying *Trichophyton* spp. isolates, the percentage that detected *T. indotineae* rose from 24.7% to 46.1%.

Conclusions

Our results reveal a marked global increase in *T. indotineae* isolation; the number of identifications rose ≈3-fold during 2022–2025. At the same time, the proportion of *T. indotineae* within the *T. mentagrophytes* complex has increased. Those findings are consistent with national or regional data that also demonstrate a temporal increase and a wide geographic distribution. Of note, the analysis of MSI data indicates *T. indotineae* was identified in countries where no cases had yet been reported, such as Bulgaria, Croatia, Colombia, Luxembourg, and Uruguay. Recent publications have already demonstrated the usefulness of MSI in identifying the first cases of *T. indotineae* in Brazil and Hungary (*10*,*11*).

The first limitation of our study is that the picture we provide of the geographic distribution of *T. indotineae* reflects both the availability of mass spectrometry devices and the use of the MSI application. Thus, no spectra were identified in Africa, where the devices are not widely available, or in well-known *T. indotineae*–endemic areas such as India and the Middle East, where few, if any, MSI users are present. Another pitfall is that the analysis is based on the number of spectra, not on the number of isolates. Inferring the number of isolates without additional data is difficult. Moreover, we do not control the conditions under which the application is used, because MSI might be used for research purposes and not exclusively for diagnostic use. Furthermore, isolates originating from a specific geographic area might be transmitted and consequently identified in another location or even another country (e.g., when isolates are sent to reference centers or used as part of research).

However, our results demonstrate that MSI can serve as a powerful interface and epidemiologic surveillance tool for emerging fungal pathogens such as *T. indotineae* or *Candida auris*. Integration of clinical and antifungal susceptibility data could enable the development of a more complete surveillance network for *T. indotineae* and bolster other initiatives, such as one supported in 2023 by the European Centre for Disease Prevention and Control that encouraged reporting of *T. indotineae* infections through EpiPulse (https://www.ecdc.europa.eu/en/publications-data/communicable-disease-threats-report-14-17-may-2023-week-20).

In non–*T. indotineae*–endemic settings, distinguishing between imported and locally acquired cases is key. The establishment of *T. indotineae* is now well documented in eastern China (*12*), and, in Germany, a growing number of infections have been reported since early 2025 among patients without recent travel history, indicating local transmission (*13*). Similarly, increased vigilance regarding transmission routes is required to improve understanding of *T. indotineae* dissemination mechanisms. Sexual transmission has recently been suggested as an underestimated route, which has been seen for *T. mentagrophytes* ITS-genotype VII (*14*). Because MSI is also used in veterinary laboratories, identifying host types could help monitor the zoonotic circulation of *T. indotineae*, because cases have been reported in dogs in India, Iran, and Egypt (*15*). Reliable and rapid identification of *T. indotineae* has direct clinical benefits, and real-time detection of *T. indotineae* cases could help identify patients for inclusion in clinical trials, which are needed given the frequent relapses observed after apparent cure with itraconazole therapy

In conclusion, we encourage microbiology laboratories to use MSI to identify dermatophytes for both individual and public health benefit. Health authorities should address this rapidly evolving international issue, which is associated with therapeutic challenges.

Members of the MSI/INuSuAle Network Database Study Group: Zeynep Yazgan (Istanbul, Turkey), Ivo Cox (Ghent, Belgium), Maxime Moniot (Clermont-Ferrand, France), Cyrille Valin (Décines-Charpieu, France), Fréderic Gabriel (Bordeaux, France), Françoise Botterel (Créteil, France), Laure Kamus (Saint-Denis de La Réunion, France), Marc Westerholt (Karlstad, Sweden), Jacinthe Gholizadeh (Levallois-Perret, France), Wouter Pyck (Oostende, Belgium), Pamela Chauvin (Toulouse, France), Sophie Cassaing (Toulouse), Caroline Mahinc (Saint-Etienne, France), Maxine Nyholm (Lund, Sweden), Karl Oldberg (Lund), Bram Vanmechelen (Brussels, Belgium), Yaye Senghor (Paris, France), Kjersti Wik Larssen (Trondheim, Norway), Emilie Sitterlé (Paris), Eric Dannaoui (Paris), Julie Bonhomme (Caen, France), Kim Camps (Antwerp, Belgium), Arthur Denoël (Noyal-Chatillon-Sur-Seiche, France), Guillaume Dumont (Tourcoing, France), Dolunay Gülmez (Ankara, Turkey), Katrien Lagrou (Leuven, Belgium), Célia Rougès (Paris), Antoine Huguenin (Reims, France), Peter Kutzer (Frankfort (Oder), Germany), Karin Van Looveren (Antwerp), Marjan Van Esbroeck (Antwerp), Noémie Coron (Mouans-Sartoux, France), Guillaume Aubin (Nantes, France), Saara J. Vainio (Nieuwegein, the Netherlands), Philippe R.S. Lagacé-Wiens (Winnipeg, MB, Canada), Fakhri Jeddi (Nantes), Damien Costa (Rouen, France), Suefay Liu (Vancouver, BC, Canada), Marthe Charles (Vancouver), Hélène Guegan (Rennes, France), Christine Bonnal (Paris), Gregory Strubbe (Ghent), Toth Zoltan (Debrecen, Hungary), Agnes Jakab (Debrecen).

The National Reference Centre INuSuAle for Digital Identification, Surveillance and Alert is funded by French Health Authorities (Santé Publique France) and is an associated laboratory to the National Reference Centre for Invasive Mycoses and Antifungals.

About the Author

Dr. Jabet is a medical mycologist in the Parasitology-Mycology Laboratory of Hôpital Universitaire Pitié Salpêtrière, Paris, France. His primary research interests are emerging fungal infections and dermatophytosis.

References

1. Jabet A, Normand AC, Brun S, Dannaoui E, Bachmeyer C, Piarroux R, et al. *Trichophyton indotineae*, from epidemiology to therapeutic. J Mycol Med. 2023;33:101383. https://doi.org/10.1016/j.mycmed.2023.101383
2. Švarcová M, Větrovský T, Kolařík M, Hubka V. Defining the relationship between phylogeny, clinical manifestation, and phenotype for *Trichophyton mentagrophytes/interdigitale* complex; a literature review and taxonomic recommendations. Med Mycol. 2023;61:myad042. https://doi.org/10.1093/mmy/myad042
3. Czerniewska A, Borman A, Abdolrasouli A, Budd EL, Fisher MC, Barton R, et al. Rapid emergence of *Trichophyton indotineae* (*Trichophyton mentagrophytes* ITS genotype VIII) observed in the United Kingdom, up to August 2025. Euro Surveill. 2025;30:2500892. https://doi.org/10.2807/1560-7917.ES.2025.30.49.2500892
4. McTaggart LR, Cronin K, Ruscica S, Patel SN, Kus JV. Emergence of terbinafine-resistant *Trichophyton indotineae* in Ontario, Canada, 2014–2023. J Clin Microbiol. 2025;63:e0153524. https://doi.org/10.1128/jcm.01535-24
5. Sacheli R, Egrek S, El Moussaoui K, Kurt B, Machowski E, Harag S, et al. National Belgian study on terbinafine resistance in *Trichophyton interdigitale/mentagrophytes/indotineae* (2022–2023): epidemiology and molecular features. J Fungi (Basel). 2025;11:676. https://doi.org/10.3390/jof11090676
6. Normand AC, Blaize M, Imbert S, Packeu A, Becker P, Fekkar A, et al. Identification of molds with matrix-assisted laser desorption ionization-time of flight mass spectrometry: performance of the newly developed MSI-2 application in comparison with the Bruker Filamentous Fungi Database and MSI-1. J Clin Microbiol. 2021;59:e0129921. https://doi.org/10.1128/JCM.01299-21
7. De Paepe R, Normand AC, Uhrlaß S, Nenoff P, Piarroux R, Packeu A. Resistance profile, terbinafine resistance screening and MALDI-TOF MS identification of the emerging pathogen *Trichophyton indotineae.* Mycopathologia. 2024;189:29. https://doi.org/10.1007/s11046-024-00835-4
8. Normand AC, Moreno-Sabater A, Jabet A, Hamane S, Cremer G, Foulet F, et al. MALDI-TOF mass spectrometry online identification of *Trichophyton indotineae* using the

MSI-2 application. J Fungi (Basel). 2022;8:1103. https://doi.org/10.3390/jof8101103
9. Normand AC, Becker P, Gabriel F, Cassagne C, Accoceberry I, Gari-Toussaint M, et al. Validation of a new web application for identification of fungi by use of matrix-assisted laser desorption ionization-time of flight mass spectrometry. J Clin Microbiol. 2017;55:2661–70. https://doi.org/10.1128/JCM.00263-17
10. Tóth Z, Ványai B, Kovács R, Jakab Á, Szegedi A, Balázs B, et al. First report of *Trichophyton indotineae* infection in Hungary. J Fungi (Basel). 2025;11:248. https://doi.org/10.3390/jof11040248
11. de Almeida JN Jr, Dos Santos AR, Trindade MRS, Gold JAW, Razo FPM, Gonçalves SS, et al. *Trichophyton indotineae* infection, São Paulo, Brazil, 2024. Emerg Infect Dis. 2025;31:1049–51. https://doi.org/10.3201/eid3105.250048
12. Xie W, Kong X, Zheng H, Mei H, Ge N, Hu S, et al. Rapid emergence of recalcitrant dermatophytosis caused by a cluster of multidrug-resistant *Trichophyton indotineae* in China. Br J Dermatol. 2024;190:585–7. https://doi.org/10.1093/bjd/ljae009
13. Uhrlaß S, Panzer R, Koch D, Mütze H, Richter S, Müller L, et al. Trichophyton mentagrophytes ITS genotype VIII/Trichophyton indotineae in Germany—revisit after 5 years [in German]. Dermatologie (Heidelb). 2025;76:551–64.
14. Jabet A, Chiarabini T, Hennequin C, Bouscarat F, Valin N, Cruchet R, et al. Autochthonous transmission of *Trichophyton indotineae* through sexual contact, France, 2024. Euro Surveill. 2025;30:2500416. https://doi.org/10.2807/1560-7917.ES.2025.30.26.2500416
15. Zineldar HA, El-Neshwy WM, Cristina RT, Abouzeid NZ, Eisa MI, Muselin F, et al. Molecular diagnostics and control of zoonotic dermatophytosis: first detection of *Trichophyton indotineae* in a dog in Africa. Animals (Basel). 2025;15:2622. https://doi.org/10.3390/ani15172622

Address for correspondence: Arnaud Fekkar, Service de Parasitologie-Mycologie, Pavillon Laveran, Hôpital de La Pitié-Salpêtrière, Boulevard de l'Hôpital, 75013 Paris, France; email: arnaud.fekkar@aphp.fr

Wickerhamomyces anomalus Pseudo-Outbreak Associated with Medical Lubricating Gel, South Africa, 2023–2024

Caroline Maluleka, Husna Ismail, Liliwe Shuping, Ruth Mpembe, Gift Sandhleni, Serisha Naicker, Tsidiso Maphanga, Nelesh P. Govender

A nationwide investigation identified 426 patients with *Wickerhamomyces anomalus* fungal cultures in South Africa; most cases clustered during May–November 2023. Case-patients lacked evidence of infection, indicating a pseudo-outbreak. Genomic and laboratory analyses implicated contaminated sterile lubricating gel. A nationwide product recall resulted in a decline in reported cases.

Wickerhamomyces anomalus, an environmental ascomycetous yeast, is associated with healthcare-associated outbreaks among critically ill or immunocompromised patients, but its sources are rarely identified (*1*–*5*). Contaminated medical gel has been implicated in healthcare-associated outbreaks caused by water-associated bacteria (*6*–*11*). In November 2023, the National Institute for Communicable Diseases (NICD) was alerted to an unusually high frequency of *W. anomalus* isolation at a laboratory in KwaZulu-Natal Province, South Africa. Two hospitals in the Western Cape Province separately identified 2 clusters during July–August 2023. One cluster was associated with recent central venous catheter placements through which blood cultures subsequently were collected; a sterile lubricating gel (Lubri-A sterile lubricating jelly; Electro-Spyres, https://www.electrospyres.com) was used in the ultrasound-guided catheter insertion procedure and was a suspected source of pseudo-infections. We investigated the extent, source, and clinical relevance of a nationwide pseudo-outbreak.

Author affiliations: National Institute for Communicable Diseases, Johannesburg, South Africa (C. Maluleka, H. Ismail, L. Shuping, R. Mpembe, G. Sandhleni, S. Naicker, T. Maphanga, N.P. Govender); University of Witwatersrand School of Pathology, Johannesburg (C. Maluleka, L. Shuping, T. Maphanga, N.P. Govender)

DOI: https://doi.org/10.3201/eid3209.260608

The Study

We reviewed National Health Laboratory Service (NHLS) records for patients at public-sector healthcare facilities with culture-confirmed *W. anomalus* from any specimen type during January 1, 2022–April 29, 2024. We removed repeat isolates from the same patient within 30 days. We contacted laboratories to determine whether increased detection coincided with introduction of the Vitek MS system (bioMérieux, https://www.biomerieux.com). We retrospectively collected clinical case data at 2 hospitals. We received *W. anomalus* isolates cultured from clinical specimens and unopened sterile lubricating gel sachets in circulation at healthcare facilities. We subcultured the isolates onto chromogenic agar (Candida CHROMagar, https://www.chromagar.com) and incubated them in ambient air at 35–37°C for 18–24 hours. We confirmed species identification by using matrix-assisted laser desorption/ionization time-of-flight mass spectrometry (MALDI BioTyper; Bruker, https://www.bruker.com). We performed antifungal susceptibility testing by using the Sensititre YeastOne method (Thermo Fisher Scientific, https://www.thermofisher.com). We interpreted MICs by using the Clinical and Laboratory Standards Institute M57S epidemiologic cutoff values (*12*).

We analyzed whole-genome sequences, generated by the NextSeq platform (Illumina, https://www.illumina.com), by using FungiPhyloGen pipeline (https://zenodo.org/records/18121445). We assessed sequence quality by using FASTQC version 0.11.9 (https://sourceforge.net/projects/fastqc.mirror/files/v0.11.9) and MultiQC version 1.13 (https://github.com/MultiQC/MultiQC/releases), followed by trimming with TrimGalore version 0.6.7 (https://github.com/FelixKrueger/TrimGalore/releases). We aligned filtered reads to a reference strain from the

United States (*W. anomalus* NRRL Y-366-8) (*13*) by using BWA version 0.7.19 (https://github.com/lh3/bwa/releases). We annotated high-confidence single-nucleotide polymorphisms (SNPs) (allele frequency >0.85) and used them for distance matrix generation and phylogenetic reconstruction with IQ-TREE version 2.2.0.3 (https://iqtree.github.io) by using 1,000 bootstrap replicates to assess clade support.

We identified 426 cases across 7 of 9 provinces in South Africa over the study period (Figure 1). Before April 1, 2023, the baseline was 2–3 cases per facility per month; 346/426 (81%) cases occurred during May–November 2023. The increase did not coincide with introduction of the Vitek MS system. The most frequent specimen categories were urine (207/426 [49%]) and blood (77/426 [18%]) (Appendix Figure 1, https://wwwnc.cdc.gov/EID/article/32/9/26-0608-App1.pdf). Gauteng Province had the highest number of cases (180/426 [42%]), and Western Cape Province had the highest number of cases from sterile sites (Appendix Figure 2).

Clinical information was available for 52/426 (12%) case-patients (Table). Median age was 23 years (interquartile range 0–47 years); 31/49 (63%) patients were male, and 21 (37%) female. Among 51 of the 52 patients, *W. anomalus* was recovered from urine (26 [51%]), tracheal aspirate (13 [26%]), peritoneal dialysis fluid (6 [12%]), and blood (4 [8%]). Among 37 patients with procedure information, 23 (62%) underwent urinary catheterization and 12 (32%) underwent endotracheal intubation; procedures were not mutually exclusive. For 48 patients whose samples were positive for *W. anomalus*, clinicians considered the positive culture as contamination in 20 (42%) and clinically relevant in 28 (58%) patients: urinary tract infection in 15 (31%), lower respiratory tract infection in 8 (17%), and bloodstream infection in 2 (4%). Antifungal treatment was administered to 10 (23%) of 44 patients for whom treatment information was available. However, objective evidence of infection such as signs of sepsis or elevated levels of inflammatory biomarkers was absent or incompletely documented. Only 5 patients had *W. anomalus* isolated from subsequent cultures. Among 50 patients with known outcomes, 30 (60%) were discharged, 6 (12%) remained hospitalized, and 14 (28%) died; available data were insufficient to attribute deaths to *W. anomalus* infection (Appendix Figure 2).

Of 86 isolates, 62 (72%) were cultured from clinical specimens and 24 (28%) from gel batches. Sealed gel sachets uniformly yielded heavy fungal growth. We confirmed 85 (99%) isolates as *W. anomalus*; we excluded 1/86 (1%) *Candida albicans* isolate. Seventeen clinical isolates and 11 gel isolates underwent susceptibility testing. Fluconazole MIC_{50} (MIC at which 50% of a specific isolate population

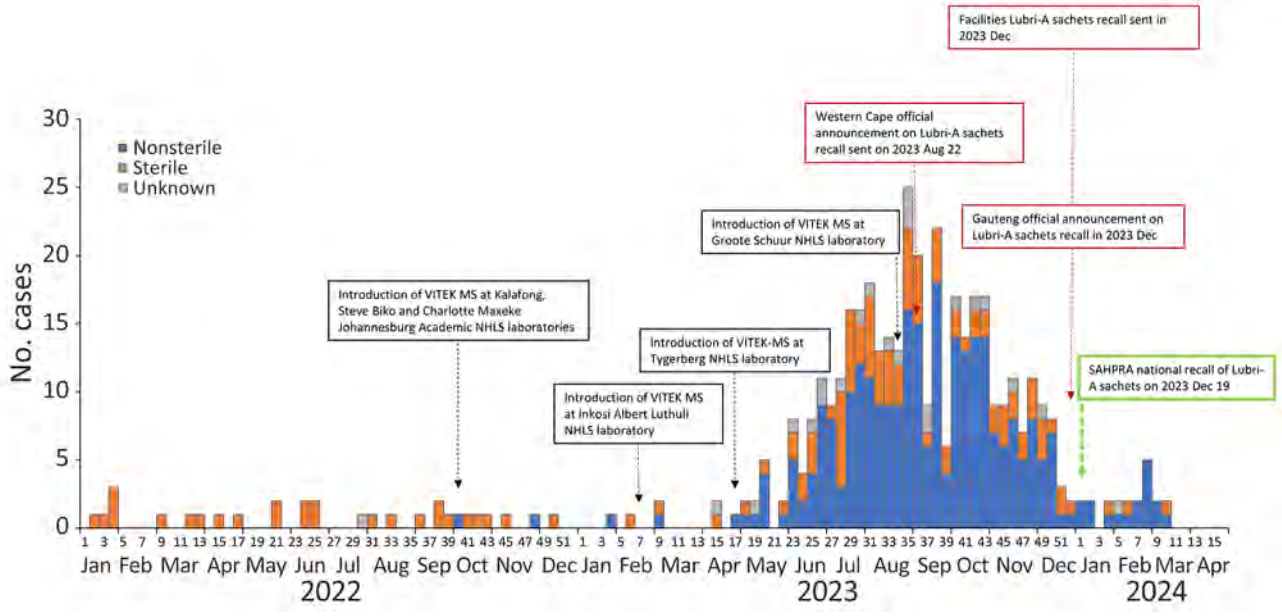

Figure 1. Annotated epidemic curve of *Wickerhamomyces anomalus* infection cases, by epidemiologic week, South Africa, January 1, 2022–April 29, 2024. Normally sterile-site specimens were those obtained from anatomical sites expected to be free of viable microorganisms. Nonsterile-site specimens were those obtained from sites normally colonized by microbiota or exposed to the external environment. Lubri-A refers to Lubri-A sterile lubricating jelly (Electro-Spyres, https://www.electrospyres.com), Vitek MS to the Vitek MS system (bioMérieux, https://www.biomerieux.com). NHLS, National Health Laboratory Service, SAPHRA, South African Health Products Regulatory Authority.

Table. Characteristics of patients with *Wickerhamomyces anomalus* infection in 2 hospitals, South Africa, August 7, 2023–January 11, 2024*

Characteristic	Value
Median age, y (IQR)	23 (0–47)
Sex, n = 49	
F	18 (37)
M	31 (63)
Underlying condition or procedure, n = 36	
HIV	6 (17)
Chronic kidney disease	7 (19)
Surgical procedure	10 (28)
Other	23 (64)
Gel-use–linked procedure, n = 38†	
Urinary catheterization	24 (63)
Endotracheal intubation	13 (48)
Ultrasound scan	10 (42)
Other‡	10 (42)
Specimen type, n = 51	
Urine	26 (51)
Tracheal aspirate	13 (26)
Peritoneal dialysis fluid	6 (12)
Blood	4 (8)
Bronchial alveolar lavage	1 (2)
Tissue	1 (2)
W. anomalus–linked diagnosis by treating clinician, n = 48	
Considered a contaminant	20 (42)
Urinary tract infection	15 (31)
Lower respiratory tract infection	8 (17)
Bloodstream infection	2 (4)
Peritonitis	3 (6)
Antifungal treatment administered, n = 44	
Yes	10 (23)
No	34 (77)
Adverse events related to *W. anomalus* infection, n = 51	
No	30 (59)
Unknown	21 (41)
Outcome, n = 50	
Still admitted	6 (12)
Discharged	30 (60)
Died	14 (28)

*Values are no. (%) except as indicated; IQR, interquartile range.
†Denominators vary because of missing data; some persons had >1 procedure linked to the use of lubricating gel.
‡Includes nasogastric tubing (n = 5), bronchoscopy (n = 1), rectal enema (n = 1), Pap smear (n = 1), vaginal examination and cardiotocography (n = 1), and tracheal dilation (n = 1).

is inhibited from growth) was 2 μg/mL for clinical and gel isolates. Fluconazole MICs were ≤2 μg/mL for 16/17 (94%) clinical isolates and 9/11 (82%) gel isolates; all were wild-type. All other azole and micafungin MICs were at or below their respective epidemiologic cutoff values. Amphotericin B MICs were ≤1 μg/mL for 15/17 (88%) clinical isolates and 9/11 (82%) gel isolates; 2/17 (12%) clinical isolates and 2/11 (18%) gel isolates had MICs >1 μg/mL. Flucytosine MICs were 0.06 μg/mL for all 17 clinical isolates, whereas 9/11 (82%) gel isolates had MICs ≥64 μg/mL (Appendix Table 1).

The phylogenetic dataset included 95 genome sequences. Of those, 72 (76%) were current outbreak isolates (GenBank BioProject no. PRJNA148538): 49 (68%) clinical, 22 (31%) gel-derived, and 1 (1%) undocumented source. The remaining 23 included 12 historic surveillance isolates from South Africa, 10 published genomes (BioProject no. PRJNA851035), and 1 reference genome (*W. anomalus* NRRL Y-366-8; RefSeq [https://www.ncbi.nlm.nih.gov/refseq] no. GCF_001661255.1). Two major clusters were separated by >10,000 SNPs; clinical and gel-derived genomes were interspersed within both clusters (Figure 2). Within-cluster diversity was <1,000 SNPs in the smaller cluster and <2,000 in the larger cluster. That finding indicated a contaminated product rather than a single local transmission chain.

The outbreak was reported to the South African Health Products Regulatory Authority and the National Department of Health on August 21, 2023. On December 8, 2023, the National Department of Health instructed facilities to stop using implicated batches, quarantine them, halt distribution, obtain alternative products, and establish case-based surveillance.

After an independent investigation, the South African Health Products Regulatory Authority later issued a Class 1 Type A nationwide recall and informed other regulatory authorities. Case counts declined sharply thereafter, although sporadic detection persisted in early 2024, probably because of remaining facility stock still in use (Figure 1).

Conclusions

Epidemiologic, microbiologic, and genomic findings identified single-use sterile lubricating gel sachets contaminated at manufacture as a source of a national pseudo-outbreak of *W. anomalus* infection. Evidence included detection across 7 provinces, recovery of the organism from sealed sachets and 3 separate batches, interspersion of clinical and gel genomes, absence of a temporal association with laboratory instrument changes, and a rapid case decline after the nationwide recall. Many positive cultures probably reflected contamination of specimens or devices rather than infection. Nonetheless, treating clinicians considered the organism clinically relevant in more than half of patients in the clinical subset, and 23% received antifungal treatment. Those findings illustrate how pseudo-outbreaks can lead to potentially unnecessary treatment. Interpretation was limited because clinical data were only available for 12% of the cases from 2 hospitals and collected retrospectively.

Healthcare facilities and diagnostic laboratories should be suspicious when unusual organisms are repeatedly detected across multiple specimen types or in geographically separate facilities. Products labeled sterile remain a risk if assurance of sterility fails during manufacturing. Strengthened procurement,

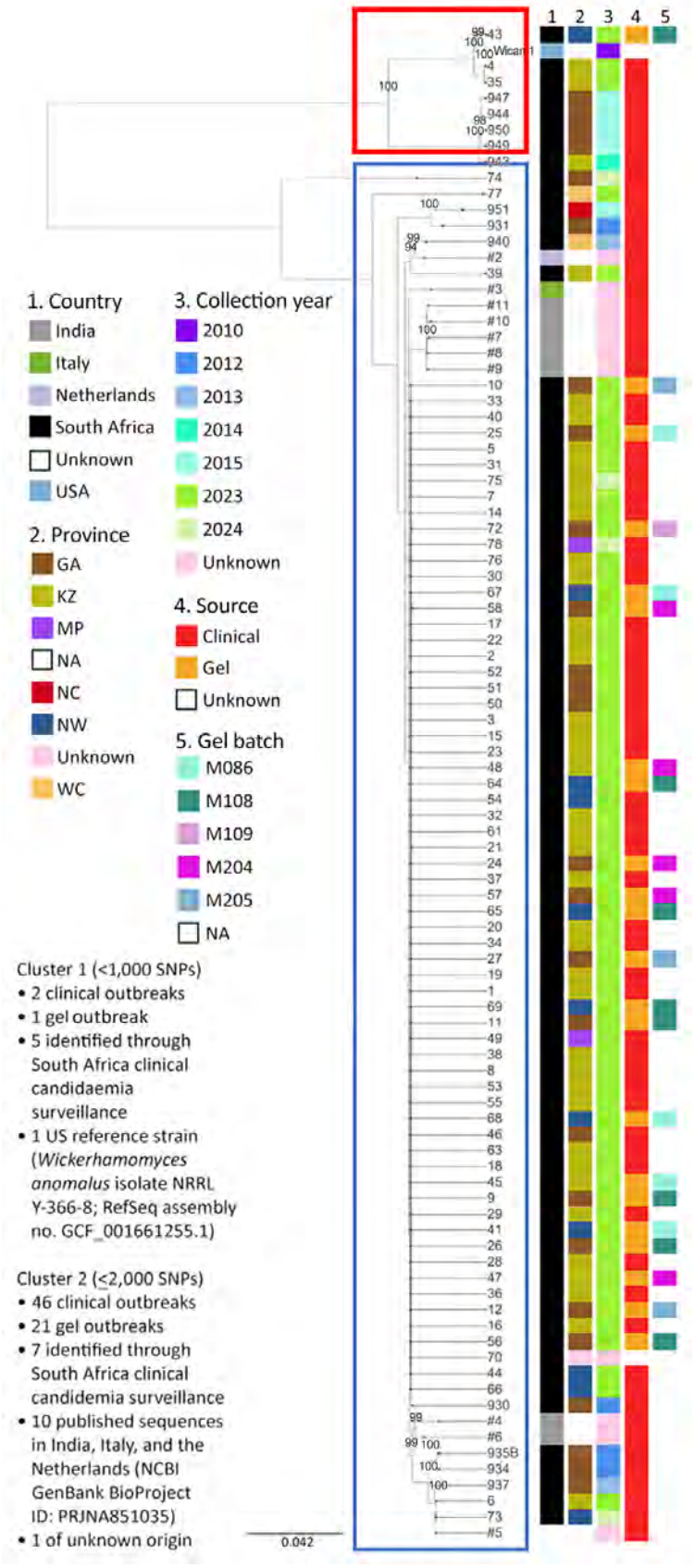

Figure 2. Whole-genome SNP phylogeny of *Wickerhamomyces anomalus* clinical, gel, surveillance, and reference isolates, South Africa. Red box indicates cluster 1; blue box indicates cluster 2. Scale bar indicates mean number of nucleotide substitutions per variable site. Node values represent ultrafast bootstrap support percentages based on 1,000 replicates. GA, Gauteng Province; KZ, KwaZulu–Natal Province; MP, Mpumalanga Province; NA, not applicable; NC, Northern Cape Province; NCBI, National Center for Biotechnology Information; NW, North West Province; WC, Western Cape Province; SNP, single-nucleotide polymorphism; USA, United States.

supplier quality assurance, product traceability, postmarket surveillance, notification, and rapid national coordination among laboratories, clinicians, infection prevention teams, public health authorities, and regulators are essential to prevent and contain similar events.

Acknowledgments

In addition to the authors, many people played a critical role in the outbreak response team. Yesholata Mahabeer, Masego Moncho, Vindana Chibabhai, and William Malebati sent isolates, assisted with outbreak management, or collated patient files for data abstraction. Staff at the NICD (Ernest Tsotetsi, Rotondwa Mudau, Miriam Mwamba, and Silondiwe Nzimande) processed isolates or performed downstream bioinformatics analyses (Stanford Kwenda). We thank all participating NHLS laboratories that submitted isolates for characterization and further analysis.

Approval for this study was granted to NICD by the Human Research Ethics Committee (Medical) at the University of Witwatersrand for essential surveillance.

The authors acknowledge the use of ChatGPT-4.0 (OpenAI, https://openai.com) during the preparation of this manuscript. The tool was only employed to assist with text editing and to improve readability and overall flow after the full manuscript had been written and the references had been verified. All generated content was critically reviewed, revised, and verified by the authors, who take full responsibility for the final version and its scientific integrity.

About the author

Dr. Maluleka is a medical microbiologist and pathologist at the Centre for Healthcare-Associated Infections, Antimicrobial Resistance and Mycoses at the National Institute for Communicable Diseases in South Africa. Her research focuses on fungal infections, antimicrobial resistance (including antifungals), and the epidemiology of healthcare-associated pathogens in low- and middle-income settings.

References

1. Kurtzman CP. Phylogeny of the ascomycetous yeasts and the renaming of *Pichia anomala* to *Wickerhamomyces anomalus*. Antonie van Leeuwenhoek. 2011;99:13–23. https://doi.org/10.1007/s10482-010-9505-6
2. Ioannou P, Baliou S, Kofteridis DP. Fungemia by *Wickerhamomyces anomalus*—a narrative review. Pathogens. 2024;13:269. https://doi.org/10.3390/pathogens13030269
3. da Silva CM, de Carvalho Parahym AMR, Leão MPC, de Oliveira NT, de Jesus Machado Amorim R, Neves RP. Fungemia by *Candida pelliculosa* (*Pichia anomala*) in a neonatal intensive care unit: a possible clonal origin. Mycopathologia. 2013;175:175–9. https://doi.org/10.1007/s11046-012-9605-0
4. Jung J, Moon YS, Yoo JA, Lim JH, Jeong J, Jun JB. Investigation of a nosocomial outbreak of fungemia caused by *Candida pelliculosa* (*Pichia anomala*) in a Korean tertiary care center. J Microbiol Immunol Infect. 2018;51:794–801. https://doi.org/10.1016/j.jmii.2017.05.005
5. Kalenic S, Jandrlic M, Vegar V, Zuech N, Sekulic A, Mlinaric-Missoni E. *Hansenula anomala* outbreak at a surgical intensive care unit: a search for risk factors. Eur J Epidemiol. 2001;17:491–6. https://doi.org/10.1023/A:1013739802940
6. Chittick P, Russo V, Sims M, Robinson-Dunn B, Oleszkowicz S, Sawarynski K, et al. An outbreak of *Pseudomonas aeruginosa* respiratory tract infections associated with intrinsically contaminated ultrasound transmission gel. Infect Control Hosp Epidemiol. 2013;34:850–3. https://doi.org/10.1086/671268
7. Yagnik KJ, Kalyatanda G, Cannella AP, Archibald LK. Outbreak of *Acinetobacter baumannii* associated with extrinsic contamination of ultrasound gel in a tertiary centre burn unit. Infect Prev Pract. 2019;1:100009. https://doi.org/10.1016/j.infpip.2019.100009
8. Hudson MJ, Park SC, Mathers A, Parikh H, Glowicz J, Dar D, et al. Outbreak of *Burkholderia stabilis* infections associated with contaminated nonsterile, multiuse ultrasound gel—10 states, May–September 2021. MMWR Morb Mortal Wkly Rep. 2022;71:1517–21. https://doi.org/10.15585/mmwr.mm7148a3
9. Angrup A, Kanaujia R, Biswal M, Ray P. Systematic review of ultrasound gel associated *Burkholderia cepacia* complex outbreaks: clinical presentation, sources and control of outbreak. Am J Infect Control. 2022;50:1253–7. https://doi.org/10.1016/j.ajic.2022.02.005
10. Arsenault C, Harel J, Doualla-Bell F, Cavayas YA, Marchand-Sénécal X, Frenette C, et al. A *Burkholderia stabilis* outbreak associated with the use of ultrasound gel in multiple healthcare centres in Montréal, Canada, May–October 2021. Can Commun Dis Rep. 2023;49:314–9. https://doi.org/10.14745/ccdr.v49i78a03
11. Solaimalai D, Devanga Ragupathi NK, Ranjini K, Paul H, Verghese VP, Michael JS, et al. Ultrasound gel as a source of hospital outbreaks: Indian experience and literature review. Indian J Med Microbiol. 2019;37:263–7. https://doi.org/10.4103/ijmm.IJMM_19_249
12. Clinical and Laboratory Standards Institute. Epidemiological cutoff values for antifungal susceptibility testing. 4th edition. Supplement M57S. Wayne (PA): The Institute; 2022.
13. Spruijtenburg B, Rudramurthy SM, Meijer EFJ, van Haren MHI, Kaur H, Chakrabarti A, et al. Application of novel short tandem repeat typing for *Wickerhamomyces anomalus* reveals simultaneous outbreaks within a single hospital. Microorganisms. 2023;11:1525. https://doi.org/10.3390/microorganisms11061525

Address for corresponding author: Caroline Maluleka, National Institute for Communicable Diseases, a division of the National Health Laboratory Service, 1 Modderfontein Rd, Sandringham, Johannesburg 2192, South Africa; email: carolinema@nicd.ac.za

Genetically Distinct African Swine Fever Virus Genotype II Variant in Wild Boar, Spain, 2025–2026

Carmina Gallardo, Marina Marcet-Houben, Montserrat Agüero, Raquel Nieto, Nadia Casado, Alejandro Soler, María José Ruano, Rubén Villalba, Jovita Fernández-Pinero, Alicia Simón, Covadonga Pérez, Concepción Gómez, Cecilia García, Mireia Labrador, Jordi Argilaguet, Liani Coronado, Natàlia Majó, Pilar Aguilera-Sepulveda, Irene Aldea, Toni Gabaldón, María Belén Gómez, Marisa Arias

African swine fever virus genotype II was detected in wild boar in Spain in 2025 after >30 years of absence. Whole-genome sequencing and molecular follow-up of 8 representative cases identified a stable 9.8-kb deletion affecting the multigene family in the left variable region, defining an ASFV genotype II variant.

African swine fever (ASF) is a highly contagious disease of domestic pigs and wild suids with major economic consequences. After the emergence of ASF virus (ASFV) genotype II in Georgia in 2007 (*1*), the virus spread across Europe and Asia and reached the Caribbean, demonstrating its capacity for transcontinental spread. In Europe, ASFV circulation is maintained in wild boar populations (*2*). On November 26, 2025, ASFV was confirmed in Spain (*3*). By May 29, 2026, a total of 326 ASFV-positive wild boar had been detected (Figure 1, panel A). Spain rapidly implemented control measures to limit wild boar movement, including carcass search and removal, reinforced passive surveillance, movement restrictions, and installation of fencing. This study describes the genomic characterization and molecular follow-up of 8 representative ASFV-positive wild boar cases detected during November 2025–February 2026, including the index cases (Figure 1, panel B).

The Study

Two freshly dead wild boar (*Sus scrofa*) were found on November 26, 2025, during passive wildlife surveillance near Barcelona, northeastern Spain (*3*). The animals were located ≈1 km apart in a periurban area with high human connectivity. We analyzed whole blood, serum, spleen, tonsil, and lymph node samples at Unitat Mixta d'Investigació Institut de Recerca i Tecnologia Agroalimentàries, Centre de Recerca en Sanitat Animal (IRTA-CReSA; Bellaterra, Spain), the Spanish National Reference Laboratory for ASF (Algete, Spain), and the European Union Reference Laboratory for ASF (EURL-ASF; Valdeolmos, Spain).

We confirmed that both animals tested ASFV-positive by World Organisation for Animal Health (WOAH) real-time PCR procedure 2; virus isolation in primary porcine alveolar macrophages showed the characteristic hemadsorption pattern. We detected ASFV-specific antibodies in both animals by WOAH indirect immunoperoxidase test; serum titers were 1:2,560.

Genotyping based on partial *B646L* (p72) sequencing assigned the virus to genotype II, which has circulated in Europe since 2007 (*4*). To determine whether the Spain ASFV corresponded to any of the 28

Author affiliations: Centro de Investigación en Sanidad Animal, Valdeolmos, Spain (C. Gallardo, R. Nieto, N. Casado, A. Soler, J. Fernandez-Pinero, A. Simón, C. Pérez, C. Gómez, P. Aguilera-Sepulveda, I. Aldea, M. Arias); Barcelona Supercomputing Center, Barcelona, Spain (M. Marcet-Houben, C. García, M. Labrador, T. Gabaldón); Institute for Research in Biomedicine, Barcelona (M. Marcet-Houben, C. García, M. Labrador, T. Gabaldón); CIBER de Enfermedades Infecciosas, Instituto de Salud Carlos III, Madrid, Spain (M. Marcet-Houben, T. Gabaldón); Laboratorio Central de Veterinaria, Algete, Spain (M. Agüero, M.J. Ruano, R. Villalba, M.B. Gómez); Unitat Mixta d'Investigació Institut de Recerca i Tecnologia Agroalimentàries–Universitat Autònoma de Barcelona en Sanitat Animal, Barcelona (J. Argilaguet, L. Coronado, N. Majó); Centre de Recerca en Sanitat Animal, Barcelona (J. Argilaguet, L. Coronado); World Organisation for Animal Health Collaborating Centre for the Research and Control of Emerging and Re-Emerging Swine Diseases in Europe, Barcelona (J. Argilaguet, L. Coronado, N. Majó); Universitat Autónoma de Barcelona, Barcelona (N. Majó); Catalan Institution for Research and Advanced Studies, Barcelona (T. Gabaldón)

DOI: https://doi.org/10.3201/eid3209.260360

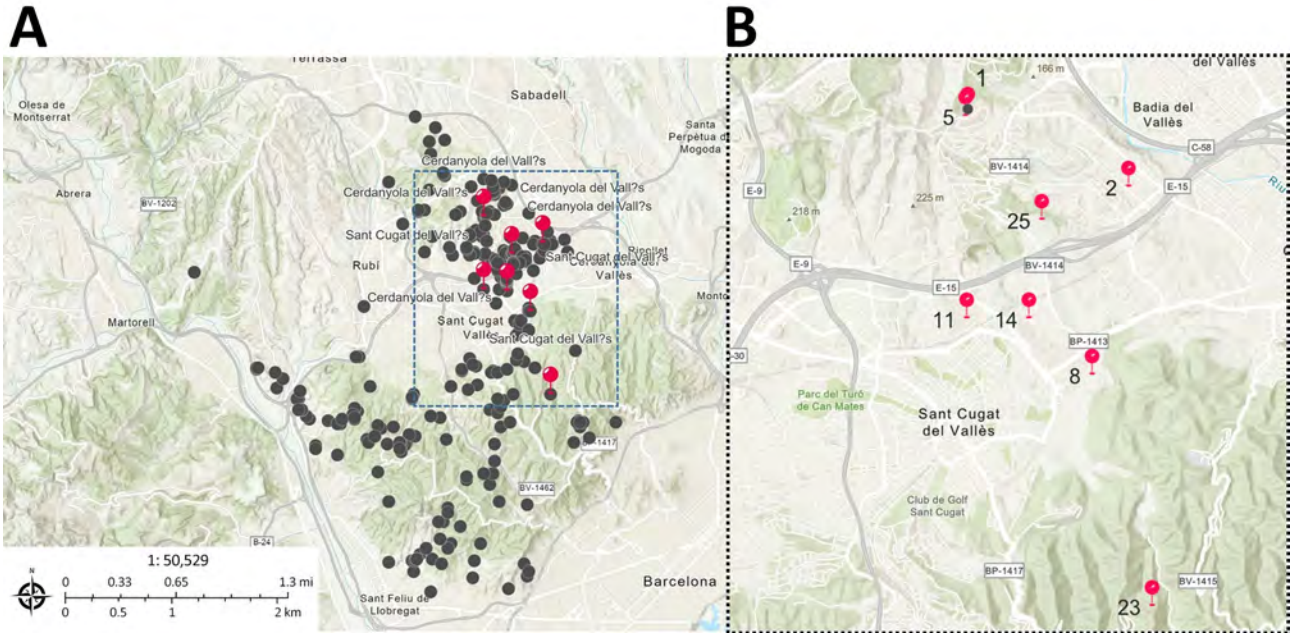

Figure 1. Spatial distribution of African swine fever virus (ASFV)–positive wild boar cases detected in northeastern Spain, 2025–2026. A) Geographic distribution of ASFV-positive wild boar cases detected during November 2025–May 2026 in the affected area in Barcelona. Red dots indicate cases selected for whole-genome sequencing. B) Enlarged view of the main affected area showing the spatial distribution of sequenced ASFV-positive wild boar cases. Numbers correspond to genome identifiers: 1, SP25WBCASE1 (index case); 2, SP25WBCASE2 (index case); 5, SP25WBCASE5 (case 0); 8, SP26WBCASE8; 11, SP26WBCASE11; 14, SP26WBCASE14; 23, SP26WBCASE23; 25, SP26WBCASE25.

genotype II genetic groups the EURL-ASF identified in Europe (Figure 2), we analyzed viruses from both index wild boar using a harmonized 6-locus framework (*5*). Comparison with 1,192 homologous genotype II sequences available in the EURL-ASF sequence database (Appendix 1 Table 1, https://wwwnc.cdc.gov/EID/article/32/9/26-0360-App1.xlsx) showed that 5 of 6 analyzed loci matched the Georgia 2007 genotype II variant 1 profile, whereas a previously undescribed G→A substitution within the MGF505-*9R/10R* intergenic region supported classification of the Spain isolate as a new genetic group, 29 (Figure 2).

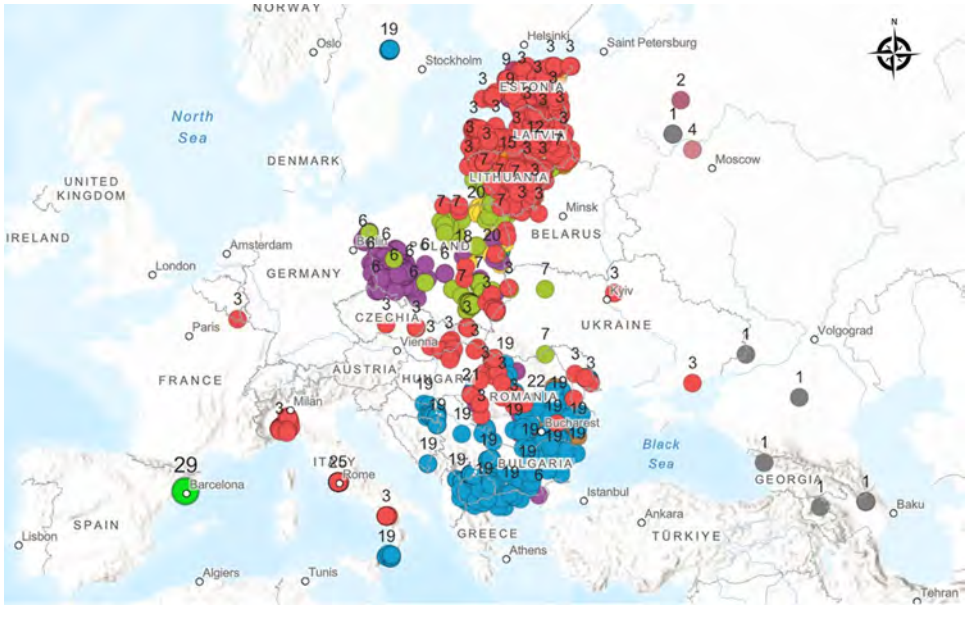

Figure 2. Geographic distribution of African swine fever (ASF) virus genotype II genetic groups in Europe, 2007–2025. We combined analysis of 6 genomic regions to define genetic groups. We assigned groups through comparison with 1,192 homologous genotype II sequences available in the European Union Reference Laboratory for ASF sequence database (Appendix 1 Table 1, https://wwwnc.cdc.gov/EID/article/32/9/26-0360-App1.xlsx). Numbers within colored circles denote genetic groups. Genetic group 29, identified in Spain in 2025, is highlighted. The analyzed regions were the central variable region within B602L; intergenic region (IGR) between I73R and I329L genes; O174L; K145R; the IGR between MGF (multigene family) 505-9R and MGF505-10R genes; and the IGR between I329L and I215L genes.

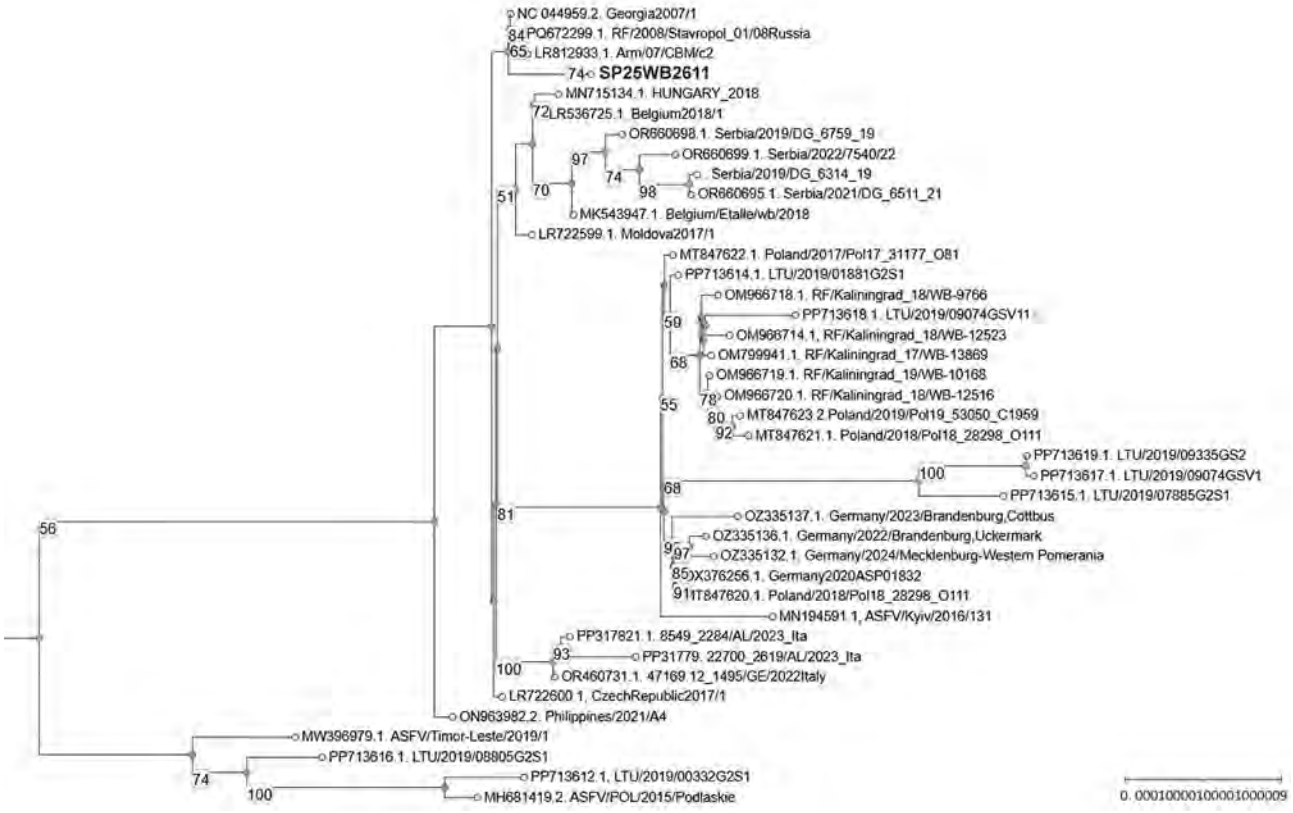

Figure 3. Maximum-likelihood phylogenetic tree based on complete genome sequences of ASFV genotype II from study of the variant in wild boar, Spain, 2025–2026. The analysis included 40 publicly available genomes retrieved from GenBank (accession numbers shown) and the consensus genome sequence SP25WB2611 from our study (bold; wild boar, Spain, 2025 case 1 and 2). We used IQ-TREE (http://www.iqtree.org) to infer the tree with the best-fitting nucleotide substitution model selected by ModelFinder (http://www.iqtree.org/ModelFinder) outside the variable regions. Branch support values are shown at nodes (10,000 ultrafast bootstrap replicates). Scale bar indicates nucleotide substitutions per site. ASFV, African swine fever virus.

We performed whole-genome sequencing to obtain higher-resolution genomic characterization of the Spain ASFV. We processed ASFV-positive blood samples using target-enriched libraries prepared with KAPA HyperCap workflow (Roche Sequencing Solutions, https://diagnostics.roche.com) and sequenced on an Illumina iSeq 100 platform (https://www.illumina.com), generating 2 × 150 bp paired-end reads. We mapped reads to the ASFV Georgia 2007/1 reference genome (GenBank accession no. FR682468.2). Both index wild boar cases yielded nearly identical genomes of 180,757 nt; mean coverage exceeded 200 times. We designated the consensus genome sequence SP25WB2611 (GenBank accession no. PZ023911).

Sequence analysis revealed a ≈9.8-kb deletion within the left variable region (LVR), spanning positions 10,264–20,087 of the reference genome. The deletion removed 21 coding sequences, predominantly members of multigene family (MGF) 110, together with MGF360-4L, MGF360-6L, and MGF100-1R (Appendix 2 Figure, https://wwwnc.cdc.gov/EID/article/32/9/26-0360-App2.pdf). Outside the deleted region, the genome retained >99.9% homology with Georgia 2007/1 with 30 differences: 18 single-nucleotide polymorphisms (SNPs) and 12 insertions or deletions.

To investigate the phylogenetic relationship of the Spanish ASFV, we retrieved 40 genotype II genomes sharing ≥99.94% nucleotide identity with the Spain isolate from GenBank. Maximum-likelihood analysis placed SP25WB2611 within the major genotype II lineage derived from Georgia 2007/1 (Figure 3). The Spain isolate clustered near historical Caucasus genotype II viruses, including Armenia 2007 and the Russian Federation 2008 Stavropol isolate, on the basis of SNP similarity outside the large LVR deletion.

To support molecular follow-up of the outbreak, we selected 6 additional ASFV-positive wild boar cases detected during November 2025–February 2026 for whole-genome sequencing (Figure 1, panel B; Appendix 1 Table 2). Those included the oldest ASFV-positive case identified during field investigation (SP25WBCASE5), considered the probable index

case of the outbreak (case 0), which had likely been dead for ≈1.5–4 months before detection. All genomes clustered within the same clade and showed the characteristic ≈9.8-kb LVR deletion and nearly identical profiles compared with SP25WB2611. The only relevant difference was a synonymous SNP in case 11 relative to the Georgia 2007/1 reference genome (C→T at position 164,421). We also observed minor variations within polynucleotide tracts. We described genomic variants and epidemiologic data (Appendix 1 Tables 2, 3). We submitted the 6 consensus genome sequences to GenBank (accession nos. PZ619929–34).

Conclusions

Genomic characterization of ASFV detected in wild boar in northeastern Spain identified a distinct genotype II variant defined by a unique multigene profile and a large LVR deletion. Outside the deleted region, although the virus remained highly similar to the Georgia 2007/1 lineage, we found 30 nt differences, together with the novel MGF signature defining genetic group 29. In whole-genome phylogenetic analysis, the study isolate clustered near early Caucasus genotype II viruses. However, that clustering should be interpreted cautiously because the large LVR deletion contributed little to the phylogenetic topology. Furthermore, genotype II ASFVs show limited genomic divergence because of their slow evolutionary rate (≈1–1.5 × 10^{-5} substitutions/site/year; ≈2 substitutions/genome/year) (*6*). Consequently, relatively few SNP differences might influence phylogenetic grouping among closely related genotype II viruses. The clustering we observed does not necessarily indicate a direct epidemiologic relationship with early Caucasus isolates.

Analysis of 6 additional ASFV-positive wild boar cases confirmed the stability of the large LVR deletion and the high genomic similarity among the Spain isolates; we detected 1 synonymous SNP within the *E423R* coding region in case 11. Of importance, case 0 already carried the same deletion, suggesting that it was present before introduction into Spain. Although the precise origin of the variant remains unresolved, our data support a long-distance, human-mediated introduction; the isolated detection in a periurban setting with high human connectivity, along with the absence of epidemiologic continuity with affected regions, support that interpretation. Contaminated pork products remain a recognized pathway for ASFV introduction (*7*–*9*).

The genomic features of the Spain ASFVs result primarily from structural changes within the LVR, particularly the deletion affecting MGF110 and MGF360 genes involved in host–virus interactions and innate immune responses (*10*,*11*). Comparable LVR deletions have been reported in ASFV field variants from Estonia and Italy with different virulence outcomes (*12*,*13*), during adaptation of genotype II viruses to continuous cell cultures (*14*), and after heat treatment (*15*). In the Spain variant, the biological consequences of such changes remain uncertain. Serologic findings during outbreak follow-up at the NRL identified ASFV-specific antibodies in 44 (32.1%) of 137 PCR-positive wild boar specimens, confirming the initial findings in the index cases. Those data suggest a more prolonged course of infection than typically observed with highly virulent genotype II ASFV strains, in which animals often die within the first week after infection, before developing detectable humoral responses. Whether the prolonged course of infection we observed in this outbreak is associated with the large LVR deletion requires confirmation through in vivo studies. Our study highlights the importance of continued epidemiologic and genomic follow-up of ASFV outbreaks to better understand the evolution, circulation, and emergence of genetically distinct genotype II variants over time.

Acknowledgments

We thank the Animal Facility Unit of IRTA-CReSA for excellent technical support.

This work was supported by the European Union Reference Laboratory for African swine fever (grant no. 101198164, EURL-ASF 2025–2027) and the Spanish Ministry of Science and Innovation (MICIU/AEI/10.13039/501100011033), grant PID2022-136312OB-I00.

The authors used ChatGPT (OpenAI, https://openai.com) for language editing and structural refinement of the manuscript. The authors take full responsibility for the content of this publication.

Author contributions: C.G., M.A., R.V., and M.Ag. conceived the study. C.G., M.A., J.F.-P., R.V., and M.Ag. designed the methodology. C.G., M.A., R.V., and M.Ag. conducted the investigation. N.C., R.N., J.A., L.C., N.M., A.S.L., A.S., C.P., C.C., M.B.G., and M.J.R. performed virus isolation and diagnostic procedures. M.M.-H., M.L., N.C., A.S., C.P., P.A., and C.Gar. carried out sequencing analyses. C.G., T.G., M.M.-H., and I.A. performed the bioinformatic analyses. C.G. and M.A. curated the data. C.G. prepared the original draft. C.G., M.A., R.V., and M.Ag. reviewed and edited the manuscript. C.G. and M.A. acquired funding. All authors read and approved the final manuscript.

About the Author

Dr. Gallardo is a senior research scientist at the Centro de Investigación en Sanidad Animal (CISA-INIA/CSIC), Madrid, Spain, and technical coordinator of both the European Union Reference Laboratory for ASF and the Food and Agriculture Organization Reference Centre for ASF. Her primary ASF work is in molecular epidemiology, diagnostics, and vaccine research. She has served as a WOAH-designated ASF expert.

References

1. Rowlands RJ, Michaud V, Heath L, Hutchings G, Oura C, Vosloo W, et al. African swine fever virus isolate, Georgia, 2007. Emerg Infect Dis. 2008;14:1870–4. https://doi.org/10.3201/eid1412.080591
2. Sukmanadi M, Khairullah AR, Mustofa I, Wiyono A, Wardhani BWK, Saepulloh M, et al. African swine fever: a highly fatal disease that is spreading globally. Open Vet J. 2025;15:3399–418. https://doi.org/10.5455/OVJ.2025.v15.i8.4
3. World Organisation for Animal Health. African swine fever (ASF) in Spain: immediate notification report. 2025 [cited 2026 Mar 9]. https://wahis.woah.org
4. Mazloum A, van Schalkwyk A, Chernyshev R, Igolkin A, Heath L, Sprygin A. A guide to molecular characterization of genotype II African swine fever virus: essential and alternative genome markers. Microorganisms. 2023;11:642. https://doi.org/10.3390/microorganisms11030642
5. Giammarioli M, Torresi C, Biccheri R, Cammà C, Marcacci M, Dondo A, et al. Genetic characterization of African swine fever Italian clusters in the 2022–2023 epidemic wave by a multi-gene approach. Viruses. 2024;16:1185. https://doi.org/10.3390/v16081185
6. Rossi G, Leitch ECM, Graham J, Biccheri R, Iscaro C, Torresi C, et al. A phylogenetic contribution to understanding the panzootic spread of African swine fever: from the global to the local scale. Virus Evol. 2026;12:veaf103. https://doi.org/10.1093/ve/veaf103
7. Lentz HHK, Bergmann H, Conraths FJ, Schulz J, Sauter-Louis C. The diffusion metrics of African swine fever in wild boar. Sci Rep. 2023;13:15110. https://doi.org/10.1038/s41598-023-42300-0
8. Mazur-Panasiuk N, Żmudzki J, Woźniakowski G. African swine fever virus—persistence in different environmental conditions and the possibility of indirect transmission. J Vet Res (Pulawy). 2019;63:303–10. https://doi.org/10.2478/jvetres-2019-0058
9. Schulz K, Calvelage S, Rogoll L, Conraths FJ, Staubach C, Albrecht K, et al. African swine fever outbreaks in German pig holdings—experiences, epidemiological considerations, and genome sequences. Sci Rep. 2026;16:4350. https://doi.org/10.1038/s41598-026-36441-1
10. Huang R, Luo R, Lan J, Lu Z, Qiu HJ, Wang T, et al. The multigene family genes-encoded proteins of African swine fever virus: roles in evolution, cell tropism, immune evasion, and pathogenesis. Viruses. 2025;17:865. https://doi.org/10.3390/v17060865
11. Zhu Z, Chen H, Liu L, Cao Y, Jiang T, Zou Y, et al. Classification and characterization of multigene family proteins of African swine fever viruses. Brief Bioinform. 2021;22:bbaa380. https://doi.org/10.1093/bib/bbaa380
12. Zani L, Forth JH, Forth L, Nurmoja I, Leidenberger S, Henke J, et al. Deletion at the 5′ end of Estonian ASFV strains associated with an attenuated phenotype. Sci Rep. 2018;8:6510. https://doi.org/10.1038/s41598-018-24740-1
13. Torresi C, Biccheri R, Cammà C, Gallardo C, Marcacci M, Zoppi S, et al. Genome-wide approach identifies natural large-fragment deletion in ASFV strains circulating in Italy during 2023. Pathogens. 2025;14:51. https://doi.org/10.3390/pathogens14010051
14. Krug PW, Holinka LG, O'Donnell V, Reese B, Sanford B, Fernandez-Sainz I, et al. The progressive adaptation of a Georgian isolate of African swine fever virus to Vero cells leads to a gradual attenuation of virulence in swine corresponding to major modifications of the viral genome. J Virol. 2015;89:2324–32. https://doi.org/10.1128/JVI.03250-14
15. Bourry O, Hutet E, Le Dimna M, Lucas P, Blanchard Y, Chastagner A, et al. Oronasal or intramuscular immunization with a thermo-attenuated ASFV strain provides full clinical protection against Georgia 2007/1 challenge. Viruses. 2022;14:2777. https://doi.org/10.3390/v14122777

Address for correspondence: Carmina Gallardo, European Union Reference Laboratory for African Swine Fever, Centro de Investigación en Sanidad Animal (CISA-INIA-CSIC), Ctra. De Algete el Casar s/n, 28130 Valdeolmos, Madrid, Spain; email: gallardo@inia.csic.es

Chronic Elbow Nodules Caused by *Fomitiporella* Fungus in Immunocompetent Patients, United States

Giannoula S. Tansarli, Bicong Wu, Stephen J. Salipante, Brad T. Cookson

We report 2 cases of chronic subcutaneous infection in immunocompetent persons caused by *Fomitiporella* spp. basidiomycetes. Both patients recovered after surgical excision without antifungal therapy. We confirmed the cause of infection using broad-range fungal PCR from formalin-fixed tissue, highlighting the value of molecular diagnostics for detecting rare environmental fungi.

Although systemic fungal infections are most often associated with immunocompromised patients, several well-described fungal diseases, such as chromoblastomycosis, mycetoma, and sporotrichosis, cause localized skin and subcutaneous infections in immunocompetent persons. The range of environmental fungi known to cause localized infections in immunocompetent persons is expanding (*1*). Such infections often follow a prolonged, indolent course and remain confined to specific organs, such as the skin and subcutaneous tissues. Subcutaneous fungal infections involve deeper layers of the skin and underlying tissues and usually result from infection by low-virulence organisms (*2*). Acquisition of fungi involved in localized infections can occur via environmental exposure, inhalation followed by localized disease, or traumatic inoculation (*1*–*3*). Traumatic inoculation is the most common portal of entry in cutaneous and subcutaneous fungal infections, frequently involving exposure to contaminated vegetation, wood, or soil.

Among the diverse fungi that cause opportunistic or localized disease, many members of the phylum Basidiomycota (basidiomycetes), including yeasts such as *Cryptococcus* and *Malassezia* as well as filamentous fungi, are environmental organisms that are rarely implicated in human disease. Filamentous basidiomycetes present a particular diagnostic challenge to clinical laboratories because they often fail to sporulate in culture; they might be mistakenly classified within the broad category of hyaline molds because they are often indistinguishable by conventional morphologic methods (*4*,*5*). Since the early 2000s, molecular techniques have increasingly been used to improve recognition and classification of such organisms (*6*); specific filamentous basidiomycetes have been implicated in hypersensitivity syndromes, chronic cough, allergic bronchopulmonary disease, sinusitis, and, rarely, invasive infections (*5*,*7*,*8*). However, the pathogenic potential for many genera within Basidiomycota remains unknown.

Fomitiporella is a genus of filamentous basidiomycetes comprising wood-decaying fungi (*9*) with no well-established role in human disease. Here, we report 2 cases of localized *Fomitiporella* infection in immunocompetent patients in the United States, both diagnosed using broad-range fungal PCR.

The Study

Case 1 was in a 46-year-old man in North Dakota, USA, who immigrated from Liberia in 2012. When he sought care in 2025, he had a 2-year history of localized pain, discomfort, and restricted movement over his right olecranon bursa. He reported no injury to the area, fever, night sweats, weight loss, or respiratory symptoms. His medical history was unremarkable, and he was taking no prescription medications. Magnetic resonance imaging demonstrated olecranon bursitis. After orthopedic evaluation, surgical excision of the bursa was conducted. Postoperative recovery was uncomplicated; sensation, motor strength, and range of motion were fully preserved.

Author affiliations: University of Washington School of Medicine, Seattle, Washington, USA (G.S. Tansarli, S.J. Salipante, B.T. Cookson); Sanford Laboratory Amber Valley, Fargo, North Dakota, USA (B. Wu)

DOI: https://doi.org/10.3201/eid3209.260263

Histopathologic examination of the removed tissue revealed multiple large expansile granulomas bordered by epithelioid histiocytes. Gram and acid-fast stains were negative; alcian blue/periodic acid–Schiff staining showed focal dermal mucin and abundant fungal hyphae, and Grocott methenamine-silver stain highlighted numerous hyphae within granulomatous areas (Figure 1). Culture was not ordered. A formalin-fixed, paraffin-embedded (FFPE) tissue block was submitted to the University of Washington (UW) Molecular Microbiology Laboratory (Seattle, WA, USA) for molecular diagnosis.

Broad-range fungal PCR (*10*) targeting the 28S rRNA gene yielded a 610-bp sequence (GenBank accession no. PX488794) with 98.2% identity to *Fomitiporella austroasiana* (accession no. MG657323) and 98.03% identity to 2 *F. austroasiana* type strain sequences (accession nos. MG657320 and NG_060440). We corroborated the result by comparing a 316-bp internal transcribed spacer (ITS1) sequence (accession no. PX596867) to the same strains, which showed 98.2% identity to *F. austroasiana* (accession no. MG657323) and 90.77% identity to 2 type strain sequences (GenBank accession nos. MG657328 and NR_158435), establishing a molecular diagnosis of *Fomitiporella* species related to *F. austroasiana*. The patient received no antifungal therapy and remained well without recurrence.

Case 2 was in a 43-year-old man in Washington who immigrated from Mexico in 2021. He sought care in 2025 for a painful, slowly enlarging nodule over his left olecranon bursa that had persisted for >5 years. He had no systemic symptoms or history of immunodeficiency. Surgical excision of the bursa was performed, and a specimen was submitted for histopathology. Immunohistochemical staining showed no infiltrative cytokeratin AE1/AE3 or CD34-positive cells. Although acid-fast staining results were negative, GMS stain revealed scattered fungal hyphae along the periphery of palisading granulomas (Figure 2). Histopathologic features were consistent with subcutaneous fungal infection. An FFPE tissue block was sent to the UW Molecular Microbiology Laboratory for broad-range fungal PCR.

A 608-bp 28S rRNA gene sequence from the specimen (GenBank accession no. PX488793) displayed 98.8% identity to *F. micropora* (accession no. MG806099). Results of 327-bp ITS sequencing of the reference strain (accession no. PX596866) provided orthologous support, showing 91.25% identity to *F. micropora* (accession no. KX181296). We established the molecular diagnosis of *Fomitiporella* species related to *F. micropora* on the basis of those results. The patient received no antifungal therapy and remained well without recurrence.

The 2 cases presented here implicate *Fomitiporella* spp. as human pathogens. In both cases, the DNA sequences identified exhibited sufficient sequence diversity from previously classified *Fomitiporella* spp. that they likely represent previously undescribed species in the genus. Case 1 involved a *F. austroasiana*–like species; case 2 involved a *F. micropora* lineage. Human infections attributed to *Fomitiporella* spp. are rarely reported in the literature; an infection involving a *F. micropora* lineage was previously identified by the UW Molecular Microbiology Laboratory in an immunocompromised patient in New York in 2025 (*11*). The cases we report demonstrate that *Fomitiporella* can cause disease in otherwise healthy hosts.

Clinicians initially considered chronic aseptic olecranon bursitis in both cases; histopathologic examination unexpectedly revealed fungal hyphae, prompting consultation with the infectious diseases service. Each of the 3 reported *Fomitiporella* infections have manifested as long-standing, localized cutaneous or subcutaneous lesions: 1 on the lower extremity (*11*) and 2, the cases we describe, involving the olecranon. That pattern suggests superficial soft tissue as a favored niche, possibly after environmental inoculation via unnoticed trauma or occupational exposure; for 1 patient, documentation indicated long-term employment in equipment assembly. In

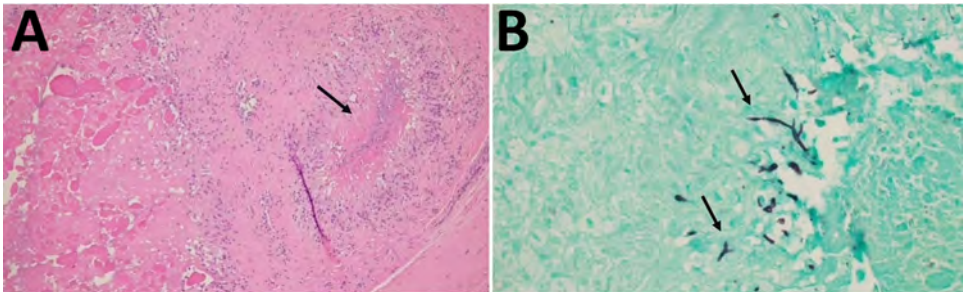

Figure 1. Images of stained tissue specimen from olecranon bursa of case-patient 1 in study of chronic elbow nodules caused by *Fomitiporella* fungus in immunocompetent patients, United States. A) Hematoxylin and eosin staining shows multiple large expansile back-to-back necrotizing granulomas surrounded by epithelioid histiocytes (arrow). Original magnification ×100. B) Grocott methenamine-silver staining shows many fungal hyphae visible throughout the granulomas (arrows). Original magnification ×400.

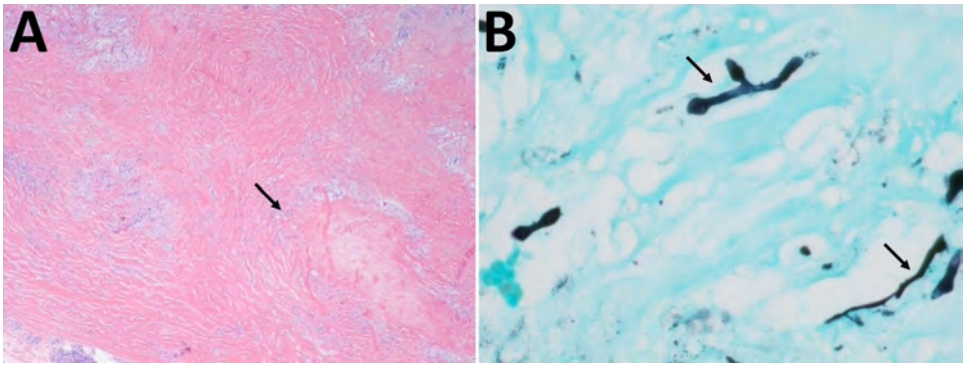

Figure 2. Images of stained tissue specimen from olecranon bursa of case-patient 2 in study of chronic elbow nodules caused by *Fomitiporella* fungus in immunocompetent patients, United States. A) Hematoxylin and eosin staining shows sclerotic granuloma (arrow). Original magnification ×20. B) Grocott methenamine-silver staining shows many fungal hyphae visible throughout the granulomas (arrows). Original magnification ×400.

other implantation mycoses, patients often do not recall a specific traumatic event. Of note, all 3 reported infections have occurred in persons who immigrated from tropical or subtropical regions (Liberia, Mexico, and Trinidad), where wood-decaying *Fomitiporella* spp. are endemic (*12*), suggesting that patients acquired the infection before immigration. However, the apparent geographic distribution might partly reflect where environmental sampling for those fungi has been conducted.

Both of the case-patients we report were treated with surgical excision and no antifungal therapy. Although long-term follow-up data were not available, the clinical course in those cases and the previously reported case (*11*) suggested that surgical excision might be sufficient for localized *Fomitiporella* infection and with antifungal therapies reserved for incomplete excision, immunosuppressed patients, or evidence of dissemination. In cases where antifungal treatment is warranted, the limited evidence suggests that infections caused by filamentous basidiomycetes usually respond well to azoles other than fluconazole (*7*,*13*).

Conclusions

Filamentous basidiomycetes are rarely implicated in human infection and are often misidentified or overlooked. Awareness of *Fomitiporella* is important for pathologists who encounter fungal hyphae in granulomatous lesions without a definitive culture result. Molecular identification should be considered when cultures are sterile or yield nonsporulating hyaline molds. Reporting additional *Fomitiporella* cases will improve understanding of epidemiology, disease spectrum, and treatment strategies.

Fomitiporella spp. infection, although exceedingly rare, can cause chronic localized lesions in both immunocompetent and immunocompromised hosts. Complete surgical excision offers excellent outcomes without antifungal therapy in most patients. Broad-range fungal PCR can identify molds and yeasts and some nonfungal eukaryotic pathogens such as oomycetes, amoebae, and parasites (*14*,*15*); therefore, it is a valuable tool for diagnosing unusual or unexpected infections, even in cases in which material is not available for microbial culture. Clinical and laboratory awareness of the pathogenic potential of *Fomitiporella* spp. will contribute to increased recognition and prevent misdiagnosis of such potentially emerging pathogens.

Acknowledgments

We thank Novae Simper for providing clinical information on one of the included cases.

About the Author

Dr. Tansarli is an acting instructor in the department of laboratory medicine and pathology at the University of Washington School of Medicine and is board-certified in clinical pathology and medical microbiology. Her research interests include molecular epidemiology of diarrheagenic *Escherichia coli*, antimicrobial resistance, and infectious disease diagnostics.

References

1. Zheng C, Li W, Gao Z, Yu Q, Yang L. Deep cutaneous fungal infection in an immunocompetent individual caused by a biological pesticide: a rare case report. BMC Infect Dis. 2025;25:341. https://doi.org/10.1186/s12879-025-10707-x
2. Ditsios K, Katsimentzas T, Pitsilos C, Koukourikos I, Christidis P, Ditsios T, et al. Deep fungal infections of the upper extremity—a review. Orthop Rev (Pavia). 2024;16:94570. https://doi.org/10.52965/001c.94570
3. Ye F, Xie JX, Zeng QS, Chen GQ, Zhong SQ, Zhong NS. Retrospective analysis of 76 immunocompetent patients with primary pulmonary cryptococcosis. Lung. 2012;190:339–46. https://doi.org/10.1007/s00408-011-9362-8
4. Brandt ME. Filamentous basidiomycetes in the clinical laboratory. Curr Fungal Infect Rep. 2013;7:219–23. https://doi.org/10.1007/s12281-013-0148-8
5. Lacaz CS, Heins-Vaccari EM, Melo NT, Hernandez-Arriagada GL. Basidiomycosis: a review of the literature. Rev Inst Med Trop São Paulo. 1996;38:379–90. https://doi.org/10.1590/S0036-46651996000500011
6. Ji XH, Vlasák J, Tian XM, Dai YC. Three new species of *Fomitiporella* (Hymenochaetales, Basidiomycota) based on

the evidence from morphology and DNA sequence data. MycoKeys. 2018;30:73–89. https://doi.org/10.3897/mycokeys.30.23109
7. Chowdhary A, Randhawa HS, Gaur SN, Agarwal K, Kathuria S, Roy P, et al. Schizophyllum commune as an emerging fungal pathogen: a review and report of two cases. Mycoses. 2013;56:1–10. https://doi.org/10.1111/j.1439-0507.2012.02190.x
8. Ogawa H, Fujimura M, Takeuchi Y, Makimura K, Satoh K. Sensitization to *Bjerkandera adusta* enhances severity of cough symptom in patients with fungus-associated chronic cough (FACC). Med Mycol J. 2011;52:205–12. https://doi.org/10.3314/mmj.52.205
9. Zhou Q, Jiang Q, Yang X, Yang J, Zhao C, Zhao J. Phylogenetic and taxonomic analyses of five new wood-inhabiting fungi of *Botryobasidium*, *Coltricia* and *Coltriciella* (Basidiomycota) from China. J Fungi (Basel). 2024;10:205. https://doi.org/10.3390/jof10030205
10. Harrington AT, Creutzfeldt CJ, Sengupta DJ, Hoogestraat DR, Zunt JR, Cookson BT. Diagnosis of neurocysticercosis by detection of *Taenia solium* DNA using a global DNA screening platform. Clin Infect Dis. 2009;48:86–90. https://doi.org/10.1086/594128
11. Jarrin Jara MD, Villanueva-Siles E, Weithorn D, Puius YA, Thwe PM. The first described case of *Fomitiporella micropora* infection in humans: a heart transplant recipient diagnosed by fungal PCR. Med Mycol Case Rep. 2025;49:100728. https://doi.org/10.1016/j.mmcr.2025.100728
12. Salvador-Montoya CA, Popoff OF, Góes-Neto A, Drechsler-Santos ER. Global phylogenetic and morphological reassessment of *Fomitiporella* s.l. (Hymenochaetales, Basidiomycota): taxonomic delimitation of *Fomitiporella* s.s. and segregation of *Rajchenbergia*, gen. nov. Plant Syst Evol. 2020;306:34. https://doi.org/10.1007/s00606-020-01648-w
13. González GM, Sutton DA, Thompson E, Tijerina R, Rinaldi MG. In vitro activities of approved and investigational antifungal agents against 44 clinical isolates of basidiomycetous fungi. Antimicrob Agents Chemother. 2001;45:633–5. https://doi.org/10.1128/AAC.45.2.633-635.2001
14. Ahuja S, Lieberman JA. Non-fungal pathogens detected by broad-range fungal polymerase chain reaction. J Clin Microbiol. 2025;63:e0008725. https://doi.org/10.1128/jcm.00087-25
15. Konnick EQ, Chow SK, Reder NP, Sengupta DJ, Hoogestraat DR, Pottinger PS, et al. Incidental identification of *Strongyloides stercoralis* infection by broad-range 28S rDNA gene sequencing in a patient with a hematolymphoid malignancy. Diagn Microbiol Infect Dis. 2016;86:362–4. https://doi.org/10.1016/j.diagmicrobio.2016.08.029

Address for correspondence: Giannoula S. Tansarli, Department of Laboratory Medicine and Pathology, Box 357110, 1959 NE Pacific St, Seattle, WA 98195–7110, USA; email: tansarli@uw.edu

etymologia revisited

Tularemia
[t-lə-rē-mē-ə]

An infectious, plaguelike, zoonotic disease caused by the bacillus *Francisella tularensis*. The agent was named after Tulare County, California, where the agent was first isolated in 1910, and Edward Francis, an Officer of the US Public Health Service, who investigated the disease. Dr. Francis first contracted deer fly fever from a patient he visited in Utah in the early 1900s. He kept a careful record of his 3-month illness and later discovered that a single attack confers permanent immunity. He was exposed to the bacterium for 16 years and even deliberately reinfected himself 4 times.

Tularemia occurs throughout North America, many parts of Europe, the former Soviet Union, the Peoples Republic of China, and Japan, primarily in rabbits, rodents, and humans. The disease is transmitted by the bites of deerflies, fleas, and ticks; by contact with contaminated animals; and by ingestion of contaminated food or water.

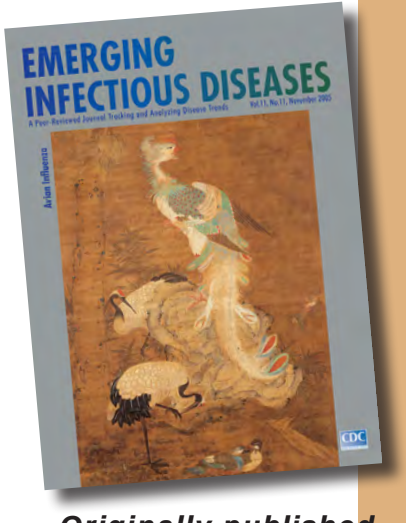

Originally published in November 2007

Reference

Dorland's illustrated medical dictionary, 31st edition. Philadelphia: Saunders; 2007; Benenson AS, editor. Control of communicable diseases manual. Washington: American Public Health Association; 1995; https://www.whonamedit.com

https://wwwnc.cdc.gov/eid/article/13/11/e1-1311_article

Pulmonary Coccidioidomycosis Linked to Shipping Containers, Taiwan, 2025

Allen C. Huang,[1] Tsung-Han Lee,[1] Min-Nan Hung, Mei-Hui Liao, Hsueh-Mei Chiang, Min-Hua Hsieh, Tein-Yao Chang, Shu-Min Lin

Author affiliations: Chang Gung University Graduate Institute of Clinical Medical Sciences, Taoyuan, Taiwan (A.C. Huang); St. Paul's Hospital, Taoyuan (A.C. Huang, S.-M. Lin); Linkou Chang Gung Memorial Hospital, Taoyuan (A.C. Huang, S.-M. Lin); Taiwan Centers for Disease Control, Taipei, Taiwan (T.-H. Lee, M.-N. Hung, M.-H. Liao, H.-M. Chiang, M.-H. Hsieh); National Defense Medical University Institute of Preventive Medicine, Taipei (T.-Y. Chang); National Defense Medical University Graduate Institute of Biodefense, Taipei (T.-Y. Chang); Chang Gung University School of Medicine, Taoyuan (S.-M. Lin)

DOI: https://doi.org/10.3201/eid3209.260714

A shipping container yard worker from Taiwan contracted laboratory-confirmed pulmonary coccidioidomycosis. He reported no travel history to endemic regions. Occupational exposure to aerosolized dust or soil residues on maritime shipping containers from endemic areas is likely. Our findings highlight international shipping as a potential pathway for introducing geographically restricted pathogens into nonendemic regions.

Coccidioidomycosis is caused by inhaling fungal spores produced by the dimorphic fungi *Coccidioides immitis* and *C. posadasii*, which inhabit arid soil primarily in the southwestern United States, northern Mexico, and parts of Central and South America (*1*). Outside those endemic areas, most cases are associated with travel or prior residence (*2*). Transmission by contaminated materials or objects from endemic regions is rare (*2*–*4*). However, increasing cargo movement from endemic regions raises the possibility that contaminated dust or soil residues might be transported and infect persons living in nonendemic regions.

In Taiwan, previously reported cases of coccidioidomycosis have been identified exclusively among persons with exposure to endemic areas (*5*). We report a case of locally acquired pulmonary coccidioidomycosis in a patient who had never traveled to the Americas. The patient provided written informed consent for the publication of his clinical history, occupational data, and relevant images.

The patient, a man in his 50s, was a smoker with no known underlying conditions. In August 2025, he sought care for a 2-week history of cough, fatigue, and intermittent dizziness. Chest radiography revealed a mass in the right upper lobe (RUL) with right hilar lymphadenopathy. Chest computed tomography (CT) revealed an RUL 3.0 × 2.0 cm solid mass touching the pleura, as well as enlarged right hilar, mediastinal lymph nodes, and multiple pulmonary nodules bilaterally (Figure 1). Because of the patient's age and smoking history, clinicians suspected a primary RUL lung malignancy with mediastinal and intrapulmonary metastases. The patient's serum tumor markers, including cancer antigen 19–9, carcinoembryonic antigen, squamous cell carcinoma antigen, and cancer antigen 125, were within reference ranges.

A flexible bronchoscopy retrieved tissue for histopathologic and microbiological evaluation. Endobronchial ultrasound did not show the pulmonary mass, precluding transbronchial biopsy. Pathologic examination of the fine-needle aspirate from the right hilar lymph node found granulomatous inflammation but no evidence of malignancy. Sputum and bronchoalveolar lavage specimens were negative for *Mycobacterium tuberculosis* by using PCR and culture. Fungal culture of bronchoalveolar lavage fluid yielded a colony morphologically consistent with *Coccidioides* spp. Serologic lateral flow assay was positive for *Coccidioides* antibodies, and enzyme immunoassay confirmed reactivity for both IgM and IgG. Because of potential serologic cross-reactivity among endemic dimorphic fungi in Taiwan, molecular testing by internal transcribed spacer sequencing and the CocciDx (Translational Genomics Research Institute, https://www.tgen.org) real-time PCR was performed, confirming *C. immitis* (*6*). The patient was treated with fluconazole and had gradual clinical and radiologic improvement.

The patient reported no travel to coccidioidomycosis-endemic regions nor indirect exposure in the month before illness onset, including contact with items brought by visitors from endemic areas or personally sourced from these regions. The patient had worked for years at a maritime container yard where shipping containers were stored, repaired, and cleaned after cargo removal. His duties included hammering deformed container panels and cleaning container surfaces by using high-pressure water jets, both performed without respiratory protection. Those activities could disturb residual soil or dust on container surfaces, aerosolizing *Coccidioides* arthroconidia spores and making them easier to inhale (Figure 2).

[1]These first authors contributed equally to this article.

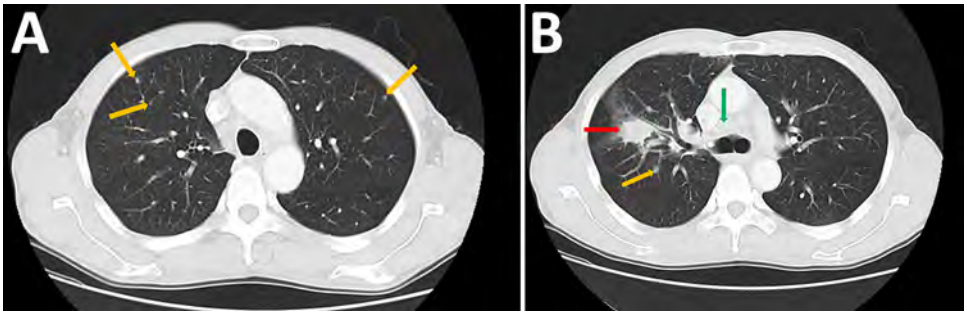

Figure 1. Chest computed tomography findings in a maritime container yard worker with pulmonary coccidioidomycosis, Taiwan, 2025. A) Axial lung-window images reveal multiple bilateral pulmonary nodules (yellow arrows). B) A 3.0 × 2.0 cm solid mass is visible in the right upper lobe (red arrow), and right hilar lymph nodes are enlarged (green arrow).

Although the specific containers involved could not be identified, the containers the patient might have worked in were associated with ports in California and Washington, USA. Because *C. immitis* is native to parts of California, Baja California, and eastern Washington (*1*), we considered the possibility of exposure to contaminated soil or dust transported in shipping containers. Our conclusion that this pathway was possible is supported by a previous report suggesting *Coccidioides* arthroconidia could be transported with shipped goods and aerosolized during container sweeping (*4*). It is also biologically plausible because of the documented environmental persistence and fomite stability of *Coccidioides* arthroconidia (*7*,*8*). Together, the absence of travel history and routine aerosol-generating container work support occupational exposure as the most likely route of acquisition.

The first limitation of our investigation is the omission of container surface environmental sampling, which precluded direct detection of aerosolized arthroconidia and prevented definitive source attribution. Second, the lack of serologic assessment among exposed co-workers limited our ability to evaluate potential shared occupational exposure. Finally, without prior serologic or clinical data, we could not distinguish recent infection from reactivation, although we considered reactivation less likely because of the absence of recognized risk factors (*9*,*10*).

With continued global commerce integration, traditional geographic boundaries of infectious diseases might be less distinct. In nonendemic regions, early diagnosis requires clinicians to consider coccidioidomycosis in patients with compatible clinical and radiologic findings and to ask about occupational exposure to imported dust- or soil-contaminated materials, including maritime containers, especially when travel history to endemic areas can be ruled out. For occupational prevention, control measures should follow the hierarchy of controls and include standardized protocols to minimize aerosolization during container maintenance, worker education and training, periodic health monitoring, and the use of fit-tested respiratory protection during high-risk activities. Surveillance in international shipping settings also might help identify exposure risks and inform strategies to prevent this emerging, potentially underrecognized occupational hazard.

Figure 2. Occupational activities at a maritime container yard in Taiwan, 2025, that might generate airborne *Coccidioides immitis* from soil or dust. A) Red arrows indicate hammers used for hammering of deformed container panels during metal surface repair. B) Green arrow indicates backsplash from high-pressure water jet cleaning of interior container surfaces. Images do not depict the patient reported in this case or any specific containers he worked on.

Acknowledgments

We thank the Taiwan Centers for Disease Control for their support of the serologic testing and species identification.

About the Author

Dr. Huang is a specialist in pulmonary and critical care medicine and director for thoracic medicine in St. Paul's Hospital, Taoyuan, Taiwan. His primary research interests are lung cancer, critical care, and interventional bronchoscopy.

References

1. Kollath DR, Miller KJ, Barker BM. The mysterious desert dwellers: *Coccidioides immitis* and *Coccidioides posadasii*, causative fungal agents of coccidioidomycosis. Virulence. 2019;10:222–33. https://doi.org/10.1080/21505594.2019.1589363
2. Desai SA, Minai OA, Gordon SM, O'Neil B, Wiedemann HP, Arroliga AC. Coccidioidomycosis in non-endemic areas: a case series. Respir Med. 2001;95:305–9. https://doi.org/10.1053/rmed.2000.1039
3. Stagliano D, Epstein J, Hickey P. Fomite-transmitted coccidioidomycosis in an immunocompromised child. Pediatr Infect Dis J. 2007;26:454–6. https://doi.org/10.1097/01.inf.0000259231.95285.bc
4. Tang THC, Tsang OTY. Images in clinical medicine. Fungal infection from sweeping in the wrong place. N Engl J Med. 2011;364:e3. https://doi.org/10.1056/NEJMicm1007348
5. Li Y-C, Lin M-W, Wu U-I, Lu C-W, Chen P-H, Tsai T-M, et al. Coccidioidomycosis: an emerging disease in Taiwan. J Formos Med Assoc. 2026;S0929-6646(26)00005-7.
6. Litvintseva AP, Marsden-Haug N, Hurst S, Hill H, Gade L, Driebe EM, et al. Valley fever: finding new places for an old disease: *Coccidioides immitis* found in Washington State soil associated with recent human infection. Clin Infect Dis. 2015;60:e1–3. https://doi.org/10.1093/cid/ciu681
7. Chow NA, Kangiser D, Gade L, McCotter OZ, Hurst S, Salamone A, et al. Factors influencing distribution of *Coccidioides immitis* in soil, Washington state, 2016. MSphere. 2021;6:e0059821. https://doi.org/10.1128/mSphere.00598-21
8. Stevens DA, Clemons KV, Levine HB, Pappagianis D, Baron EJ, Hamilton JR, et al. Expert opinion: what to do when there is *Coccidioides* exposure in a laboratory. Clin Infect Dis. 2009;49:919–23. https://doi.org/10.1086/605441
9. Bhardwaj S, Tewari A, Tewari R, Kogan S. The fungus among us: latency, reactivation, and the expanding clinical spectrum of coccidioidomycosis. Cureus. 2026;18:e107243. https://doi.org/10.7759/cureus.107243
10. Crum NF. Coccidioidomycosis: a contemporary review. Infect Dis Ther. 2022;11:713–42. https://doi.org/10.1007/s40121-022-00606-y

Address for correspondence: Min-Nan Hung, Taiwan Centers for Disease Control, No. 6, Linsen S Rd, Jhongjheng District, Taipei 100008, Taiwan; email: mnhung@cdc.gov.tw

Southern Tick–Associated Rash Illness in Pediatric Patient, New York, USA, 2025

Andrew S. Handel, Sophia Ahmed, Ilia Rochlin, Hwan Keun Kim

Author affiliations: Stony Brook University Renaissance School of Medicine, Stony Brook, New York, USA (A.S. Handel); Stony Brook University, Stony Brook (S. Ahmed, I. Rochlin, H.K. Kim)

DOI: https://doi.org/10.3201/eid3209.260871

Southern tick–associated rash illness (STARI) is a tickborne disease of unknown etiology characterized by an erythema migrans–like skin lesion. We report a STARI case in New York in a child after an *Amblyomma americanum* tick bite; we detected *Borrelia lonestari*, a disputed cause of STARI, in the tick.

Southern tick–associated rash illness (STARI) is a tickborne disease of unknown etiology. Its hallmark finding is an erythema migrans (EM)–like skin lesion after a lone star tick (*Amblyomma americanum*) bite. Although it is considered self-limited, STARI is difficult to diagnose and manage because of characteristics similar to Lyme disease. STARI is not known to cause any sequelae after rash resolution; the role of antimicrobial drugs in proven cases is therefore undetermined (*1*).

Previous descriptions of STARI focused on the southern United States. Because lone star tick populations have increased in the mid-Atlantic and northeastern United States, regions highly endemic to Lyme disease, differentiating STARI from Lyme disease has become a challenge (*2*). We describe the case of a child evaluated in Long Island, New York, USA for an EM-like skin lesion.

An 8-year-old girl with a history of asthma and allergic rhinitis living in eastern Long Island was brought in June 2025 for evaluation of a recent EM-like lesion. Approximately 2 weeks before her visit, she had a 5-cm annular lesion with peripheral erythema and a central nodule on the upper back (Figure 1). She also experienced low-grade fever, posterior cervical lymphadenopathy, and myalgia. A tick had been removed from the lesion site and stored in a sealed bag 12 days before the rash began. The patient did not receive doxycycline postexposure prophylaxis. Because early localized Lyme disease was suspected, her pediatrician prescribed a 2-week course of amoxicillin. The rash and associated symptoms resolved within 1 week. She was asymptomatic at the time of the follow-up consultation.

Although care providers initially suspected Lyme disease, the biting tick was identified as an adult male lone star tick (Figure 2), which does not transmit *Borrelia burgdorferi*, which mean the patient's signs and symptoms were consistent with a diagnosis of STARI. We extracted DNA from the tick, performed nested PCR targeting the *Borrelia* flagellin gene (*3*), and confirmed the presence of a *B. lonestari*–specific sequence (GenBank accession no. PZ457021).

A. americanum, an aggressive tick species, has expanded across the United States (*2*,*3*). In the US Northeast, diagnosing STARI is challenging because of a high rate of *B. burgdorferi*–infected *Ixodes scapularis* ticks (*2*). As *A. americanum* tick populations have increased across Long Island, the proportion of EM lesions caused by Lyme disease has decreased, likely because of higher STARI incidence (*2*). National STARI incidence remains unknown because the condition is not reportable and is often presumed to be the result of *B. burgdorferi* infection.

STARI was described in 1995 in 45 patients with EM-like lesions in Missouri, USA, in a region without Lyme disease (*4*). Study participants had negative serology results for Lyme disease and negative *B. burgdorferi* culture results from skin lesion biopsies, which raised suspicion of an alternative diagnosis (*4*). *B. lonestari* was identified as a potential cause of STARI after it was identified in both skin biopsy and the associated tick in a patient bitten by a female *A. americanum* tick in North Carolina (*5*). A subsequent Missouri study assessed *B. burgdorferi* and *B. lonestari* in skin biopsies from patients with EM-like lesions (*6*); results from 16S eubacterial rDNA PCR, *glpQ* PCR for *B. lonestari* DNA detection, and *B. burgdorferi* culture were negative (*6*). In a later study, 16s rRNA metagenomic sequencing of blood samples collected during 2018–2019 from STARI patients did not identify any tickborne bacteria (*7*). Consequently, it has been suggested that STARI is caused not by an infection but rather a hypersensitivity reaction (*8*), possibly related to alpha-gal syndrome, which is also caused by the bite of a lone star tick (*8*). *B. lonestari* prevalence on Long Island is uncommon (detected in 1% of *A. americanum* ticks) (*9*), which made identification in our case particularly interesting. Because our patient did not undergo testing for *B. lonestari* infection, we cannot determine if that bacterium caused her symptoms.

STARI diagnosis is difficult because it shares features with Lyme disease; however, subtle clinical differences exist. Compared with EM patients from New York, a highly Lyme disease–endemic state, patients from Missouri, who presumably had STARI, experienced a shorter duration from tick bite to skin lesion onset; had fewer associated symptoms; were less likely to experience multiple lesions; had

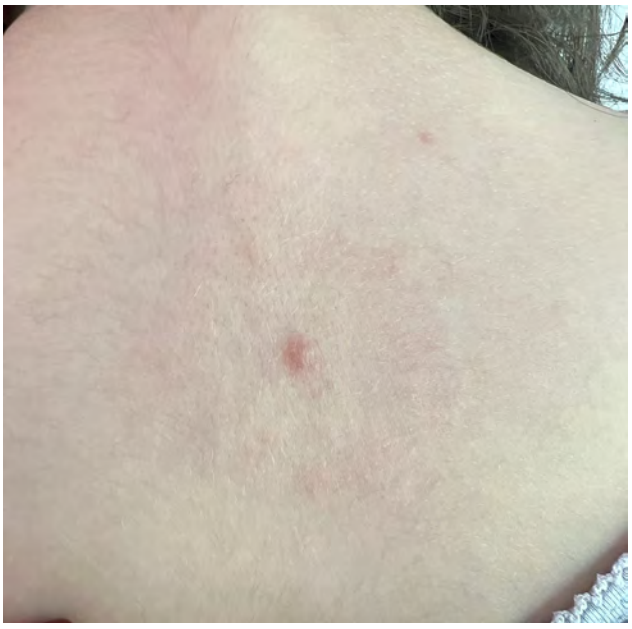

Figure 1. Erythema migrans–like skin lesion at the site of a tick bite on patient's upper back in study of southern tick–associated rash illness in pediatric patient, New York, USA, 2025.

Figure 2. Adult male lone star tick (*Amblyomma americanum*) from study of southern tick–associated rash illness in pediatric patient, New York, USA, 2025. The tick was removed from the patient 12 days before rash onset.

lesions that were smaller, more circular, and had more central clearing; and recovered more quickly (*10*). Although withholding antimicrobial treatment might be reasonable in confirmed cases of STARI, doing so in *B. burgdorferi*–endemic regions poses the risk of undertreating Lyme disease. As our case demonstrated, STARI can be diagnosed only if a lone star tick is identified, underscoring the importance of preserving the biting tick.

The etiology of STARI remains unknown; whether *B. lonestari* is the causative agent is not clear (*5*,*6*). Although detection of *B. lonestari* does not establish it as the cause, our findings raise questions about *B. lonestari* pathogenicity and underscore the need for improved diagnostics for patients with EM-like lesions.

Acknowledgments

We thank Jorge Benach for his critical review of this manuscript.

The patient's parent or guardian provided written permission to publish this case report.

We are grateful for ongoing research support from the Long Island Network for Clinical and Translational Science fellowship (A.S.H.), National Institute of Allergy and Infectious Diseases of the National Institutes of Health (grant nos. AI152208 and AI179732 to H.K.K.), and Stony Brook University (A.S.H., H.K.K.). The funders had no role in study design, data collection, interpretation, or the decision to submit the work for publication. The authors declare no competing interests.

A.S.H. has received honoraria from GSK for serving in an expert panel on invasive meningococcal disease.

About the Author

Dr. Handel is a clinical associate professor of pediatrics in the Division of Infectious Diseases at the Renaissance School of Medicine at Stony Brook University in New York, USA. His research focuses on recognized and emerging tickborne infections and congenital cytomegalovirus.

References

1. Lantos PM, Rumbaugh J, Bockenstedt LK, Falck-Ytter YT, Aguero-Rosenfeld ME, Auwaerter PG, et al. Clinical practice guidelines by the Infectious Diseases Society of America (IDSA), American Academy of Neurology (AAN), and American College of Rheumatology (ACR): 2020 guidelines for the prevention, diagnosis and treatment of Lyme disease. Clin Infect Dis. 2021;72:e1–8. https://doi.org/10.1093/cid/ciaa1215
2. Schutzer SE, Wellins A-M, Dattwyler RJ. *Borrelia burgdorferi* infection and erythema migrans. N Engl J Med. 2026;394:302–3. https://doi.org/10.1056/NEJMc2508805
3. Stromdahl EY, Williamson PC, Kollars TM Jr, Evans SR, Barry RK, Vince MA, et al. Evidence of *Borrelia lonestari* DNA in *Amblyomma americanum* (Acari: Ixodidae) removed from humans. J Clin Microbiol. 2003;41:5557–62. https://doi.org/10.1128/JCM.41.12.5557-5562.2003
4. Campbell GL, Paul WS, Schriefer ME, Craven RB, Robbins KE, Dennis DT. Epidemiologic and diagnostic studies of patients with suspected early Lyme disease, Missouri, 1990–1993. J Infect Dis. 1995;172:470–80. https://doi.org/10.1093/infdis/172.2.470
5. James AM, Liveris D, Wormser GP, Schwartz I, Montecalvo MA, Johnson BJB. *Borrelia lonestari* infection after a bite by an *Amblyomma americanum* tick. J Infect Dis. 2001;183:1810–4. https://doi.org/10.1086/320721
6. Wormser GP, Masters E, Liveris D, Nowakowski J, Nadelman RB, Holmgren D, et al. Microbiologic evaluation of patients from Missouri with erythema migrans. Clin Infect Dis. 2005;40:423–8. https://doi.org/10.1086/427289
7. Lindell K, Sheldon S, Kingry L, Mead PS, Molins C, Hinckley AF. Epidemiologic and clinical characteristics and outcomes of patients diagnosed with southern tick–associated rash illness (STARI), 2018–2019. Diagn Microbiol Infect Dis. 2025;113:116928. https://doi.org/10.1016/j.diagmicrobio.2025.116928
8. Wormser GP, Shishido A. Could alpha-gal syndrome be the cause of southern tick-associated rash illness (STARI)? Wien Klin Wochenschr. 2025;137:800–1. https://doi.org/10.1007/s00508-025-02584-w
9. Sanchez-Vicente S, Tagliafierro T, Coleman JL, Benach JL, Tokarz R. Polymicrobial nature of tick-borne diseases. MBio. 2019;10:e02055-19. https://doi.org/10.1128/mBio.02055-19
10. Wormser GP, Masters E, Nowakowski J, McKenna D, Holmgren D, Ma K, et al. Prospective clinical evaluation of patients from Missouri and New York with erythema migrans-like skin lesions. Clin Infect Dis. 2005;41:958–65. https://doi.org/10.1086/432935

Address for correspondence: Andrew S. Handel, Stony Brook University Renaissance School of Medicine, 101 Nicolls Rd, HSC-T11, Stony Brook, NY 11794, USA; email: andrew.handel@stonybrookmedicine.edu

Pediatric Tuberculosis Care Outcomes in a Tertiary Care Center, France, 2014–2024

Diane Franco, Luc Panetta, Florence Ader, Antoine Ouziel, Yves Gillet, Côme Horvat

Author affiliations: Hospices Civils de Lyon, Lyon, France (D. Franco, L. Panetta, F. Ader, A. Ouziel, Y. Gillet, C. Horvat); Centre Hospitalier Universitaire Sainte-Justine, Montreal, Quebec, Canada (L. Panetta).

DOI: https://doi.org/10.3201/eid3209.260600

We evaluated pediatric tuberculosis treatment outcomes in a tertiary care center in France during 2014–2024 by using updated World Health Organization definitions. Among 123 children, 60.9% were successfully treated. Unfavorable outcomes reflected suboptimal adherence, dosing errors, and incomplete follow-up, highlighting the need for implementation and evaluation of optimized care processes.

Pediatric tuberculosis (TB) remains a major global health concern; an estimated 1.2 million new cases and 174,300 deaths were reported in 2024 (*1*). Treatment regimens are well-standardized and updated by the World Health Organization (WHO) (*2*). However, research and implementation efforts predominantly focus on high-incidence countries. Data from pediatric cohorts in high-income, low-incidence settings remain scarce, reporting overall success rates around 90% (*3*,*4*), but provide very limited insights into the quality of care, treatment pathways, and potential barriers. We describe TB treatment outcomes in a tertiary pediatric center in France over a 10-year period by using the updated WHO treatment–outcome definitions as a standardized framework.

We conducted a retrospective cohort study at a tertiary pediatric hospital in Lyon, France, including all patients <18 years of age treated for TB during January 1, 2014–December 31, 2024. TB diagnosis was consistent with WHO guidelines (*2*). To achieve comprehensive case identification, we cross-matched 4 institutional databases, including microbiology, pharmacy, administrative records, and pediatric infectious disease consultations, and then conducted a systematic manual review of each medical record.

We collected data on demographics, signs and symptoms, treatment, and outcomes by using standardized definitions (*2*,*5*–*7*). We classified treatment outcomes according to WHO definitions as favorable (cured or treatment completed) or unfavorable (treatment failure, lost to follow-up, or death) (Appendix Table, http://wwwnc.cdc.gov/EID/article/32/9/26-0600-App1.pdf) (*8*). To further elucidate the care process, we captured secondary analytic outcomes. Those outcomes included dosing adequacy, assessed according to WHO-recommended weight-based drug dosages and, when available, therapeutic drug monitoring for rifampin or isoniazid; treatment nonadherence (intake <80% or treatment interruption for ≥2 consecutive weeks (*6*); follow-up nonadherence (any missed scheduled visit); microbiological failure; treatment prolongation; modification of the initial regimen (excluding adaptations on the basis of drug susceptibility); and treatment-related adverse events (*7*).

Among 123 children with TB, 13 were not evaluated according to WHO outcome definitions because they were transferred to another facility. Of the 110 evaluable children, 67 (60.9%) had favorable treatment outcomes and 43 (39.1%) had unfavorable treatment outcomes, including 34 with treatment failures, 9 who were lost to follow-up, and 2 with documented microbiological failure (Figure). Treatment failure was related to radiological failure (32.6%, n = 14), clinical failure (16.3%, n = 7), or treatment nonadherence or underdosing (23.3%, n = 10). Underdosing was documented in 28 (25.4%) children, 11 (10%) with subtherapeutic drug concentrations and 17 (15.5%) with subrecommended weight-based dosing. Overdosing was documented in only 1 child. Therapeutic nonadherence was reported in 17 (15.5%) children, and follow-up nonadherence was reported in 67 (60.9%) children. Thirteen (11.8%) children experienced adverse events, including hepatotoxicity (8.2%, n = 9), agranulocytosis (2.7%, n = 3), peripheral neuropathy (0.9%, n = 1), and optic toxicity under ethambutol (0.9%, n =1). Nearly half of the adverse events (46%, n = 6) led to permanent discontinuation of the implicated drug.

Of the 110 evaluable children, the median age was 5 years; 61 (55.5%) were male and 49 (45.5%) female (Table). Malnutrition was documented in 10 (9.1%) children, and 4 (3.6%) children were co-infected with HIV. Isolated thoracic disease was documented in 78 (70.9%) children, including 50 children with severe forms of the disease. Extrapulmonary TB was reported in 32 (29.1%) children. We obtained microbiological confirmation from 58 (52.7%) children and documented index cases in 43 (39.1%) children. Five (4.5%) TB strains were resistant: 3 resistant to isoniazid, 1 resistant to ethambutol, and 1 multidrug-resistant. Most (57.3%, n = 63) children were treated with the standard 6–month regimen;

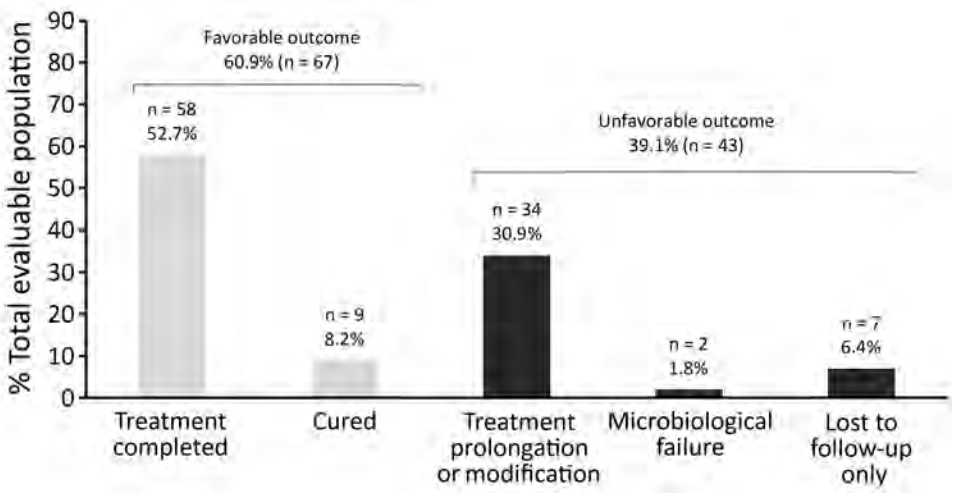

Figure. Distribution of pediatric tuberculosis care outcomes in a tertiary care center, France, 2014–2024. Light gray bars indicate favorable outcomes and black bars unfavorable outcomes, as defined by the World Health Organization. Percentage values reflect the percentage of the total evaluable population (n = 110).

only 1 received the 4–month regimen, and 13 (11.8%) children with severe disease required prolonged treatment for 9–12 months (2).

By using standardized WHO definitions in a high-income, low-incidence setting, we found nearly 40% of children had unfavorable treatment outcomes. Care-process gaps were frequent: 1 in 4 children were underdosed, treatment nonadherence was documented in 1 in 6 children, and ≈66% of children had suboptimal follow-up attendance. Those findings underscore that many unfavorable outcomes reflect elements of care that can be improved rather than intrinsic disease severity or care access.

Our results are in striking contrast with reported success rates ≈90% in similar settings, largely on the basis of heterogeneous or earlier outcome definitions (3,4), highlighting how updated WHO definitions go beyond death or microbiological failure to capture

Table. Population characteristics of pediatric patients with TB, France, 2014–2024*

Characteristics	No. (%) patients		
	Total, n = 110	Favorable outcome, n = 67	Unfavorable outcome, n = 43
Age group, y			
<1	11 (10.0)	7 (10.4)	4 (9.3)
1–5	46 (41.8)	28 (41.8)	18 (41.9)
5–10	20 (18.2)	13 (19.4)	7 (16.3)
10–18	33 (30)	19 (28.4)	14 (32.5)
Sex			
M	61 (55.5)	40 (59.7)	21 (48.8)
F	49 (45.5)	27 (41.3)	22 (51.2)
Underlying conditions			
Malnutrition	10 (9.1)	6 (9.0)	4 (9.3)
HIV co-infection	4 (3.6)	2 (3.0)	2 (4.7)
Extrapulmonary tuberculosis complications			
Isolated thoracic TB	78 (70.9)	52 (77.6)	26 (60.5)
Peripheral lymphadenitis	18 (16.4)	8 (7.3)	10 (9.1)
Central nervous system TB	6 (5.5)	4 (3.6)	2 (1.8)
Osteoarticular TB	6 (5.5)	4 (3.6)	2 (1.8)
IRIS	8 (7.3)	2 (3.0)	6 (14.0)
BCG vaccination	45 (40.9)	36 (53.7)	9 (20.9)
Microbiologic characteristics			
Microbiological confirmation	58 (52.7)	31 (46.3)	27 (62.8)
Identified index case	43 (39.1)	32 (47.8)	11 (25.6)
Drug-resistant strain	5 (4.5)	2 (3.0)	3 (7.0)
Initial treatment characteristics			
Planned treatment duration, mo			
≤6	64 (58.2)	55 (82.1)	9 (20.9)
>6	13 (11.8)	12 (17.9)	1 (2.3)
Initial treatment regimen			
Standard 4-drug regimen: HRZE	62 (56.4)	38 (56.7)	24 (55.8)
Standard 3-drug regimen: HRZ	46 (41.8)	27 (40.3)	19 (44.2)
Other treatment regimen	2 (1.8)	2 (3.0)	0

* BCG, Bacille Calmette-Guérin; HRZ, isoniazid, rifampin, and pyrazinamide; HRZE, isoniazid, rifampin, pyrazinamide, and ethambutol; IRIS, immune reconstitution inflammatory syndrome; TB, tuberculosis

suboptimal treatment processes. Furthermore, the low relevance of the cured category, because of limited microbiological documentation in children (*9*), reinforces the value of treatment completed as a more meaningful indicator in pediatric TB.

Although the retrospective and single-center design of our study limits its generalizability, its decade-long timespan, exhaustive case identification, and rigorous application of standardized WHO definitions strengthen our findings. Similar concerns have been raised in other high-income settings, where organizational models of TB care have influenced treatment outcomes (*10*).

In conclusion, applying updated WHO definitions revealed a high proportion of unfavorable outcomes in a high-income, low-incidence setting. This revelation supports the implementation and evaluation of optimized care processes focused on treatment adherence, accurate weight-based drug dosing, and structured follow-up.

Acknowledgments

We are thankful to Oana Dumitrescu for her support with laboratory database extraction; the Department of Medical Information, particularly Balthazar Ntab, and Philippe Reix for administrative database support and data access agreement; and the hospital pharmacy team, including Elise Galoustian-Estéphani, Pauline Rascle, and Laura Delpech, for their assistance with pharmacy data extraction.

This study was approved by the local ethics committee, complied with data protection regulations in France, and was registered on ClinicalTrials.gov (trial no. NCT07357844).

About the Author

Dr. Franco is a pediatric resident at Hospices Civils de Lyon, France, pursuing specialization in pediatric infectious diseases. Her research interests include pediatric tuberculosis.

References

1. World Health Organization. Global tuberculosis report 2025 [cited 2025 Dec 9]. https://iris.who.int/server/api/core/bitstreams/e97dd6f4-b567-4396-8680-717bac6869a9/content
2. World Health Organization. WHO operational handbook on tuberculosis. Module 5: management of tuberculosis in children and adolescents. 1st edition. Geneva: The Organization; 2022.
3. Gafar F, Van't Boveneind-Vrubleuskaya N, Akkerman OW, Wilffert B, Alffenaar JC. Nationwide analysis of treatment outcomes in children and adolescents routinely treated for tuberculosis in the Netherlands. Eur Respir J. 2019; 54:1901402. https://doi.org/10.1183/13993003.01402-2019
4. Abubakar I, Laundy MT, French CE, Shingadia D. Epidemiology and treatment outcome of childhood tuberculosis in England and Wales: 1999–2006. Arch Dis Child. 2008;93:1017–21. https://doi.org/10.1136/adc.2008.139543
5. World Health Organization. WHO child growth standards: length/height-for-age, weight-for-age, weight-for-length, weight-for-height and body mass index-for-age: methods and development. [cited 2025 Jul 26]. https://www.who.int/publications/i/item/924154693X
6. Observance and treatment follow-up [in French]. Med Mal Infect. 2004;34:386–90.7. National Cancer Institute. PRO-CTCAE measurement system terminology [cited 2025 Jul 23]. https://evs.nci.nih.gov/ftp1/CTCAE/About.html
8. World Health Organization. WHO consolidated operational handbook on tuberculosis. Module 4 treatment and care. Geneva: The Organization; 2025.
9 Gupta N, Kashyap B, Dewan P, Hyanki P, Singh NP. Clinical spectrum of pediatric tuberculosis: a microbiological correlation from a tertiary care center. J Trop Pediatr. 2019;65:130–8. https://doi.org/10.1093/tropej/fmy026
10. Guido G, Di Gennaro F, Cavallin F, Pisaturo M, Onorato L, Zimmerhofer F, et al. Team-based, hybrid, or standard of care? Organizational models of tuberculosis care on tuberculosis outcomes in eleven Italian hospital. Clin Microbiol Infect. 2025;31:2033–40. https://doi.org/10.1016/j.cmi.2025.08.020

Address for correspondence: Diane Franco, Equipe Mobile d'Infectiologie Pédiatrique & Urgences Pédiatriques, Hôpital Femme Mère Enfant, Hospices Civils de Lyon, 59 Boulevard, Pinel 69500 Bron, France; email: diane.franco@chu-lyon.fr

Powassan Virus in *Ixodes scapularis* Tick Populations, Illinois, USA, 2025

Aurora Marguccio, Lance E. Jones, Brian Wilm, Arif Ciloglu, Valeria Trivellone, Millon Blackshear, Tomas Rodriguez, April Holmes, Samantha Kerr, Chang-Hyun Kim, Chris M. Stone

Author affiliations: Prairie Research Institute, University of Illinois Urbana-Champaign, Champaign, Illinois, USA (A. Marguccio, L.E. Jones, B. Wilm, A. Ciloglu, V. Trivellone, M. Blackshear, T. Rodriguez, C.-H. Kim, C.M. Stone); Faculty of Veterinary Medicine, Erciyes University, Kayseri, Türkiye (A. Ciloglu); Illinois Department of Public Health, Springfield, Illinois, USA (A. Holmes, S. Kerr)

DOI: http://doi.org/10.3201/eid3209.260812

Powassan virus is a tickborne flavivirus that can cause severe encephalitis in humans. After the first known human case in Illinois, USA, we detected Powassan virus in adult *Ixodes scapularis* ticks collected from 2 sites in northern Illinois during 2025. Phylogenetic analysis confirmed the virus as Powassan virus lineage II.

Powassan virus (POWV; Flaviviridae: *Orthoflavivirus*) is a member of the tick-borne encephalitis serocomplex of flaviviruses and, although rare, poses a serious public health risk. Common symptoms include encephalitis and meningitis. Infection often results in considerable sequelae and, in ≈10% of cases, can be fatal (*1*). Reports have documented the distribution of POWV in the United States through case reports and studies of ticks and vertebrate hosts (*1*–*3*). US regions with cases of recorded POWV include those in the mid-Atlantic, Northeast, and Midwest, and the past decade has seen a consistent rise in human cases (*4*).

POWV consists of 2 clinically indistinguishable lineages: lineage I (POWV prototype) and lineage II (deer tick virus [DTV]) (*5*,*6*). Lineage I is maintained predominantly in an enzootic cycle involving *Ixodes cookei* ticks and woodchucks (*Marmota monax*), whereas lineage II is maintained in a cycle involving *Ixodes scapularis* ticks and white-footed mice (*Peromyscus leucopus*) (*1*). The first case of POWV in Illinois occurred in 2025, involving a resident from Tazewell County, although exposure may have occurred out of state (*7*). In response, we expanded our tick surveillance to assess the presence and distribution of POWV in *I. scapularis* tick populations in central and northwestern counties in Illinois and determine the phylogenetic lineages of detected strains.

We performed tick drags during October and November 2025 in 14 Illinois counties (Figure 1). We selected outdoor recreational areas containing woodland habitats as sampling locations. Within each county, 1 or 2 sites were visited 1–3 times, with at least five 150-m transects per visit. We used a 1-m^2 white cloth drag attached to a wooden dowel for collection, according to previously established methods (*8*), and placed ticks in vials containing 85% ethanol. We sampled a total of 21 sites across 14 counties for *I. scapularis* ticks. We identified ticks according to species, life stage, and sex by light microscopy and then placed them in RNAlater solution (Thermo Fisher Scientific, https://www.thermofisher.com) and stored at −80°C until processing.

We extracted nucleic acids individually from ticks using the MagMAX Viral/Pathogen Ultra Nucleic Acid Isolation kit (Thermo Fisher Scientific) after crushing each specimen on liquid nitrogen. We screened extracts for POWV RNA presence by quantitative reverse transcription PCR (qRT-PCR) using an existing primer and probe set (*9*). We then reverse transcribed the extracts of qRT-PCR–positive samples (quantification cycle values <37) using the PrimeScript 1st strand cDNA Synthesis Kit (Takara Bio USA, https://www.takarabio.com) and amplified using an existing primer set (*5*). We slightly modified the reverse primer (5′-AGCGGGTGTTT TTCCGAGTCACWCA-3′) to detect both POWV lineage I and lineage II. When direct PCR failed, we ran a nested PCR using nested primer pairs POWVUTR-NestSeqF

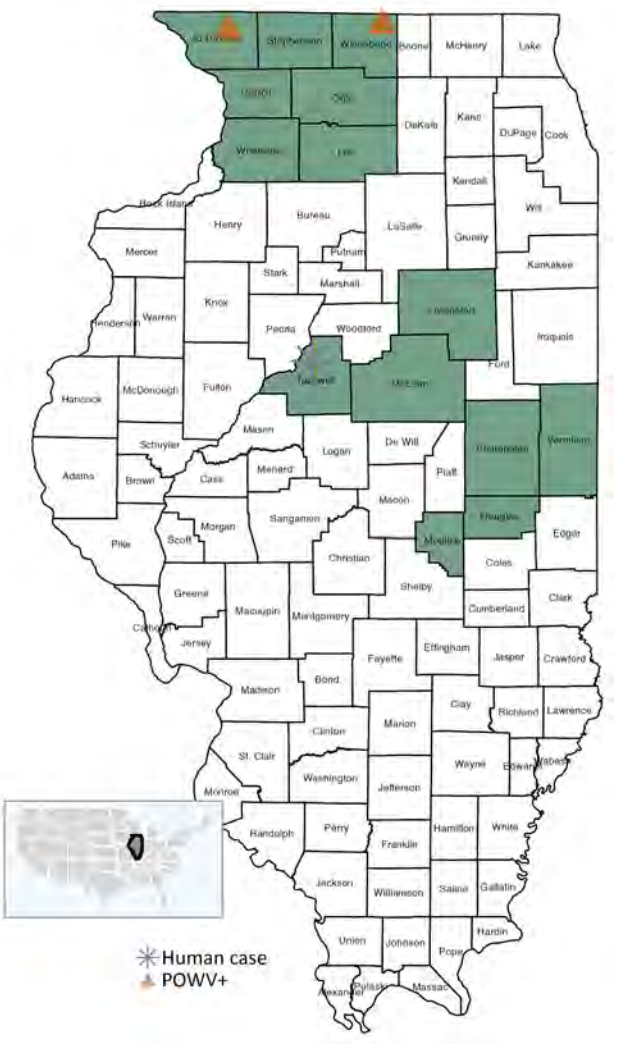

Figure 1. Geographic information from study of Powassan virus (POWV) in *Ixodes scapularis* tick populations, Illinois, USA, 2025. Green shading shows counties in Illinois where *I. scapularis* tick active surveillance included POWV testing. Orange triangles indicate locations where POWV-positive ticks were detected. Asterisk indicates county in which a human case was reported in 2025 (placed at random location within the county).

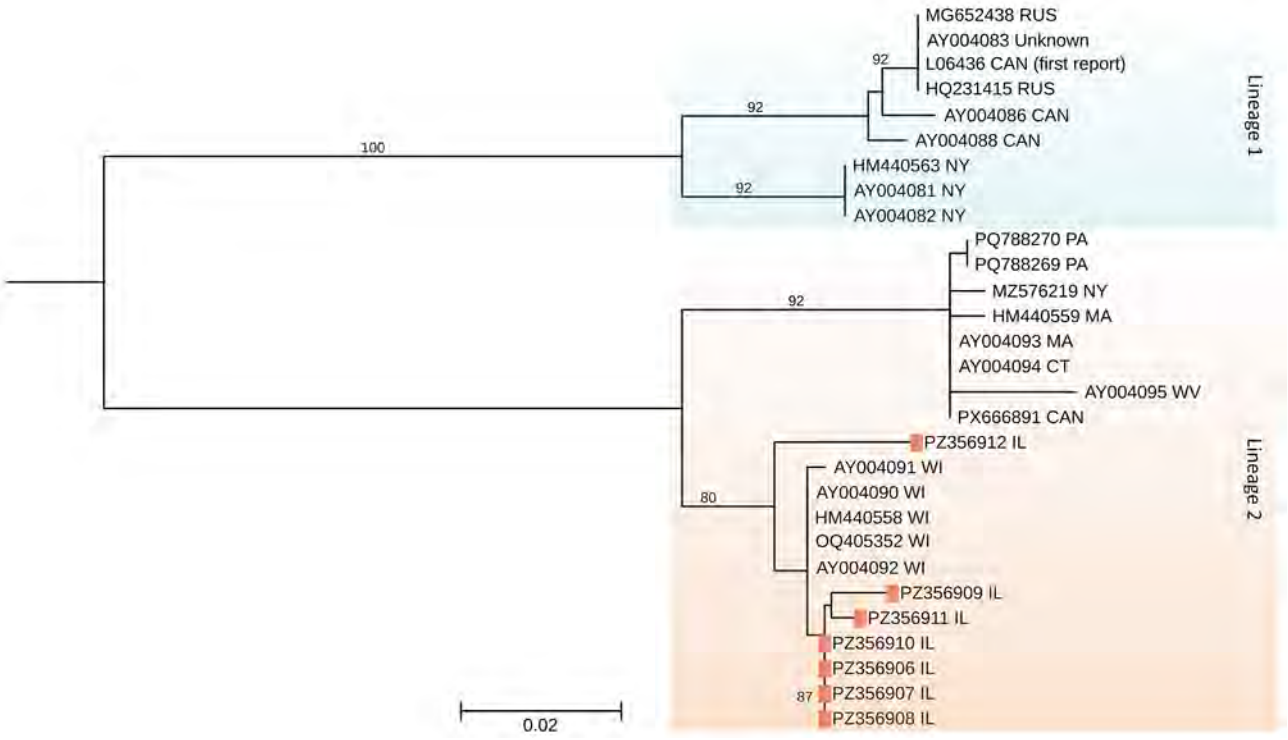

Figure 2. Maximum-likelihood phylogenetic tree of Powassan 3′ untranslated region created for study of Powassan virus in *Ixodes scapularis* tick populations, Illinois, USA, 2025. Branch lengths estimated using Hasegawa-Kishino-Yano substitution model with a gamma-distributed rate variation across 4 site categories. Bootstrap values >80% (1,000 replicates) are shown. Orange squares indicate samples from this study, clustering within lineage II together with samples previously detected in Wisconsin, USA. CAN, Canada; RUS, Russia.

(5′-AGCATGACTGAACAGTCAAAAGA-3′) and POWVUTR-NestSeqR (5′-TTGTCAGGCTATCTGTGCC-3′). Amplicons were Sanger sequenced at the University of Illinois Urbana-Champaign Roy J. Carver Biotechnology Center (Champaign, Illinois, USA). We queried consensus sequences ranging 446–519 bp against the National Center for Biotechnology Information BLAST search tool (https://blast.ncbi.nlm.nih.gov). We considered only samples confirmed by both qRT-PCR and sequencing to be positive.

We generated sequence alignments using MAFFT (https://mafft.cbrc.jp/alignment/software) and a maximum-likelihood phylogenetic tree using IQ-TREE software (https://iqtree.github.io) with 1,000 bootstrap replicates for branch support. Phylogenetic reconstruction incorporated reference strains from various US states and localities in Canada and Russia (Appendix Table 1, https://wwwnc.cdc.gov/EID/article/32/9/26-0812-App1.pdf).

All collected ticks were adult *I. scapularis*, with the exception of a single *I. scapularis* nymph and a single *Dermacentor albipictus* male tick. We established density data for the female ticks collected (Appendix Table 2). We detected POWV in *I. scapularis* adults at single sites in Jo Daviess and Winnebago counties. The ticks determined to be positive for POWV (confirmed by sequencing) included 1 female and 2 male ticks from Winnebago collected on October 23, two male ticks from the same site collected on October 31, and 2 male ticks collected from a site in Jo Daviess on October 30. The prevalence of infection for adult *I. scapularis* ticks was 0.059 (Wilson CI 0.025–0.13) in Winnebago and 0.064 (Wilson CI 0.018–0.207) in Jo Daviess. POWV lineage I and lineage II reference strains were recovered as monophyletic clades (Figure 2), and the Illinois field samples clustered within lineage II. Within the DTV branch, we detected a cluster consisting of primarily northeastern United States samples, whereas Illinois samples clustered together with Wisconsin sequences.

Finding POWV-positive *I. scapularis* ticks in Illinois has relevance for healthcare providers, who may need to consider POWV exposure in establishing diagnoses, and also for health officials in crafting public health messaging to include such information as duration of tick attachment required for POWV transmission (*9*). The locations where we detected POWV-positive ticks were close to the Wisconsin border, where foci of POWV have previously been described (*1*). Of note, the prevalence in the positive counties was higher than that reported from a stable focus in Wisconsin, where the prevalence was 1.3% (*10*). An

important question we pondered is whether POWV has been present, undetected, in Illinois for longer than the recent emergence our findings suggest. Increased surveillance and genomic analysis may elucidate POWV prevalence and phylogeographic history in this area of ongoing *I. scapularis* tick expansion.

Our investigation was supported through an agreement with the Illinois Department of Public Health. Points of view or opinions expressed in this document are those of the authors and do not necessarily represent the official position or policies of the Illinois Department of Public Health. The Illinois Natural History Survey Medical Entomology Lab (Prairie Research Institute) is additionally supported through the State of Illinois Used Tire Management and Emergency Public Health Funds.

About the Author

Ms. Marguccio is a laboratory technician at the University of Illinois Urbana-Champaign. Her research interests include the evolutionary relationships among arboviruses and how human activity shapes patterns of disease ecology.

References

1. Ebel GD. Update on Powassan virus: emergence of a North American tick-borne flavivirus. Annu Rev Entomol. 2010;55:95–110. https://doi.org/10.1146/annurev-ento-112408-085446
2. Khan M, Beckham JD, Piquet AL, Tyler KL, Pastula DM. An overview of Powassan virus disease. Neurohospitalist. 2019;9:181–2. https://doi.org/10.1177/1941874419844888
3. Hermance ME, Thangamani S. Powassan virus: an emerging arbovirus of public health concern in North America. Vector Borne Zoonotic Dis. 2017;17:453–62. https://doi.org/10.1089/vbz.2017.2110
4. Centers for Disease Control and Prevention. 2025. Powassan virus—historic data (2004–2024) [cited 2026 Jun 3]. https://www.cdc.gov/powassan/data-maps/historic-data.html
5. Ebel GD, Spielman A, Telford SR. Phylogeny of North American Powassan virus. J Gen Virol. 2001;82:1657–65. https://doi.org/10.1099/0022-1317-82-7-1657
6. Beasley DWC, Suderman MT, Holbrook MR, Barrett ADT. Nucleotide sequencing and serological evidence that the recently recognized deer tick virus is a genotype of Powassan virus. Virus Res. 2001;79:81–9. https://doi.org/10.1016/S0168-1702(01)00330-6
7. Illinois Department of Public Health. IDPH reminds Illinois residents to take precautions against tick bites. 2025 [cited 2026 Jun 3]. https://dph.illinois.gov/resource-center/news/2025/september/release-20250922.html
8. Tuten HC, Burkhalter KL, Noel KR, Hernandez EJ, Yates S, Wojnowski K, et al. Heartland virus in humans and ticks, Illinois, USA, 2018–2019. Emerg Infect Dis. 2020;26:1548–52. https://doi.org/10.3201/eid2607.200110
9. Ebel GD, Kramer LD. Short report: duration of tick attachment required for transmission of Powassan virus by deer ticks. Am J Trop Med Hyg. 2004;71:268–71. https://doi.org/10.4269/ajtmh.2004.71.3.0700268
10. Brackney DE, Nofchissey RA, Fitzpatrick KA, Brown IK, Ebel GD. Stable prevalence of Powassan virus in *Ixodes scapularis* in a northern Wisconsin focus. Am J Trop Med Hyg. 2008;79:971–3. https://doi.org/10.4269/ajtmh.2008.79.971

Address for correspondence: Chris M. Stone, Illinois Natural History Survey, Prairie Research Institute, University of Illinois Urbana-Champaign, 1816 South Oak St, Champaign IL 61820, USA; email: cstone@illinois.edu

Outbreak of Brazilian Spotted Fever, Southeastern Brazil, 2018

Jardel Brasil, Rodrigo N. Angerami, Maria R. Donalisio

Author affiliations: Municipal Health Department, Americana, Brazil (J. Brasil); State University of Campinas, Campinas, Brazil (J. Brasil, R.N. Angerami, M.R. Donalisio)

DOI: https://doi.org/10.3201/eid3209.260548

Brazilian spotted fever is a severe tickborne rickettsial disease endemic to Brazil. We report the clinical and epidemiological characteristics of an outbreak of 15 cases of Brazilian spotted fever caused by *Rickettsia rickettsii* in 2018 with high lethality. Our report highlights the need for early diagnosis to avert deaths.

Brazilian spotted fever (BSF) is caused by *Rickettsia rickettsii* bacteria and transmitted in endemic areas of the interior of São Paulo state, southeastern Brazil, by *Amblyomma sculptum* ticks. Transmission typically occurs in forested areas along rivers and streams inhabited by capybaras, which are the main host for the tick vector and an amplifier host for *Rickettsiae* (*1*–*3*). We describe a BSF outbreak characterized by a high number of confirmed cases, specific circumstances of transmission, and associated deaths.

An eco-epidemiologic investigation in 2018 in the municipality of Americana, Brazil, identified a cluster of 15 laboratory-confirmed cases of BSF in a periurban area (*3*) (Appendix Figure, http://wwwnc.cdc.gov/EID/article/32/9/26-0548-App1.pdf). The outbreak lasted

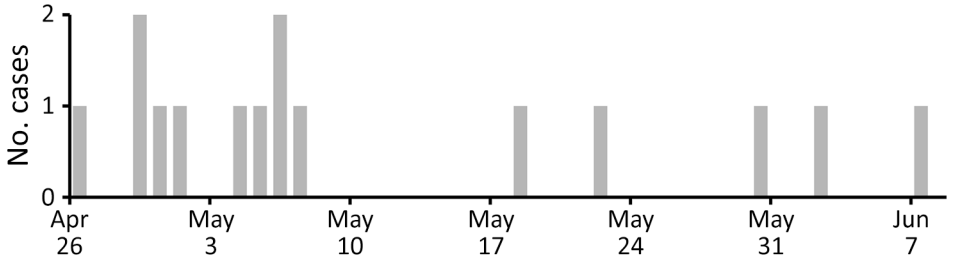

Figure. Temporal distribution of Brazilian spotted fever cases, by date of onset of symptoms, during outbreak in Americana, Brazil, 2018.

43 days, from April 26, 2018, the date of symptom onset of the index case, to June 7, 2018, when symptom onset occurred in the last reported case (Figure). We applied Brazilian Ministry of Health criteria to confirm each case (*4*) (Appendix Table 1). This study was approved by the Research Ethics Committee of the Faculty of Medical Sciences of the State University of Campinas (protocol no. 5,474,734).

We noted the most prevalent symptoms in each case included fever, headache, and myalgia. We also observed an increased frequency in symptom severity, including respiratory failure, renal dysfunction, jaundice, neurologic symptoms, shock, and hemodynamic instability at the time of suspicion (Appendix Table 2). There were 11 deaths out of 15 cases. Of note, severe febrile-icteric and hemorrhagic syndromes were prevalent.

The case-patients' mean age was 37 years (range 2–65 years); 14 were male and 1 female, and 6 were persons of color (Table). The case-patients had a median of 3 (range 1–4) medical consultations before hospitalization, indicating diagnostic delay. The 12 patients who were hospitalized had a median of 4 (range 2–11) days from symptom onset to hospitalization. Among the hospitalized patients who survived, the length of hospital stay was 10–14 (median 12) days. Among patients with fatal outcomes, the median duration from symptom onset to death was 6 days (range 4–10 days), whereas the median time between hospitalization and death was 1 day (range 1–5 days).

Most patients were working-age adults (20–59 years), although the inclusion of children is notable. Previous studies suggest severe manifestations and mortality reaching 80% in children (*5*–*7*). We found that the low frequency of widespread skin rashes (5 of 15 in general, 1 of 6 in patients of color), a clinical clue for BSF suspicion even in cases that already showed signs of severity, might have contributed to late suspicion with a consequent high mortality rate.

Survivors sought care during the first 3 days of symptoms and received doxycycline at median day 3 (range 2–4) compared with day 6 (range 4–9) for nonsurvivors. Time from onset to hospitalization was also shorter among survivors (3 vs. 5 days). We found that early identification of the disease during the prodromal phase, especially when associated with nonspecific clinical symptoms and a history of exposure to tick habitats, ideally by day 3 of symptom onset, can provide an opportunity for immediate outpatient treatment with oral antimicrobial drugs to avoid hospitalization (*4*).

During the investigation, the municipal epidemiologic surveillance team gathered information from patients and family members. Eight patients reported the occurrence of tick bites. All patients had a history of engaging in outdoor leisure activities (e.g., fishing, hiking) ≤15 days before symptom onset in a waterside

Table. Patient demographics and outcomes during a Brazilian spotted fever outbreak, Americana, Brazil, 2018*

Age, y/sex	Race or skin color	Onset of symptoms	No. medical consultations before diagnosis	Hospitalization date	Treatment start date†	Clinical outcome	Date of outcome
45/M	White	Apr 26	2	May 7	May 7	Cure	May 21
23/M	White	Apr 29	2	May 3	May 3	Death	May 4
53/M	White	Apr 29	4	May 4	May 5	Death	May 5
7/F	White	Apr 30	3	May 4	May 4	Death	May 4
51/M	Brown	May 01	1	NA	May 2	Cure	NA
65/M	Black	May 04	3	May 13	May 14	Death	May 14
45/M	Brown	May 05	3	May 9	May 9	Death	May 14
6/M	White	May 06	2	May 8	May 9	Cure	May 18
60/M	White	May 06	4	May 8	May 10	Death	May 11
59/M	White	May 07	2	May 11	May 11	Death	May 11
4/M	Brown	May 18	2	May 23	May 24	Death	May 24
37/M	Brown	May 22	1	May 27	May 28	Death	May 28
2/M	White	May 30	3	NA	Jun 3	Death	Jun 3
49/M	White	Jun 02	2	NA	Jun 7	Death	Jun 7
49/M	Brown	Jun 07	1	NA	Jun 9	Cure	NA

*NA, not applicable.
†Treatment with doxycycline or chloramphenicol.

forest area located at the confluence of the Atibaia and Jaguari Rivers. An acarological survey that applied a CO_2 trap technique conducted at 10 sites in this area on June 14, 2018, collected 403 *A. sculptum* ticks (277 larvae, 110 nymphs, and 16 adults) and 82 *A. dubitatum* ticks (30 larvae, 49 nymphs, and 3 adults). We did not test ticks for *R. rickettsii* bacteria.

Unlike what we observed in this outbreak, in endemic areas of BSF where *A. sculptum* ticks are the vector, cases typically concentrate during July– November, when nymphs, the main life stage involved in transmitting *R. rickettsii* to humans, are most abundant in the environment (*2*,*4*,*8*). High infestation by immature stages (larvae and nymphs) of the vector in the environment and high turnover of capybaras susceptible to infection are factors that possibly enabled the occurrence of this outbreak outside the expected epidemiologic pattern, instead during the seasonal peak of larval abundance (*8*).

Even though this region has a long history of BSF endemicity, during this outbreak, the alerts were not timely enough for healthcare professionals in the region. We noted delays in clinical suspicion and diagnosis of BSF in most patients who died, highlighting that BSF remains a relevant public health challenge for health services and that early diagnosis is necessary to avert deaths.

Acknowledgments

We would like to thank the Americana Municipal Health Department for supporting this study.

About the Author

Mr. Brasil is a doctoral student in the postgraduate program in public health at the State University of Campinas, Brazil. His research interests include entomology and zoonoses in public health.

References

1. Labruna MB. Ecology of rickettsia in South America. Ann N Y Acad Sci. 2009;1166:156–66. https://doi.org/10.1111/j.1749-6632.2009.04516.x
2. Foley J, López-Pérez AM, Álvarez-Hernández G, Labruna MB, Angerami RN, Zazueta OE, et al. A wolf at the door: the ecology, epidemiology, and emergence of community- and urban-level Rocky Mountain spotted fever in the Americas. Am J Vet Res. 2025;86:1–12. https://doi.org/10.2460/ajvr.24.11.0368
3. Brasil J, Soares S, Brites-Neto J. Clinical and epidemiological aspects of a cluster of Brazilian spotted fever, which occurred in the city of Americana, São Paulo, Brazil, 2018. Journal of Health & Biological Sciences. 2020;8:1–5. https://doi.org/10.12662/2317-3076jhbs.v8i1.3037.p1-5.2020
4. Brazilian Ministry of Health. Spotted fever in Brazil: epidemiology, clinical manifestations and environment, 2022 [cited 2026 Jan 11]. https://www.gov.br/saude/pt-br/centrais-de-conteudo/publicacoes/svsa/febre-maculosa/febre-maculosa-aspactos-epidemiologicos-clinicos-e-ambientais.pdf
5. Chiang L, Ramchandar N, Aramkul J, Fireizen Y, Beatty ME, Monroe M, et al. Rocky Mountain spotted fever in children along the US–Mexico border, 2017–2023. Emerg Infect Dis. 2024;30:2288–93. https://doi.org/10.3201/eid3011.231760
6. de Oliveira SV, Willemann MCA, Gazeta GS, Angerami RN, Gurgel-Gonçalves R. Predictive factors for fatal tick-borne spotted fever in Brazil. Zoonoses Public Health. 2017;64:e44–50. https://doi.org/10.1111/zph.12345
7. Nogueira Angerami R, Oliveira Morais E, Katz G, Jacintho da Silva L. Brazilian spotted fever in the paediatric age-segment in the State of São Paulo, southeastern Brazil, 2003–2006. Clin Microbiol Infect. 2009;15(Suppl 2):205–6. https://doi.org/10.1111/j.1469-0691.2008.02728.x
8. Brasil J, Pinter A, Angerami RN, Donalisio MR. Spatial and temporal distribution of Brazilian spotted fever in an endemic area: epidemiological profile of a zoonosis in constant adaptation to anthropogenic actions. Rev Bras Epidemiol. 2026;29:e260020. https://doi.org/10.1590/1980-549720260020.2

Address for correspondence: Jardel Brasil, Health Surveillance Unit, Av. Paschoal Ardito, 1221, Americana, Brazil; email: 13473-010j061638@dac.unicamp.br

Pediatric *Rickettsia massiliae* Infection, Spain, 2023

Jorge Martín-Trueba, Isabel Jado, María Elena Andrés-Galván, Rosa M. González-Martín-Niño, Inés Martín-Martín, Marcos López-de-Felipe Escudero, María Teresa Llorente, José María Serrano-Romero, Antonio Sampedro, Raquel Andrade-Lobato, Coral García-Esteban, Judit Gil-Zamorano, María Isabel Hurtado-Gavilán, David González-Barrio

Author affiliations: Instituto de Salud Carlos III, Madrid, Spain (J. Martín-Trueba, I. Jado, M.E Andrés-Galván, R.M. González-Martín-Niño, I. Martín-Martín, M. López-de-Felipe Escudero, M.T. Llorente, J. Gil-Zamorano, M.I. Hurtado-Gavilán, D. González-Barrio); Consortium for Biomedical Research in Infectious Diseases, Madrid (I. Martín-Martín, D. González-Barrio); Hospital Universitario Virgen de las Nieves, Granada, Spain (J.M. Serrano-Romero, A. Sampedro); Biosanitary Institute of Granada, Granada (A. Sampedro); Hospital Universitario de Móstoles, Madrid (R. Andrade-Lobato); Hospital Universitario de Getafe, Madrid (C. García-Esteban)

DOI: https://doi.org/10.3201/eid3209.260035

Rickettsial disease caused by *Rickettsia massiliae* is rare in humans; only 6 cases have been reported since 2006. We report a case of *R. massiliae* infection in a pediatric patient in Spain with symptoms suggestive of rickettsiosis. Our results suggest that *R. massiliae* is an emerging tickborne rickettsial pathogen.

The increasing incidence and transmission of tickborne diseases is a major public health challenge. Although surveillance contributes to understanding the distribution and ecology of tickborne diseases, they remain underdiagnosed (*1*). *Rickettsia massiliae*, a spotted fever group *Rickettsia* species, is a human pathogen that was first isolated from *Rhipicephalus* spp. ticks in France in the 1990s (*2*). Since then, *R. massiliae* has been identified in questing and feeding ticks from a variety of animal hosts and in asymptomatic humans across regions of Europe, Africa, Asia, and limited areas of the Americas (*3*). *R. massiliae* was first recognized as a human pathogen in 2006 (*4*). Only 6 confirmed cases of *R. massiliae* caused rickettsiosis have been reported, highlighting its emergence as a tickborne rickettsial pathogen (*5*–*7*).

R. massiliae infection often causes clinical symptoms similar to other rickettsial infections, including fever, muscle pain, rash, hepatomegaly, scalp bedsores, neck lymphadenopathy, and eye issues such as retinal vasculitis, conjunctivitis, and vision loss (*8*). Although ticks of the genus *Rhipicephalus* are the primary vectors (*9*), the tick species responsible for the transmission of *R. massiliae* to humans has not been identified. We report a laboratory-confirmed case of *R. massiliae* infection in a patient from southern Spain.

In January 2023, a pediatric patient was brought to medical care for a dark eschar on the right hemiscrotum, associated with pruritus, pain, and local inflammation. The patient reported travel 2 weeks before seeking medical attention to a periurban area of Granada Province, southern Spain, where he had contact with a domestic dog but no known arthropod exposure. He remained afebrile, except for a single temperature of 38°C on the day of admission. Laboratory test results were unremarkable, including a leukocyte count of 8.9 × 10^3 cells/μL (68.4% neutrophils), platelet count of 266 × 10^3/μL, and hemoglobin level of 13.9 g/dL. The C-reactive protein result was elevated (51.8 mg/L; reference range <5.0 mg/L). Scrotal ultrasonography revealed thickening of the tunica vaginalis with mild hyperemia, but the testes were unaffected. Serologic testing for *Borrelia burgdorferi*, *Coxiella burnetii*, and *Rickettsia conorii* yielded negative results. The patient was treated with intravenous amoxicillin/clavulanic acid (25 mg/kg/8 h for 3 d), leading to clinical improvement. Before he was discharged, a lesion scraping was collected for microbiological analysis. Patient follow-up was conducted at the Pediatric Infectious Diseases outpatient clinic (Granada, Spain); the patient was treated with oral amoxicillin/clavulanic acid (25 mg/kg/8 h for 1 wk). Twenty days after symptom onset and confirmed rickettsial infection, the patient was prescribed doxycycline (100 mg/12 h for 3 d), leading to complete resolution of symptoms and signs.

Biopsy material was submitted to the Special Pathogens Reference and Research Laboratory, National Center for Microbiology (Madrid, Spain) for the detection of tickborne pathogens. We extracted DNA from the biopsy sample by using the QIAamp Tissue Kit (QIAGEN, https://www.qiagen.com) according to the manufacturer's instructions. We detected DNA from *Rickettsia* spp. by performing PCR amplification of fragments from the 23S–5S rRNA intergenic spacer and the outer membrane protein A (*ompA*) gene (*10*). We purified PCR amplicons and sequenced the amplicons bidirectionally by capillary electrophoresis by using BigDye Terminator chemistry on an ABI PRISM 3130 automated sequencer (Thermo Fisher Scientific, https://www.thermofisher.com).

We generated a consensus sequence for the 23S–5S rRNA intergenic spacer (GenBank accession no. PV679725) by aligning the sequence fragments to reference sequences retrieved from the GenBank database. We determined sequence similarity by using BLASTn (https://blast.ncbi.nlm.nih.gov). The sequence shared 100% identity with *R. massiliae* strain MTU5 (GenBank accession no. AY125013) and with an *R. massiliae* isolate (accession no. PP263054) detected in a tick belonging to the *Rhipicephalus sanguineus* complex from Spain. The consensus sequence also shared >99% identity with *Rickettsia* spp. isolated from ticks collected in Romania (accession no. MG450328) and Tunisia (accession no. KF245444) and the *R. massiliae* B29 strain isolated from Spain (accession no. AY125014).

We detected *R. massiliae* DNA from a skin biopsy of a patient with signs and symptoms consistent with rickettsial infection. The sequence we generated shared 99%–100% identity with *R. massiliae* strains previously isolated from ticks in other regions of Spain and Mediterranean countries. Our findings provide evidence that *R. massiliae* is an emerging cause of human rickettsiosis and highlight the diagnostic relevance of eschars in rickettsial infections. Eschars can be clinical indicators for early recognition, enabling prompt antimicrobial therapy, improving patient outcomes, and enhancing epidemiologic surveillance of emerging rickettsial infections.

The limited number of reported cases of *R. massiliae* in humans, despite the high prevalence in *Rhipicephalus* ticks, might reflect underdiagnosis because of nonspecific clinical signs and symptoms and limited molecular testing. Limited human–tick contact might also contribute to the lack of cases, because some *Rhipicephalus* species have limited anthropophilic behavior and exposure is likely concentrated in periurban settings. Because of the complexity of pathogen–vector–host interactions and the potential for severe clinical outcomes, *R. massiliae* should be considered an emerging public health concern in Mediterranean regions.

Acknowledgments

We thank the healthcare professionals of the Spanish National Health System, particularly those at the National Center for Microbiology (Instituto de Salud Carlos III, Spain), for their commitment and collaboration, which made the collection of the data and samples used in this study possible.

This study was based on the routine diagnostic program of the Special Pathogens Research and Reference Laboratory based at the National Center for Microbiology, Madrid, Spain. Written informed consent could not be obtained because the patient was not reachable despite repeated efforts. Data has been fully anonymized, and its publication is justified because of its public health importance.

This study was supported by the Instituto de Salud Carlos III, Ministry of Science, Innovation and Universities (grant no. PI23CIII/00052 to D.G.-B.).

About the Author

Dr. Martín-Trueba is a health biologist specializing in microbiology at the Instituto de Salud Carlos III, National Center for Microbiology, Majadahonda, Madrid, Spain. His research focuses on the surveillance of ticks in the Iberian Peninsula and the management of emerging tickborne infectious diseases in public health.

References

1. Boulanger N, Iijima H, Doi K, Watari Y, Kwak M, Nakao R, et al. Ticks and tick-borne diseases in the northern hemisphere affecting humans. Front Microbiol. 2025; 16:1632832. https://doi.org/10.3389/fmicb.2025.1632832
2. Beati L, Raoult D. *Rickettsia massiliae* sp. nov., a new spotted fever group *Rickettsia*. Int J Syst Bacteriol. 1993;43:839–40. https://doi.org/10.1099/00207713-43-4-839
3. Pustijanac E, Buršić M, Millotti G, Paliaga P, Iveša N, Cvek M. Tick-borne bacterial diseases in Europe: threats to public health. Eur J Clin Microbiol Infect Dis. 2024;43:1261–95. https://doi.org/10.1007/s10096-024-04836-5
4. Jumpertz M, Sevestre J, Luciani L, Houhamdi L, Fournier PE, Parola P. Bacterial agents detected in 418 ticks removed from humans during 2014–2021, France. Emerg Infect Dis. 2023;29:701–10. https://doi.org/10.3201/eid2904.221572
5. Vieira Lista MC, Belhassen-García M, Vicente Santiago MB, Sánchez-Montejo J, Pedroza Pérez C, Monsalve Arteaga LC, et al. Identification and distribution of human-biting ticks in northwestern Spain. Insects. 2022;13:469. https://doi.org/10.3390/insects13050469
6. Vitale G, Mansuelo S, Rolain JM, Raoult D. *Rickettsia massiliae* human isolation. Emerg Infect Dis. 2006;12:174–5. https://doi.org/10.3201/eid1201.050850
7. Moerbeck L, Domingos A, Antunes S. Tick-borne rickettsioses in the Iberian Peninsula. Pathogens. 2022;11:1377. https://doi.org/10.3390/pathogens11111377
8. Monterde-Álvarez ML, Calbet-Ferré C, Rius-Gordillo N, Pujol-Bajador I, Ballester-Bastardie F, Escribano-Subías J. Rickettsiosis after tick bite: a subtle clinic picture on many occasions, we must be vigilant [in Spanish]. Enferm Infecc Microbiol Clin. 2017;35:100–3.
9. Matsumoto K, Ogawa M, Brouqui P, Raoult D, Parola P. Transmission of *Rickettsia massiliae* in the tick, *Rhipicephalus turanicus*. Med Vet Entomol. 2005;19:263–70. https://doi.org/10.1111/j.1365-2915.2005.00569.x
10. Ramos JM, Pérez-Tanoira R, Martín-Martín I, Prieto-Pérez L, Tefasmariam A, Tiziano G, et al. Arthropod-borne bacteria cause nonmalarial fever in rural Ethiopia: a cross-sectional study in 394 patients. Vector Borne Zoonotic Dis. 2019;19:815–20. https://doi.org/10.1089/vbz.2018.2 396

Address for correspondence: David González Barrio, National Centre for Microbiology, Instituto de Salud Carlos III, Carretera de Pozuelo, 28, 28222 Majadahonda, Madrid, Spain; email: david.gonzalezb@isciii.es

Gulf Coast Ticks (*Amblyomma maculatum*) and *Rickettsia parkeri*, Ohio, USA, 2020

Risa Pesapane, Kaylee Shrock, Cece Bryant, Andrew J. Rosendale

Author affiliations: The Ohio State University, Columbus, Ohio, USA (R. Pesapane, K. Shrock, C. Bryant); Mount St. Joseph University, Cincinnati, Ohio, USA (A.J. Rosendale)

DOI: https://doi.org/10.3201/eid3209.260632

We report the establishment of the Gulf Coast tick (*Amblyomma maculatum*) and *Rickettsia parkeri* bacteria in Ohio, USA. We collected host-seeking ticks through surveillance in 2020–2021. Our discovery of established populations in 2 Ohio counties highlights a medically critical vector–pathogen system with serious public health implications.

The Gulf Coast tick (*Amblyomma maculatum*) is a 3-host ixodid tick of increasing medical and veterinary note (*1*). Historically, this species inhabited only coastal regions of the southeastern United States from Florida to Virginia (*2*), but its geographic range has expanded in recent years to include portions of the Midwest and Northeast (*3*–*7*). Because the geographic distribution of this tick species is expanding, so might the distribution of its associated pathogens. Gulf Coast ticks are the vector for *Rickettsia parkeri*, a causative agent of rickettsiosis (*1*).

The state of Ohio Department of Health has received sporadic reports of Gulf Coast ticks since 1990 (Figure), but the tick was not yet documented as established (the collection of ≥6 ticks of >1 life stage within a county during a 12-month period) (*8*). The reports were limited, involving a total of 29 Gulf Coast tick records from 22 counties, often with only 1 tick reported in any county each year. However, unverified reports of increasing Gulf Coast tick detections in southwestern Ohio prompted our investigation into whether self-sustaining populations and their associated pathogens were present.

We collected host-seeking ticks from vegetation in Butler County, Ohio, USA, in July 2020 and Hamilton County, Ohio, USA, in September 2020 by flagging or dragging vegetation along walking trails in public recreational areas (Appendix, http://wwwnc.cdc.gov/EID/article/32/9/26-0632-App1.pdf). We also received unfed ticks collected by a citizen scientist at a neighborhood green space in Madison County, Ohio, USA, in June and July 2021.

We obtained 41 adult *A. maculatum* ticks from 3 counties for this study (Figure): 30 (8 male, 22 female) from Hamilton County, 7 (1 male, 6 female) from Butler County, and 4 (1 male, 3 female) from Madison County. The collections met the criteria for establishment in Hamilton and Butler counties but not Madison County. We extracted DNA from 37 specimens for pathogen testing by real-time PCR (Appendix). Of the 29 specimens we tested from the Hamilton County site, 15 (51.7%) were positive for *R. parkeri* bacteria.

Established Gulf Coast tick populations have recently been documented in several states outside of the species' historical range, including Indiana in 2020 (*3*); Illinois, Connecticut, and New York in 2021 (*4*,*5*,*7*); and New Jersey in 2022 (*6*). Those reports indicate rapid range expansion of Gulf Coast ticks in the northeastern and midwestern United States. Through active surveillance, we collected enough Gulf Coast ticks to document established populations in 2 Ohio counties in 2020; passive submissions also documented the species in a third county in 2021. Those findings suggest Gulf Coast tick establishment in Ohio occurred before 2021.

We also detected *R. parkeri* bacteria in host-seeking ticks, revealing the presence of a tick vector and its primary human pathogen in Ohio. Human

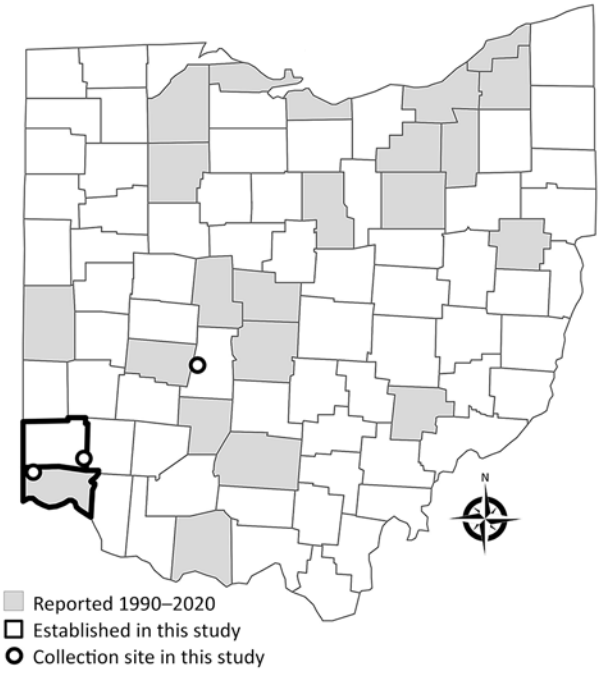

Figure. Reports of Gulf Coast ticks (*Amblyomma maculatum*) in Ohio, USA. Map highlights counties with previous reports of 1–2 Gulf Coast tick detections from the Ohio Department of Health (1990–2020), the collection sites from this study of active and passive Gulf Coast tick detections (2020–2021), and the counties we determined to have an established population (≥6 adults) of Gulf Coast ticks.

and animal health providers should remain vigilant for locally acquired cases of *R. parkeri* caused rickettsiosis. The Ohio Department of Health has reported spotted fever rickettsiosis cases in Hamilton and Butler counties (*9*). Although those cases are presumed to represent Rocky Mountain spotted fever associated with *R. rickettsii* bacteria from *Dermacentor variabilis* ticks, *R. parkeri* bacteria antibodies might cross-react with antigens used in routine serologic assays for other spotted fever group *Rickettsia.* Cross-reactivity would make the causative agent and vector difficult to distinguish (*10*). Our detection of *R. parkeri*–infected Gulf Coast ticks emphasizes the need to consider alternative spotted fever group rickettsiae when interpreting human spotted fever rickettsiosis surveillance data in Ohio.

Gulf Coast tick populations might have become established before 2020 but remained undetected because of limitations in active surveillance activities. Although we collected our samples in 2020–2021, they remain relevant as historical records documenting established populations rather than as transient introductions. Our records also help define the chronology of the tick species' spread. Our findings further underscore the value of passive tick surveillance through public submission programs in which the public submits ticks for identification as a complement to active surveillance, particularly in areas with limited surveillance capability experiencing tick range expansion.

Acknowledgments

We are grateful to Julia Beckett for her assistance in the laboratory and to Douglas Sweet for his contributions to our public tick submission program.

This work was supported by the US Department of Agriculture National Institute of Food and Agriculture, through Hatch Act appropriations (project no. NE2443). R.P. received funding from The Ohio State University College of Food, Agricultural, and Environmental Sciences and from The Ohio State University College of Veterinary Medicine.

The authors acknowledge using AI tools for editing the R code of the figure.

About the Author

Dr. Pesapane is an associate professor at The Ohio State University specializing in arthropods of medical and veterinary importance. Her research program focuses on vector-host-pathogen relationships, range expansion dynamics, and integrated pest management.

References

1. Paddock CD, Goddard J. The evolving medical and veterinary importance of the Gulf Coast tick (Acari: Ixodidae). J Med Entomol. 2015;52:230–52. https://doi.org/10.1093/jme/tju022
2. Hooker WA, Bishopp FC, Wood HP. The life history and bionomics of some North American ticks. Washington: US Department of Agriculture, Bureau of Entomology; 1912 [cited 2026 Apr 8]. https://www.biodiversitylibrary.org/bibliography/65064
3. Wojan C, Thrasher T, Lacey E, Clay K. Distribution, dynamics, and diversity of questing ticks in the lower Midwest. J Med Entomol. 2022;59:273–82. https://doi.org/10.1093/jme/tjab155
4. Phillips VC, Zieman EA, Kim CH, Stone CM, Tuten HC, Jiménez FA. Documentation of the expansion of the Gulf Coast tick (*Amblyomma maculatum*) and *Rickettsia parkeri*: first report in Illinois. J Parasitol. 2020;106:9–13. https://doi.org/10.1645/19-118
5. Molaei G, Little EAH, Khalil N, Ayres BN, Nicholson WL, Paddock CD. Established population of the Gulf Coast tick, *Amblyomma maculatum* (Acari: Ixodidae), infected with *Rickettsia parkeri* (Rickettsiales: Rickettsiaceae), in Connecticut. J Med Entomol. 2021;58:1459–62. https://doi.org/10.1093/jme/tjaa299
6. Musnoff BL, Cuadera MKQ, Birney MR, Zipper L, Nicholson W, Ayres B, et al. The first record of an established population of *Amblyomma maculatum* (Acari: Ixodidae) in New Jersey, USA. J Med Entomol. 2024;61:1081–5. https://doi.org/10.1093/jme/tjae056
7. Ramírez-Garofalo JR, Curley SR, Field CE, Hart CE, Thangamani S. Established populations of *Rickettsia parkeri*-infected *Amblyomma maculatum* ticks in New York City, New York, USA. Vector Borne Zoonotic Dis. 2022;22:184–7. https://doi.org/10.1089/vbz.2021.0085
8. Dennis DT, Nekomoto TS, Victor JC, Paul WS, Piesman J. Reported distribution of *Ixodes scapularis* and *Ixodes pacificus* (Acari: Ixodidae) in the United States. J Med Entomol. 1998;35:629–38. https://doi.org/10.1093/jmedent/35.5.629
9. Ohio Department of Health. Rocky Mountain spotted fever in Ohio map, 2025 [cited 2026 Apr 8]. https://odh.ohio.gov/know-our-programs/zoonotic-disease-program/media/rmsf-map
10. Drexler NA, Dahlgren FS, Heitman KN, Massung RF, Paddock CD, Behravesh CB. National surveillance of spotted fever group rickettsioses in the United States, 2008–2012. Am J Trop Med Hyg. 2016;94:26–34. https://doi.org/10.4269/ajtmh.15-0472

Address for correspondence: Risa Pesapane, The Ohio State University, 1920 Coffey Rd, Columbus, OH 43210, USA; email: pesapane.1@osu.edu

Emergence of Oropouche Virus, Venezuela, 2025

Pierina D'Angelo,[1] Lieska Rodríguez,[1] Víctor Alarcón, Yoneira Sulbarán, Norca García, Giulianna Antonelli, Marwan Aguilar, Martha Bravo, Zoila C. Moros, Carmen L. Loureiro, Ferdinando Liprandi, José L. Zambrano, Rossana C. Jaspe, Flor H. Pujol

Author affiliations: Instituto Nacional de Higiene "Rafael Rangel," Caracas, Venezuela (P. D'Angelo, L. Rodríguez, V. Alarcón, N. García, G. Antonelli, M. Aguilar, M. Bravo); Instituto Venezolano de Investigaciones Científicas, Caracas (Y. Sulbarán, Z.C. Moros, C.L. Loureiro, F. Liprandi, J.L. Zambrano, R.C. Jaspe, F.H. Pujol)

DOI: https://doi.org/10.3201/eid3209.250678

We describe 5 cases of human Oropouche virus infection detected in rural Venezuela in 2025. All isolates belonged to the $OROVBr_{2015–2024}$ reassortant lineage linked to the 2024–2025 epidemic. Our results emphasize ongoing transmission, which highlights the need for strengthened surveillance and laboratory capacity in South America.

Oropouche virus (OROV) is an arthropodborne virus and member of the family Peribunyaviridae, genus *Orthobunyavirus*; the species is *Orthobunyavirus oropoucheense*. The genome consists of 3 segments of a linear negative-stranded RNA: small, medium, and large (*1*). Several outbreaks of OROV infection have occurred in the Amazon region since 1960. The largest OROV outbreak has been ongoing since 2022 (*1*). By February 2025, a total of 9 countries in the Americas reported autochthonous cases of OROV. Meanwhile Canada, Cayman Islands, the United States, Germany, Italy, and Spain also reported 30 imported cases, mostly in travelers returning from Cuba (*2*).

The National Institute of Hygiene Rafael Rangel (Caracas, Venezuela) has been detecting OROV by using reverse transcription PCR since 2023. Beginning in 2024, a total of 25% of the samples negative for dengue, chikungunya, and Zika viruses were tested for Mayaro and Oropouche viruses by quantitative reverse transcription PCR (qRT-PCR) (*3*). During the first trimester of 2025, five samples tested positive for OROV by qRT-PCR in 2 states of Venezuela, Miranda and Portuguesa (Figure 1). After the first case of OROV was detected in January 2025, all the samples negative for the 3 other arboviruses from January–March 2025 were retrospectively tested for Mayaro virus and OROV, which were all negative. This study was approved

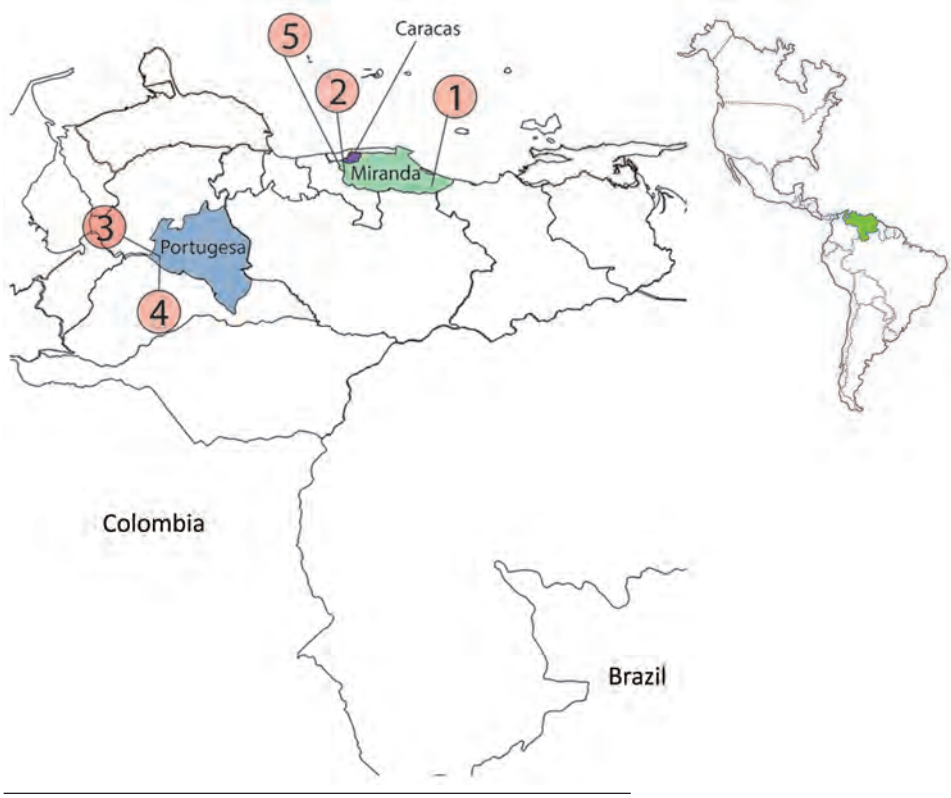

Figure 1. Locations of Oropouche virus cases detected in Venezuela, 2025. The numbers represent the cases detected. The cases were detected in the Portugesa and Miranda states. The first detected Oropouche virus case was from January 27, 2025, although official notification was performed in March 2025, when sequences were available. Inset shows location of Venezuela in the Americas.

[1]These first authors contributed equally to this article.

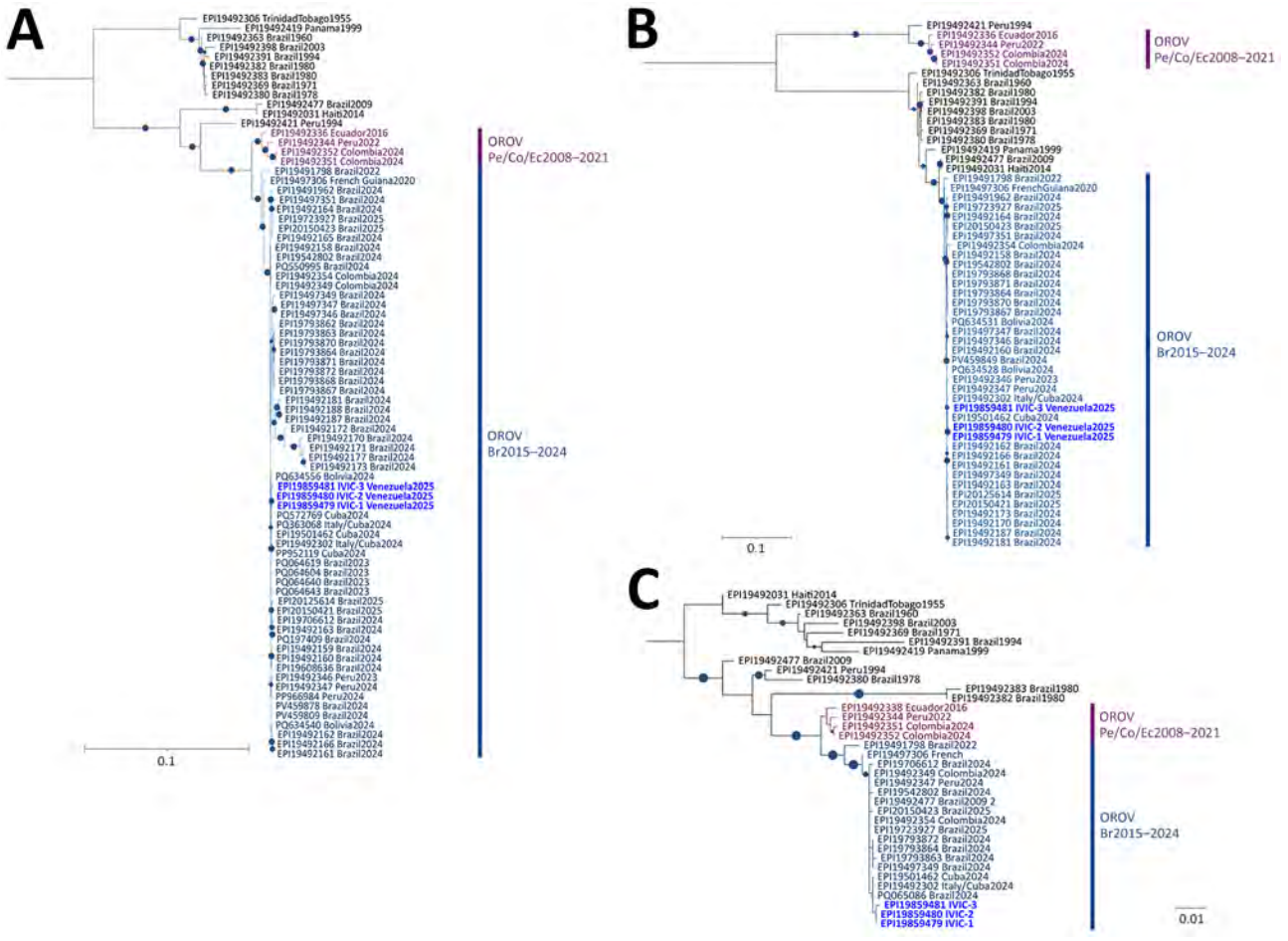

Figure 2. Phylogenetic analysis of OROV cases in Venezuela, 2025. Maximum-likelihood phylogenetic analysis for each genomic segment of the OROV genome: A) large genome segment sequences; B) medium genome segment sequences; C) small genome segment sequences. The isolates are named according to their accession number in GenBank or GISAID (https://www.gisaid.org), including the country and year of collection of each sample. Blue indicates the $OROV_{BR2015–2024}$ clade and purple the $OROV_{Pe/Co/Ec2008–2021}$ clade. Bold indicates the sequences of the Venezuela isolates. The tree scale indicates the average number of nucleotide substitutions per site. Blue circles indicate bootstrap values >80. OROV, Oropouche virus.

by the Bioethical Committee of Instituto Venezolano de Investigaciones Científicas (protocol no. CBioEtIVIC-2022–001): written informed consent was obtained in OROV-positive human cases. We described the clinical findings of the 5 patients in accordance with the Pan American Health Organization guidelines (Appendix Table 1, http://wwwnc.cdc.gov/EID/article/32/9/25-0678-App.pdf) (*2*). We observed no neurologic compromise in those cases. For the first case, the patient had a possible relapse 3 weeks later, although qRT-PCR was negative. Recurrence seems to be a frequent phenomenon in OROV infection (*4*).

We collected serum samples 2 or 3 days after the appearance of acute febrile illness. We performed genome sequencing on an Illumina iSeq platform (Illumina, https://www.illumina.com) by using a COVIDSeq library and primers specific for the OROV genome (Appendix Table 2) (*2*). We assembled genome sequences by using both Genome Detective (https://www.genomedetective.com) and INSaFLUTELEVIR bioinformatic tools (https://insaflu.insa.pt).

We deposited complete genome sequences into the GISAID database (accession nos. EPI_ISL_19859479–81), and in GenBank (GenBank accession nos. PX494099–101, PX495048–50 and PX495206–8). We aligned sequences by using MAFFT (*5*) and performed phylogenetic analysis by using IQTree with 1000 bootstrap replicas (Appendix) (*6*).

Our phylogenetic analysis of 3 complete viral genome segments revealed that the isolates from Venezuela grouped in the $OROV_{BR2015–2024}$ clade, a dominant lineage associated with current outbreaks (*1*). The sequences from Venezuela were

related to OROV isolates from Cuba. However, the small segment sequences were also closely related to sequences from Brazil (Figure 2). A large outbreak of OROV occurred in Cuba in 2024, with 626 confirmed cases, and was still ongoing in 2025 (*2*). Since late 2022, an unprecedented epidemic of OROV infection is still ongoing in Brazil (*1*,*2*,*7*). However, no history of travel outside the country was reported for the cases in Venezuela.

A close relative of OROV, Madre de Dios Virus, was isolated from a monkey (*Cebus olivaceus*) during an epizootic outbreak in the Eastern region of Venezuela in 2010 (*8*). Animal reservoirs, such as nonhuman primates and sloths, cannot be excluded in other rural regions of Venezuela and might be involved in a spillover OROV event to humans (*9*). However, the relatedness of the sequences to the $OROV_{BR2015–2024}$ clade suggests an introduction from the countries with OROV outbreaks. The 2 cases from Portuguesa state were from close localities, in contrast with the cases from Miranda state. No secondary cases were found among febrile persons in the localities where the OROV positive cases were found. However, secondary asymptomatic cases (*10*) cannot be ruled out. Epidemiologic surveillance of OROV infection is challenging because of the dengue virus epidemic in Venezuela. Some OROV cases might be underreported because they are misdiagnosed as dengue virus, or because they were asymptomatic (*10*). Two additional OROV infections were reported in April 2025 in Portuguesa state.

In conclusion, we detected OROV in Venezuela in 2025. Although underreporting of OROV cases cannot be ruled out, the epidemiologic pattern of this viral infection in Venezuela does not appear to be as pervasive compared with other countries such as Brazil and Cuba. We believe continued surveillance in the region is necessary to reduce outbreak risk.

Acknowledgments

We wish to express our gratitude to Gonzalo Bello and Felipe Naveca for advice on the generation and assembly of sequences. We also thank Valeria Bonetti for providing us access to IQTree.

This study was supported by the Ministerio del Poder Popular para la Salud and the Ministerio del Poder Popular de Ciencia, Tecnología e Innovación of Venezuela. We are also thankful for the Pan American Health Organization regional genomic surveillance network for the next-generation sequencing reagents.

About the Author

Mrs. D'Angelo is the coordinator of the virology department at the National Institute of Hygiene Rafael Rangel, of the National Polio Laboratory, and a member of the National Committee for Poliovirus Containment in Venezuela. Her research interests include viral genomic surveillance and the detection of emerging and reemerging viral pathogens.

References

1. Naveca FG, Almeida TAP, Souza V, Nascimento V, Silva D, Nascimento F, et al. Human outbreaks of a novel reassortant Oropouche virus in the Brazilian Amazon region. Nat Med. 2024;30:3509–21. https://doi.org/10.1038/s41591-024-03300-3
2. Pan American Health Organization/World Health Organization. Oropouche epidemiological update in the Americas region, 11 February 2025. Washington: The Organizations; 2025.
3. Naveca FG, Nascimento VAD, Souza VC, Nunes BTD, Rodrigues DSG, Vasconcelos PFDC. Multiplexed reverse transcription real-time polymerase chain reaction for simultaneous detection of Mayaro, Oropouche, and Oropouche-like viruses. Mem Inst Oswaldo Cruz. 2017;112:510–3. https://doi.org/10.1590/0074-02760160062
4. Pastula DM, Beckham JD, Tyler KL. Oropouche virus: an emerging neuroinvasive arbovirus. Ann Neurol. 2024;97:28–33. https://doi.org/10.1002/ana.27139
5. Katoh K, Rozewicki J, Yamada KD. MAFFT online service: multiple sequence alignment, interactive sequence choice and visualization. Brief Bioinform. 2019;20:1160–6. https://doi.org/10.1093/bib/bbx108
6. Trifinopoulos J, Nguyen LT, von Haeseler A, Minh BQ. W-IQ-TREE: a fast online phylogenetic tool for maximum likelihood analysis. Nucleic Acids Res. 2016;44(W1):W232-5. https://doi.org/10.1093/nar/gkw256
7. Scachetti GC, Forato J, Claro IM, Hua X, Salgado BB, Vieira A, et al. Re-emergence of Oropouche virus between 2023 and 2024 in Brazil: an observational epidemiological study. Lancet Infect Dis. 2025;25:166–75. https://doi.org/10.1016/S1473-3099(24)00619-4
8. Navarro JC, Giambalvo D, Hernandez R, Auguste AJ, Tesh RB, Weaver SC, et al. Isolation of Madre de Dios virus (*Orthobunyavirus*; *Bunyaviridae*), an *Oropouche virus* species reassortant, from a monkey in Venezuela. Am J Trop Med Hyg. 2016;95:328–38. https://doi.org/10.4269/ajtmh.15-0679
9. Sciancalepore S, Schneider MC, Kim J, Galan DI, Riviere-Cinnamond A. Presence and multi-species spatial distribution of Oropouche virus in Brazil within the One Health framework. Trop Med Infect Dis. 2022;7:111. https://doi.org/10.3390/tropicalmed7060111
10. Manuli ER, Hua X, Scachetti GC, Forato J, Claro IM, Pereira GM, et al. Transmission dynamics of Oropouche virus in Latin America and the Caribbean. Nat Med. 2026;32:1383–92. https://doi.org/10.1038/s41591-026-04221-z

Address for correspondence: Flor H. Pujol and Rossana Jaspe, Laboratorio de Virología Molecular, CMBC, IVIC, Apdo 21827, Caracas 1020A, Venezuela; email: fhpujol@gmail.com and rossanajaspesec@gmail.com

Autochthonous Canine Pythiosis Linked with Freshwater Exposure, Italy, 2021–2024

Andrea Peano, Anna Rita Molinar Min, Patrizia Danesi, Francesco Albanese, Nicla Furiani, Moira Monaco, Fabiano Necci, Chiara Noli, Sofia Sgubin, Antonella Varina, Mario Pasquetti

Author affiliations: Universita degli Studi di Torino, Torino, Italy (A. Peano, A.R. Molinar Min, M. Pasquetti); Istituto Zooprofilattico Sperimentale delle Venezie, Legnaro, Italy (P. Danesi, S. Sgubin); CDVet—Laboratorio Analisi Veterinarie, Rome, Italy (F. Albanese, F. Necci); Clinica Veterinaria Città dei Papi, Viterbo, Italy (N. Furiani); Veterinaria Cetego, Rome, Italy (M. Monaco); Ospedale Veterinario Anubi Bluvet, Ca'Zampa, Torino (C. Noli); private practice, Torino (A. Varina)

DOI: http://doi.org/10.3201/eid3209.260354

We report 7 recognized autochthonous cases of canine pythiosis, a fungal disease, identified in Italy during 2021–2024. All infected dogs had freshwater exposure. Cases involved multiple lakes and occurred over consecutive years. Sequenced isolates clustered within clade IV of the *Pythium insidiosum* complex, currently designated *Pythium periculosum*.

Pythiosis is a severe fungal disease caused by pathogenic oomycetes of the genus *Pythium* and is classically associated with tropical and subtropical climates and freshwater environments (*1*,*2*). The disease affects mainly humans, horses, and dogs and is typically linked to exposure to stagnant or slow-moving freshwater habitats that support production of infective zoospores. Most mammalian infections involve the *Pythium insidiosum* complex, although there have been occasional reports citing additional pathogenic oomycetes (*3*,*4*).

Increasing reports from regions outside traditionally recognized endemic areas, including northern areas of the United States and Japan, suggest a broader global distribution of pythiosis (*2*). Europe, however, remains exceptionally affected. A recent systematic review identified Spain as the only country in Europe in which locally acquired human pythiosis cases had been documented (*2*,*5*). In 2023, we reported 2 autochthonous canine cutaneous pythiosis cases in Italy, which were linked to recurrent exposure to Lake Bracciano in central Italy (*6*). Those initial observations suggested the possible presence of a local ecologic niche favorable to pathogenic *Pythium* species. We subsequently identified 5 additional canine cases diagnosed during 2021–2024, bringing the total number of recognized locally acquired canine cases in Italy to 7. None of the dogs had traveled outside Italy before disease onset, supporting the notion of locally acquired infection.

All dogs had histories of repeated exposure to natural freshwater environments. Reported sites included Lake Bracciano (5 cases), Lake Bolsena (1 case), and Lake Viverone in northern Italy (1 case) (Figure 1). Distinct cases linked to Lake Bracciano were recognized from 2021 through 2024, suggesting persistent local environmental conditions favorable to pathogenic *Pythium* species. In addition, identification of a case associated with Lake Viverone expands the geographic range of recognized exposure sites by >300 km. Although environmental investigations were outside the scope of this study, all implicated sites feature shallow, near-shore areas that undergo marked seasonal warming during summer months. Such conditions may favor persistence or proliferation of pathogenic *Pythium* species (*1*). All factors considered, we believe that our findings support the presence of ecologic niches potentially suitable for

Figure 1. Freshwater sites associated with autochthonous canine pythiosis cases for a study of autochthonous canine pythiosis linked with freshwater exposure, Italy, 2021–2024. Dots indicate lakes linked to reported exposure histories. Labels summarize the number and year(s) of associated cases; asterisk indicates that 2 previously published cases (*6*) were included in the total count for that lake. Base map adapted from Wikimedia Commons (https://commons.wikimedia.org)

pathogenic oomycetes in different regions of Italy despite the absence of traditionally recognized tropical climatic conditions.

Six of the 7 infected dogs were German shepherds. Although the number of cases remains limited, this predominance is noteworthy and suggest that factors beyond environmental exposure alone might contribute to disease occurrence. Published canine series from endemic regions show variable breed distributions, suggesting that disease emergence likely reflects a multifactorial interplay between environmental exposure, host-related factors, and clinical recognition patterns. Clinical manifestations were predominantly cutaneous and characterized by chronic nodules, plaques, ulceration, and draining tracts (Figure 2); 1 dog later developed gastrointestinal involvement. Researchers have described similar cutaneous and gastrointestinal manifestations in canine pythiosis occurring in other regions of the world (*7*–*9*). The predominance of cutaneous presentations in our series may reflect route of exposure through damaged skin or recognition bias, because gastrointestinal disease may be less readily diagnosed. In

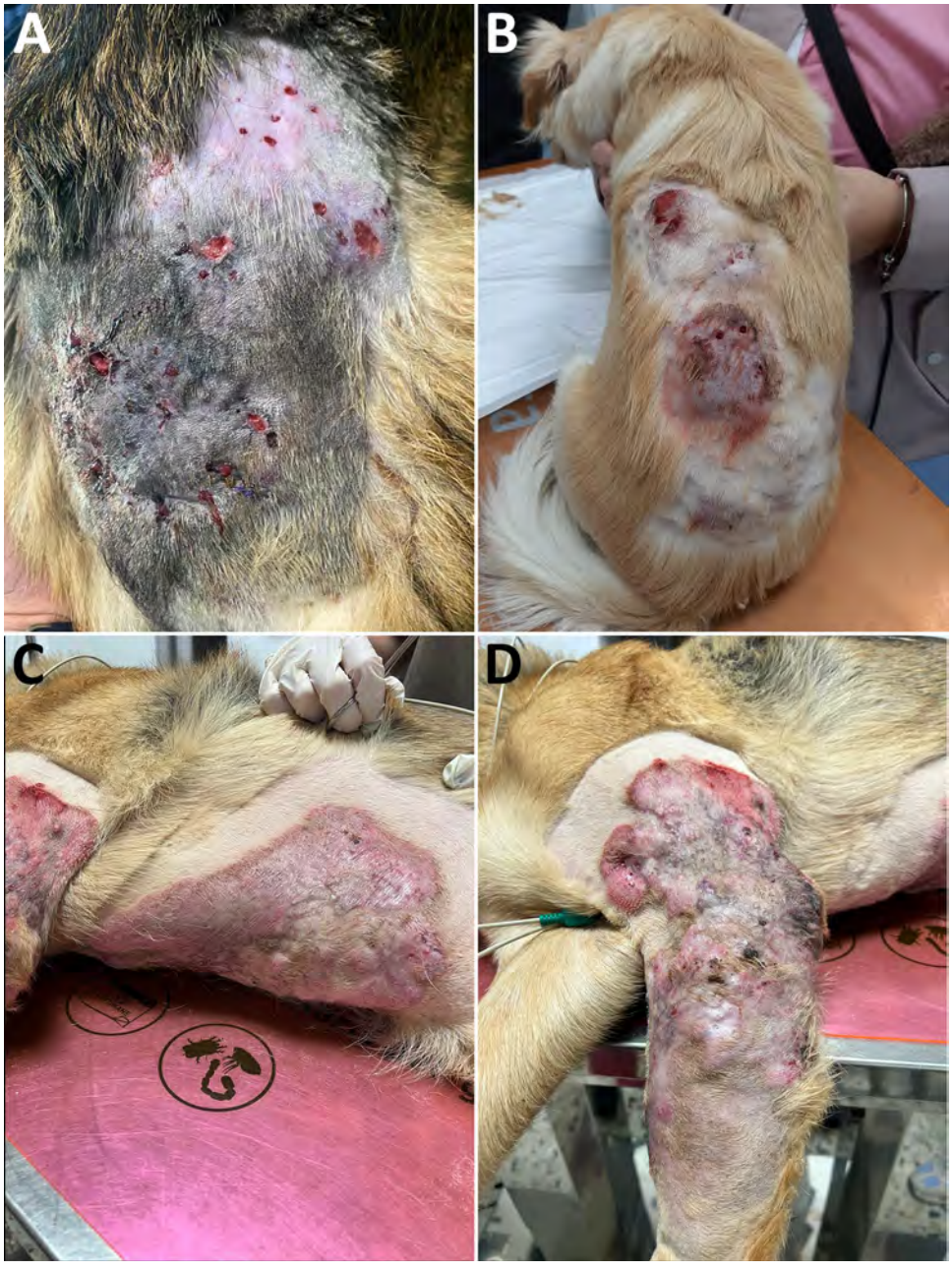

Figure 2. Representative cutaneous manifestations of canine pythiosis for a study of autochthonous canine pythiosis linked with freshwater exposure, Italy, 2021–2024. Lesions were characterized by chronic ulceration, nodules or plaques, draining tracts, and extensive proliferative to necrotizing cutaneous involvement. A) Extensive ulcerative and proliferative lesions involving the dorsal region. B) Ulcerative plaque affecting the dorsal thoracic region. C) Extensive ventral cutaneous involvement with ulcerative and proliferative lesions. D) Severe chronic ulcerative and exudative lesion affecting the left forelimb.

several cases, the initial clinical manifestation suggested inflammatory or bacterial disorders, and empirical treatment and, in some cases, repeated surgery preceded definitive diagnosis (Appendix, https://wwwnc.cdc.gov/EID/article/32/9/26-0354-App1.pdf).

We established diagnosis by combinations of cytology, histopathology, culture, and sequencing (Appendix). Cytologic and histologic examination showed broad, irregular, sparsely septate, hyphae-like structures associated with pyogranulomatous inflammation. Internal transcribed spacer sequence data were available for 6 cases, and those isolates clustered within clade IV of the *P. insidiosum* complex, corresponding to the lineage currently designated *Pythium periculosum*. (*10*) We conducted phylogenetic analysis using representative reference sequences spanning the 4 major clades recognized within the complex (Appendix Figure). All sequences from Italy grouped within clade IV, consistent with the broader extra-American representation previously observed for this clade (*10*). One additional case, for which only large subunit sequence data were available, showed highest similarity to isolates previously assigned to the same lineage. The sequences from Italy also showed limited divergence from one another and appeared closely related within the clade IV framework, suggesting a geographically related cluster.

Our findings provide further evidence that canine pythiosis can occur in temperate settings outside traditionally recognized endemic areas. Recurrent identification of cases associated with freshwater exposure suggests that suitable environmental niches may exist in multiple regions of Italy despite the absence of classically tropical climatic conditions. From a One Health perspective, dogs may act as sentinels of environmental exposure risk relevant to multiple hosts and may contribute to recognition of previously underappreciated ecologic niches favorable to pathogenic oomycetes. Increased awareness among veterinary and human healthcare professionals will be important for earlier recognition of this emerging disease in Europe.

The authors used ChatGPT (OpenAI, https://www.openai.com) for language editing and technical guidance in figure formatting but performed all data collection, analyses, interpretations, and figure preparation themselves. No images, data, or scientific content were generated by AI.

About the Author

Dr. Peano is an assistant professor in the Department of Veterinary Sciences, University of Turin, Italy. His research focuses on fungal diseases of domestic and wild animals, with particular interest in their epidemiology and One Health implications.

References

1. Gaastra W, Lipman LJ, De Cock AW, Exel TK, Pegge RB, Scheurwater J, et al. *Pythium insidiosum*: an overview. Vet Microbiol. 2010;146:1–16. https://doi.org/10.1016/j.vetmic.2010.07.019
2. Yolanda H, Krajaejun T. Global distribution and clinical features of pythiosis in humans and animals. J Fungi (Basel). 2022;8:182. https://doi.org/10.3390/jof8020182
3. Calvano TP, Blatz PJ, Vento TJ, Wickes BL, Sutton DA, Thompson EH, et al. *Pythium aphanidermatum* infection following combat trauma. J Clin Microbiol. 2011;49:3710–3. https://doi.org/10.1128/JCM.01209-11
4. Farmer AR, Murray CK, Driscoll IR, Wickes BL, Wiederhold N, Sutton DA, et al. Combat-related *Pythium aphanidermatum* invasive wound infection: case report and discussion of utility of molecular diagnostics. J Clin Microbiol. 2015;53:1968–75. https://doi.org/10.1128/JCM.00410-15
5. Bernheim D, Dupont D, Aptel F, Dard C, Chiquet C, Normand AC, et al. Pythiosis: case report leading to new features in clinical and diagnostic management of this fungal-like infection. Int J Infect Dis. 2019;86:40–3. https://doi.org/10.1016/j.ijid.2019.06.011
6. Peano A, Min ARM, Fondati A, Romano E, Brachelente C, Porcellato I, et al. Cutaneous pythiosis in 2 dogs, Italy. Emerg Infect Dis. 2023;29:1447–50. https://doi.org/10.3201/eid2907.230320
7. Oldenhoff W, Grooters A, Pinkerton ME, Knorr J, Trepanier L. Cutaneous pythiosis in two dogs from Wisconsin, USA. Vet Dermatol. 2014;25:52–e21. https://doi.org/10.1111/vde.12101
8. Berryessa NA, Marks SL, Pesavento PA, Krasnansky T, Yoshimoto SK, Johnson EG, et al. Gastrointestinal pythiosis in 10 dogs from California. J Vet Intern Med. 2008;22:1065–9. https://doi.org/10.1111/j.1939-1676.2008.0123.x
9. Billings P, Walton S, Shmalberg J, Santoro D. The use of mefenoxam to treat cutaneous and gastrointestinal pythiosis in dogs: a retrospective study. Microorganisms. 2023;11:1726. https://doi.org/10.3390/microorganisms11071726
10. Miraglia BM, Mendoza L, Rammohan R, Vilela L, Vilela C, Vilela G, et al. *Pythium insidiosum* complex hides a cryptic novel species: *Pythium periculosum.* Fungal Biol. 2022;126:366–74. https://doi.org/10.1016/j.funbio.2022.03.002

Address for correspondence: Andrea Peano, Dipartimento di Scienze Veterinarie, Largo P. Braccini 2, 10095 Grugliasco, Torino, Italy; email: andrea.peano@unito.it

Pulmonary Histoplasmosis, Taiwan, 1997–2024

Chih-Wei Liang, Chieh Yu Hsieh, Shang-Yi Lin

Author affiliations: Division of Infectious Diseases, Kaohsiung Medical University Hospital, Kaohsiung Medical University, Kaohsiung, Taiwan (C.-W. Liang, S.-Y. Lin); Kaohsiung Municipal Siaogang Hospital, Kaohsiung (C.-Y. Hsieh)

DOI: https://doi.org/10.3201/eid3209.260437

To the Editor: We read with interest about the cases of *Histoplasma capsulatum* infection in Taiwan, described by Kao et al. (*1*). However, molecular characterization of clinical isolates from Taiwan remains limited.

We report a case of disseminated histoplasmosis diagnosed in southern Taiwan in 2024. A 57-year-old man had persistent fever, weight loss, and progressive dyspnea. He had no history of diabetes, autoimmune disease, immunosuppressive therapy, or HIV infection. Imaging revealed diffuse pulmonary infiltrates and hepatosplenomegaly. Laboratory tests showed pancytopenia, hyperferritinemia, hypertriglyceridemia, and elevated liver enzymes, raising suspicion for hemophagocytic lymphohistiocytosis. Bone marrow examination demonstrated intracellular yeast forms within histiocytes, and metagenomic next-generation sequencing detected *H. capsulatum* fungi. The patient received liposomal amphotericin B (3 mg/kg/d) for 10 days, followed by oral itraconazole (200 mg 2×/d), with gradual clinical improvement. A bone marrow fungal culture yielded *H. capsulatum* fungi 28 days after sample collection. The patient never traveled to histoplasmosis-endemic regions, but he did engage in vegetable gardening on farmland in suburban Kaohsiung, where bat activity has been documented, although he reported no direct contact with bat guano, bird roosts, or imported animals.

Our phylogenetic analysis showed that the isolate clustered within the Latin American A1 lineage, together with reference strains from Mexico and Honduras (Figure). That finding was unexpected because most Asia isolates belong to the Eurasian clade (*2*). Possible explanations include imported infection, historical introduction, or unrecognized environmental reservoirs. Because *H. capsulatum* fungi commonly inhabit soil enriched with bat guano or bird droppings, suitable ecological niches might exist in subtropical Taiwan (*2*–*4*). Our findings suggest that lineage diversity of *H. capsulatum* fungi circulating in Asia might be underestimated.

Our findings provide molecular epidemiologic evidence of an unexpected *H. capsulatum* Latin American A1 lineage in Taiwan. Given the increase in histoplasmosis in Taiwan (*1*,*5*), expanded molecular surveillance and environmental sampling are needed to clarify the geographic distribution and transmission ecology of *H. capsulatum* fungi.

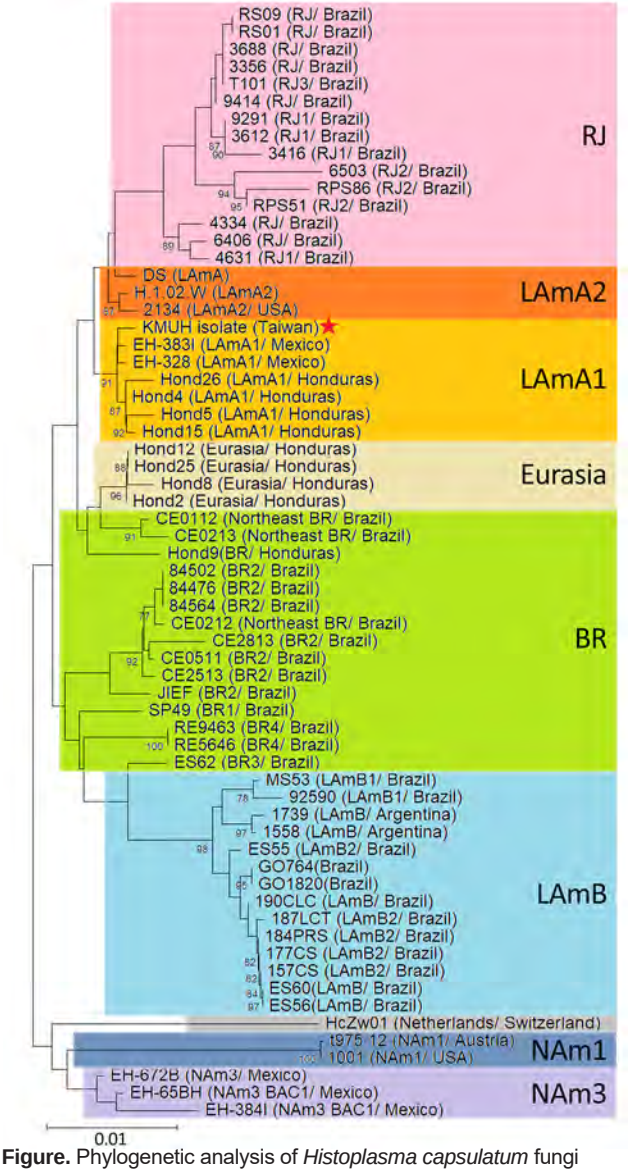

Figure. Phylogenetic analysis of *Histoplasma capsulatum* fungi sequences from a case of disseminated histoplasmosis, Taiwan, 2024. Phylogenetic tree was constructed by using the neighbor-joining method on the basis of concatenated multilocus sequence typing analysis of 4 genes (*arf*, *H-anti*, *ole*, and *tub*). Bootstrap support for the relevant internal node was 91% on the basis of 1,000 replicates. Red star indicates isolate sequenced from our study (GenBank accession nos. PX954369 [*arf*], PX954370 [*H-anti*], PX954371 [*ole*], and PX954372 [*tub*]). Scale bar indicates nucleotide substitutions per site. BR, Brazilian; LAmA1, Latin American A1; LAmA2, Latin American A2; LAmB, Latin American B; NAm1, North American 1; NAm3, North American 3; RJ, Rio de Janeiro.

We used ChatGPT (OpenAI, https://openai.com) to assist with English-language editing. All authors reviewed and approved the final manuscript and take full responsibility for its content.

References

1. Kao TW, Yang SC, Hu HW, Huang YT, Shu CC, Sheng WH. Pulmonary histoplasmosis, Taiwan, 1997–2024. Emerg Infect Dis. 2026;32:7–14. https://doi.org/10.3201/eid3201.251091
2. Teixeira MM, Patané JS, Taylor ML, Gómez BL, Theodoro RC, de Hoog S, et al. Worldwide phylogenetic distributions and population dynamics of the genus *Histoplasma.* PLoS Negl Trop Dis. 2016;10:e0004732. https://doi.org/10.1371/journal.pntd.0004732
3. Taylor ML, Reyes-Montes MDR, Estrada-Bárcenas DA, Zancopé-Oliveira RM, Rodríguez-Arellanes G, Ramírez JA. Considerations about the geographic distribution of *Histoplasma* species. Appl Environ Microbiol. 2022;88:e0201021. https://doi.org/10.1128/aem.02010-21
4. Galgiani JN, Kauffman CA. Coccidioidomycosis and histoplasmosis in immunocompetent persons. N Engl J Med. 2024;390:536–47. https://doi.org/10.1056/NEJMra2306821
5. Hsu JC, Chang PH, Tai CH, Chen YC. Histoplasmosis in Taiwan: case summary and literature review. Life (Basel). 2024;14:738. https://doi.org/10.3390/life14060738

Address for correspondence: Shang-Yi Lin, Division of Infectious Diseases, Department of Internal Medicine, Kaohsiung Medical University Hospital, Kaohsiung Medical University, Kaohsiung, 100 Tzyou 1st Rd, Kaohsiung City, Taiwan; email: amoe616@gmail.com

Ting-Wei Kao, Shang-Chen Yang, Hsiang-Wei Hu, Yu-Tsung Huang, Chin-Chung Shu, Wang-Huei Sheng

Author affiliations: National Taiwan University Hospital, Department of Internal Medicine, National Taiwan University College of Medicine, Taipei, Taiwan (T.-W. Kao, S.-C. Yang, C-.C. Shu, W.-H. Sheng); National Taiwan University Hospital, Department of Pathology, Taipei (H.-W. Hu); National Taiwan University Hospital, Department of Laboratory Medicine, National Taiwan University College of Medicine, Taipei (Y.-T. Huang); Graduate Institute of Clinical Medicine, National Taiwan University College of Medicine, Taipei (C.-C. Shu); National Taiwan University Hospital Hsinchu Branch, Department of Internal Medicine, Hsinchu, Taiwan (W.-H. Sheng)

DOI: https://doi.org/10.3201/eid3209.261249

In Response: We sincerely thank Lin et al. for their insightful comments on our article (*1*) and for providing valuable molecular epidemiologic evidence regarding *Histoplasma capsulatum* in Taiwan. The identification of a Latin American A1 lineage isolate in a patient without a travel history raises interesting questions regarding the local epidemiology of histoplasmosis. Their report highlights the increasing role of molecular approaches in understanding transmission dynamics and phylogeography of *Histoplasma* spp. fungi. Such molecular characterization might represent a necessary direction for future epidemiologic investigations. However, our retrospective study spanned nearly 3 decades, during which fungal isolates were not routinely preserved for molecular characterization. Consequently, comparable genomic data were unavailable for most patients.

The case report shared notable similarities with our findings. Both studies identified patients with histoplasmosis without a travel history, supporting the possibility of local acquisition or previously unrecognized environmental exposure. Also, both studies demonstrate that histoplasmosis is not restricted to immunocompromised persons and should not be regarded only as an imported infection in Taiwan. The report used molecular analysis to characterize a fungal isolate obtained from culture. In contrast, fungal cultures were infrequently positive in our cohort, highlighting one of the major diagnostic challenges encountered in routine clinical practice.

Whether these cases reflect local environmental reservoirs, historical introduction events, or previously unrecognized transmission pathways remains unclear. Expanded environmental sampling, preservation of fungal isolates, and molecular surveillance are needed to clarify the geographic distribution, lineage diversity, and transmission ecology of *Histoplasma* spp. fungi in Taiwan and other traditionally nonendemic regions. That limitation also could contribute to underrecognition of locally acquired histoplasmosis.

References

1. Kao TW, Yang SC, Hu HW, Huang YT, Shu CC, Sheng WH. Pulmonary histoplasmosis, Taiwan, 1997–2024. Emerg Infect Dis. 2026;32:7–14. https://doi.org/10.3201/eid3201.251091

Chin-Chung Shu, Division of Pulmonary and Critical Care Medicine, Department of Internal Medicine, National Taiwan University Hospital, No. 7, Chung-Shan South Rd, Taipei, Taiwan; email: ccshu@ntu.edu.tw

Recent *Mycobacterium tuberculosis* Transmission, United States, 2018–2022

Rohma Zubairi

Author affiliation: Jinnah Sindh Medical University, Karachi, Pakistan

DOI: https://doi.org/10.3201/eid3209.261176

To the Editor: A recent article published in June 2026 described the characteristics of plausible source cases responsible for recent *Mycobacterium tuberculosis* transmission in the United States by using national surveillance and whole-genome sequencing data (*1*). The authors expertly applied molecular epidemiology and machine-learning methods to identify factors associated with tuberculosis (TB) transmission and demonstrated the heterogeneity of transmission events.

The study relied on a plausible source–case algorithm incorporating spatial proximity, temporal linkage, and genomic similarity. Although that information is valuable for surveillance, recent evidence suggests that TB transmission networks are often more complex than can be captured by predefined genomic thresholds and hierarchical source assignment rules. Contemporary transmission-reconstruction approaches integrate genomic, epidemiologic, and spatial data to account for incomplete sampling, undetected intermediaries, and within-host evolution. Consequently, some transmission events might have been misclassified, potentially influencing estimates of source-case characteristics (*2*,*3*).

Although the adaptive boosting model demonstrated good discriminatory performance, its generalizability remains uncertain because validation was restricted to the study dataset. Predictive models frequently experience performance degradation when applied to populations with different demographic compositions, healthcare access patterns, and transmission dynamics. External validation across diverse settings is essential before such models are used to prioritize public health interventions (*4*).

Finally, several social and healthcare-system factors that influence TB transmission, including diagnostic delay, were not included. Untreated disease increases opportunities for transmission and might contribute to highly infectious disease phenotypes, including cavitary disease and sputum smear positivity. Because populations facing barriers to healthcare access often experience longer diagnostic delays, some associations between demographic characteristics, markers of infectiousness, and source-case attribution might reflect prolonged infectious periods rather than independent transmission-promoting effects. Diagnostic delay remains a critical but underrecognized target for tuberculosis control interventions (*5*).

Despite those considerations, the study provides evidence on persons contributing most to ongoing TB transmission. Future investigations incorporating transmission-reconstruction methods, diagnostic-delay metrics, and external validation of predictive models might strengthen TB prevention and control.

References

1. Kammerer S, Flanagan D, Raz K, Shaw T, Wortham J, Talarico S. Characteristics of plausible source cases responsible for recent *Mycobacterium tuberculosis* transmission, United States, 2018–2022. Emerg Infect Dis. 2026;32:880–93. https://doi.org/10.3201/eid3206.260104
2. Sobkowiak B, Romanowski K, Sekirov I, Gardy JL, Johnston JC. Comparing *Mycobacterium tuberculosis* transmission reconstruction models from whole genome sequence data. Epidemiol Infect. 2023;151:e105. https://doi.org/10.1017/S0950268823000900
3. Lan Y, Rancu I, Chitwood MH, Sobkowiak B, Nyhan K, Lin HH, et al. Integrating genomic and spatial analyses to describe tuberculosis transmission: a scoping review. Lancet Microbe. 2025;6:101094. https://doi.org/10.1016/j.lanmic.2025.101094
4. Liu ZZ, Yuan Q, Zhang YD, Zhang XD, Liu J, Yan JW, et al. Validation and interpretation of machine-learning models for rapid identification of active tuberculosis infection using routine laboratory indicators. Front Cell Infect Microbiol. 2025;15:1718614. https://doi.org/10.3389/fcimb.2025.1718614
5. Getnet F, Demissie M, Assefa N, Mengistie B, Worku A. Delay in diagnosis of pulmonary tuberculosis in low-and middle-income settings: systematic review and meta-analysis. BMC Pulm Med. 2017;17:202. https://doi.org/10.1186/s12890-017-0551-y

Address for correspondence: Rohma Zubairi, Jinnah Sindh Medical University, Rafiqui (H.J.) Shaheed Road, Karachi 75510, Sindh, Pakistan; email: zubairirohma@gmail.com

Steve Kammerer

Author affiliation: Centers for Disease Control and Prevention, Atlanta, Georgia, USA

DOI: https://doi.org/10.3201/eid3209.261478

In Response: We thank Dr. Zubairi for raising the points in his letter (1). We view those methodological considerations as valid questions within the context of applying our results to tuberculosis (TB) prevention and control.

We agree that transmission networks can be more complex than are represented by our plausible source case algorithm and use of whole-genome single nucleotide polymorphism distances to assess genomic similarity. However, our integration of spatial and temporal proximity with genomic similarity represents our best estimates of recent transmission, which were validated with locally provided contact investigation data from multiple sites in the United States. In addition, we accept that those estimates can misclassify cases as false-positive or false-negative transmission events. Validation of the algorithm demonstrated an accuracy of 95.8% compared with on-the-ground epidemiologic data, with sensitivity of 79.1% and specificity of 97.7% (S. Kammerer, unpub. data)

Regarding external validation of the adaptive boosting machine learning model, our study examined the epidemiology of TB transmission in the United States. Generalization to other settings with different transmission dynamics, demographics, genomic diversity, healthcare utilization, and public health infrastructure, including settings that do not genotype nearly all isolates from culture-confirmed cases, would not be appropriate. Our findings are appropriate to consider for prioritizing interventions in the United States. The methodological approach could also be a starting place for a similar analysis in other settings with similar epidemiology and genotyping coverage.

We agree that diagnostic delay is a major driver of TB transmission; however, we did not have reliable data regarding symptom onset to assess in our study. Accurate data regarding symptom onset are challenging to obtain in clinical settings. However, we did consider objective clinical findings associated with diagnostic delay and advanced disease (e.g., sputum smear positivity), and those findings were associated with plausible source cases in our analysis.

References

1. Zubairi R. Recent *Mycobacterium tuberculosis* transmission, United States, 2018–2022. Emerg Infect Dis. 2026;32:1531. https://doi.org/10.3201/eid3209.261176

Address for correspondence: Steve Kammerer, Centers for Disease Control and Prevention, 1600 Clifton Rd NE, Mailstop V24-3, Atlanta, GA 30329-4018, USA; email: fzk3@cdc.gov

etymologia revisited

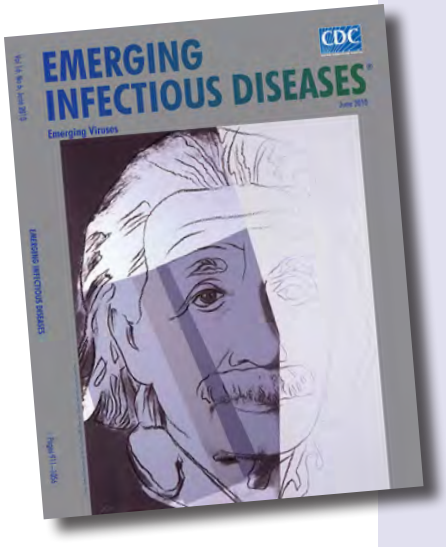

Originally published in June 2010

Lassa Virus

[lah sə] virus

This virus was named after the town of Lassa at the southern end of Lake Chad in northeastern Nigeria, where the first known patient, a nurse in a mission hospital, had lived and worked when she contracted this infection in 1969. The virus was discovered as part of a plan to identify unknown viruses from Africa by collecting serum specimens from patients with fevers of unknown origin. Lassa virus, transmitted by field rats, is endemic in West Africa, where it causes up to 300,000 infections and 5,000 deaths each year.

References:

1 Frame JD, Baldwin JM Jr, Gocke DJ, Troup JM. Lassa fever, a new virus disease of man from West Africa. I. Clinical description and pathological findings. Am J Trop Med Hyg. 1970;19:670–6
2. Mahy BW. The dictionary of virology, 4th ed. Burlington (MA): Elsevier; 2009.

https://wwwnc.cdc.gov/eid/article/16/6/et-1606_article

Jörg Braumeister, *Stadtbibliothek im Bildungscampus Nürnberg*, *Amb. 317.2°*, *Folio 60 recto*, 1437 (detail). Pen and ink on parchment. 287 mm × 205 mm (11.3 in × 8.1 in). Collection: The Hausbücher der Nürnberger Zwölfbrüderstiftungen. Nuremberg Twelve Brothers House Books, Nuremberg, Germany.

Liquid Bread and Invisible Worlds—Beer, Fungi, and the Origins of Microbial Control

Nicolas Hoffmann

Beer is among humanity's oldest inventions. Academic debate continues over what came first, beer or bread, and one leading hypothesis suggests beer itself evolved from earlier accidents: perhaps from grain stores that became wet and spontaneously fermented, or from observations of mead, when honey and rainwater were colonized by wild yeasts. Whatever the precise origin, the result was the same. Humans began cultivating a process they did not yet understand.

This month's cover image captures that prescientific moment. A lone figure stands before fire and liquid, engaged in a process both ordinary and profound—the production of a beverage essential for hydration, nutrition, and safety in medieval life. The brewer does not know it, but the labor is shared with unseen fungal partners.

The illustration comes from the *Hausbücher der Nürnberger Zwölfbrüderstiftungen* (Nuremberg Twelve Brothers House Books, Nuremberg, Germany), a set of illuminated manuscripts compiled during 1426–1806 to document the trades of craftsmen supported by the Mendel and Landauer charitable foundations in Nuremberg. Each folio depicts a single artisan at work, accompanied by a brief biographical entry. The illustrators are largely anonymous, and individual attribution is rarely possible. The manuscripts are held by the Stadtbibliothek Nürnberg and have been fully digitized (https://www.nuernberger-hausbuecher.de).

Author affiliation: Marist School, Atlanta, Georgia, USA; Georgia Gwinnett College, Lawrenceville, Georgia, USA

DOI: https://doi.org/10.3201/eid3209.AC3209

The brewer here is a layman—not, despite popular association, a monk—supported by the foundation in old age. According to the description on the obverse, "Jörg Breu was the first almshouse brother of whom it is recorded—according to the inscription—that he was discharged from the Twelve Brothers' House due to illness; in this instance, he was transferred to the St. Jobst Leper Hospital."

He stirs a heated vessel while smaller tubs await the finished product, the fire beneath carefully controlled. The scene conveys method, repetition, and accumulated knowledge. Yet it also reflects a world in which craft knowledge far outpaced scientific explanation. Brewers understood the process; they did not understand the how.

For most of human history, fermentation was observed rather than understood. Grain was soaked, bread dissolved, liquid boiled, and time did the rest. What transformed that mixture was not magic but fungi. Yeast, single-celled fungi of the genus *Saccharomyces*, consume sugars and produce alcohol and carbon dioxide, converting grain into something stable, caloric, and safer to drink. But yeast do not act alone. They exist within a microbial ecosystem that includes bacteria and other fungi; some contribute desirable flavors, others spoil the batch, and still others, introduced through contaminated water or poorly managed fermentation, can cause illness.

The fungal kingdom occupies a peculiar place in human history, both intimate and dangerous. Fungi make possible some of humanity's most important foods—bread, beer, cheese—yet they are also notable agents of disease. Recent estimates attribute ≈3.8 million deaths annually to invasive fungal infection, and roughly 2.5 million are directly caused by fungal pathogens such as *Candida*, *Aspergillus*, *Cryptococcus*, and *Pneumocystis*. In 2022, the World Health Organization issued its first fungal priority pathogens list, recognizing rising antifungal resistance and the scarcity of diagnostic and therapeutic tools. Mycotoxins compound the burden; ergot alkaloids in contaminated grain, for example, have historically caused outbreaks of mass poisoning and hallucination.

To premodern populations, such outcomes were indistinguishable in cause. The same unseen forces that produced nourishment could also produce sickness. Beer sat at that intersection, a product of controlled fungal activity whose safety depended on keeping other microbial actors in check.

By the early 16th Century, brewers in the German states attempted to impose order on this unpredictable system. The Reinheitsgebot of 1516 limited beer ingredients to water, grain, and hops. Notably absent was yeast, which, although essential, remained invisible to science. The law is often remembered as a cultural constraint, but in practice it functioned as risk reduction. Brewers had long experimented with additives—some harmless, others toxic—and by restricting ingredients, the law lowered the likelihood of contamination, poisoning, and unintended fermentation. Hops in particular contain antimicrobial compounds that inhibit bacterial growth, helping stabilize beer and extend its shelf life. Without knowing it, brewers were practicing infection control.

Beer's role in survival reaches even further back. In ancient Egypt, laborers were partly compensated in beer rations: thick, nutritious, and calorically dense, fermented from bread and grain. That early beer was, quite literally, liquid bread, and it offered a crucial advantage: relative safety. In environments where waterborne pathogens were common, fermentation, boiling, alcohol, and acidity all inhibited microbial growth. Beer was not sterile, but it was often safer than the available water.

That relationship changed in the 19th Century, when Louis Pasteur demonstrated that fermentation was driven by living microorganisms, specifically, by yeast. Yeast could now be isolated, cultivated, and standardized; contamination could be identified and spoilage prevented with intention. What had once been an uncertain collaboration became a controlled partnership.

The brewer in this image stands at a moment before germ theory, before microbiology, before fungi were understood as either allies or pathogens. Yet he works within that system reliably, and with consequences that continue to shape human health. Beer represents one of humanity's earliest and most successful negotiations with fungi, harnessing some organisms to create stability while suppressing others that might cause harm. It is a story not of elimination but of coexistence, and one that remains unfinished. As antifungal resistance grows and invasive mycoses claim millions of lives each year, the brewer's vat reminds us that managing fungi has always been, and remains, a public health enterprise.

Bibliography

1. Denning DW. Global incidence and mortality of severe fungal disease. Lancet Infect Dis. 2024;24:e428–38. https://doi.org/10.1016/S1473-3099(23)00692-8
2. World Health Organization. WHO fungal priority pathogens list to guide research, development and public health action [cited 2026 May 6]. https://www.who.int/publications/i/item/9789240060241

Address for correspondence: Nicolas Hoffmann, Marist School, 3790 Ashford Dunwoody Rd, Atlanta, GA 30319, USA; email: nhoffmann@gmail.com, hoffmannn@marist.com

EMERGING INFECTIOUS DISEASES®

Upcoming Issue
Vaccine-Preventable Diseases • October 2026

- Reassortment of High Pathogenicity Avian Influenza as a Driver for Zoonotic Spillover, Asia
- Meta-Analysis of Maternal and Fetal Outcomes of Crimean-Congo Hemorrhagic Fever during Pregnancy
- Detection of *Anaplasma capra* in Patients with Suspected Crimean-Congo Hemorrhagic Fever, Turkey, 2022
- Systematic Review and Meta-Analysis of Group B *Streptococcus* Recto-Vaginal Colonisation Rates and Serotype Distribution among Pregnant Women in the Asia-Pacific Region
- Detection, Notification, and Response Timeliness during a Cross-Border Bundibugyo Virus Disease Outbreak, Uganda, 2026
- Multiple Introductions and Cross-Sector Transmission of *Salmonella enterica* Serovar *Infantis* Carrying $bla_{\text{CTX-M-65}}$ Gene, South Korea, 2022–2024
- Molecular Epidemiology and Evolution of Swine Influenza A Viruses in Vietnam, 2020–2024
- Genomic Epidemiology of Persistent Strain of *Salmonella* Hadar Linked to Poultry-Associated Salmonellosis Outbreaks
- Persistent *Bartonella quintana* Infection in Japanese Macaques Housed at Primate Research Institute in Japan
- Isothermal Detection of Influenza D Virus using RT-LAMP
- Multi-Sectoral Emergence of a Multidrug-Resistant *Campylobacter coli* ST-10042 Lineage, Europe, 2018–2025
- Meta-Analysis of Asymptomatic Monkeypox Virus Prevalence in Nonendemic Regions, 2022–2024
- Human Myiasis Due to Reemergence of *Cochliomyia hominivorax*, Mexico, 2025–2026
- Wastewater Surveillance to Track a Resurgent Outbreak of Measles, Ontario, Canada, 2025
- Surface Sampling for Mpox Virus in Multiple Healthcare Settings, Sierra Leone, June 2025
- Detection of Divergent Highly Pathogenic Avian Influenza (H5N1) Clade 2.3.4.4b Virus, São Paulo, Brazil, 2025
- Highly Pathogenic Avian Influenza Virus (H5N1) Detected in Cat and Rats during Backyard Poultry Outbreak, United States, 2025
- *Chlamydia psittaci* Meningitis, Chile, 2023
- Emergence of Macrolide-Resistant *Bordetella pertussis* in Peru
- Baloxavir-Based Treatment Combinations Provide Robust Protection against Clade 2.3.4.4b H5N1 Virus Infection in Mice
- Emergence of a Genotype 2.3.1 Multidrug-Resistant *Salmonella enterica* Serotype Typhi Strain, West Africa, 2021–2025
- Clinical Characterization, Diagnostic Gaps, and Transmission-Setting Determinants of Invasive Meningococcal Disease during the 2026 Tashkent Outbreak
- Emergence of Rabies in Cape Fur Seals, South Africa
- Emergence of *Plasmodium malariae* and Co-Endemicity of 3 *Plasmodium* Species Parasites, Khanh Hoa Province, Vietnam, 2023–2025
- Fatal Infection with Dengue Virus and Avian Orthoavulavirus 1 in Traveler from Saudi Arabia, 2025
- Transmission Characteristics and Superspreading Potential of Andes Virus Human-to-Human Transmission
- Highly Pathogenic Avian Influenza Virus Subtype 5 in Cetaceans, Brazil
- *Trichodysplasia spinulosa* Virus Not Detectable in Inflammatory Dermatoses by RNAscope
- Genomic and Phylogenetic Characterization of Human Mpox Clade 1b in Uganda and Co-Circulation with Varicella Zoster Virus
- Human Infection with Japanese Encephalitis Virus Genotype V, China, 2025
- Age Shift in Epidemiology of Pertussis Epidemics in New South Wales, Australia, 2015 and 2024
- Transmissibility and Case-Fatality of Bundibugyo Virus Estimated from the First Outbreak, Uganda, 2007
- *Haemophilus ducreyi* as Cause of a Cutaneous Ulcer Outbreak in Children, Sierra Leone, December 2025
- In Memoriam: The Enduring Influence of Nancy J. Cox (1948–2026)
- Smallpox Military Policy and Decisive Actions of George Washington

Complete list of articles in the October issue at
http://www.cdc.gov/eid/#issue-336

Earning CME Credit

To obtain credit, you should first read the journal article. After reading the article, you should be able to answer the following, related, multiple-choice questions. To complete the questions (with a minimum 80% passing score) and earn continuing education (CE) credit, please visit CDC TRAIN (https://www.train.org/cdctrain/welcome) and search for the course in the Course Catalog using SCJA5063. Follow the steps below by August 31, 2027. Credit cannot be obtained for tests completed on paper, although you may use the worksheet below to keep a record of your answers.

1. Register for and complete the course.
2. Pass the post-assessment at 80%.
   All CDC continuing education courses allow two attempts to pass the post-assessment. If you do not pass on the first attempt, you have 30 days to retake it. Failing both attempts will result in a failed course status, and the course cannot be retaken during the current accreditation period. Please refer to the course description page for specific start and end dates.
3. Complete the evaluation.
4. Visit Your Learning to access your certificates and transcript.

Only one answer is correct for each question. Once you successfully answer all posttest questions and course evaluation, you will be able to view and print your certificate. No fees are charged for CDC's CE activities.

For questions regarding this activity, contact the accredited provider, https://www.cdc.gov/cdc-train/contact. For technical assistance, contact https://www.cdc.gov/cdc-train/contact.

Article Title

Neoehrlichiosis Causing Hemolytic Anemia in Patients Treated with Rituximab, Norway, 2024–2025

CME Questions

1. Which of the following statements about neoehrlichiosis is most accurate?

a) Neoehrlichiosis is a mild and self-limiting illness.
b) Signs and symptoms of neoehrlichiosis include fever, malaise, fatigue, night sweats, myalgia, skin rashes, and vascular events.
c) Neoehrlichiosis is more likely to affect immunocompetent persons.
d) Neoehrlichiosis is easily detectable by blood culture.

2. Identify two primary neoehrlichiosis risk factors that were common among all three patients described in this study.

a) Immunocompromised and history of cancer
b) Cardiovascular disease and renal disease
c) Previous vascular events and international travel
d) Splenomegaly and previous treatment with rituximab

3. According to the report *Neohehrlichia mikurensis* bacteria can cause latent infections that can reactivate when B-cell immunity is suppressed by rituximab.

a) True
b) False

4. A clinical team observes hemolytic anemia, vasculitis resembling giant cell arteritis, and splenomegaly in a patient reporting fever, night sweats, and fatigue. The patient has a history of tick bites without erythema migrans. A direct antiglobulin test (DAT) returns negative results. The patient reported receiving rituximab treatment for rheumatoid arthritis. The care team suspects neoehrlichiosis. What additional diagnostic testing could confirm neoehrlichiosis?

a) PCR of EDTA blood samples for tickborne pathogens
b) Blood culture for bacterial pathogens
c) Flow cytometry of bone marrow aspirate
d) Abdominal PET-CT scan

5. After confirming neoehrlichiosis in the three patients in this study, which of the following successfully treated the infection and improve hemolysis?

a) Oral methotrexate
b) Intravenous immunoglobin
c) Oral doxycycline
d) Splenectomy